UNIVERSITY OF COPENHAGEN
DEPARTMENT OF BIOLOGY

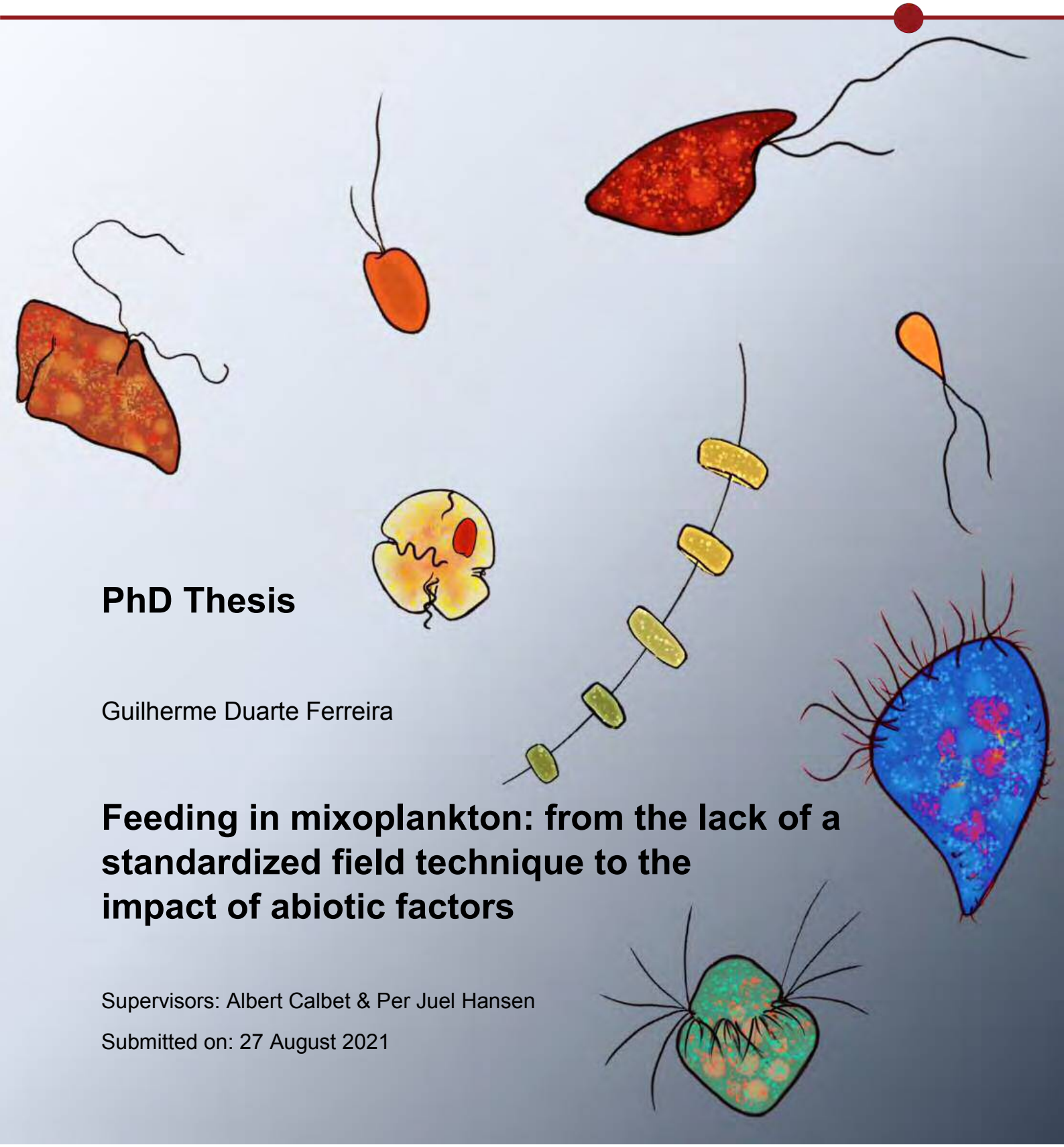

PhD Thesis

Guilherme Duarte Ferreira

Feeding in mixoplankton: from the lack of a standardized field technique to the impact of abiotic factors

Supervisors: Albert Calbet & Per Juel Hansen

Submitted on: 27 August 2021

UNIVERSITY OF COPENHAGEN

Name of department:	Department of Biology
Author:	Guilherme Duarte Ferreira
Title:	Feeding in mixoplankton: from lack of a standardized field technique to the impact of abiotic factors
Supervisors:	Prof. Per Juel Hansen Marine Biological Section Department of Biology Københavns Universitet, Denmark Dr. Albert Calbet Institut de Ciències del Mar Department of Marine Biology and Oceanography Consejo Superior de Investigaciones Científicas, Spain
Submitted on:	27 August 2021
Assessment committee:	Nina Lundholm (Chair) Natural History Museum of Denmark Department of Botany Københavns Universitet, Denmark Torkel Gissel Nielsen (Opponent) National Institute of Aquatic Resources DTU Aqua Danmarks Tekniske Universitet, Denmark Diane Stoecker (Opponent) University of Maryland Center for Environmental Science Horn Point Laboratory University of Maryland, United States

This thesis has been submitted to the PhD school of The Faculty of Science, University of Copenhagen

Preface

This thesis represents the work done during my years as a PhD fellow at the University of Copenhagen. This project has received funding from the European Union's Horizon 2020 research and innovation programme under the Marie Skłodowska-Curie grant agreement No. 766327. This document reflects only the author's view; the REA and the European Commission are not responsible for any use that may be made of the information it contains. This work was done under the joint supervision of Per Juel Hansen and Albert Calbet, at the Marine Biological Section in Helsingør, Denmark, and at the Institut de Ciències del Mar, CSIC, Barcelona, Spain, respectively.

The original title of this thesis was "Top-down control of marine protists by mixotrophs". The aim was to explore predator-prey interactions where mixotrophs are the predators, with the final objective of quantifying their *in situ* impact on other protists. Although not entirely deviated from the original scope, this thesis started with an international cooperation that clarified the nomenclature surrounding these fascinating organisms. Therefore, and as I had the opportunity of collaborating with an amazing array of international researchers, this thesis developed into something that would be quite underscored by the original title.

I am very happy with the path that led me down this road although this was a rather bumpy road, if I may say so myself. Long hours in the laboratory, spectacular failures, repeated experiments, lost cultures, etc… You name it. Still, I think that one can never fully appreciate the good things in life if one does not experience the other side. It is, thus, not surprising to find myself eager to start whatever path life has designated for me, knowing beforehand that I am going to grow from the experience, and that my supervisors will continue to have my back.

Ourém, Portugal, August 2021

Table of Contents

List of papers 1

Abstract 2

Danske Resumé 4

1. Introduction 6

2. Specific aims of the thesis and papers included 14

Paper I 18

Paper II 50

Paper III 72

Paper IV 102

3. Conclusions and future perspectives 126

References 129

Supplementary Information for Paper I 135

Supplementary Information for Paper III 137

Supplementary Information for Paper IV 144

Acknowledgments 148

List of papers

Paper I

Ferreira G.D., Calbet A., 2020. Caveats on the use of rotenone to estimate mixotrophic grazing in the oceans. *Scientific Reports*, 10, 3899.

Paper II

Ferreira G.D., Figueira J., Marques S.C., Hansen P.J., Calbet A. The strengths and weaknesses of Live Fluorescently Labelled Algae (LFLA) to estimate herbivory in protozooplankton and mixoplankton. Under revision for publication in *Marine Environmental Research*.

Paper III

Ferreira G.D., Romano F., Medić N., Pitta P., Hansen P.J., Flynn K.J., Mitra A., Calbet A. Integrating phago-mixotrophy in dilution grazing experiments. Under revision for publication in *Scientific Reports*.

Paper IV

Ferreira G.D., Grigoropoulou A., Saiz E., Calbet A. The effect of short-term temperature changes on key physiological processes of mixoplankton and protozooplankton grazers. Manuscript.

Additional work done during the PhD not to be included in the evaluation of the thesis

Appendix

Flynn K.J., Mitra A., Anestis K., Anschütz A.A., Calbet A., **Ferreira G.D.**, Gypens N., Hansen P.J., John U., Martin J.L., Mansour J.S., Maselli M., Medić N., Norlin A., Not F., Pitta P., Romano F., Saiz E., Schneider L.K., Stolte W., Traboni C., 2019. Mixotrophic protists and a new paradigm for marine ecology: where does plankton research go now? *Journal of Plankton Research*, 41, 375-391.

Abstract

The purpose of this PhD thesis is to contribute to the understanding of the recently formulated “mixoplankton paradigm” (**Appendix**). This paradigm recognises the importance of phago-mixotrophs in marine waters and stresses the importance of including them in biogeochemical models in the future. The first objective was to study techniques to quantify grazing by different types of mixoplankton. Therefore, I explored three independent approaches to quantify the grazing impact of mixoplankton in the field and attempted to characterise the consequences of light and temperature on the obtained rates. I started by following the incorporation of Live Fluorescently Labelled Algae (LFLA) over time (**Paper I**) in several protistan grazers, attempting to determine possible caveats of the technique in the determination of mixoplanktonic herbivory. The results indicate that LFLA can be used to track diel ingestion and digestion rates in several species. However, I also showed that LFLA must be used with caution in the field, due to issues surrounding selectivity and feeding mechanisms. Therefore, as this method was far from perfect, I also explored a different approach, which relied on the selective inhibition of the mitochondria by rotenone (**Paper II**). According to the mechanism of action, rotenone was expected to display a stronger effect on protozooplankton than on mixoplankton. The results demonstrated that, at low concentrations of rotenone, mixoplankters survived better than protozooplankters, despite not being able to feed. As the latter was still able to eat at inhibiting concentrations for mixoplankton, rotenone could not be used to discriminate between trophic modes of nutrition. The final attempt focused on the ubiquitously used dilution technique (**Paper III**). The results of a laboratory food web simulation, including mixoplankton as well as protozooplankton as grazers, evidenced that chlorophyll is an inadequate proxy for phytoplankton biomass when mixoplankton are present. In addition, the results showed that selectivity and intraguild predation affect the outcome of the technique. Still, the data produced may be of much help for building *in silico* models able to disentangle the grazing impact exerted by mixoplankton and protozooplankton in the field. The second objective of the thesis was to understand how light and temperature modulate grazing in mixoplankton and protozooplankton. The former was addressed by conducting day/night incubations with a few species (**Papers I** and **III**), but also in the complete absence of light during an entire day (**Paper III**). The results support the existence of diel feeding rhythms, which are partly retained in the

absence of light, even though this factor is critical for the correct expression of feeding for both protozooplankton and mixoplankton. The experiments from **Paper IV** enabled the determination of the effect of temperature on mixoplankton and protozooplankton in terms of growth and grazing, but also in terms of carbon dioxide sequestration and production. The results of this last paper showed that mixoplankton (but not protozooplankton) deviate from the canonical Metabolic Theory of Ecology. Indeed, the former become more phototrophic in a warming scenario, unlike past assumptions, which supported a higher degree of phagotrophy at higher temperatures. Protozooplankton displayed higher optimal temperatures for both growth and ingestion than their mixoplanktonic counterparts did. Altogether, this thesis contributed to the ongoing process of unveiling the ecological role of mixoplankton, in particular in the situations where their grazing impact is concerned.

Danske Resumé

Formålet med denne PhD thesis er at bidrage til forståelsen af det nyligt formulerede ”mixoplankton paradigma” (**Appendix**). Dette paradigma anerkender betydningen af “fago-mixotrofer” i havets frie vandmasser, og påpeger vigtigheden af at inkludere dem i fremtidige biogeokemiske modeller. Mit første formål var at studere og udvikle teknikker til kvantifikation af fødeoptagelsen hos forskellige typer af mixoplankton. Jeg benyttede 3 uafhængige metoder til at kvantificere mixoplanktons græsningsrater i felten, og forsøgte at karakterisere indflydelsen af lysintensitet and temperatur på disse rater. Jeg undersøgte først optagelsen af fluorescens-mærkede levende alger (kaldet LFLA) som funktion af inkubationstiden hos udvalgte fagotrofe protister, for at undersøge mulighederne for at anvende denne teknik til målinger af mixoplankton græsningsrater (**Artikel I**). Resulterne indikerede at LFLA kan benyttes til at måle døgnvariationer i fødeoptagelse og fordøjelse i udvalgte arter. Dog viste data også at LFLA skal bruges med forsigtighed i felten, pga problemer omkring bytteselektivitet og fødeoptagelses-mekanismer. Metoden er derfor langt fra perfekt. Jeg forsøgte mig derfor med en anden tilgang, som bygger på selektiv inhibition af mitokondrier ved brug af kemikaliet rotenon (**Artikel II**). Pga stoffet virkningsmekanisme var det forventet at rotenon skulle have en stærkere effekt på protozooplankton end på mixoplankton. Resulterne viste mixoplankton overlevede bedre end protozooplankton ved lave koncentrationer of rotenon, selvom de stoppede med at optage føde. Da protozooplankton stadig var i stand til at optage føde ved koncentrationer som inhiberede fødeoptagelsen hos mixoplankton, kunne rotenon ikke bruges til at diskriminere mellem de to gruppers måde at ernære sig på. Det sidste forsøg på at måle græsningsrater fra mixoplankton fokuserede på “fortyndingsteknikken” (**Artikel III**). Resultaterne af en fødenets-simulering i laboratoriet, som inkluderede både mixoplankton og protozooplankton som græssere, viste at klorofyl ikke kan bruges som proxy for fytoplankton biomasse, når mixoplankton er tilstede. Forsøgene viste også at bytte-selektivitet og intern græsning påvirker resultaterne ved brug af denne metode. Dog, kunne data der kom frem ved sådanne forsøg bidrage til opstilling af “*in silico* modeller” ved at skelne mellem græsningen fra hhv mixoplankton og protozooplankton i felten. Det andet formål med denne afhandling var at studere hvordan lys og temperatur påvirker græsningen hos hhv mixoplankton og protozooplankton. Betydningen af lys blev adresseret ved at udføre dag/nat (**Artiklerne I** og **III**), og 24 timers mørke inkubationer

med udvalgte arter (**Artikel III**). Resulterne støttede eksistensen af døgnrytmer i fødeoptagelsen hos protister, der delvist blev opretholdt i fravær af lys, selvom denne faktor er kritisk for korrekte målinger af fødeoptagelsen hos begge grupper. I **Artikel IV** blev temperatureffekter på kulstofoptag, kulstofudnyttelse, vækst og græsning hos mixoplankton og protozooplankton undersøgt. Resultaterne af denne sidste artikel viste at mixoplankton (men ikke protozooplankton) afviger fra den såkaldte "Metabolic Theory of Ecology". Mixoplankton blev mere afhængige af fototrofi i et "varmere klimascenarie", hvilket er i modstrid med tidligere formodninger, der forudsagde en højere grad af fagotrofi ved højere temperaturer. Protozooplankton udviste højere optimale temperaturer mht både vækst og fødeoptagelse end deres mixoplanktoniske modparter. Alt i alt bidrager denne afhandling til en stadig vedvarende proces med at fastlægge mixoplanktons rolle i fødenettet, især mht til deres rolle som græssere i det marine fødenet.

1. Introduction

Attempting to determine the ecological role of marine microorganisms has been a major driver of biological oceanographic research since Azam *et al.* (1983) coined the term “microbial loop” (Azam *et al.* 1983, Fenchel 2008). Many years have passed since the advent of this “paradigm shift” in marine ecology and, nowadays, the reassement of marine microbial ecology is of a different nature. The photosynthetic activity of marine phytoplankton is responsible for nearly half of the carbon (C) sequestration by autotrophs on Earth. Most of this C will be processed in the food web by microzooplankton (Calbet & Landry 2004, Schmoker *et al.* 2013); however, it is currently accepted that a substantial part of this grazing activity might be mediated by phagotrophic “phytoplankton” (Jeong *et al.* 2010).

Still, it would require almost 25 years for these phagotrophic “phytoplankton” to force a paradigm shift in marine ecology, away from the traditional phyto/zooplankton dichotomy (Flynn *et al.* 2013). Alongside the collaborators of the MixITiN project, we have coined the term mixoplankton to describe single-celled organisms that have the potential to simultaneously express phototrophy and phagotrophy (Flynn *et al.* 2019, see **Appendix**). By definition, the passive uptake of dissolved organic C sources by some photoautotrophs such as diatoms (Lewin 1953) can be regarded as mixotrophy. Nevertheless, osmotrophy is likely ubiquitous and used to mitigate against metabolite leakage (Flynn & Berry 1999), whereas phagotrophy involves the capture, ingestion, and digestion of other organisms, thus affecting the structure and functioning of food webs. As such, this distinction is crucial for the understanding of marine food webs and the development of climate change and fisheries models, among others. Thus, for clarity, I will hereafter refer to mixoplankton as the protists, which combine photo-autotrophy, osmo-heterotrophy, and phago-heterotrophy. Likewise, organisms that combine the former two modes of nutrient acquisition are going to be termed phytoplankton whereas if the latter two modes are combined, the organisms are going to be referred to as protozooplankton (**Figure 1-1**).

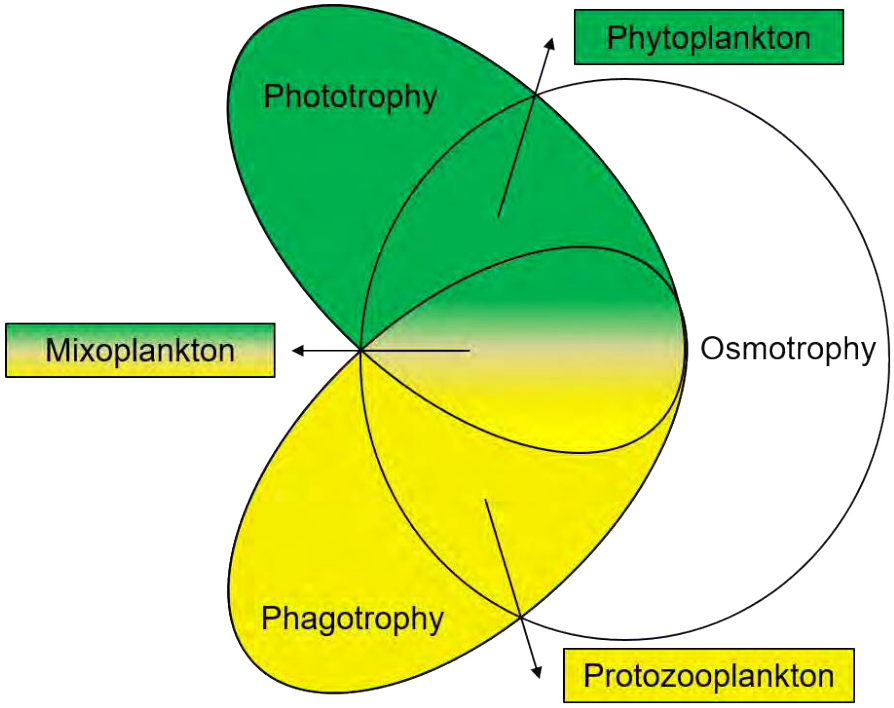

Figure 1-1 Venn diagram of overlaps between phototrophy, osmotrophy, and phagotrophy. Mixoplankton are, by definition, capable of all three modes. Phytoplankton are mixotrophic by virtue of phototrophy and osmotrophy but cannot conduct phagocytosis. Protozooplankton are incapable of phototrophy. Modified from Flynn *et al.* (2019).

Mixoplankton can be divided according to their acquisition of chloroplasts into two major functional groups, the Constitutive and the Non-Constitutive mixoplankton (CM and NCM, respectively, see Mitra *et al.* 2016). CMs possess their own chloroplasts, while NCMs have to retain them from ingested photosynthetic prey. The latter can be further divided by the specificity of the prey required for the retention of the plastids. If a wide array of prey can be used to provide plastids to the predator, the term General NCM (GNCM) should be used (e.g., *Strombidium rassoulzadegani* – Schoener & McManus 2012). If the choice of prey is narrow due to species-specific interactions (e.g., *Mesodinium rubrum* – Yih *et al.* 2004), then the term Specialist NCM (SNCM) is more adequate. Finally, SNCMs may retain only the plastids or the entire prey cell as a symbiont, becoming either plastidic SNCM (pSNCM) or endosymbiotic SNCM (eSNCM). It is important to notice that, although grouped by their functionality, the benefits of photo- and phagotrophy vary qualitatively as well as quantitatively within each group (Stoecker *et al.* 2017).

Still, the description of several functional groups within mixoplankton does not imply that they are a group worthy of inclusion in traditional food webs. However, mixoplankton are not only ubiquitous (Leles *et al.* 2017, 2019, Faure *et al.* 2019) but also phylogenetically diverse, and can be found across a wide size spectrum (Flynn *et al.*

2019, see **Appendix**). Therefore, mixoplankton are expected to be very important grazers in marine systems, and even dominant in some (Mitra *et al.* 2014). Yet, their inclusion in traditional food webs is not an easy task as it is not only a matter of adding organisms but also a matter of adding functions to pre-existing ones. The issue escalates when we move from conceptual food webs (**Figure 1-2**) to large-scale ecosystem models.

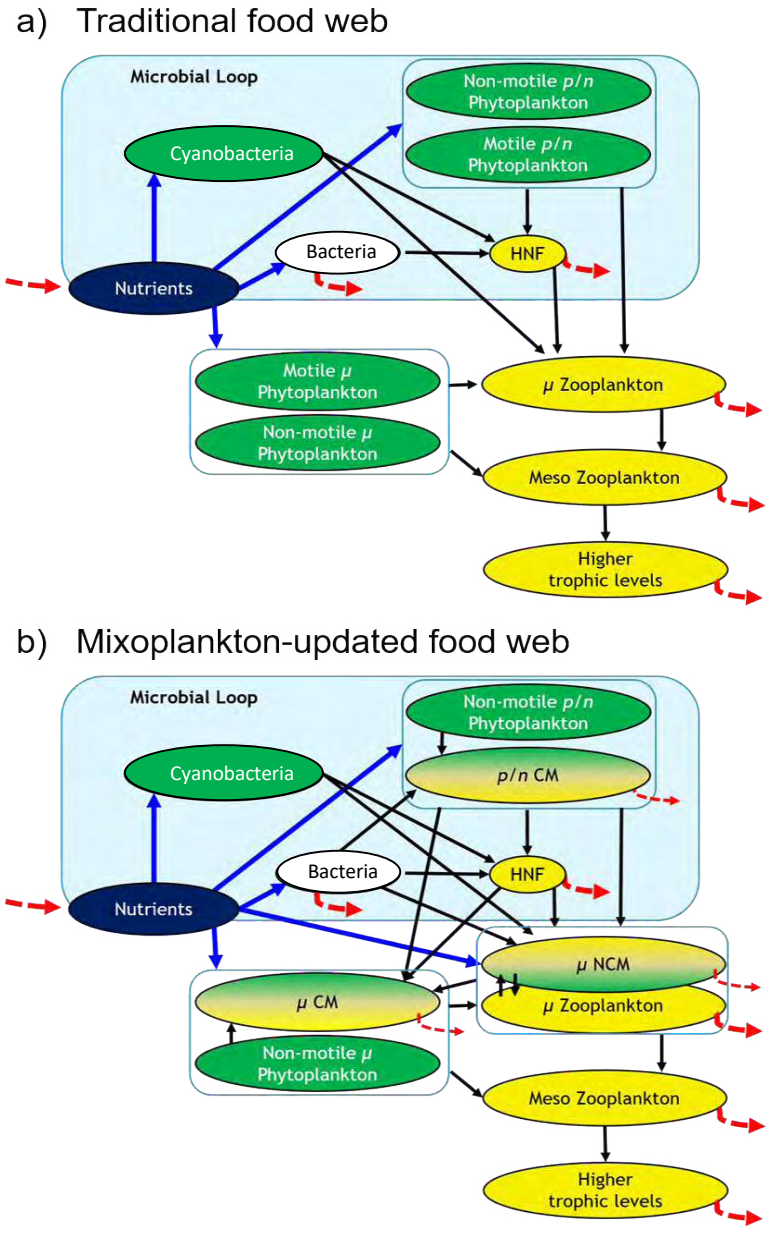

Figure 1-2 Differences between a conceptual food web a) before and b) after the inclusion of the mixoplankton paradigm. The microbial food web components are within the blue boxes. Red dashed arrows indicate input and outputs of dissolved (in)organic, blue arrows imply the uptake of nutrients, and black arrows indicate grazing routes. The colours used to distinguish the different groups of organisms correspond to their mode of nutrition as described in **Figure 1-1**. HNF: heterotrophic nanoflagellates; p/n: pico/nano-sized organisms, μ: micro-sized organisms. Modified from Flynn *et al.* (2019).

Indeed, the presence of mixoplankton impairs most of the current models for nutrient cycling dynamics (Yool *et al.* 2013), the management of fisheries (Plagányi 2007), or climate change projections (Arora *et al.* 2013), as they are still based on the traditional phyto/zooplankton dichotomy (Flynn *et al.* 2013). Furthermore, the combination of all three previously-mentioned trophic modes of nutrition may enhance a predators' gross growth efficiency (Mitra *et al.* 2016, Stoecker *et al.* 2017), which have consequences on models' forecasting abilities.

One of the greatest limitations to the advance of mixoplankton-inclusive models is the difficulty in accurately measuring the grazing impact of mixoplankton in the field, as it is challenging to ascertain when organisms are actively feeding or not (Anderson *et al.* 2017, Stoecker *et al.* 2017, Beisner *et al.* 2019, Flynn *et al.* 2019). The fact that diel feeding rhythms are non-negligible both in protozooplankton and mixoplankton (e.g., Strom 2001, Jakobsen & Strom 2004, Ng *et al.* 2017, Arias *et al.* 2020, 2021) complicate the matter even further when conducting field studies. Indeed, a single sampling event is likely to over/underestimate the measured predation based on the organisms that are feeding the most at that time of the day (e.g., Anderson *et al.* 2017).

Moreover, classic methods for estimating primary or secondary productivity do not recognise the complexity of involving mixoplankton growth (Mitra *et al.* 2014), and the numerous approaches to quantify grazing fail to distinguish mixoplanktonic and protozooplanktonic activities (Flynn *et al*. 2019, Wilken *et al.* 2019). In this latter group of techniques that quantify grazing, the dilution grazing technique (Landry & Hassett 1982) is perhaps the best example of a great technique (with more than 100 studies on the topic – Schmoker *et al.* 2013) that is systematically beset by the presence of mixoplankton, among other factors that have been extensively discussed in the past (e.g., Gallegos 1989, Dolan *et al.* 2000, Dolan & McKeon 2005, Calbet & Saiz 2013, 2018). In the original description, the growth of the "phytoplankton" prey was assessed by using chlorophyll *a* (Chl *a*) as a proxy for its biomass, and grazing was assumed to be exclusively due to the predatory activity of "microzooplankton" (i.e., *de facto* protozooplankton). The rationale behind the method comes from the decreased encounter rates between predators and their prey as the whole community is diluted. Additionally, it assumes that phytoplankton growth is affected neither by the dilution factor nor by the presence of other phytoplankton species/individuals (Landry & Hassett 1982). Thus, the afore-mentioned physiological characteristics of mixoplankton make this technique blind to their presence since they are simultaneously considered prey and predators in dilution experiments (Calbet *et al.* 2012, Schmoker *et al.* 2013).

As such, to address the mixoplankton paradigm properly, we are in dire need of a technique that can measure their grazing impact *in situ* and retain its effectiveness under the different scenarios that modulate grazing. Therefore, in this thesis, I explored three independent approaches that, if successful in the laboratory, could be used to determine mixoplankton's grazing impact in the field. For the first approach (**Paper I**), we used Live Fluorescently Labelled Alagae (LFLA) as tracers for grazing (e.g., Li *et al.* 1996,

Kamiyama 2000, Calbet *et al.* 2012, Martínez *et al.* 2014). The second methodology (**Paper II**) was conceptually similar to those of early authors who attempted to measure bacterivory using selective metabolic inhibitors for prokaryotes and/or eukaryotes (e.g., Newell *et al.* 1983, Fuhrman & McManus 1984, Sanders & Porter 1986, Sherr *et al.* 1986). Finally, the third approach (**Paper III**) to measure mixoplankton's grazing impact *in situ* considered the mathematical disentangling of mixoplankton and protozooplankton grazing in a traditional dilution experiment (Landry & Hassett 1982).

We started by focusing our efforts on the LFLA technique (**Paper I**). This technique operates at an individual rather than at a community level (Beisner *et al.* 2019, Wilken *et al.* 2019), as those described in **Paper II** and **III**. The use of live prey is an advantage over using heat-killed organisms as suggested by Rublee & Gallegos (1989), in the formulation of its predecessor (the FLA technique). Additionally, this technique can be easily deployed in remote field locations (Li *et al.* 1996) and, as it relies on microscopy, the results have a high taxonomic resolution, in terms of both predators and prey. Finally, due to the short-term nature of these experiments, it is easier to assess effects such as the relevance of diel feeding rhythms for a given organism/community (Martínez *et al.* 2014). Therefore, we used several mixoplanktonic and protozooplanktonic grazers of different taxonomic groups and feeding mechanisms and conducted short-term (ca. 5 h) incubations with LFLA.

This approach proved to be a fairly good solution to the determination of mixoplankton's grazing impact if a given number of criteria was met. Still, we encountered several issues that questioned the viability of the technique and, as such, directed our attention to a novel approach that would not, *a priori*, be hindered by those issues. Given that the dilution technique has proven to be simple and useful but is blind to the presence of mixoplankton, it would be very useful to develop a modified version of it that can uncouple mixoplankton and protozooplankton grazing rates. Therefore, a method that discriminates between trophic modes or one able to disrupt one of them would be extremely useful. Rotenone (2R,6aS,12aS)-1,2,6,6a,12,12a-hexahydro-2-isopropenyl-8,9-dimethoxychromeno[3,4-b]furo(2,3-h)chromen-6-one) is a compound that inhibits the electron transport chain in the mitochondria by blocking the transmission of electrons from complex I to ubiquinone (Palmer *et al.* 1968). Therefore, rotenone discontinues oxidative phosphorylation and ATP synthesis in this organelle. According to the mode of action, organisms relying exclusively on mitochondria for ATP synthesis (such as

protozooplankton) are likely more vulnerable to rotenone than chloroplast-bearing organisms, which can also use chloroplasts to produce ATP in the light phase of the photosynthesis (Kohzuma *et al.* 2017).

Rotenone has already been suggested to eliminate unwanted predation by rotifers in microalgae cultures, as the latter are seemingly unaffected (Van Ginkel *et al.* 2015, 2016, El-Sayed *et al.* 2018). Nevertheless, direct evidence of the effects of rotenone on chloroplast-bearing organisms is scarce despite the common assumption that these organisms are largely unaffected. If this assumption is confirmed, from a theoretical point of view, natural food webs (on a dilution experiment) could be modified by suppressing protozooplanktonic grazers (Schmoker *et al.* 2013). Therefore, we have investigated the effects of rotenone on phytoplankton, mixoplankton, and protozooplankton species in the laboratory under acute assays (ca. 24 h), using growth and ingestion as endpoints for toxicity (Ferreira & Calbet 2020, **Paper II**).

Nevertheless, despite being a novel approach with good theoretical foundations for the discrimination between protozooplankton and mixoplankton, we encountered some issues that made rotenone an impossible solution to the quantification of mixoplanktonic grazing. Given the diversity of grazers in natural communities and the array of preferred prey that each particular species possesses, it is logical to think that dilution experiments (Landry & Hassett 1982) will capture the net community response properly. This conclusion is also extended to properly capturing the grazing impact of mixoplankton. Nevertheless, as mentioned before, the parameters that are traditionally used to interpret a dilution experiment conceal the presence/absence of mixoplankton.

With these matters in mind, we conducted several dilution grazing experiments in the laboratory, with mixtures of phytoplankton, mixoplankton, and protozooplankton species (**Paper III**). The experiments were conducted under regular diel light cycle conditions, and also in complete darkness, because light can act both as a resource for phototrophic growth and as a modulating factor for grazing (Arias *et al.* 2020, Morison *et al.* 2020). Dark incubations could serve to provide information on the contribution of mixoplanktonic activity into dilution grazing experiments. Additionally, we prepared control treatments (that cannot be included in field experiments) containing only prey, and combinations of a single predator with the prey, to explore individual dynamics during the incubation. These additional experiments, as controlled scenarios, provide added information for interpreting the otherwise hidden dynamics of multi-organism dilution

grazing experiments and could ultimately, be used for *in silico* simulations of dilution grazing experiments.

Parallel to light, which was studied in **Paper III**, the temperature is perhaps the most important abiotic factor that can affect the balance between nutrition modes (i.e., phototrophy and phagotrophy) on a given mixoplanktonic species, irrespective of its taxonomic group (e.g., Princiotta *et al.* 2016). In this regard, both autotrophic and heterotrophic processes (like photosynthesis and ingestion, respectively) are predicted to increase in response to temperature albeit at different rates (Regaudie-de-Gioux & Duarte 2012). In particular, the Metabolic Theory of Ecology (MTE, Gillooly *et al.* 2001, Brown *et al.* 2004) predicts that the Activation Energy (*Ea*) for the rate-limiting biochemical reactions of photosynthesis is significantly lower than the value for heterotrophic activities such respiration and grazing (Allen *et al.* 2005, López-Urrutia *et al.* 2006, Rose & Caron 2007, Regaudie-de-Gioux & Duarte 2012). Therefore, heterotrophic processes are expected to increase faster than autotrophic ones in response to increasing temperatures, which would shift the balance of photo/phagotrophy in mixoplankton towards the latter mode of nutrition. In fact, one of the major drivers motivating research on mixoplankton is the quantification of this balance on a given species among different groups of protists such as dinoflagellates (e.g., Adolf *et al.* 2006, Riisgaard & Hansen 2009, Berge & Hansen 2016) and ciliates (e.g., Stoecker *et al.* 1988, Stoecker & Michaels 1991, Yih *et al.* 2004). Such differences may strongly impact the flow of matter and energy within the food web and complicate their accurate integration into biogeochemical models (Mitra *et al.* 2014). Nevertheless, at the moment, the data on the effects of temperature on key physiological parameters of mixoplankton is rather scarce and conflicting (e.g., Wilken *et al.* 2013, Princiotta *et al.* 2016, Cabrerizo *et al.* 2019, González-Olalla *et al.* 2019), which precludes a proper speculation on the topic.

One particular issue that brings the temperature to the spotlight is the increasing evidence that climate change will have profound impacts on marine ecosystems, namely due to short-term extreme climate events (such as marine heatwaves), which are projected to increase both in frequency and intensity (Oliver *et al.* 2019). To understand how short-term (ca. 24 h) changes in temperature affect mixoplankton and protozooplankton species, we measured growth, grazing, respiration, and photosynthetic rates (**Paper IV**). Through the comparison of the dependency of these processes on temperature, we hope to continue the (far from complete) process of integrating mixoplankton within biogeochemical models, by placing them properly in the MTE.

Page deliberately left in blank

2. Specific aims of the thesis and papers included

This thesis had two major objectives:

- To develop a technique to measure mixoplankton's grazing in the field
- To determine the different responses of mixoplankton and protozooplankton to abiotic factors, such as light and temperature

For the first objective, we have explored three independent approaches, which can be found in **Papers I**, **II**, and **III**. The first (using LFLA) and the second (the addition of rotenone) approaches were deemed circumstantially effective and ineffective, respectively. The third and final approach (integration of mixoplankton in a dilution model) has two phases, an *in vitro* (the one included in this thesis), and an *in silico* (still under development). The combination of the two phases is promising and could, in a near future, be used to determine mixoplankton's grazing in the field.

For the second objective, we have attempted to understand how light and temperature modulate grazing in mixoplankton and protozooplankton. The former was addressed both as an exogenous and endogenous factor, by conducting day/night incubations with a few species (**Papers I** and **III**), but also in the complete absence of light during an entire day (**Paper III**). At last, we have dwelled on the effects of temperature on mixoplankton and protozooplankton not only in terms of growth and grazing but also in terms of carbon dioxide sequestration and production (**Paper IV**).

Paper I

The strengths and weaknesses of Live Fluorescently Labelled Algae (LFLA) to estimate herbivory in protozooplankton and mixoplankton

The LFLA technique (Li *et al.* 1996) offers the possibility to directly visualize whether or not prey have been ingested using epifluorescence microscopy while retaining its effectiveness under the different scenarios that modulate grazing. Still, this technique has limitations that need to be properly discussed in light of the mixoplankton paradigm.

This manuscript aimed to assess the strengths and weaknesses of the method in light of the aforementioned paradigm. To address this, we conducted several short-term incubations with LFLA in the laboratory, comprising protists from different taxonomic groups and trophic modes of nutrition. Moreover, we addressed how do different feeding mechanisms affect the outcome of the technique.

Paper II

Caveats on the use of rotenone to estimate mixotrophic grazing in the oceans

Rotenone has already been suggested to eliminate unwanted predation by rotifers in microalgal cultures, as the latter are seemingly unaffected (El-Sayed *et al.* 2018). However, the effect of rotenone on protozooplankton and mixoplankton is unknown. From a theoretical point of view, natural food webs could be modified with rotenone by suppressing protozooplanktonic grazers with minor effects on mixoplankton.

The main aim of this study was the evaluation of rotenone as a potential protozooplankton deterrent. Accordingly, we studied the acute effects (ca. 24 h) of rotenone on phytoplankton, mixoplankton, and protozooplankton in the laboratory. Furthermore, on a parallel and independent experiment, we evaluated whether the physiological condition of an organism affected its tolerance to rotenone.

Paper III

Integrating phago-mixotrophy in dilution grazing experiments

In situ measurements of protist grazing are often obtained using the dilution technique developed by Landry & Hassett (1982). Still, the technique is not free from artefacts and the interpretation of the results is not easy, in particular when mixoplankton are present. These artefacts include the use of Chl *a* as a proxy for phytoplankton biomass and the assumption that grazing is exclusive to protozooplankton.

This paper aimed to provide a framework for interpreting the hidden dynamics within dilution experiments. As such, we constructed artificial food webs with known mixtures of phytoplankton, protozooplankton, and mixoplankton under different light regimes. The species-specific results that we obtained could, ultimately, be used *in silico* to simulate dilution grazing experiments.

Paper IV

The effect of short-term temperature exposure on key physiological processes of mixoplankton and protozooplankton grazers

Future climate change projections state that marine heatwaves will be intensified, both in frequency and magnitude (Oliver *et al.* 2019). Additionally, the MTE (Brown *et al.* 2004) predicts that, in a rising temperature scenario, heterotrophic processes increase more rapidly than phototrophic ones. It is currently unknown how mixoplankton will react to these changes.

The aim of this paper was two-fold: 1) to determine short-term (ca. 24 h) thermal performance curves for key protozooplankton and mixoplankton species and 2) to compare the degree of phototrophy/heterotrophy within mixoplankton in varying temperatures. These results can start to unravel the place of mixoplankton within the MTE and in future climate change models.

Page deliberately left in blank

Paper I

The strengths and weaknesses of Live Fluorescently Labelled Algae (LFLA) to estimate herbivory in protozooplankton and mixoplankton

Guilherme D. Ferreira, Joana Figueira, Sónia C. Marques, Per J. Hansen, Albert Calbet

Abstract

The Live Fluorescently Labelled Algae (LFLA) technique has been used numerous times in the past to estimate microzooplankton herbivory. Yet, it is unknown how mixoplankton, single-cells that have the potential to express phototrophy and phagotrophy simultaneously, affect the outcome of this technique. Hence, we aimed to conduct a broad-spectrum assessment of the strengths and weaknesses of the LFLA technique. Thus, we used several mixoplanktonic and protozooplanktonic grazers, from different taxonomic groups and feeding mechanisms, and prepared three independent short-term experiments (ca. 5 h) in the laboratory. First, we evaluated the effects of prey concentration and incubation time on the incorporation of LFLA. We recommend a maximum 1h incubation time for the use of LFLA to estimate grazing rates irrespective of the prey concentration. We also concluded that the LFLA technique, due to its short-term nature, can be an effective tracker of diel ingestion and digestion rates, as well as to detect new mixoplanktonic predators. Nevertheless, our results also call for caution whenever using LFLA to track feeding in the field. In particular, feeding mechanisms other than direct engulfment (like peduncle feeding) may provide severely biased ingestion rates. Furthermore, size and species selectivity are very hard to circumvent. To reduce the effects of selectivity, we propose the combined use of two distinctly coloured fluorochromes with a similar emission spectrum in the future. With this modification, one could either label different size ranges of prey or account for species-specific interactions in the food web.

Graphical Abstract

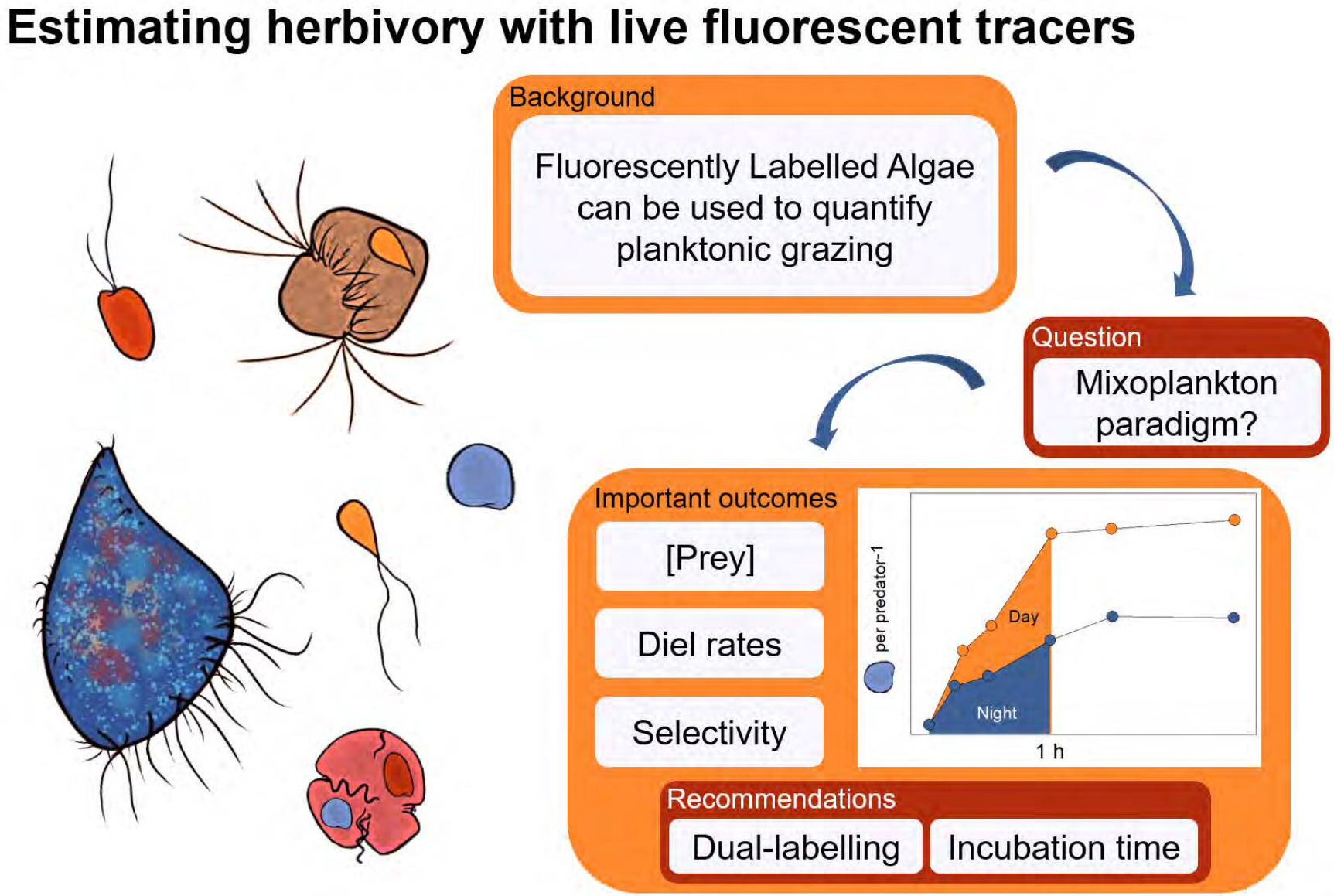

Introduction

Attempting to determine the ecological role of marine microorganisms has been a major driver of biological oceanographic research since Azam *et al.* (1983) coined the term “microbial loop” (Azam *et al.* 1983, Fenchel 2008). At the time, it was difficult to quantify bacterial biomass and production rates but the thirst for knowledge was unequivocally there (e.g., Hagström *et al.* 1979, Krambeck *et al.* 1981). The most successful approaches relied on the use of radioactive isotopes (Fuhrman & Azam 1980, 1982), but the fate of the apparently substantial bacterial production remained a mystery until Fenchel (1982) clarified the role of flagellates as important consumers of pelagic bacteria.

Logically, scientists became eager to develop methods to quantify predation rates on bacteria and the first techniques were quickly developed. Some immediate solutions were based on the disappearance of bacterial biomass through direct cellular counts (Landry *et al.* 1984, Wright & Coffin 1984), or on the use of radioisotopes (Lessard & Swift 1985). Alternative approaches included the use of selective metabolic inhibitors for prokaryotes and/or eukaryotes (Newell *et al.* 1983, Fuhrman & McManus 1984, Sanders & Porter 1986, Sherr *et al.* 1986), or the use of fluorescent tracer particles like minicells (Wikner *et al.* 1986) or fluorescent latex beads (Børsheim 1984, Cynar & Sieburth 1986, McManus & Fuhrman 1986). Yet, the true game-changer came with the paper by Sherr *et al.* (1987), who suggested the replacement of latex beads with natural bacteria, which were previously heat-killed and labelled with the fluorochrome 5-(4,6-dichlorotriazin-2-yl) aminofluorescein (DTAF).

The major advantages offered by this methodology (Fluorescently Labelled Bacteria, FLB) were i) avoiding a negative selection towards inert particles like the latex beads (e.g., Sherr *et al.* 1987, Nygaard *et al.* 1988, Epstein & Rossel 1995; Jürgens & DeMott 1995), and ii) offering consistently-sized particles thus enabling cross-laboratory comparisons, which unevenly sized beads did not allow (e.g. Chrzanowski & Šimek 1990, Gonzalez *et al.* 1990, Monger & Landry 1991, 1992, Kinner *et al.* 1998).

FLBs are still used nowadays both in marine (e.g., Avrahami & Frada 2020) and freshwater systems (e.g., Izaguirre *et al.* 2021), despite the cumulative evidence that bacterivores may favour live over heat-killed bacteria (e.g., Gonzalez *et al.* 1993, Landry *et al.* 1991, Ishii *et al.* 2002, Fu *et al.* 2003, Bochdansky & Clouse 2015, Bock *et al.* 2021). A very detailed description of the how to obtain bacterivory rates using FLB can be found

in Caron (2001). For an overview of current methodologies that can be employed to determine bacterivory rates, see the reviews by Beisner *et al.* (2019) and Wilken *et al.* (2019), as I will not explore the matter further.

Shortly after the paper by Sherr *et al.* (1987), Rublee & Gallegos (1989) used the same protocol (with minor differences in the centrifugation steps) to stain algae instead of bacteria (Fluorescently Labelled Algae, FLA). DTAF-stained FLA possess similar advantages and disadvantages to DTAF-stained FLB and, consequently, this method has been used in 33 (as far as I am aware of) studies across the world to quantify protistan herbivory rates. Interestingly, more than half of the studies that used DTAF-stained algae were published within the first decade after the original description of the method, and only 4 were published after 2010. At the time of the development of the FLA technique, chemosensory selectivity had already been confirmed in ciliates (e.g., Stoecker *et al.* 1981, Verity 1988) and dinoflagellates (e.g., Hauser *et al.* 1974, Spero 1985), which together would later be acknowledged as the major herbivores on a global scale (Calbet & Landry 2004, Schmoker *et al.* 2013). Therefore, the question of whether dead algae would be ideal tracers was quickly raised, and answered.

Based on the screening for vital stains conducted by Harman & Stasz (1988), and on the confirmed ability to stain freshwater ciliates (Graham 1990), Putt (1991) proposed the utilization of the “vital” stain hydroethidine to label algae as an alternative to DTAF. Despite successfully staining cells, hydroethidine was seemingly toxic as it significantly decreased the motility and photosynthesis of the prey (*Isochrysis galbana*). Additionally, hydroethidine fluoresced in a bright red colour (like the autofluorescence of chloroplasts), and faded within ca. 1 h after fixation, rendering this stain unusable for field studies. Further, Dolan & Coats (1991) proposed an indirect live-staining technique to study ingestion rates on ciliates by predacious ciliates using microspheres. The technique was well-received by the scientific community (see also Cleven 1996 and Smalley *et al.* 1999 for variations), but it required knowledge on the turnover rates of ingested beads by the prey. Therefore, it is not surprising that simpler alternatives were proposed, bringing the DNA-specific stain DAPI (2,4-diamidino-6-phenylindole) into the spotlight as a live-stain (Kenter *et al.* 1996, Lessard *et al.* 1996, Pfister & Arndt 1998).

Still, it was Lessard *et al.* (1996) who first introduced DAPI as a live-stain, successfully using it to label 8 protozooplankton and 4 phytoplankton species. Premke & Arndt (2000) extended the count for DAPI-labelled protozooplankton species by 6. It may

be noteworthy to mention that the latter authors managed to use DTAF as a live-stain for most of their species as well. Yet, DAPI-stained samples needed to be kept away from bright light, as DAPI is light sensitive and faded quickly (Lessard *et al.* 1996). At the same time, Li *et al.* (1996) suggested an alternative to DAPI by using the cytoplasmic stain CMFDA (5-chloromethyl-fluorescein diacetate), originating what would later become known as the Live FLA (LFLA) technique. This stain performs better than DAPI in terms of stain retention and fading (Li *et al.* 1996, Kamiyama 2000, Kamiyama *et al.* 2001), and toxicity (e.g., Stoecker *et al.* 2000). In addition, CMFDA was soon incorporated in studies targeting phagotrophic "phytoplankton" (e.g., Li *et al.* 1996, Kamiyama 2000, Stoecker *et al.* 2000, Kamiyama *et al.* 2001, Johnson *et al.* 2003), whose importance within the microbial loop was gathering attention. Still, it would require almost 25 years to acknowledge the importance of these phagotrophic "phytoplankton" (hereafter termed mixoplankton, single-celled organisms that have the potential to simultaneously express phototrophy and phagotrophy - Flynn *et al.* 2019), and to force a paradigm shift in marine ecology, away from the traditional phyto/zooplankton dichotomy (Flynn *et al.* 2013). Mixoplankton can be divided according to their acquisition of chloroplasts into two major groups, the Constitutive and the Non-Constitutive mixoplankton (CM and NCM, respectively, see Mitra *et al.* 2016 and Flynn *et al.* 2019). CMs possess their own chloroplasts, while NCMs have to retain them from ingested photosynthetic prey. It is important to mention that, although grouped by their functionality, the benefits of photo- and phagotrophy vary qualitatively as well as quantitatively within each group (Stoecker *et al.* 2017).

Accounting for the grazing impact of mixoplankton in the field is not an easy task. It is difficult to ascertain when organisms are actively feeding or not (Anderson *et al.* 2017, Beisner *et al.* 2019, Flynn *et al.* 2019, Stoecker *et al.* 2017), although recent attempts have been made (e.g., Ferreira and Calbet 2020, Ferreira *et al.* submitted – **Paper III**). The fact that diel feeding rhythms are non-negligible both in protozooplankton and mixoplankton (e.g., Arias *et al.* 2020a, Arias *et al.* 2021, Ferreira *et al.* submitted – **Paper III**, Jakobsen & Strom 2004, Ng *et al.* 2017, Strom 2001) complicate the matter even further when conducting field studies. Indeed, a single sampling event is likely to over/underestimate the measured predation based on the organisms that are feeding the most at that time of the day.

To address the mixoplankton paradigm properly, we are in need of a technique that can measure their grazing impact and retain its effectiveness under the different

scenarios that affect grazing. This is exactly what the fluorescent labelling of live algae (LFLA) technique offers, within its own limitations that need to be properly discussed in light of the mixoplankton paradigm. Thus, the aim of this manuscript was to determine, in the laboratory, the strengths and weaknesses of the method with the description of a sound protocol for the incorporation of this methodology in situ to account for mixoplankton's grazing in the field. For that we used protist grazers of different taxonomic and trophic groups and conducted short-term incubations with LFLA.

Methods

Cultures

We used protozooplankton and mixoplankton species, encompassing several taxonomic groups and feeding strategies to provide an overview of natural populations. For protozooplankton we used the dinoflagellates *Oxyrrhis marina* (strain ICM-ZOO-OM001, ESD = 16.5 µm), *Gyrodinium dominans* (strain ICM-ZOO-GD001, ESD = 17.8 µm), and *Lessardia elongata* (strain ICM-ZOO-LSP001, ESD = 11.0 µm). The first two species feed by direct engulfment of prey, whereas the latter feeds using a peduncle. We also used a protozooplanktonic ciliate, *Strombidium arenicola* (strain ICM-ZOO-SA001, ESD = 32.3 µm), which feeds by direct engulfment.

Regarding CMs, we used the dinoflagellates *Karlodinium armiger* (peduncle feeder, strain ICM-ZOO-KA001, ESD = 17.8 µm) and *Karlodinium veneficum* (peduncle feeder strain ICMB-274, ESD = 12.8 µm). In addition, we used *Gymnodinium litoralis* (strain CGA, ESD = 19.7 µm), which we discovered is a CM mixoplankton species that feed using a peduncle. For NCMs, the chosen species were the pSNCM dinoflagellate *Dinophysis acuminata* (strain FR101009, ESD = 29.0 µm) and the pSNCM ciliate *Mesodinium rubrum* (strain DK-2009, ESD = 19.9 µm). At last, we used the GNCM ciliate *Strombidium basimorphum* (ESD = 39.9 µm). The former feeds using a peduncle and the latter two feed by direct engulfment of the prey.

K. veneficum, *M. rubrum*, and *S. basimorphum* were offered *Teleaulax amphioxeia* (cryptophyte, strain K-1837 from the NIVA culture collection of algae, ESD = 4.7 µm) as prey. *D. acuminata* was maintained with *M. rubrum* as prey. All other predators except *G. litoralis* were offered *Rhodomonas salina* (cryptophyte, strain K-0294 from NIVA, ESD = 7.5 µm) instead. *G. litoralis* was maintained as a unialgal culture, as were the prey algae

T. amphioxeia, *R. salina*, *Isochrysis galbana* (strain CCMP 1323, ESD = 4.5 µm), *Tetraselmis chuii* (ESD = 9.2 µm), and *Heterocapsa* sp. (ESD = 13.4 µm), i.e., kept in f/2 medium (Guillard 1975) at 100-200 µmol photons m^{-2} s^{-1} (provided by cool white fluorescent lights). To ensure that cultures were always in exponential growth, we replenished ca. 30 % of the culture with fresh medium on a daily basis. All predators were kept in autoclaved 0.1 µm-filtered seawater at 35-55 µmol photons m^{-2} s^{-1}. *S. basimorphum*, *D. acuminata* and their prey in their respective experiments were kept in a temperature-controlled room at 15°C with a 14:10 L/D cycle, at a salinity of 15. All other cultures were kept in a temperature-controlled room at 19°C with a 10:14 L/D cycle, at a salinity of 38.

Preparation of LFLA

I. galbana, *T. chuii*, *Heterocapsa* sp., and *M. rubrum* were fluorescently labelled following the guidelines by Martínez *et al.* (2014) with slight modifications. Briefly, cells were stained overnight with the fluorochrome CellTracker™ Blue CMAC (7-amino-4-chloromethylcoumarin), a vital cytoplasmic stain, at a final concentration of 10 µM. After the staining period, the excess stain was removed from the medium by centrifugation (1000 g) for 10 min for all species except for *M. rubrum*, due to its fragility. The supernatant was discarded and the cells were re-suspended in 0.1 µm filtered seawater. This clean-up process was repeated twice, to reduce the carryover of stain, which can enter predator cells and mask the actual ingestion of LFLA. *M. rubrum* cells were picked individually with a drawn Pasteur pipette and transferred through five wells of 0.1 µm filtered seawater to get rid of the stain.

Exp. 1 – The effects of prey concentration and time on LFLA incorporation

For this experiment, we used the protozooplankton *O. marina*, *G. dominans*, and *S. arenicola*, while *K. armiger*, *K. veneficum*, and *M. rubrum* were chosen as representatives of mixoplankton. During the experiments, all predators were offered a mixture of the LFLA *I. galbana* and the respective cryptophyte prey as described before (the final percentage of LFLA was approximately 30 % of the total - Martínez *et al.* 2014). For the detailed prey concentrations and proportions between LFLA and cryptophytes, see **Table SI-1** in the Supplementary Information. The final predator concentrations were adjusted to avoid the depletion of prey at the target concentration. Additionally, we prepared a second incubation for *M. rubrum*, where we only offered it the LFLA (i.e., 100 % of the offered prey were labelled *I. galbana*).

Experiments were conducted in 0.1 µm filtered seawater (i.e., without added nutrients) inside 75 mL Nunc™ Non-treated flasks (Thermo Scientific™). Each experiment was carried out at two concentrations of prey, one saturating ([Prey] = High) and one non-saturating ([Prey] = Low) (see also **Table SI-1**). The experimental bottles were prepared in duplicates and filled in two to three steps using a common suspension containing both predator and prey at the target concentrations. The suspension was gently mixed between fillings avoiding the formation of air bubbles (Broglio *et al.* 2004). The bottles were incubated on a plankton wheel (0.2 rpm) at 19°C at an irradiance of 35-55 µmol photons m^{-2} s^{-1}. Each experimental bottle was sampled (9-45 mL depending on final predator concentration) every 20 min during the first 2 h of incubation, and then after 3 and 5 h. The samples were fixed with cold glutaraldehyde (4°C, final concentration of 1 %) for ca. 2 h and then filtered with a vacuum pump onto 2 µm pore-size black polycarbonate filters, which were later mounted on microscope slides. Before filtration, these filters were placed on top of support Whatman® GF/C glass microfiber filters to ensure the homogeneity of the filtrate. The first 100 predators encountered on each slide were examined for the presence or absence of ingested prey, determined as blue-fluorescent inclusions (BFI).

In the incubations where the two prey species were of different sizes (i.e., when the cryptophyte prey was *R. salina*), an initial and a final sample were also collected from each experimental bottle and the cells were quantified using a Beckman Coulter Multisizer III particle counter. This data was used to calculate clearance rates using the Frost (1972) equations, as modified by Heinbokel (1978), to account for the growth of protistan predators. From the calculated clearance rates, we estimated the selection coefficient (*Wi*) and the electivity index (*Ei**) according to Vanderploeg & Scavia (1979). The former is calculated according to **Equation I.1**

$$\frac{\quad}{\quad}$$

where *Fi* is the clearance rate for a given food type *i* and Σ*Fi* is the sum of clearance rates on all food types. The latter is calculated using **Equation I.2**

where *n* is the total number of food types. Negative values imply active avoidance of prey, whereas the opposite implies selection for a given species.

Exp. 2 – The effects of diel feeding rhythms on prey incorporation and digestion

For this experiment, we used *S. basimorphum*. This species was maintained on *T. amphioxeia* before the experiment according to Maselli *et al.* (2020) but was allowed to decrease its prey to negligible levels before the onset of the incubations. We conducted two independent incubations with the LFLA *T. chuii* in a proportion of ca. 5 prey per predator under non-saturating concentrations, one incubation during the day and one during the night. The experiments were always conducted in 0.1 µm filtered seawater.

We prepared triplicate experimental bottles, filled as described before, containing the mixture of the GNCM predator and the LFLA. We coordinated the experiment so that the initial samples for both the day and night periods would be as close as possible to the lights-on/lights-off event in the temperature-controlled chamber. Both incubations lasted 5 h and were sampled hourly except for the second sampling point, which occurred within 30 min of incubation. The fixation and processing of the samples were as in Exp. 1. The ingested volume of LFLA stained prey (μm^3 BFI^{-1}) was obtained from linear dimensions of the cells measured on photographs using the Fiji software (Schindelin *et al.* 2012) and its decrease rate was used as a measure of digestion (Strom 2001). Carbon contents for *T. chuii* were estimated using the equation of Menden-Deuer & Lessard (2000) for chlorophytes.

Exp. 3 – The effects of peduncle feeding on the LFLA technique

As suggested before by Archer *et al.* (1996), there could be issues concerning the feeding mechanism of the predator when quantifying ingestion rates based on fluorescent tracers. Accordingly, we prepared an experiment to ascertain whether the feeding mechanism could be an issue when using LFLA as tracer particles, by selecting known peduncle feeders and offering them labelled prey. This experiment was designed to be qualitative instead of quantitative like the previous two experiments and, thus, the prey was always offered in a proportion of ca. 1 prey per predator.

The species that were chosen for this experiment were the protozooplankton *L. elongata*, and three mixoplanktonic species, *K. armiger*, *D. acuminata*, and *G. litoralis*. *L. elongata* and *K. armiger* were fed the LFLA *I. galbana* during the experiment. *D. acuminata* was maintained as described by Nielsen *et al.* (2012) and Rusterholz *et al.* (2017) and fed fluorescently labelled *M. rubrum*. The co-existent unlabelled prey was removed before the incubation with labelled *M. rubrum* using a similar approach as used for the cleaning of extra stain in *M. rubrum*, as previously described. Lastly, *G. litoralis* was offered the LFLA *Heterocapsa* sp. during the experiment. Yet, food vacuoles in this species were first noticed in a monoculture that was kept under complete darkness for two days (cannibalism) and, later, in a mixed culture with *T. amphioxeia* in 0.1 µm filtered seawater (**Figure SI-1** in the Supplementary Information).

Calculations of clearance and grazing rates using LFLA

The average number of BFI per protist was determined using UV light by epifluorescence microscopy on samples collected at several time points. Plotting this information versus time (h) typically yields a linear relationship for the initial time points, levelling off as the experiment progresses due to digestion of ingested algae (Rublee & Gallegos 1989, Caron 2001). The slope of the linear portion of this regression yields the ingestion of LFLA predator^{-1} h^{-1}. This value can be converted to total algae ingested per predator per hour by multiplying it by the unlabelled algae:LFLA ratio assuming that there is no discrimination for or against fluorescently labelled tracers (e.g., Kamiyama 2000, Johnson *et al.* 2003, Martínez *et al.* 2014). Clearance rates (both LFLA-specific and total) are determined by dividing the ingestion rates by the concentration of LFLA or by the total concentration of prey (Frost 1972, Heinbokel 1978). In the field, estimates of community-level herbivory are obtained by multiplying group-specific clearance rates by the abundance of each group, determining the latter with standard microscopic methods (Caron 2001).

Results

Exp. 1 – The effects of prey concentration and time on LFLA incorporation

All dinoflagellates exhibited a significantly ($P < 0.01$ for all species) higher LP_{max} (maximum number of labelled prey inside a predator) at high food concentrations than when the concentration of prey was low (**Figure I-1**). *G. dominans* was the predator with the largest difference between high and low concentrations, being followed by *O. marina* (ca. 6.05 and 2.05x more LFLA ingestion at the highest prey concentration, respectively; **Figure I-1a,b**). Conversely, mixoplanktonic species displayed lower LP_{max} differences between concentrations, being *K. armiger* the species exhibiting the lowest fold-increase (ca. 1.57x). *K. veneficum* increased its LP_{max} by ca. 1.76x. The differences obtained in the half-satiation times (Km_t, i.e., incubation time needed to reach half of LP_{max}) between saturating and non-saturating conditions were never statistically significant ($P > 0.05$).

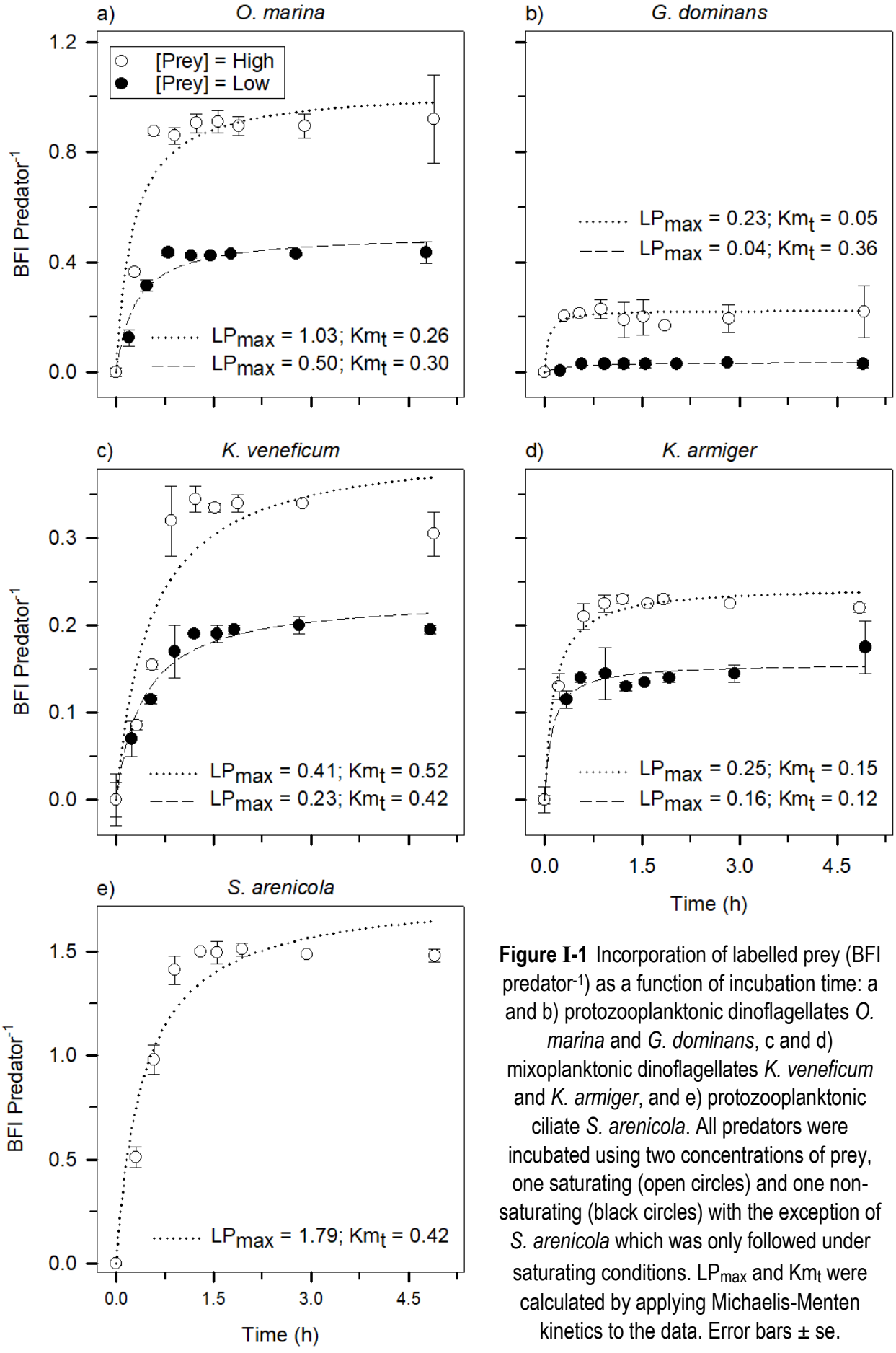

Figure I-1 Incorporation of labelled prey (BFI predator^{-1}) as a function of incubation time: a and b) protozooplanktonic dinoflagellates *O. marina* and *G. dominans*, c and d) mixoplanktonic dinoflagellates *K. veneficum* and *K. armiger*, and e) protozooplanktonic ciliate *S. arenicola*. All predators were incubated using two concentrations of prey, one saturating (open circles) and one non-saturating (black circles) with the exception of *S. arenicola* which was only followed under saturating conditions. LP_{max} and Km_t were calculated by applying Michaelis-Menten kinetics to the data. Error bars ± se.

Overall, all species reached the plateau phase of the tracer incorporation curve within 45 min irrespective of the prey concentration. Accordingly, from the portion of the curves before the plateau phase, we can estimate ingestion rates on the LFLA. These values can then be converted to total ingestion and clearance rates, as summarised in **Table I-1**. Irrespective of the predator species, higher prey concentrations resulted in higher ingestion and lower clearance rates.

Table I-1 Ingestion (Total prey predator^{-1} h^{-1}) and clearance (µL predator^{-1} h^{-1}) rates for each predator depicted in **Figure I-1**. These rates were calculated as described in the Methods Section. The calculation considered only the initial time points where a linear relationship between time and BFI predator^{-1} can be seen (Rublee & Gallegos 1989, Caron 2001). We used actual unlabelled algae:LFLA ratios from each individual incubation for the calculation of both rates and assumed no discrimination for or against LFLA.

Species	[Prey] = Low		[Prey] = High	
	Total prey predator^{-1} h^{-1}	µL predator^{-1} h^{-1}	Total prey predator^{-1} h^{-1}	µL predator^{-1} h^{-1}
Oxyrrhis marina	2.249	472.682	4.271	48.648
Gyrodinium dominans	0.112	26.564	2.205	24.027
Karlodinium veneficum	0.612	120.479	1.179	67.556
Karlodinium armiger	1.168	138.371	1.812	15.873
Strombidium arenicola	-------	-------	5.808	78.776

As mentioned in Methods Section, we also used the pSNCM *M. rubrum* in the first experiment. Nevertheless, in addition to the incubation with the LFLA *I. galbana* as a tracer, i.e., provided in a mixture containing *T. amphioxeia* as well, we incubated it with LFLA as the sole prey. This ciliate was therefore excluded from **Figure I-1** and displayed separately in **Figure I-2**.

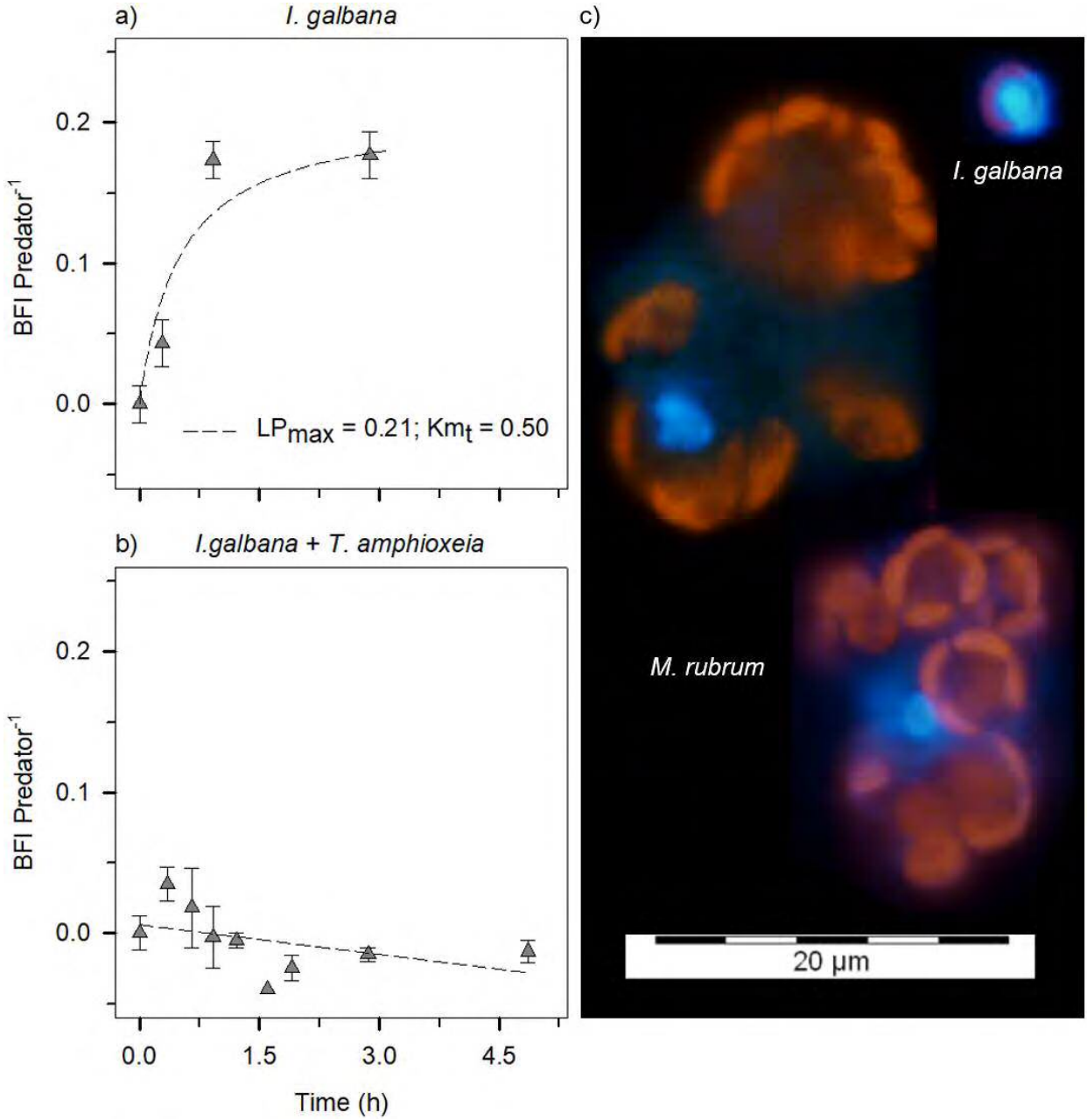

Figure I-2 Incorporation of labelled prey (BFI predator^{-1}) by the pSNCM *M. rubrum* as a function of incubation time: a) *I. galbana* was the only prey offered – LP_{max} and Km_t were calculated by applying Michaelis-Menten kinetics to the data; b) the LFLA *I. galbana* was offered as a tracer particle, i.e., *T. amphioxeia* was also present in the mixture of prey and c) epifluorescence pictures from the experiment without *T. amphioxeia* obtained under UV light excitation where BFI can be seen inside *M. rubrum*. Error bars ± se.

When *I. galbana* was offered without an alternative prey (**Figure I-2a,c**), *M. rubrum* ingests it and the incorporation of BFI per predator followed the typical satiation pattern described before. On the other hand, if *T. amphioxeia* was provided in the mixture of prey (being *I. galbana* used only as a tracer, i.e., using the regular protocol for LFLA), the incorporation of BFI per predator is negligible (**Figure I-2b**). From the first experiment,

we were also able to assess the selection for or against the tracer particle due to the size differences between the LFLA and the cryptophyte *R. salina*. Accordingly, the *Ei** (as calculated using **Equations I.1** and **I.2**) for *S. arenicola*, *O. marina*, *G. dominans*, and *K. armiger* were summarised in **Figure I-3**.

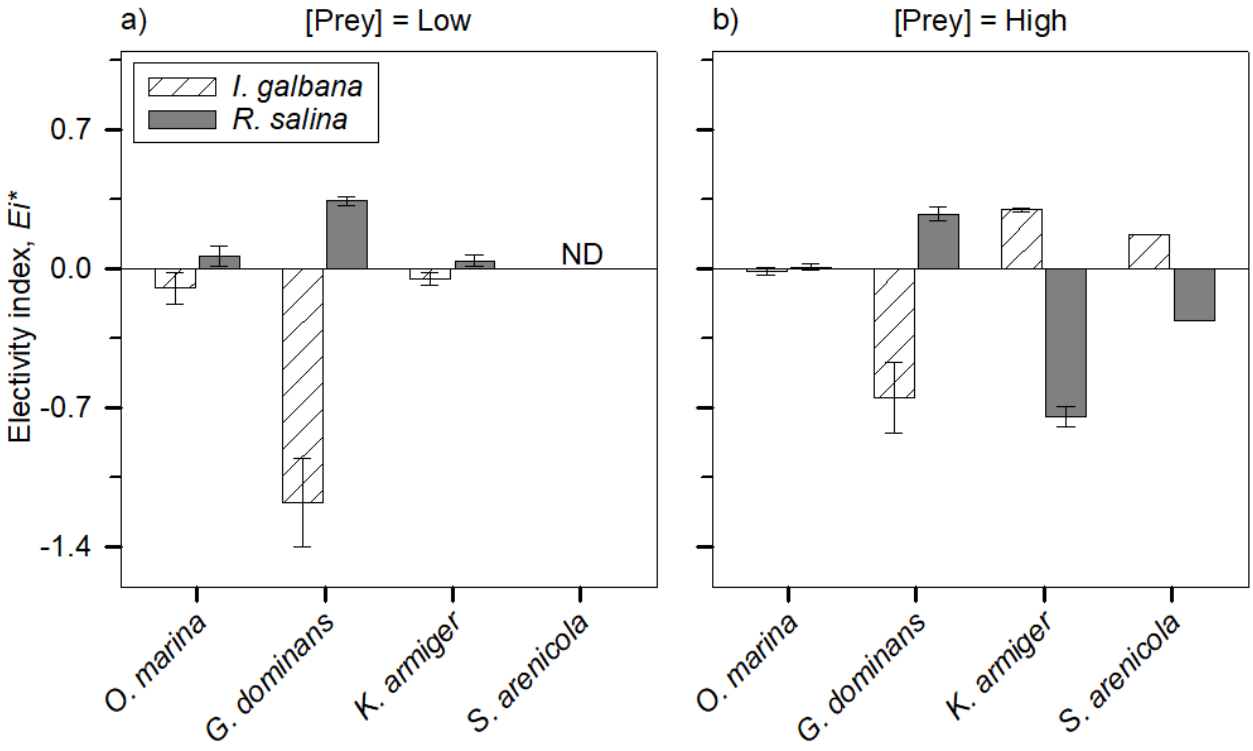

Figure I-3 Electivity indexes calculated for *I. galbana* and *R. salina* for *O. marina*, *G. dominans*, *K. armiger*, and *S. arenicola* under a) non-saturating food conditions and b) saturating food conditions. Negative values imply a negative selection and vice-versa. ND = not determined. Error bars ± se.

Under non-saturating prey conditions (**Figure I-3a**), the electivity indexes for all three dinoflagellates were positive for *R. salina* (i.e., the cryptophyte was the preferred prey species). For both *O. marina* and *K. armiger*, the *Ei** value was close to 0, which suggests a negligible prey preference in these conditions for the two dinoflagellates. For *G. dominans* on the other hand, there was a marked preference for *R. salina*, as seen by an *Ei** value for *I. galbana* lower than 1.

At the highest prey concentration (**Figure I-3b**), *G. dominans* was still feeding preferentially on *R. salina* (i.e., *Ei** > 0), although the avoidance of *I. galbana* was less evident (as seen by an *Ei** value closer to 0). Also, *K. armiger* shifted from a non-selective predator at low prey concentrations to a highly selective one at saturating conditions. Contrary to *G. dominans*, *K. armiger* favoured *I. galbana* as prey over *R. salina* under

saturating food conditions. The ciliate *S. arenicola* also shared a preference for *I. galbana*, albeit to a smaller extent than *K. armiger*.

Exp. 2 – The effects of diel feeding rhythms on prey incorporation and digestion

A very similar procedure was applied to follow the diel incorporation of the LFLA *T. chuii* by the NCM *S. basimorphum* (**Figure I-4**). The LP_{max} obtained during the day incubation was ca. 1.93x higher than the one obtained during the night ($P < 0.01$) but the half-satiation constants were similar ($P = 0.97$). Regarding volume changes in the ingested BFIs over time (**Figure I-4b,d**), the first two hours induced an average reduction of 18.68 μm^3 BFI^{-1} during the day and 7.55 μm^3 during the night. Nevertheless, the parameters in both decay curves were not statistically different, likely due to the variability of the data, except for the one controlling the initial volume of the BFI. Still, from the combined information (and normalized to C units) of **Figure I-4a** and **Figure I-4b**, one can estimate digestion rates by calculating the differences between the estimated and observed pg C per BFI. Despite having statistically insignificant decay parameters, the fact that diurnal ingestion rates were higher than the nocturnal ones resulted in significantly higher (ca. 2.88x) digestion rates between the day and the night (**Figure I-4c**, $P < 0.01$).

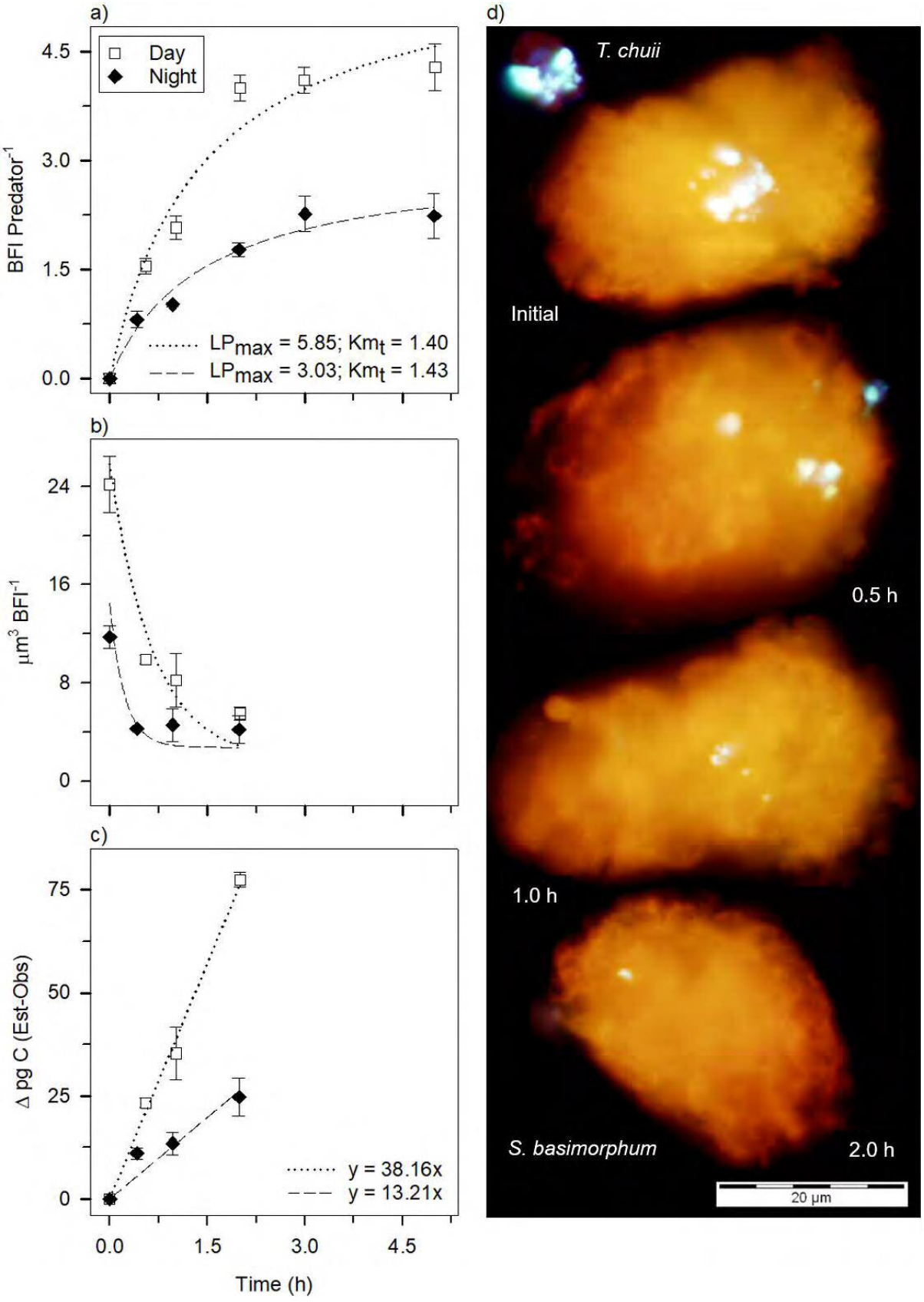

Figure I-4 Incubation of the GNCM *S. basimorphum* with labelled *T. chuii*. White square points correspond to day samples, whereas black diamond points correspond to night ones. a) incorporation of prey over time (BFI predator^{-1}); b) changes in the average fluorescent volume inside a ciliate (µm^3 BFI^{-1}); c) differences between estimated and observed C content in the ingested prey (i.e., digestion rate); d) epifluorescence pictures obtained under UV light in the day samples at sequential sampling occasions. Error bars ± se.

Exp. 3 – The effects of peduncle feeding on the LFLA technique

To answer the question of whether the feeding mechanism could impact the conclusions drawn from an experiment with LFLA, we prepared a qualitative experiment with known tube-feeding dinoflagellates (**Figure I-5**). The major issue demonstrated by this experiment is the complete cytoplasm staining, noticeable irrespective of the chosen predator (i.e., an uncountable amount of prey inside), despite being particularly evident in *D. acuminata* (**Figure I-5d**). The least affected predator was *K. armiger* (**Figure I-5a**), whose cytoplasm staining was heavily dependent on the elapsed time after the beginning of the incubation. The experiment with *G. litoralis* (**Figure I-5c**) demonstrated the same issues as those mentioned before; however, as the prey offered was similarly sized to the predator, it was common to find half-eaten prey in the filter and/or more than one predator feeding on a single prey, further impairing the estimation of grazing rates. The experiment with *L. elongata* (**Figure I-5b**) demonstrated that using LFLA to quantify grazing in peduncle feeding protozooplankton is even more difficult than in mixoplankton. It seems that the incorporation of LFLA by the former is further masked by the lack of naturally occurring pigments i.e., the result is a completely blue predator irrespective of the feeding condition, either due to auto-fluorescence or to the complete staining of the cytoplasm due to ingestion.

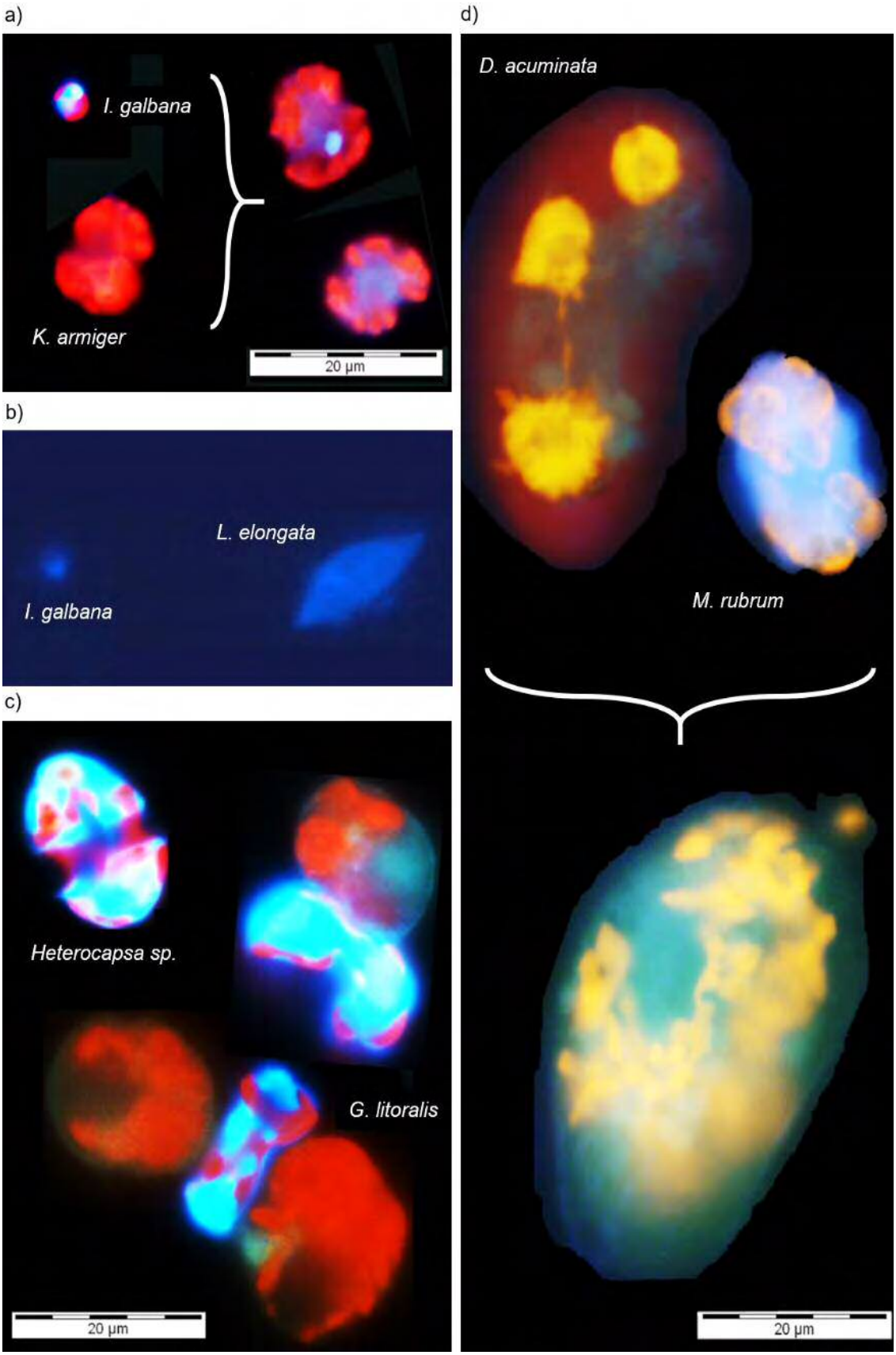

Figure I-5 Examples of tube-feeding dinoflagellates, a) *K. armiger*; b) *L. elongata;* c) *G. litoralis*; d) *D. acuminata,* before and after LFLA addition as seen under UV light in epifluorescence. The red colour in this figure is due to the autofluorescence of Chl *a*, orange implies the presence of phycoerythrin, and blue is due to the presence of the fluorochrome CMAC. The common result is the total staining of the predator's cytoplasm instead of the expected countable number of BFI.

Discussion

The LFLA technique as proposed by Li *et al.* (1996) offered unique possibilities that distinguished it (although not necessarily improved) from other techniques which had been previously developed for the estimation of protist herbivory (e.g., the dilution technique - Landry & Hassett 1982; quantitative protargol staining – Montagnes & Lynn 1987). For instance, the dilution technique estimates bulk community rates with a rather simple experimental protocol but does not differentiate the protist assemblage composition unless specifically desired (e.g., Arias *et al.* 2020b, Ferreira *et al.* submitted – **Paper III**). On the other hand, the quantitative protargol staining protocol is incredibly challenging to follow and can take up to 27 h to completely produce a permanent microscope slide (e.g., Skibbe 1994) despite enabling an accurate taxonomic resolution (e.g., Bockstahler & Coats 1993a,b). In this regard, the LFLA technique stands somewhere in between the two other methods, being more complicated than the technique by Landry & Hassett (1982), but less than that of Montagnes & Lynn (1987), and vice-versa for taxonomic resolution.

It is its ability to deal with mixoplankton that gives LFLA an edge against other techniques. In their particular case, where knowing who is there is arguably not as important as knowing what are they doing and at what rate (Flynn *et al.* 2019), being able to observe phagocytosis is paramount. Therefore, relying on microscopy (i.e., by providing a direct visualisation of organisms) is an advantage as it enables a species/community-specific analysis (Caron 2001). Indeed, it was only due to the use of microscopes that we were able to undeniably detect *T. amphioxeia* inside the dinoflagellate *G. litoralis* (**Figure SI-1b**), due to the different photosynthetic pigment that each organism possesses. Feeding in this dinoflagellate had never been reported before and, thus, it can be moved from the phyto- into the mixoplankton group, namely into the CM group as it possesses its own chloroplasts (Mitra *et al.* 2016).

Nevertheless, the technique was not free from issues, as pointed out by its developers. For instance, Li *et al.* (1996) stated that their stain, the green CMFDA, faded quickly in the light, which would be a major issue if attempting to conduct incubations over large periods. Still, some authors were able to use anti-fading substances successfully, such as propylgallate at trace concentrations (e.g., Schumann *et al.* 2003). Nevertheless, Martínez *et al.* (2014) confirmed that the blue stain CMAC (our stain), was better on this specific issue, in particular when following their optimised staining protocols. Indeed, we

experienced no issues regarding stain bleaching or fading, both during the actual experiments (at irradiances between 35 and 55 µmol photons m^{-2} s^{-1}) and during the processing of the samples under the epifluorescence microscope. Furthermore, the fact that predators typically reach the plateau phase (i.e., LP_{max}) within 45 min irrespective of prey concentration, trophic mode, and taxonomic group (see **Figures I-1** and **I-2a**) seems to put this problem on a secondary level. That is, of course, if prey incorporation experiments are conducted instead of prey disappearance ones (see the discussion on FLB by Caron 2001).

As confirmed by our first and second experiments, there are several protist predators which incorporate LFLA without major issues and under different experimental conditions (**Figures I-1** and **I-4a**). We have also confirmed the usefulness of the technique on the quantification of diel ingestion and digestion rates on an NCM species (**Figure I-4b,c**). We strongly believe that this is a close-to universal utility of the technique, as pigments/fluorescent tracers have been used numerous times to estimate digestion rates (e.g., Dolan & Šimek 1998, Li *et al.* 2001, Nishibe *et al.* 2002, Setälä *et al.* 2005). Nevertheless, even when the incorporation of prey followed the typical satiation pattern, and maximum ingestion rates and half-saturation constants could be estimated, we encountered selectivity issues, both for and against the tracer algae (**Figure I-3**).

One of the assumptions that is crucial for the estimation of grazing rates is that the tracer is incorporated at similar rates as the remaining prey. In fact, these issues are far from negligible as they question the foundations of the technique and, above everything else, are species-specific and unpredictable without experimentation. This is an issue that, as far as we know, has not been thoroughly evaluated in the past, although it must be said that both Calbet *et al.* (2012) and Martínez *et al.* (2014) did not overlook this factor, as evidenced by the use of two distinctly sized LFLA in the field. Still, most efforts focused on the selection of prey based on the presence of the fluorochrome. For example, Kamiyama (2000) confirmed experimentally that stained and unstained algae were ingested at similar rates by *Schmidingerella taraikaensis* (previously known as *Favella taraikaensis*). Likewise, Martínez *et al.* (2014) demonstrated that *O. marina* ingested labelled *I. galbana* and *T. chuii* as it did on unlabelled prey. However, in the same study, *G. dominans* seemed to have a slight preference for fluorescent over unlabelled prey.

In our experiments, *G. dominans* was the species displaying the largest differences on both LP_{max} and Km_t between saturating and non-saturating food concentrations. Additionally, this dinoflagellate exhibited a marked selectivity against labelled *I. galbana*, which was partly dependent on the concentration of prey (**Figure I-3**). The opposite (i.e., preference for *I. galbana*) was observed in *K. armiger* at saturating, but not at low food concentrations, whereas *O. marina*'s species preference was unaffected by the concentration of prey (**Figure I-3**). Despite not having been strongly emphasized in the past (but see Jürgens & DeMott 1995 and Dolan & Šimek 1999), this concentration-dependent selectivity could partially explain the massive dissimilarities seen in the LP_{max} and Km_t parameters for *G. dominans*. We are unable to confirm whether the results with *G. dominans* are a consequence of size or fluorochrome selectivity, although size appears to be the main driver (as per the results of Martínez *et al.* 2014). However, we can undeniably state that the measured ingestion rate using the LFLA methodology fails to represent the total ingestion of prey by *G. dominans* (see **Table I-1**). To illustrate the importance of considering size selectivity towards or against the tracer, let us consider the scenario where *G. dominans* was offered a mix of the two prey at the highest prey concentration. Assuming that there was no discrimination between the two prey species, we obtained a total ingestion rate of ca. 2.2 prey predator^{-1} h^{-1} (**Table I-1**). If we take the negative selection against the tracer into consideration (i.e., a ca. 7.4x higher clearance rate on *R. salina* than on *I. galbana*), the total ingestion rate is ca. 11.9 prey predator^{-1} h^{-1}, a value ca. 5.4x higher than the original estimation.

Similarly, the results obtained with *Karlodinium* spp. suggest that there could be problems in the extrapolation of community grazing rates for these species if selectivity is ignored. For instance, we know that one *K. armiger* ingests ca. 8-10 *R. salina* d^{-1} at saturating food conditions (Berge *et al.* 2008b, Arias *et al.* 2020a), a value which is ca. 7-9x higher than the one obtained for *K. veneficum* on the same prey (listed as K21 - Calbet *et al.* 2011). Yet, the results from the LFLA experiment at the same concentrations yielded a total ingestion rate only 1.6x higher for *K. armiger* (selectivity issues ignored, **Table I-1**), besides estimating a higher LP_{max} for *K. veneficum* (**Figure I-1c,d**). Nevertheless, it must be noted that *K. veneficum* was offered *T. amphioxeia* instead of *R. salina* (i.e., no size differences between the LFLA and the cryptophyte during the incubations). Thus, the values displayed for *K. veneficum* in **Table I-1** are probably quite accurate, whereas if

selectivity is considered, the total ingestion rates for *K. armiger* become only ca. 0.5 cells predator^{-1} h^{-1}. As such, these results suggest that using a small-sized LFLA like *I. galbana* favours the estimation of grazing in *K. veneficum* over its larger congener, *K. armiger*, which is unsurprising since size preferences are typically directly correlated with one's own size (e.g., Hansen *et al.* 1994).

A way to circumvent the size-selectivity issue could have been to use two different sizes of labelled prey (e.g., Calbet *et al.* 2012, Martínez *et al.* 2014). Ideally, both prey would be simultaneously labelled with fluorochromes whose emission spectrum would coincide but differing in the emitted fluorescent colour (Shields & Smith 2008, Nelson *et al.* 2009). For example, *I. galbana* could be labelled with CMFDA (green fluorescence, viable labelling - e.g., Li *et al.* 1996) and *T. chuii* could be simultaneously labelled with CMAC (blue fluorescence, viable labelling - e.g., Calbet *et al.* 2012, Martínez *et al.* 2014). It should be noted, however, that cryptophytes (like our secondary prey *R. salina* and *T. amphioxeia*) remain elusive in terms of fluorochrome retention (being proflavine the only compound successfully retained by *R. salina* – Johnson *et al.* 2018) and are still typically detected using their signature pigment, phycoerythrin (e.g., Li *et al.* 1996, 2001, Adolf *et al.* 2008, Johnson 2015, **Figure SI-1**). For an objective analysis of species that can (or cannot) be stained with CMFDA, see figure 4 in MacIntyre & Cullen (2016).

Still, even if a sample is dually labelled there may be a selection for or against the labelled prey due to the presence of the fluorochrome. In the cases where there is a positive/negative selection for the fluorochrome, an alternative could be to incorporate the fluorescent tracer on the genome of the tracer algae (for example, by fusing a green fluorescent protein, GFP, to a housekeeping gene). This is an advantage even over vital stains (Epstein & Rossel 1995) and is getting attention from the scientific community since the GFP vector is very bright and easily detectable, besides being photo-stable (Bochdansky *et al.* 2015). Despite being highly promising, this approach is only publicly available for bacteria at the time of writing (e.g., Ishii *et al.* 2002, Fu *et al.* 2003, Bochdansky *et al.* 2015). Still, it is important to mention that Zhang *et al.* (2013) state that they have successfully inserted GFP on a strain of *Hemiselmis virescens* and detected it inside three mixoplanktonic dinoflagellates, *Prorocentrum donghaiense*, *Karenia mikimotoi*, and *Alexandrium catenella*.

Aside from size selectivity, the experiments with the pSNCM *M. rubrum* confirmed that species selectivity is a problem that cannot be circumvented. When its preferential

prey was absent (see for example Yih *et al.* 2004 and Smith & Hansen 2007) the number of BFI per *M. rubrum* followed the typical satiation pattern (**Figure I-2a**). However, when *T. amphioxeia* was present, BFI were mostly absent inside *M. rubrum* (**Figure I-2b**). In the laboratory, it is possible to control both the grazer and the prey but in the field, one cannot choose which species will be present. As the functional group name suggests, *M. rubrum* is a specialised predator and retains chloroplasts mostly from a specific clade of cryptophytes, which include *T. amphioxeia* among others (e.g., Myung *et al.* 2011, Hansen *et al.* 2012). Still, *M. rubrum* can ingest some other flagellates as well (Park *et al.* 2007, Hansen *et al.* 2012, Ferreira & Calbet 2020, this study), and can retain chloroplasts from *Rhodomonas* spp. for short periods (Myung *et al.* 2011). Accordingly, our results with *I. galbana* are not surprising. Yet, in the field, the presence of *M. rubrum* is typically correlated with the presence of cryptophytes (e.g., Johnson *et al.* 2018), which means that it is extremely unlikely that a field experiment will be able to capture the feeding process of this ciliate using a tracer particle that is not its preferred prey.

Another far from a negligible issue with this technique that we have shown in our experiments concerns tube-feeding dinoflagellates. Indeed, as confirmed with 4 independent predator-prey combinations from distinct trophic modes, predators that feed using a peduncle tend to become entirely stained themselves instead of displaying individualized (and countable) BFIs. In addition, the low grazing rates obtained with *K. armiger* (**Figure I-1d**) may have been because this dinoflagellate feeds using a peduncle (Berge *et al.* 2008a). Based on our results with tube feeders, it is likely that some *K. armiger* did contain LFLA but we were unable to see them because of the dispersal of the fluorochrome through the predator's cytoplasm. This issue appears to become more relevant over time, as some *K. armiger* cells did, on the other hand, contain easily distinguishable and countable BFIs (see **Figure I-5a,c**). To further complicate the peduncle feeding matter, it should be mentioned that the incorporation of ingested material through a peduncle may flow into a single (e.g., Calado & Moestrup 1997) or several (smaller) food vacuoles (e.g., Hansen 1991). Also, small cells like *I. galbana* (ESD ca. 4.5 µm) may be taken whole through a peduncle in some cases (e.g., Calado & Moestrup 1997), explaining why *K. veneficum* was, apparently, issue-free.

Tube feeding is a common characteristic in both naked and thecate dinoflagellates (Hansen & Calado 1999), suggesting that this caveat of the technique may be a truly important factor to take into consideration when applying this technique in mixed

assemblages in the field. One other long-known feeding mechanism in dinoflagellates (in particular in the genus *Protoperidinium* spp.) is through the deployment of a pallium, which liquefies the cytoplasmic contents of the prey extracellularly (Gaines & Taylor 1984, Jacobson & Anderson 1986). Accordingly, pallium feeders do not transport particles into the main cell body and thus lack food vacuoles (Archer *et al.* 1996, Hansen & Calado 1999). We did not experiment on pallium feeders and, as such, we can only simply hypothesize on these organisms. Still, it seems reasonable to assume that these dinoflagellates would probably appear as a very intense and uniformly bright cell, due to even incorporation of the fluorochrome. On a similar, albeit almost species-specific note, comes the feeding by toxic mucus traps. This feeding mechanism has only been reported, as far as we know, in the species *Alexandrium pseudogonyaulax* (Blossom *et al.* 2012, 2017) and on a *Prorocentrum* sp. (Michaela E. Larsson, MixITiN Symposium, pers. comm.). *A. pseudogonyaulax* consumes whole cells through the sulcus but is unable to capture individual, motile prey cells. Therefore, it deploys a mucus trap that immobilises (but does not kill on a short time scale) prey and, by swimming with it attached to its own body, oftentimes end up entrapping several prey inside. Accordingly, these predators may affect the availability of prey without exhibiting food vacuoles or, even if showing clear and distinguishable BFIs, provide unrealistic grazing rates.

Conclusion

Altogether, the LFLA technique appears to be only directly applicable to organisms that feed by direct engulfment of prey. Indeed, all other feeding mechanisms (present both in protozoo- and mixoplanktonic dinoflagellates) result in biased or even unmeasurable ingestion rates. In this regard, we must stress the fact that most predators reached the plateau phase of LFLA incorporation within 45 minutes (**Figure I-1**) and that digestion of prey is usually quite fast (faster during the day than during the night – **Figure I-4b,c**). Therefore, to provide accurate grazing estimates and avoid finding organisms that display no food vacuoles due to digestion (e.g., Adolf *et al.* 2006, Matantseva & Skarlato 2013), we recommend that all samples of a given LFLA experiment should be collected in short intervals (e.g., 10 minutes) and within a maximum period of 1 h.

At last, we have provided clear evidence that there are omnipresent size and species-specific selectivity processes that are hard to circumvent. As seen in the *Teleaulax-Isochrysis-Mesodinium* incubation (and, on a qualitative extent, also on the

Mesodinium-Dinophysis interaction), these predators exhibit species-specific selectivity, which hindered the quantification of ingested tracer prey. This conclusion is likely valid for all the specialised protist predators that exist on Earth and implies that they may be systematically discriminated against if one decides to use LFLA in the field. Nevertheless, we proved that *M. rubrum* can be effectively labelled with CMAC, which proves that it is not impossible to determine grazing rates for species-specific predators if their specific prey is offered as a labelled tracer. In addition, we propose that dually labelling samples with CMFDA and CMAC should become routine when applying the LFLA technique in the field. The combined use of these two fluorochromes can either be used to distinguish different prey size ranges or account for species-specific grazing within a given water column.

References

Adolf J.E., Bachvaroff T., Place A.R., 2008. Can cryptophyte abundance trigger toxic *Karlodinium veneficum* blooms in eutrophic estuaries? *Harmful Algae*, **8**: 119-128.

Adolf J.E., Stoecker D.K., Harding Jr L.W., 2006. The balance of autotrophy and heterotrophy during mixotrophic growth of *Karlodinium micrum* (Dinophyceae). *J. Plankton Res.*, **28**: 737-751.

Anderson R., Jürgens K., Hansen P.J., 2017. Mixotrophic phytoflagellate bacterivory field measurements strongly biased by standard approaches: a case study. *Front. Microbiol.*, **8**: 1398.

Archer S.D., Leakey R.J.G., Burkill P.H., Sleigh M.A., 1996. Microbial dynamics in coastal waters of East Antarctica: herbivory by heterotrophic dinoflagellates. *Mar. Ecol. Prog. Ser.*, **139**: 239-255.

Arias A., Saiz E., Calbet A., 2020a. Towards an understanding of diel feeding rhythms in marine protists: consequences of light manipulation. *Microb. Ecol.*, **79**: 64-72.

Arias A., Saiz E., Tiselius P., Calbet A., 2020b. Trophic interactions and diel feeding rhythms of microzooplankton in a productive Swedish Fjord. *ICES J. Mar. Sci.*, **77**: 2718-2728.

Arias A., Selander E., Saiz E., Calbet A., 2021. Predator chemical cue effects on the diel feeding behaviour of marine protists. *Microb. Ecol.*, 10.1007/s00248-020-01665-9.

Avrahami Y., Frada M.J., 2020. Detection of phagotrophy in the marine phytoplankton group of the coccolithophores (Calcihaptophycidae, Haptophyta) during nutrient replete and phosphate limited growth. *J. Phycol.*, **56**: 1103-1108.

Azam F., Fenchel T., Field J.G., Gray J.S., Meyer-Reil L.A., Thingstad F., 1983. The ecological role of water-column microbes in the sea. *Mar. Ecol. Prog. Ser.*, **10**: 257-263.

Beisner B.E., Grossart H.-P., Gasol J.M., 2019. A guide to methods for estimating phago-mixotrophy in nanophytoplankton. *J. Plankton Res.*, **41**: 77-89.

Berge T., Hansen P.J., Moestrup Ø., 2008a. Feeding mechanism, prey specificity and growth in light and dark of the plastidic dinoflagellate *Karlodinium armiger*. *Aquat. Microb. Ecol.*, **50**: 279-288.

Berge T., Hansen P.J., Moestrup Ø., 2008b. Prey size spectrum and bioenergetics of the mixotrophic dinoflagellate *Karlodinium armiger*. *Aquat. Microb. Ecol.*, **50**: 289-299.

Blossom H.E., Bædkel T.D., Tillmann U., Hansen P.J., 2017. A search for mixotrophy and mucus trap production in *Alexandrium* spp. and the dynamics of mucus trap formation in *Alexandrium pseudogonyaulax*. *Harmful Algae*, **64**: 51-62.

Blossom H.E., Daugbjerg N., Hansen P.J., 2012. Toxic mucus traps: A novel mechanism that mediates prey uptake in the mixotrophic dinoflagellate *Alexandrium pseudogonyaulax*. *Harmful Algae*, **17**: 40-53.

Bochdansky A.B., Clouse M.A., 2015. New tracer to estimate community predation rates of phagotrophic protists. *Mar. Ecol. Prog. Ser.*, **524**: 55-69.

Bock N.A., Charvet S., Burns J., Gyaltshen Y., Rozenberg A., Duhamel S., Kim E., 2021. Experimental identification and in silico prediction of bacterivory in green algae. *ISME J.*, 10.1038/s41396-021-00899-w.

Bockstahler K.R., Coats D.W., 1993a. Grazing of the mixotrophic dinoflagellate *Gymnodinium sanguineum* on ciliate populations of Chesapeake Bay. *Mar. Biol.*, **116**: 477-487.

Bockstahler K.R., Coats D.W., 1993b. Spatial and temporal aspects of mixotrophy in Chesapeake Bay dinoflagellates. *J. Eukaryot. Microbiol.*, **40**: 49-60.

Børsheim K.Y., 1984. Clearance rates of bacteria-sized particles by freshwater ciliates, measured with monodisperse fluorescent latex beads. *Oecologia*, **63**: 286-288.

Broglio E., Saiz E., Calbet A., Trepat I., Alcaraz M., 2004. Trophic impact and prey selection by crustacean zooplankton on the microbial communities of an oligotrophic coastal area (NW Mediterranean Sea). *Aquat. Microb. Ecol.*, **35**: 65-78.

Calado A.J., Moestrup Ø., 1997. Feeding in *Peridiniopsis berolinensis* (Dinophyceae): new observations on tube feeding by an omnivorous, heterotrophic dinoflagellate. *Phycologia*, **36**: 47-59.

Calbet A., Bertos M., Fuentes-Grünewald C., Alacid E., Figueroa R., Renom B., Garcés E., 2011. Intraspecific variability in *Karlodinium veneficum*: Growth rates, mixotrophy, and lipid composition. *Harmful Algae*, **10**: 654-667.

Calbet A., Landry M.R., 2004. Phytoplankton growth, microzooplankton grazing, and carbon cycling in marine systems. *Limnol. Oceanogr.*, **49**: 51-57.

Calbet A., Martínez R.A., Isari S., Zervoudaki S., Nejstgaard J.C., Pitta P., Sazhin A.F., Sousoni D., Gomes A., Berger S.A., 2012. Effects of light availability on mixotrophy and microzooplankton grazing in an oligotrophic plankton food web: evidences from a mesocosm study in Eastern Mediterranean waters. *J. Exp. Mar. Biol. Ecol.*, **424**: 66-77.

Caron D.A., 2001. Protistan herbivory and bacterivory. In: J.H. Paul (Ed), Marine Microbiology. Academic Press, Florida, USA, pp 289-315.

Chrzanowski T.H., Šimek K., 1990. Prey size selection by freshwater flagellated protozoa. *Limnol. Oceanogr.*, **35**: 1429-1436.

Cleven E.-J., 1996. Indirectly fluorescently labelled flagellates (IFLF): a tool to estimate the predation on free-living heterotrophic flagellates. *J. Plankton Res.*, **18**: 429-442.

Cynar F.J., Sieburth J.M., 1986. Unambiguous detection and improved quantification of phagotrophy in apochlorotic nanoflagellates using fluorescent microspheres and concomitant phase contrast and epifluorescence microscopy. *Mar. Ecol. Prog. Ser.*, **32**: 61-70.

Dolan J.R., Coats D.W., 1991. A study of feeding in predacious ciliates using prey ciliates labeled with fluorescent microspheres. *J. Plankton Res.*, **13**: 609-627.

Dolan J.R., Šimek K., 1998. Ingestion and digestion of an autotrophic picoplankter, *Synechococcus*, by a heterotrophic nanoflagellate, *Bodo saltans*. *Limnol. Oceanogr.*, **43**: 1740-1746.

Dolan J.R., Šimek K., 1999. Diel periodicity in *Synechococcus* populations and grazing by heterotrophic nanoflagellates: analysis of food vacuole contents. *Limnol. Oceanogr.*, **44**: 1565-1570.

Epstein S.S., Rossel J., 1995. Methodology of *in situ* grazing experiments: evaluation of a new vital dye for preparation of fluorescently labeled bacteria. *Mar. Ecol. Prog. Ser.*, **128**: 143-150.

Fenchel T., 1982. Ecology of heterotrophic microflagellates. IV. Quantitative occurrence and importance as bacterial consumers. *Mar. Ecol. Prog. Ser.*, **9**: 5.

Fenchel T., 2008. The microbial loop – 25 years later. *J. Exp. Mar. Biol. Ecol.*, **366**: 99-103.

Ferreira G.D., Calbet A., 2020. Caveats on the use of rotenone to estimate mixotrophic grazing in the oceans. *Sci. Rep.*, **10**: 3899.

Flynn K.J., Hansen P.J., 2013. Cutting the canopy to defeat the "selfish gene"; conflicting selection pressures for the integration of phototrophy in mixotrophic protists. *Protist*, **164**: 811-823.

Flynn K.J., Mitra A., Anestis K., Anschütz A.A., Calbet A., Ferreira G.D., Gypens N., Hansen P.J., John U., Martin J.L., Mansour J.S., Maselli M., Medić N., Norlin A., Not F., Pitta P., Romano F., Saiz E., Schneider L.K., Stolte W., Traboni C., 2019. Mixotrophic protists and a new paradigm for marine ecology: where does plankton research go now? *J. Plankton Res.*, **41**: 375-391.

Frost B.W., 1972. Effects of size and concentration of food particles on the feeding behavior of the marine planktonic copepod *Calanus pacificus*. *Limnol. Oceanogr.*, **17**: 805-815.

Fu Y., O'Kelly C., Sieracki M., Distel D.L., 2003. Protistan grazing analysis by flow cytometry using prey labeled by in vivo expression of fluorescent proteins. *Appl. Environ. Microbiol.*, **69**: 6848.

Fuhrman J.A., Azam F., 1982. Thymidine incorporation as a measure of heterotrophic bacterioplankton production in marine surface waters: evaluation and field results. *Mar. Biol.*, **66**: 109-120.

Fuhrman J.A., McManus G.B., 1984. Do bacteria-sized marine eukaryotes consume significant bacterial production? *Science*, **224**: 1257-1260.

Gaines G., Taylor F.J.R., 1984. Extracellular digestion in marine dinoflagellates. *J. Plankton Res.*, **6**: 1057-1061.

Gonzalez J.M., Sherr E., Sherr B.F., 1993. Differential feeding by marine flagellates on growing versus starving, and on motile versus nonmotile, bacterial prey. *Mar. Ecol. Prog. Ser.*, **102**: 257-267.

Gonzalez J.M., Sherr E.B., Sherr B.F., 1990. Size-selective grazing on bacteria by natural assemblages of estuarine flagellates and ciliates. *Appl. Environ. Microbiol.*, **56**: 583.

Graham J.M., 1990. Measurement of grazing rates on ciliates by freshwater copepods. Conference abstract: Society of Protozoologists 43rd Annual Meeting Proceedings doi: .

Guillard R.R.L., 1975. Culture of phytoplankton for feeding marine invertebrates. In: W.L. Smith, M.H. Chanley (Eds), Culture of marine invertebrate animals. Plenum Press, New York, NY, pp 29-60.

Hagström Å., Larsson U., Hörstedt P., Normark S., 1979. Frequency of dividing cells, a new approach to the determination of bacterial growth rates in aquatic environments. *Appl. Environ. Microbiol.*, **37**: 805.

Hansen B., Bjornsen P.K., Hansen P.J., 1994. The size ratio between planktonic predators and their prey. *Limnol. Oceanogr.*, **39**: 395-403.

Hansen P.J., 1991. Quantitative importance and trophic role of heterotrophic dinoflagellates in a coastal pelagial food web. *Mar. Ecol. Prog. Ser.*, **73**: 253-261.

Hansen P.J., Calado A.J., 1999. Phagotrophic mechanisms and prey selection in free living dinoflagellates *J. Eukaryot. Microbiol.*, **46**: 382-389.

Hansen P.J., Moldrup M., Tarangkoon W., Garcia-Cuetos L., Moestrup Ø., 2012. Direct evidence for symbiont sequestration in the marine red tide ciliate *Mesodinium rubrum*. *Aquat. Microb. Ecol.*, **66**: 63-75.

Harman G.E., Stasz T.E., 1988. Fluorescent vital stains for complementary labelling of protoplasts from *Trichoderma* spp. *Stain Technol.*, **63**: 241-247.

Hauser D.C., Levandowsky M., Hutner S.H., Chunosoff L., Hollwitz J.S., 1974. Chemosensory responses by the heterotrophic marine dinoflagellate *Crypthecodinium cohnii*. *Microb. Ecol.*, **1**: 246-254.

Heinbokel J.F., 1978. Studies on the functional role of tintinnids in the Southern California Bight. I. Grazing and growth rates in laboratory cultures. *Mar. Biol.*, **47**: 177-189.

Ishii N., Takeda H., Doi M., Fuma S., Miyamoto K., Yanagisawa K., Kawabata Z.i., 2002. A new method using enhanced green fluorescent protein (EGFP) to determine grazing rate on live bacterial cells by protists. *Limnology*, **3**: 47-50.

Izaguirre I., Unrein F., Schiaffino M.R., Lara E., Singer D., Balagué V., Gasol J.M., Massana R., 2021. Phylogenetic diversity and dominant ecological traits of freshwater Antarctic Chrysophyceae. *Polar Biol.*, **44**: 941-957.

Jacobson D.M., Anderson D.M., 1986. Thecate heterophic dinoflagellates: Feeding behavior and mechanisms. *J. Phycol.*, **22**: 249-258.

Jakobsen H.H., Strom S.L., 2004. Circadian cycles in growth and feeding rates of heterotrophic protist plankton. *Limnol. Oceanogr.*, **49**: 1915-1922.

Johnson M.D., 2015. Inducible mixotrophy in the dinoflagellate *Prorocentrum minimum*. *J. Eukaryotic Microbiol.*, **62**: 431-443.

Johnson M.D., Beaudoin D.J., Frada M.J., Brownlee E.F., Stoecker D.K., 2018. High grazing rates on cryptophyte algae in Chesapeake Bay. *Front. Mar. Sci.*, **5**.

Johnson M.D., Rome M., Stoecker D.K., 2003. Microzooplankton grazing on *Prorocentrum minimum* and *Karlodinium micrum* in Chesapeake Bay. *Limnol. Oceanogr.*, **48**: 238-248.

Jürgens K., DeMott W.R., 1995. Behavioral flexibility in prey selection by bacterivorous nanoflagellates. *Limnol. Oceanogr.*, **40**: 1503-1507.

Kamiyama T., 2000. Application of a vital staining method to measure feeding rates of field ciliate assemblages on a harmful alga. *Mar. Ecol. Prog. Ser.*, **197**: 299-303.

Kamiyama T., Takayama H., Nishii Y., Uchida T., 2001. Grazing impact of the field ciliate assemblage on a bloom of the toxic dinoflagellate *Heterocapsa circularisquama*. *Plankton Biol. Ecol.*, **48**: 10-18.

Kenter U., Zimmermann U., Müller H., 1996. Grazing rates of the freshwater ciliate *Balanion planctonicum* determined by flow cytometry. *J. Plankton Res.*, **18**: 1047-1053.

Kinner N.E., Harvey R.W., Blakeslee K., Novarino G., Meeker L.D., 1998. Size-selective predation on groundwater bacteria by nanoflagellates in an organic-contaminated aquifer. *Appl. Environ. Microbiol.*, **64**: 618-625.

Krambeck C., Krambeck H.-J., Overbeck J., 1981. Microcomputer-assisted biomass determination of plankton bacteria on scanning electron micrographs. *Appl. Environ. Microbiol.*, **42**: 142.

Landry M.R., Haas L.W., Fagerness V.L.I., 1984. Dynamics of microbial plankton communities: experiments in Kaneohe Bay, Hawaii. *Mar. Ecol. Prog. Ser.*, **16**: 127.

Landry M.R., Hassett R.P.I., 1982. Estimating the grazing impact of marine micro-zooplankton. *Mar. Biol.*, **67**: 283-288.

Landry M.R., Lehner-Fournier J.M., Sundstrom J.A., Fagerness V.L., Selph K.E., 1991. Discrimination between living and heat-killed prey by a marine zooflagellate, *Paraphysomonas vestita* (Stokes). *J. Exp. Mar. Biol. Ecol.*, **146**: 139-151.

Lessard E.J., Martin M.P., Montagnes D.J.S., 1996. A new method for live-staining protists with DAPI and its application as a tracer of ingestion by walleye pollock (*Theragra chalcogramma* (Pallas)) larvae. *J. Exp. Mar. Biol. Ecol.*, **204**: 43-57.

Lessard E.J., Swift E., 1985. Species-specific grazing rates of heterotrophic dinoflagellates in oceanic waters, measured with a dual-label radioisotope technique. *Mar. Biol.*, **87**: 289-296.

Li A., Stoecker D.K., Coats D.W., 2001. Use of the 'food vacuole content' method to estimate grazing by the mixotrophic dinoflagellate *Gyrodinium galatheanum* on cryptophytes. *J. Plankton Res.*, **23**: 303-318.

Li A., Stoecker D.K., Coats D.W., Adam E.J., 1996. Ingestion of fluorescently labeled and phycoerythrin-containing prey by mixotrophic dinoflagellates. *Aquat. Microb. Ecol.*, **10**: 139-147.

MacIntyre H.L., Cullen J.J., 2016. Classification of phytoplankton cells as live or dead using the vital stains fluorescein diacetate and 5 chloromethylfluorescein diacetate. *J. Phycol.*, **52**: 572-589.

Martínez R.A., Isari S., Calbet A., 2014. Use of live, fluorescently-labeled algae for measuring microzooplankton grazing in natural communities. *J. Exp. Mar. Biol. Ecol.*, **457**: 59-70.

Maselli M., Altenburger A., Stoecker D.K., Hansen P.J., 2020. Ecophysiological traits of mixotrophic *Strombidium* spp. *J. Plankton Res.*, **42**: 485-496.

Matantseva O.V., Skarlato S.O., 2013. Mixotrophy in microorganisms: ecological and cytophysiological aspects. *J. Evol. Biochem. Physiol.*, **49**: 377-388.

McManus G.B., Fuhrman J.A., 1986. Bacterivory in seawater studied with the use of inert fluorescent particles. *Limnol. Oceanogr.*, **31**: 420-426.

Menden-Deuer S., Lessard E.J., 2000. Carbon to volume relationships for dinoflagellates, diatoms, and other protist plankton. *Limnol Oceanogr*, **45**: 569-579.

Mitra A., Flynn K.J., Tillmann U., Raven J.A., Caron D., Stoecker D.K., Not F., Hansen P.J., Hallegraeff G., Sanders R.W., Wilken S., McManus G., Johnson M., Pitta P., Våge S., Berge T., Calbet A., Thingstad F., Jeong H.J., Burkholder J., Glibert P.M., Granéli E., Lundgren V., 2016. Defining planktonic protist functional groups on mechanisms for energy and nutrient acquisition: incorporation of diverse mixotrophic strategies. *Protist*, **167**: 106-120.

Monger B.C., Landry M.R., 1991. Prey-size dependency of grazing by free-living marine flagellates. *Mar. Ecol. Prog. Ser.*, **74**: 239-248.

Monger B.C., Landry M.R., 1992. Size-selective grazing by heterotrophic nanoflagellates: an analysis using live-stained bacteria and dual-beam flow cytometry. *Arch. Hydrobiol., Beih.*, **37**: 173-185.

Montagnes D.J.S., Lynn D.H., 1987. A quantitative protargol stain (QPS) for ciliates: Method description and test of its quantitative nature. *Mar. Microb. Food Webs*, **2**: 83-93.

Myung G., Kim H.S., Park J.S., Park M.G., Yih W., 2011. Population growth and plastid type of *Myrionecta rubra* depend on the kinds of available cryptomonad prey. *Harmful Algae*, **10**: 536-541.

Nelson B.N., Lemieux E.J., Drake L., Kulis D., Burns K., Anderson D., Welshmeyer N., Smith S., Scianni C., Wier T., 2009. Phytoplankton enumeration and evaluation experiments. Woods Hole Oceanographic Institute, Moss Landing Marine Laboratory, Naval Research Laboratory, Fluid Imaging Technologies, Key West, FL. 33040.

Newell S.Y., Sherr B.F., Sherr E.B., Fallon R.D., 1983. Bacterial response to presence of eukaryote inhibitors in water from a coastal marine environment. *Mar. Environ. Res.*, **10**: 147-157.

Ng W.H.A., Liu H., Zhang S., 2017. Diel variation of grazing of the dinoflagellate *Lepidodinium* sp. and ciliate *Euplotes* sp. on algal prey: the effect of prey cell properties. *J. Plankton Res.*, **39**: 450-462.

Nielsen L.T., Krock B., Hansen P.J., 2012. Effects of light and food availability on toxin production, growth and photosynthesis in *Dinophysis acuminata*. *Mar. Ecol. Prog. Ser.*, **471**: 37-50.

Nishibe Y., Kawabata Z.i., Nakano S.-i., 2002. Grazing on *Microcystis aeruginosa* by the heterotrophic flagellate *Collodictyon triciliatum* in a hypertrophic pond. *Aquat. Microb. Ecol.*, **29**: 173-179.

Nygaard K., Børsheim K.Y., Thingstad T.F., 1988. Grazing rates on bacteria by marine heterotrophic microflagellates compared to uptake rates of bacterial-sized monodisperse fluorescent latex beads. *Mar. Ecol. Prog. Ser.*, **44**: 159-165.

Park J.S., Myung G., Kim H.S., Cho B.C., Yih W., 2007. Growth responses of the marine photosynthetic ciliate *Myrionecta rubra* to different cryptomonad strains. *Aquat. Microb. Ecol.*, **48**: 83-90.

Pfister G., Arndt H., 1998. Food selectivity and feeding behaviour in omnivorous filter-feeding ciliates: A case study for *Stylonychia*. *Eur. J. Protistol.*, **34**: 446-457.

Premke K., Arndt H., 2000. Predation on heterotrophic flagellates by protists: food selectivity determined using a live-staining technique. *Arch. Hydrobiol.*, **150**: 17-28.

Putt M., 1991. Development and evaluation of tracer particles for use in microzooplankton herbivory studies. *Mar. Ecol. Prog. Ser.*, **77**.

Rublee P.A., Gallegos C.L., 1989. Use of fluorescently labelled algae (FLA) to estimate microzooplankton grazing. *Mar. Ecol. Prog. Ser.*: 221-227.

Rusterholz P.M., Hansen P.J., Daugbjerg N., 2017. Evolutionary transition towards permanent chloroplasts?-Division of kleptochloroplasts in starved cells of two species of *Dinophysis* (Dinophyceae). *PLoS One*, **12**: e0177512.

Sanders R.W., Porter K.G., 1986. Use of metabolic inhibitors to estimate protozooplankton grazing and bacterial production in a monomictic eutrophic lake with an anaerobic hypolimnion. *Appl. Environ. Microbiol.*, **52**: 101-107.

Schindelin J., Arganda-Carreras I., Frise E., Kaynig V., Longair M., Pietzsch T., Preibisch S., Rueden C., Saalfeld S., Schmid B., 2012. Fiji: an open-source platform for biological-image analysis. *Nat. Methods*, **9**: 676.

Schmoker C., Hernández-León S., Calbet A., 2013. Microzooplankton grazing in the oceans: impacts, data variability, knowledge gaps and future directions. *J. Plankton Res.*, **35**: 691-706.

Schumann R., Schiewer U., Karsten U., Rieling T., 2003. Viability of bacteria from different aquatic habitats. II. Cellular fluorescent markers for membrane integrity and metabolic activity. *Aquat. Microb. Ecol.*, **32**: 137-150.

Setälä O., Autio R., Kuosa H., 2005. Predator–prey interactions between a planktonic ciliate *Strombidium sp.* (Ciliophora, Oligotrichida) and the dinoflagellate *Pfiesteria piscicida* (Dinamoebiales, Pyrrophyta). *Harmful Algae*, **4**: 235-247.

Sherr B.F., Sherr E.B., Andrew T.L., Fallon R.D., Newell S.Y., 1986. Trophic interactions between heterotrophic protozoa and bacterioplankton in estuarine water analyzed with selective metabolic inhibitors. *Mar. Ecol. Prog. Ser.*, **32**: 169-179.

Sherr B.F., Sherr E.B., Fallon R.D., 1987. Use of monodispersed, fluorescently labeled bacteria to estimate *in situ* protozoan bacterivory. *Appl. Environ. Microbiol.*, **53**: 958-965.

Shields A.R., Smith W.O., 2008. An examination of the role of colonial *Phaeocystis antarctica* in the microbial food web of the Ross Sea. *Polar Biol.*, **31**: 1091-1099.

Skibbe O., 1994. An improved quantitative protargol stain for ciliates and other planktonic protists. *Arch. Hydrobiol.*, **130**: 339-347.

Smalley G.W., Coats D.W., Adam E.J., 1999. A new method using fluorescent microspheres to determine grazing on ciliates by the mixotrophic dinoflagellate *Ceratium furca*. *Aquat. Microb. Ecol.*, **17**: 167-179.

Smith M., Hansen P.J., 2007. Interaction between *Mesodinium rubrum* and its prey: importance of prey concentration, irradiance and pH. *Mar. Ecol. Prog. Ser.*, **338**: 61-70.

Spero H.J., 1985. Chemosensory capabilities in the phagotrophic dinoflagellate *Gymnodinium fungiforme*. *J. Phycol.*, **21**: 181-184.

Stoecker D., Guillard R.R.L., Kavee R.M., 1981. Selective predation by *Favella ehrenbergii* (Tintinnia) on and among dinoflagellates. *Biol. Bull.*, **160**: 136-145.

Stoecker D.K., Hansen P.J., Caron D.A., Mitra A., 2017. Mixotrophy in the marine plankton. *Annu. Rev. Mar. Sci.*, **9**: 311-335.

Stoecker D.K., Stevens K., Gustafson Jr D.E., 2000. Grazing on *Pfiesteria piscicida* by microzooplankton. *Aquat. Microb. Ecol.*, **22**: 261-270.

Strom S.L., 2001. Light-aided digestion, grazing and growth in herbivorous protists. *Aquat. Microb. Ecol.*, **23**: 253-261.

Vanderploeg H.A., Scavia D., 1979. Two electivity indices for feeding with special reference to zooplankton grazing. *J. Fish. Res. Bd. Can.*, **36**: 362-365.

Verity P.G., 1988. Chemosensory behavior in marine planktonic ciliates. *Bull. Mar. Sci.*, **43**: 772-782.

Wikner J., Andersson A., Normark S., Hagström A., 1986. Use of genetically marked minicells as a probe in measurement of predation on bacteria in aquatic environments. *Appl. Environ. Microbiol.*, **52**: 4-8.

Wilken S., Yung C.C.M., Hamilton M., Hoadley K., Nzongo J., Eckmann C., Corrochano-Luque M., Poirier C., Worden A.Z., 2019. The need to account for cell biology in characterizing predatory mixotrophs in aquatic environments. *Phil. Trans. R. Soc. B*, **374**: 20190090.

Wright R.T., Coffin R.B., 1984. Measuring microzooplankton grazing on planktonic marine bacteria by its impact on bacterial production. *Microb. Ecol.*, **10**: 137-149.

Yih W., Kim H.S., Jeong H.J., Myung G., Kim Y.G., 2004. Ingestion of cryptophyte cells by the marine photosynthetic ciliate *Mesodinium rubrum*. *Aquat. Microb. Ecol.*, **36**: 165-170.

Zhang Q.-C., Song J.-J., Yu R.-C., Yan T., Wang Y.-F., Kong F.-Z., Zhou M.-J., 2013. Roles of mixotrophy in blooms of different dinoflagellates: Implications from the growth experiment. *Harmful Algae*, **30**: 10-26.

Paper II

Caveats on the use of rotenone to estimate mixotrophic grazing in the oceans

Guilherme D. Ferreira, Albert Calbet

Abstract

Phagotrophic mixotrophs (mixoplankton) are now widely recognised as important members of food webs, but their role in the functioning of food webs is not yet fully understood. This is due to the lack of a well-established technique to estimate mixotrophic grazing. An immediate step in this direction would be the development of a method that separates mixotrophic from heterotrophic grazing that can be routinely incorporated into the common techniques used to measure microplankton herbivory (e.g., the dilution technique). This idea was explored by the addition of rotenone, an inhibitor of the respiratory electron chain that has been widely used to selectively eliminate metazoans, both in the field and in the laboratory. Accordingly, rotenone was added to auto-, mixo-, and heterotrophic protist cultures in increasing concentrations (ca. 24 h). The results showed that mixotrophs survived better than heterotrophs at low concentrations of rotenone. Nevertheless, their predation was more affected, rendering rotenone unusable as a heterotrophic grazing deterrent. Additionally, it was found that rotenone had a differential effect depending on the growth phase of an autotrophic culture. Altogether, these results suggest that previous uses of rotenone in the field may have disrupted the planktonic food web.

Introduction

The photosynthetic activity of marine phytoplankton is responsible for nearly half of the carbon (C) sequestration by autotrophs on Earth. Most of this C will be processed in the food web by microzooplankton (Calbet & Landry 2004, Schmoker *et al.* 2013); however, it is currently accepted that a substantial part of this grazing activity might be mediated by phagotrophic "phytoplankton" (Jeong *et al.* 2010). Therefore, the flux of C throughout the food web becomes more complicated than predicted when considering only the phytoplankton-zooplankton dichotomy, as this type of plankton is concurrently a primary and a secondary producer (Flynn *et al.* 2013).

Mixotrophy is a globally ubiquitous nutritional strategy (Leles *et al.* 2017, Faure *et al.* 2019) that defies the traditional auto- and heterotroph classification by combining both nutritional modes (Stoecker *et al.* 2017) and can be found among phylogenetically diverse organisms whose sizes occupy four orders of magnitude (Flynn *et al.* 2019). Mixotrophy is traditionally defined as the use of both inorganic and organic C-forms but can also include the incorporation of other nutrients (Stoecker *et al.* 2017). By definition, the passive uptake of dissolved organic C sources by some photoautotrophs such as diatoms (Lewin 1953) can be regarded as mixotrophy, although this trait is not useful for discriminating among trophic strategies (Flynn *et al.* 2013). Thus, for the purpose of clarity, this paper will hereafter only address phago-mixotrophs, which have recently been termed mixoplankton (Flynn *et al.* 2019). Mixoplankton can be divided according to their physiological traits of chloroplast acquisition into two major groups, the Constitutive and the Non-Constitutive mixoplankton (CM and NCM, respectively) (Mitra *et al.* 2016). CMs possess an innate ability to photosynthesize, whereas NCMs acquire their C-fixation mechanisms from ingested prey.

The presence of mixoplankton, with this trophic mode being the rule rather than the exception (Flynn *et al.* 2013), impairs most of the current models for nutrient cycling dynamics (Yool *et al.* 2013), fishery management (Plagányi 2007), and climate change predictions (Arora *et al.* 2013). Indeed, mixoplankton may affect the stability of the food web (Mitra *et al.* 2014) while enhancing predators' gross growth efficiencies and nutrient cycling (Mitra *et al.* 2016, Stoecker *et al.* 2017), which have consequences on models' forecasting abilities. In addition, despite knowing that mixotrophy is abundant, it is still very difficult to quantify the degree of functional mixotrophy in a given microplankton assemblage (Flynn *et al.* 2019). Indeed, the traditional methods for estimating primary production in aquatic environments (such as ^{14}C) do not disentangle the contribution of

pure autotrophs and mixoplankton (Flynn *et al.* 2019, Wilken *et al.* 2019). Similarly, the methods aiming at measuring the grazing and secondary production by phagotrophs fail, once again, to discriminate the contribution of mixoplankton (Flynn *et al.* 2019). It becomes thus clear that a better performance of ecosystem predictive models depends on a proper approach to the mixoplankton paradigm.

Therefore, to understand the contribution of mixoplankton to the trophic interactions of any given system, the quantification of auto- and heterotrophic processes is needed either at a community or individual level (Beisner *et al.* 2019, Wilken *et al.* 2019). At the community level, the major issue regarding mixoplankton is the change in bulk nutrient circulation whereas at the individual level is to elucidate how mixoplankton affect the structure and biodiversity of a community (Beisner *et al.* 2019).

Several methodologies to measure mixotrophic grazing in the field do exist, in particular targeting bacterivorous nanoflagellates (reviewed recently in Wilken *et al*. 2019 and Beisner *et al*. 2019). The techniques with the highest success rate rely on fluorescent particles that are used as tracers (such as Fluorescently Labelled Bacteria – Beisner *et al.* 2019), and Live Fluorescently Labelled Algae – Li *et al.* 1996), especially because of the applicability to remote field locations (Wilken *et al.* 2019). These approaches have a high taxonomic resolution, both in terms of predators and prey. Additionally, due to the short-term nature of these experiments, it is easier to assess effects such as the relevance of diel feeding rhythms for a given organism/community (Stoecker *et al.* 1997). Yet, as these methods rely on microscopy, a few disadvantages emerge and can restrict their application. The major disadvantage is the shortage of properly trained taxonomists who can readily identify mixoplankton within the samples (Flynn *et al.* 2019). Other important disadvantages include the lack of evidence of selectivity of grazers towards or against the labelled prey, the artificial increase in natural prey densities (Li *et al.* 1996, Martínez *et al.* 2014), and the possible coincidental overlap of prey and predator cells upon filtration (Wilken *et al.* 2019).

An approach that does not possess any of the above mentioned disadvantages while retaining a short-term nature is the one that relies on the selective action of acidotropic probes (e.g. LysoTracker Green) on food vacuoles (Rose *et al.* 2004, Martinez-Garcia *et al.* 2012, Anderson *et al.* 2017). This fluorochrome can be coupled to flow cytometry, yielding a good discrimination of both mixo- and heterotrophic nanoflagellates communities (Martinez-Garcia *et al.* 2012) and even estimates of *in situ* bacterivory rates by both groups (Anderson *et al.* 2017). Yet, it relies on the maintenance

of the membrane potential, which is disrupted by fixation methods, restraining its use to live samples (Rose *et al.* 2004). Additionally, the use of a flow cytometer is highly limited by the size of the particles, as larger and less abundant organisms such as dinoflagellates and ciliates (likely the major algal grazers) are mostly missed. Finally, unspecific fluorescence may occur on pigmented cells (e.g. fluorescence by silica frustule of diatoms – Martínez *et al.* 2014, acidic thylakoid lumens – Wilken *et al.* 2019, or autophagy of cellular components – Johnson *et al.* 2014).

Regarding community level approaches (which do not possess any of the above mentioned disadvantages but cannot provide differentiation between groups), the most widely used technique to measure microplankton herbivory in the field (the dilution technique(Landry & Hassett 1982)) is blind to mixotrophy (see Schmoker *et al.* 2013 for a review of the assumptions, details, and caveats of the methodology).

Should a natural sample contain mixoplankton (the most usual condition in marine waters), the mortality of prey measured on a standard dilution setting would not just be attributable to heterotrophic life-forms but also to mixoplanktonic organisms (Stoecker & Pierson 2019). Additionally, knowing that both CMs and NCMs possess chlorophyll, mixoplankton act simultaneously both as prey and predators in the dilution technique, biasing the grazing estimates (Schmoker *et al.* 2013).

It becomes thus evident that new approaches to estimate mixotrophic grazing *in situ* are required. Given that the dilution technique has proven to be a simple and useful technique but does not discriminate between mixo- and heterotrophic grazing, it would be very useful to develop a modified version of this technique that is capable of uncoupling the grazing rates for both groups. Therefore, a method that discriminates between trophic modes or one able to disrupt one of them would be extremely useful. In this regard, rotenone (IUPAC: (2R,6aS,12aS)-1,2,6,6a,12,12a-hexahydro-2-isopropenyl-8,9-dimethoxychromeno[3,4-b]furo(2,3-h)chromen-6-one) is a compound that inhibits the electron transport chain in the mitochondria by blocking the transmission of electrons from complex I to ubiquinone (Palmer *et al.* 1968). Therefore, rotenone discontinues oxidative phosphorylation and ATP synthesis in this organelle. According to the mode of action, organisms relying exclusively on mitochondria for ATP synthesis (heterotrophs) are likely more vulnerable to rotenone than chloroplast-bearing organisms, which can also use chloroplasts to produce ATP in the light phase of the photosynthesis (Kohzuma *et al.* 2017).

Rotenone has already been suggested to eliminate unwanted predation by rotifers in microalgae cultures, as microalgae are seemingly unaffected (Van Ginkel *et al.* 2015, 2016, El-Sayed *et al.* 2018). Nevertheless, direct evidence of the effects of rotenone on chloroplast-bearing organisms is scarce despite the common assumption that these organisms are largely unaffected. If this assumption is confirmed, from a theoretical point of view, natural food webs could be modified by suppressing heterotrophic grazers (Schmoker *et al.* 2013). It is important to mention that, also from a theoretical point of view, a dose of rotenone could diminish the pool of available ATP for chloroplast-bearing organisms as well, which ultimately may affect their grazing performance, both in the laboratory and in the field.

Therefore, the present study investigates the effects of rotenone on auto-, mixo- and heterotrophs in the laboratory under acute assays (ca. 24 h), using growth and ingestion as endpoints. The main aim of this study was to evaluate whether rotenone could be tentatively added to a standard dilution setting to uncouple mixo- and heterotrophic grazing rates. Furthermore, on a parallel and independent experiment, it was evaluated whether the physiological condition of an organism (assessed by a differential growth phase) affected its tolerance to rotenone.

Methods

Cultures

The experiments were conducted with two protozooplankton, the dinoflagellate *Gyrodinium dominans* (strain ICM-ZOO-GD001) and the ciliate *Strombidium arenicola* (strain ICM-ZOO-SA001); two mixoplankton, the CM dinoflagellate *Karlodinium armiger* (strain ICM-ZOO-KA001) and the pSNCM ciliate *Mesodinium rubrum* (strain DK-2009); two phytoplanktonic flagellates, *Rhodomonas salina* (strain K-0294) and *Tetraselmis chuii*, and one phytoplanktonic diatom, *Conticribra weissflogii* (previously known as *Thalassiosira weissflogii*). All cultures were kept in a controlled-temperature room at 19°C with a 10:14 L/D cycle. Additionally, all cultures were maintained at a salinity of 38.

R. salina, *T. amphioxeia*, and *T. chuii* were kept in f/2 medium (Guillard 1975) under exponential growth conditions. These organisms were irradiated at 100-200 µmol photons m^{-2} s^{-1} provided by cool white fluorescent lights. *C. weissflogii* was grown under the same conditions with the exception that silicate was added to the medium and bubbling was applied to maintain cells in suspension. *G. dominans*, *S. arenicola*, and *K.*

armiger were kept at a PFD of 35-55 µmol photons m^{-2} s^{-1} in autoclaved 0.1 µm-filtered seawater that contained EDTA and trace metals in accordance with f/2 medium. *R. salina* was offered as prey to all three species *ad libitum*. *M. rubrum* was grown under the same light conditions though kept in autoclaved 0.1 µm filtered seawater without the addition of metals and supplied with *T. amphioxeia* as prey at a proportion of ca. 5 prey per predator (Smith & Hansen 2007).

Rotenone effects on growth and grazing rates

Rotenone solutions were prepared according to the guidelines provided by El-Sayed *et al.* (2018). Briefly, a stock solution of 1 g L^{-1} (2.535 mM) was prepared by dissolving 0.05 g of rotenone (≥ 95 %, Sigma-Aldrich) in 50 mL of dimethylsulfoxide (DMSO) (≥ 99.5 %, PanReac AppliChem) and stored at -20°C while not in use. Standard solutions of 50 mg L^{-1} were prepared on the days of the experiments by diluting the stock solution 20 times with deionized water.

The experiments were conducted in 132 mL Pyrex bottles and consisted of three concentrations of rotenone (0.5, 1.0 and 2.0 mg L^{-1}, i.e., 1.27 to 5.08 µM), and two controls, one containing only water (0 mg L^{-1}) and another with DMSO (solvent control). DMSO controls comprised only the highest concentration of DMSO (ca. 0.2 %) used with the rotenone solutions of 2.0 mg L^{-1}. Additionally, experimental and control suspensions were prepared in f/40 to guarantee that the incubated prey was not nutrient limited during the experimental period.

Each treatment with rotenone was conducted in triplicate experimental (predator and prey) and control bottles (only prey) and mounted on a plankton wheel (0.2 rpm). The incubations begun shortly after the onset of the light period to maximise the odds of survival for chloroplast-bearing organisms by enabling a longer period for ATP synthesis using the light phase of photosynthesis (Dawson *et al.* 1991, El-Sayed *et al.* 2018). The bottles were incubated for ca. 24 h at 19°C with a 10:14 L/D cycle. At the same time, as the preparation of the triplicate experimental and control bottles, a fourth bottle of each treatment was also prepared for sacrifice as an initial bottle. All bottles were filled gradually, in three to four steps, before being capped. The suspension was gently stirred between fillings. The formation of air bubbles during the filling and capping processes was avoided because shear may damage the organisms (Broglio *et al.* 2004) and thus bias the measured rates. Rotenone was added to the bottles with an automatic pipette

just before capping them to avoid exposing the organisms to very high concentrations of the compound, though only temporarily.

For mixoplankton and protozooplankton, prey was added at saturating concentrations (**Table II-1**) to minimise the effect of different food concentrations on the measured ingestion rate. Predator concentrations were adjusted to allow for ca. 30 % prey depletion after the incubation time (Calbet *et al.* 2013). All organisms were counted, and their volumes were assessed using a Beckman Coulter Multisizer III particle counter, with the exception of *M. rubrum*, which can escape the current flow generated by the particle counter due to their shear sensitivity (Fenchel & Hansen 2006). Aliquots of the experiments with *M. rubrum* were therefore fixed in acidic Lugol's (final concentration 5 %) and enumerated manually using a Sedgwick-Rafter counting chamber. A minimum of 300 cells (of both predator and prey) were counted using a 10x objective on an inverted microscope.

Table II-1 Summary of the prey and predator concentrations used for the acute toxicity assays with rotenone for the mixoplankton *M. rubrum* and *K. armiger*, and protozooplankton *S. arenicola* and *G. dominans*.

Species	Target concentration, Cells mL^{-1}		Reference
	Prey	Predator	
Gyrodinium dominans	100 000	1 500	Calbet *et al.* 2013
Mesodinium rubrum	15 000	1 500	Smith & Hansen 2007
Karlodinium armiger	100 000	3 750	Berge *et al.* 2008b
Strombidium arenicola	100 000	400	Ferreira *et al.* submitted

Grazing rates and average prey concentrations were calculated using Frost (1972) equations; the average concentration of grazers in each replicate was used to assess the grazing per predator (Heinbokel 1978). The magnitude of the effects of the different concentrations of rotenone on the grazing impact reduction (GIR, %) on the prey populations was assessed separately for each grazer species by **Equation II.1**

where $<C>$ and I are the mean predator concentration (Cells mL^{-1}) during the incubation period and the average ingestion rate (Cells Ind^{-1} d^{-1}) measured for each treatment i ($<C>_0$ and I_0 refer to the control treatment of 0 mg L^{-1}). The control suspensions with only DMSO added (no rotenone) were considered a treatment. Non-significant ingestion rates (see the Methods Section) were considered 0 for the calculation of the GIR.

Physiological condition effects on the response to rotenone

Additionally, whether the physiological condition of an organism affected its response to rotenone was assessed. The experiments were conducted with *R. salina,* which was exposed to rotenone both during the exponential and stationary growth phases, with all target concentrations tested at once. The experimental protocol was the same as described before.

Statistical analysis

Species-specific effects of rotenone on growth were analysed using One-Way ANOVAs followed by Tukey's HSD post hoc tests (n = 15 for each treatment; Zar 2010). In the case of *S. arenicola*, in which the assumptions of homoscedasticity were not met, the non-parametric Kruskal-Wallis test was applied, followed by the Games-Howell post hoc test (n =15; Zar 2010).

Ingestion rates were deemed significant only when the prey growth rates in the control and experimental bottles were significantly different (two-tailed Student's t-test, n = 6 for each treatment) (Saiz *et al.* 2014). Subsequently, the results for this parameter were analysed with the same procedure as described for growth rates, with the normality and homoscedasticity assumptions met and Tukey's HSD post hoc tests applied (Zar 2010). Finally, the effects of rotenone on the exponential and stationary *R. salina* were analysed separately for each growth phase using One-Way ANOVAs followed by Tukey's HSD post hoc tests. The interaction between growth phases and treatment was assessed using a two-way ANOVA followed by Bonferroni post hoc tests due to the unequal sample size between factors (Zar 2010). Calculations were conducted using IBM SPSS Statistics 25, and all the results were considered significant at $P < 0.05$.

Results

Rotenone effects on growth rates

The increase in rotenone concentration progressively reduced the growth rates of the two autotrophic flagellates tested (**Figure II-1a,b**). The response was more drastic in *T. chuii*, which even displayed mortality at the lowest concentration (**Figure II-1b**). Conversely, at the same concentration, *R. salina* was not significantly affected (**Figure II-1a**; Tukey HSD, P = 0.261). On the other hand, the diatom *C. weissflogii* was unaffected by all concentrations of rotenone (One-Way ANOVA, P = 0.792; **Figure II-1c**). DMSO at ca. 0.2 % had no visible effect in any of the target autotrophic species when compared to the treatment with 0 mg L^{-1} (Tukey HSD tests, P > 0.05 in all cases). The mixoplankton *M. rubrum* and *K. armiger* were not significantly affected by the presence of DMSO or by the lowest concentration of rotenone, although a negative tendency was observed for *K. armiger* in this last instance (**Figure II-2**; Tukey HSD, P = 0.098). However, higher concentrations of the chemical compound severely reduced the growth rates of both protists, even resulting in mortality (**Figure II-2**).

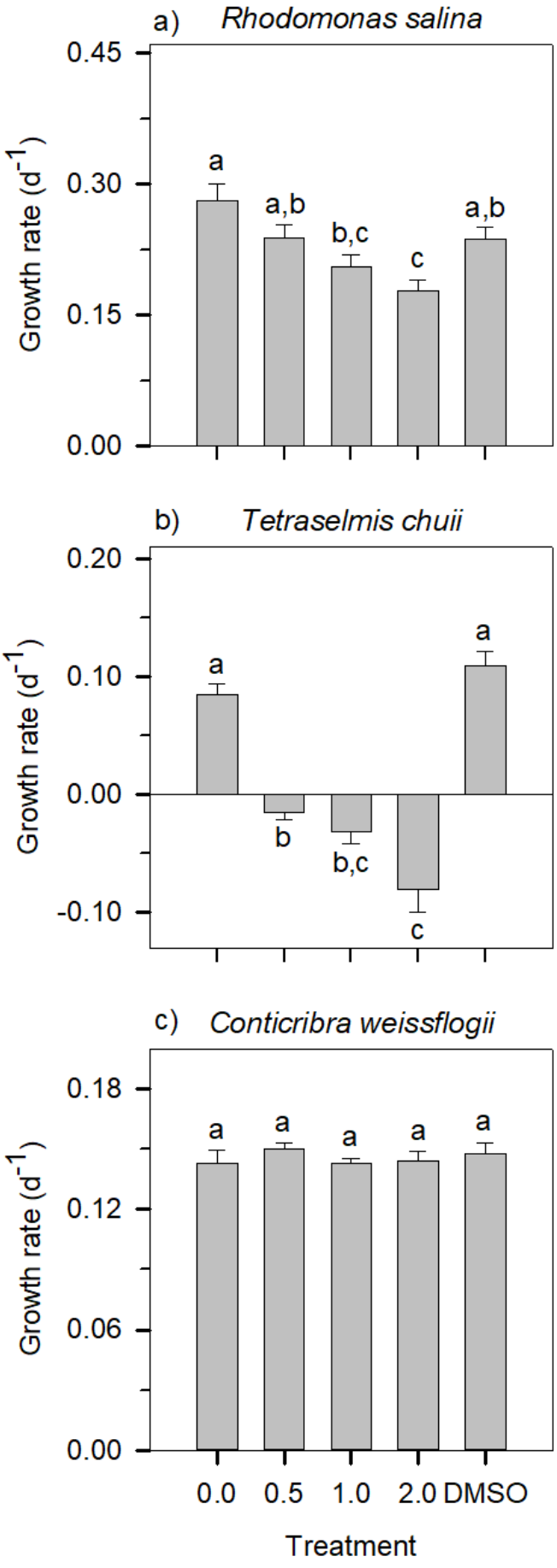

Figure II-1 Growth rate (d^{-1}) of the phytoplankton species a) *R. salina*, b) *T. chuii*, and c) *C. weissflogii* upon exposure to increasing concentrations of rotenone. The data plotted for *R. salina* include all the results for the experiments with the different grazers. Different letters within the same organism indicate statistically significant differences (Tukey HSD, $P < 0.05$). Error bars ± se.

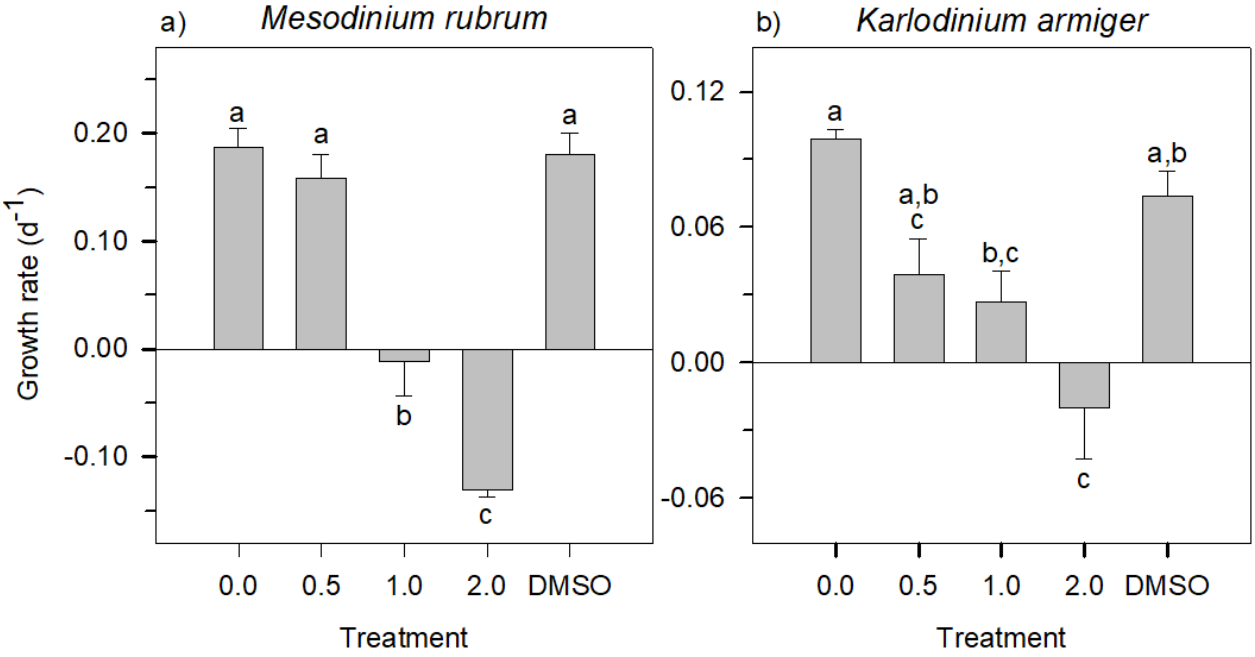

Figure II-2 Growth rate (d^{-1}) of the mixoplankton species a) *M. rubrum* and b) *K. armiger* upon exposure to increasing concentrations of rotenone. Different letters within the same organism indicate statistically significant differences (Tukey HSD, $P < 0.05$). Error bars ± se.

The growth of the heterotrophic species was, on average, the most affected by rotenone (**Figure II-3**). For the protozooplanktonic dinoflagellate *G. dominans*, the maximum growth inhibition was achieved immediately at the lowest concentration tested (0.5 mg L^{-1}); at this concentration, however, the ciliate *S. arenicola* still exhibited positive growth, although it was almost 80% lower than that under the control condition of 0 mg L^{-1}. This ciliate species appeared to be particularly sensitive, being the only species significantly affected by the sole presence of DMSO in the water (Games-Howell, $P = 0.017$). Further supporting a high sensitivity of *S. arenicola*, the ciliates that remained alive after the 24 h were nearly immotile, suggesting severe deleterious effects. Independent of the trophic mode, all motile species exhibited a reduction in the speed of displacement in the presence of the highest concentrations of rotenone, although the magnitude of the reduction was not quantified.

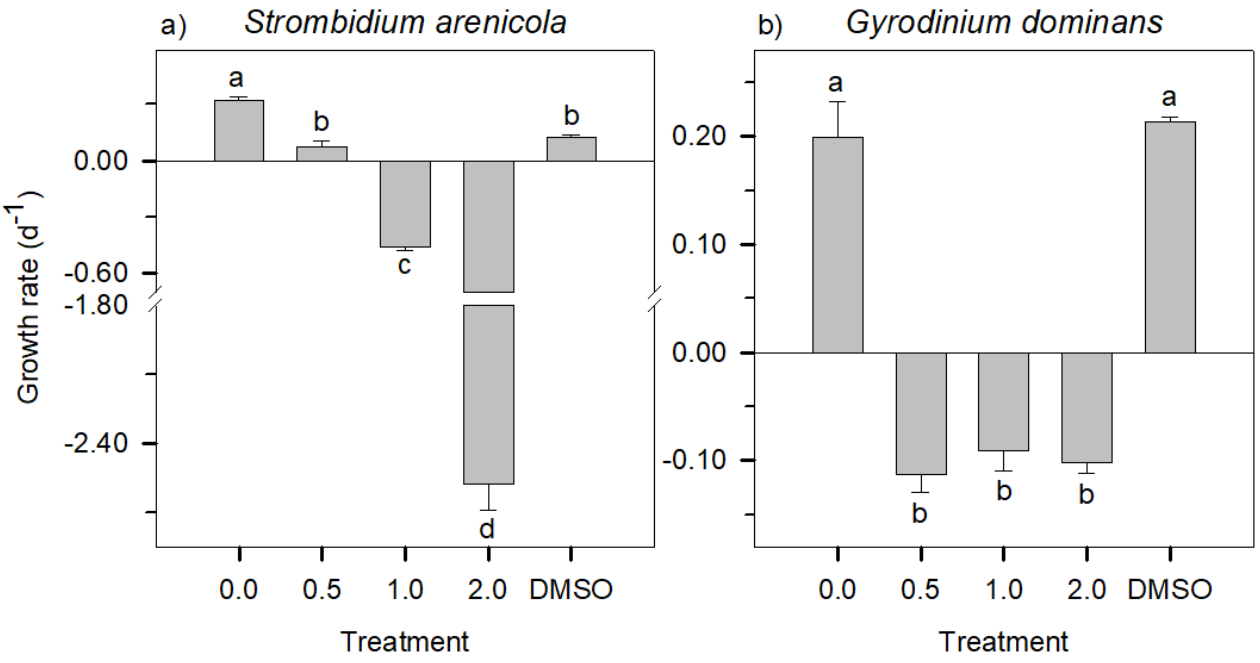

Figure II-3 Growth rate (d^{-1}) of the protozooplankton species a) *S. arenicola* and b) *G. dominans* upon exposure to increasing concentrations of rotenone. Different letters within the same organism indicate statistically significant differences (Tukey HSD, $P < 0.05$). Error bars ± se.

Rotenone effects on ingestion rates

The presence of rotenone impaired feeding in both ciliates, *M. rubrum* (**Figure II-4a**) and *S. arenicola* (**Figure II-4c**), regardless of the trophic mode of nutrition. The responses varied between no significant grazing (two-tailed Student's t-tests, $P > 0.05$ in all cases) and significantly negative ingestion rates (Tukey HSD tests, $P < 0.05$ in all cases). A significantly negative ingestion rate (1.0 and 2.0 mg L^{-1} for *M. rubrum*, and 0.5 and 1.0 mg L^{-1} for *S. arenicola*) implies a positive growth of the prey in the experimental with respect to the control bottles, and likely results from an increase in the nutrient pool originating from the dead grazers. The presence of DMSO also deterred the feeding of these two species, with *M. rubrum* being the most affected (**Figure II-4a,c**). On the other hand, neither the mixoplanktonic *K. armiger* (**Figure II-4b**) nor the protozooplanktonic *G. dominans* (**Figure II-4d**) were significantly affected by the DMSO treatment (Tukey HSD tests, $P > 0.05$ in all cases). Rotenone, however, did affect the feeding rates of these dinoflagellates. *K. armiger* displayed no evidence of feeding whenever rotenone was present, and *G. dominans* showed null ingestion rates at 2.0 mg L^{-1} of rotenone (two-tailed Student's t-tests, $P > 0.05$ in all cases).

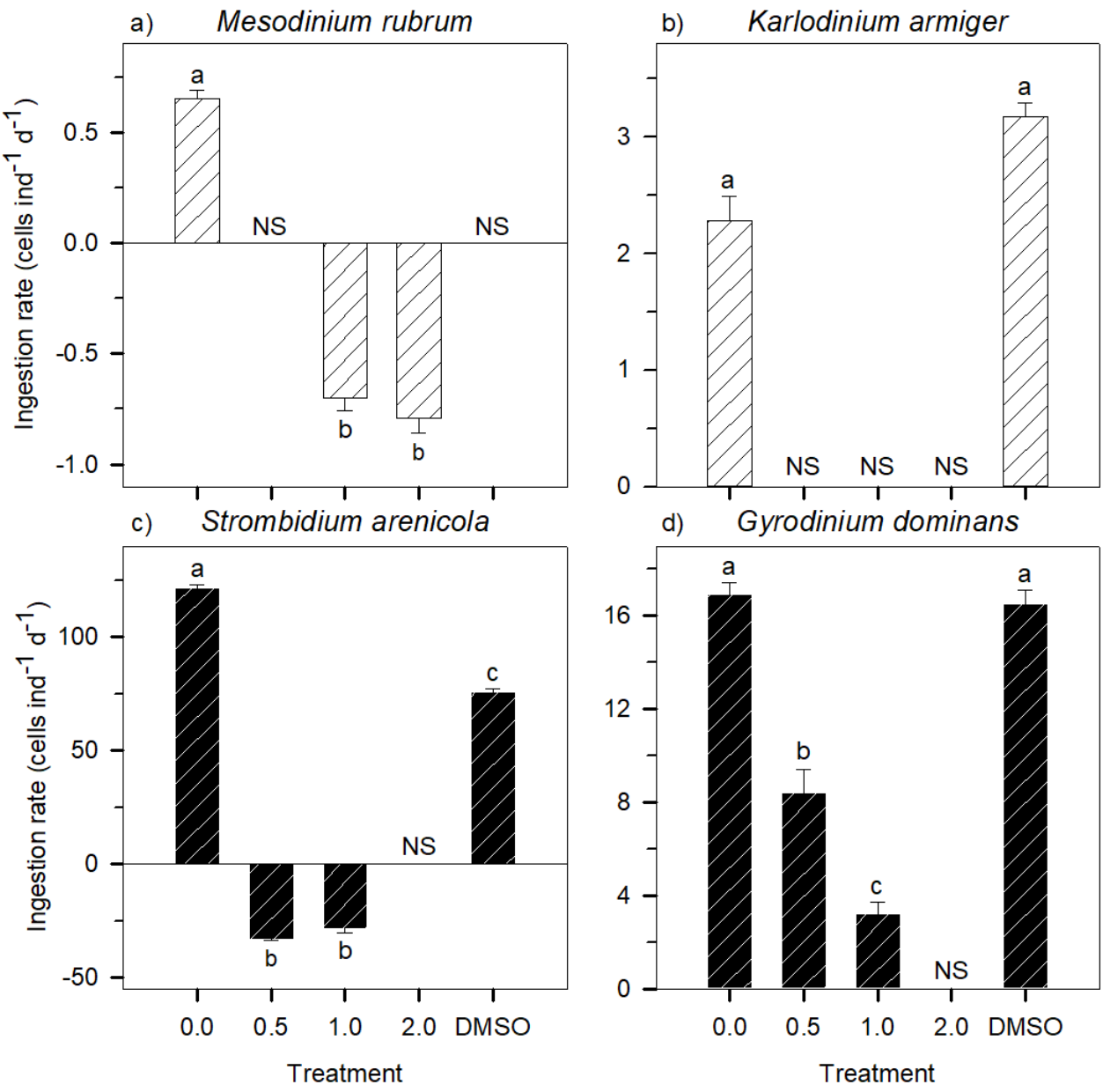

Figure II-5 Ingestion rate (Cells Ind^{-1} d^{-1}) of the mixoplankton (▨) a) *M. rubrum* and b) *K. armiger*, and protozooplankton (■) c) *S. arenicola* and d) *G. dominans* upon exposure to increasing concentrations of rotenone. All organisms were fed *R. salina* during the exposure period. Different letters within the same organism indicate significant differences (Tukey HSD, $P < 0.05$). NS represents the non-significant ingestion rates (two-tailed Student's t-test, $P > 0.05$). Error bars ± se.

Rotenone effects on the overall grazing impact

The reduction in the impact of the chosen predators on the standing stock of *R. salina*, defined using **Equation II.1** as the combined effect of feeding rates and grazer abundances during the incubations, is summarised in **Table II-2**. Regardless of the trophic mode of nutrition, the grazing pressure by dinoflagellates was overall less inhibited by rotenone than that exhibited by ciliates.

Table II-2 Combined effects of rotenone on grazer survival and on their feeding rates on *R. salina* (GIR, %) throughout the incubation. The values were calculated using **Equation II.1**. Non-significant ingestion rates were considered 0, and GIR was thus capped at 100% in these situations, with the values highlighted with an *. No effect of the treatment on the overall grazing impact is indicated by a zero in the table.

Species	Grazing Impact Reduction (GIR), %				
	0.0 mg L^{-1}	0.5 mg L^{-1}	1.0 mg L^{-1}	2.0 mg L^{-1}	DMSO
Gyrodinium dominans	0.00	56.83	83.62	100.00*	0.15
Strombidium arenicola	0.00	123.07	114.80	100.00*	45.59
Karlodinium armiger	0.00	100.00*	100.00*	100.00*	0.00
Mesodinium rubrum	0.00	100.00*	197.07	202.77	100.00

Effects of physiological conditions on the resistance to rotenone

Rotenone affected *R. salina* in different ways depending on its physiological condition (**Figure II-6**). During the deceleration phase, the flagellate was roughly unaffected by the presence of rotenone, independent of the concentration (One-Way ANOVA, P = 0.071). On the other hand, during exponential growth, progressively higher concentrations of rotenone diminished the growth of this cryptophyte up to a maximum of ca. 40% lower than that under the control treatment with 0 mg L^{-1} (Tukey HSD test, P = 0.000).

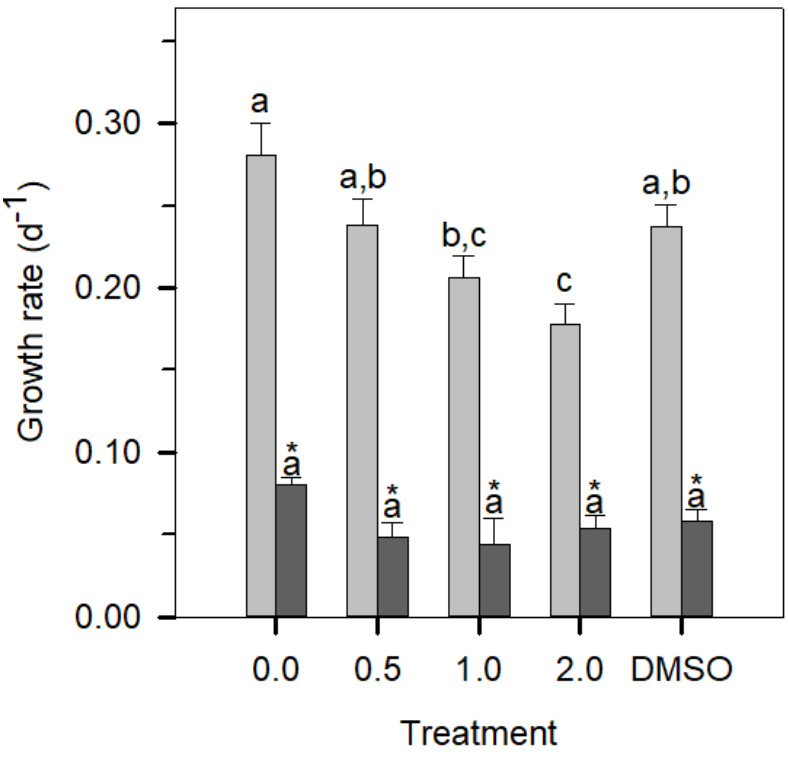

Figure II-5 Growth rate (d^{-1}) of the phytoplanktonic *R. salina* upon exposure to increasing concentrations of rotenone on the exponential (▒) and deceleration (■) growth phases. The data regarding the exponential phase are the same as those displayed in **Figure II-2a**. Different letters within the same growth phase indicate significant differences (Tukey HSD, $p < 0.05$). *Indicates statistically significant differences between exponential and deceleration phases for each individual treatment (Bonferroni, $P < 0.05$). Error bars ± se.

Discussion

As expected, phytoplankton species were more resistant to rotenone, with the exception of *T. chuii*. Other species of the genus *Tetraselmis* are also reported to be more vulnerable to rotenone than other algae species, such as the marine *Nannochloropsis oculata* (Van Ginkel *et al.* 2016) and the freshwater *Chlorella kessleri* (Van Ginkel *et al.* 2015). This observation suggests that there may be a factor that is common to the genus *Tetraselmis* that enhances cellular susceptibility to this compound, although it is currently unknown. Conversely, the diatom and *R. salina* were quite resistant to rotenone effects. In the particular case of the cryptophyte, the effects of this compound were only evident during the exponential growth phase.

Cells undergo drastic metabolic changes when switching from exponential to stationary phases. For example, photosynthesis and respiration rates are, on average, higher during the exponential growth phase for phyto- and mixoplanktonic species (López-Sandoval *et al.* 2014). Similarly, protozooplanktonic ciliates and flagellates displayed higher respiration rates when actively growing than when stationary (Fenchel & Finlay 1983). Therefore, it seems that the increased respiratory chain activity during the exponential phase enhances an organism's susceptibility to rotenone. This conclusion aligns with the mechanism of action of rotenone, which, among other effects, is known to inhibit the synthesis of ATP (Palmer *et al.* 1968). A consequence of the reduced pool of available ATP can be seen in the assembly of microtubules, which becomes impaired and ultimately results in mitotic arrest and inhibition of cell proliferation (Srivastava & Panda 2007). Without these processes, the cell cannot divide, which would have a much higher impact on actively growing cells than on those progressing towards stationary phase.

The observed differences between growth phases under exposure to rotenone may have important consequences for the interpretation of laboratory and field experiments on single-celled organisms, not only with rotenone but with other toxic compounds as well. Despite having data exclusively from *R. salina* (which forces caution in the extrapolation of conclusions to other species), the results indicate that the effect of pollutants should always be tested using the same physiological conditions to minimise intra-specific differences. In the laboratory, this can be easily accomplished by controlling sampling times and/or by using a single batch of cultured organisms (as used in the experiments with mixo- and protozooplankton). On the other hand, for field work this may

represent a challenge. Nonetheless, organisms in the field are likely living on an almost constant exponential growth phase (e.g. Dortch *et al*. 1983), diminishing the risk of comparisons.

A major result of the study is the high sensitivity of the ciliate *S. arenicola* to rotenone, in particular compared to the other protozooplanktonic predator tested, the dinoflagellate *G. dominans*. In fact, *G. dominans*, displayed a peculiar response to rotenone, showing negative growth rates and high ingestion rates at the lowest concentration, and similar growth rates and non-significant ingestion rates (two-tailed Student's t-test, P = 0.114) at the highest. These results suggest that this dinoflagellate may be able to tolerate the presence of rotenone up to a concentration of 1.0 mg L^{-1} by maintaining key cellular processes (like phagocytosis) active while avoiding expensive ones such as cellular division. This could be a mechanism of survival that enables the endurance of harsh conditions for short time periods. Nonetheless, more data is needed to validate this hypothesis. On the other hand, planktonic ciliates are known to be highly susceptible to several chemical compounds, such as hydrocarbons and chemical dispersants (Almeda *et al.* 2014, Schmoker *et al.* 2016), but also to DMSO, although the toxicity of the latter is usually evidenced at higher concentrations than the ones used in this study (Fok & Valin 1983, Rajini *et al.* 1989). Indeed, the ciliate *S. arenicola* was the only species whose growth was reduced by ca. 60% solely by the presence of DMSO.

Analogous to the results observed for protozooplankton, with the ciliate being more sensitive than the dinoflagellate, the pSNCM *M. rubrum* was more sensitive than *K. armiger*. In fact, the ingestion rate of *M. rubrum* was already negligible even with DMSO as the only added compound (**Figure II-4a**). Indeed, DMSO hindered the ingestion of prey for both ciliates (**Figure II-4a,c**). In this regard, a precursor of DMSO, β-dimethylsulfoniopropionate (DMSP), reduced the feeding of protozooplanktonic marine ciliates by 50-75%, whereas for dinoflagellates of the same trophic mode, this reduction was 28-40% (Fredrickson & Strom 2009).

Overall, chloroplast-bearing predators displayed better resilience than protozooplankton at a concentration of 0.5 mg of rotenone L^{-1}. However, their feeding rates were more affected, rendering the overall mixoplankton grazing impact on prey populations considerably lower than that of protozooplanktonic species. In particular, *K. armiger* did not exhibit any evidence of feeding in the presence of rotenone (irrespective

of concentration), while displaying only a slight negative growth rate in the highest concentration. These results are in agreement with those of previous studies on this species, in which it has been observed that *K. armiger* can survive long starvation periods using only chloroplasts for C acquisition, although barely dividing in the absence of food (Berge & Hansen 2016), comparable to the non-significant ingestion rates observed in this study in the presence of rotenone.

One of the main motivations of this study was to test the effectiveness of the use of rotenone combined with the dilution technique to determine mixoplanktonic grazing. For the method to be useful, protozooplanktonic grazing should be impaired while leaving mixoplankton grazing unaffected. Despite the promising results for the effects of rotenone in terms of growth rates (with perhaps the caveat of the high sensitivity of *T. chuii*), the analysis of the effects of this compound on grazing highlighted severe limitations that were not predicted by the theoretical mechanism of action for rotenone (see **Table II-2**). For instance, one of the assumptions of the study was that chloroplast-bearing organisms would be less affected by rotenone despite likely displaying a reduced ATP pool. A question that remains unanswered by this assumption is how large is the dependence of mixoplankton grazing processes on the ATP produced by the oxidative phosphorylation. In other words, can the photo phosphorylation supply enough ATP to maintain basal functions while enabling phagocytosis? The answer, at least from the present experiments, seems to be no, as explained next.

At 30 µmol photons m^{-2} s^{-1} (the experimental conditions used in the present study), a well-fed *K. armiger* fixes C at a higher rate than the maximum observed for unfed cells, and the chlorophyll *a* content is close to the maximum registered (Berge & Hansen 2016). These observations suggest that this dinoflagellate maximises the use of the chloroplasts in situations akin to those used on the present study. Therefore, it seems plausible to assume that these conditions are less prone to magnify potential negative effects of rotenone on the behaviour of the CM.

For *M. rubrum*, it is known that the photosynthetic capacities depend on the quality of the chloroplasts acquired through the ingestion of cryptophytes from the genera *Teleaulax*, *Plagioselmis* or *Geminigera* (Hansen *et al.* 2012), and peak around 30 µmol photons m^{-2} s^{-1} (Moeller *et al.* 2011). Ultimately, the sequestered chloroplasts require the presence of active cryptophyte nuclei, and start to lose photosynthetic efficiency after 3

days without the adequate food source (Kim *et al.* 2017). Accordingly, during the exposure to rotenone, the chloroplasts of the NCM were also likely close to their full potential despite being fed with *R. salina*.

Contrary to all other tested predators, *G. dominans* was still able to ingest *R. salina* under concentrations of rotenone up to 1.0 mg L^{-1} (although with ca. 9% mortality and a grazing impact reduction, GIR, of ca. 83%). Indeed, it is important to note that with a concentration of 0.5 mg L^{-1}, the absolute number of *R. salina* cells ingested per *G. dominans* was approximately 3.8× higher than that of *K. armiger* and 13.2× higher than that of *M. rubrum* in their respective control situations.

Thus, despite the fact that the chloroplasts of both mixoplankton tested here should have been in good conditions and that the available ATP pool for *G. dominans* was (likely) severely reduced during the exposure to rotenone, field grazing estimates using rotenone would be, at best, conservative. Indeed, the analysis of the GIR suggests that in a hypothetical dilution setting with rotenone (0.5 mg L^{-1}) and all 3 predators, *G. dominans* would still be the major grazer. Hence, mixoplanktonic grazing is clearly affected by the reduced ATP concentration, although future physiological studies are required to elucidate the actual contribution of the oxidative phosphorylation for mixoplankton and its role on phagotrophy.

An example that further corroborates that protozooplanktonic dinoflagellates can display a substantial grazing impact on natural populations (thus further complicating the use of a protozooplanktonic grazing deterrent such as rotenone) is the fact that some areas of the Mediterranean Sea possess a biomass of protozooplanktonic dinoflagellates approximately 4× higher than that of phytoplanktonic (with high potential for phagotrophy, Jeong *et al.* 2010) and mixoplanktonic species combined when not blooming (Ignatiades 2012). Additionally, the average C-specific ingestion rate of protozooplanktonic dinoflagellates is ca. 4.5× higher than that of their mixoplankton counterparts (see Figure 10 in Calbet *et al*. 2011 and references therein), meaning that one can assume that protozooplankton would impact prey nearly 20× more than mixoplankton. Assuming that *G. dominans* is a good representative of protozooplanktonic dinoflagellates (Kim & Jeong 2004), the presence of 0.5 mg L^{-1} would still render their impact (see **Table II-2**) on prey populations ca. 11× higher than that of mixoplankton, which would be virtually zero (as

per *K. armiger* results). Thus, rotenone cannot be used as an addition to the standard dilution technique for the purpose of deterring heterotrophic predation.

On an ecological note, rotenone has been used for decades to kill undesirable fish species *in situ*, and typical concentrations varied between 0.5 and 5.0 mg L^{-1}, depending on the sensitivity of the target species (Hinson 2000). However, as evidenced by the results of this study, considerably lower concentrations cause nefarious or even lethal effects on several planktonic species of distinct taxonomic groups. Additionally, the half-life of rotenone in aquatic environments ranges from hours to weeks (Dawson *et al.* 1991) and depends on several factors, namely temperature and pH, increases in which quicken degradation (El-Sayed *et al.* 2018). Hence, this information, together with the data gathered in this study for protists, and previous studies on zooplankton (Naess 1991, Beal & Anderson 1993) and rotifers (Van Ginkel *et al.* 2015, 2016) suggest that the indiscriminate use of this compound in the past may have had disastrous consequences for aquatic food webs, whose extent is largely unknown.

Despite the inability of acting as a deterrent of protozooplanktonic grazing (noticed by the stronger effect on mixoplanktonic predation), rotenone can still be used as a good algal crop protector, especially if the predator is a sensitive organism like a ciliate (our study) or a rotifer (Van Ginkel *et al.* 2015, 2016). Nevertheless, future measures should always assess the effect of rotenone on the specific organism that is plaguing the algal culture, as differences in the sensitivity towards the compound are expected, as highlighted by our results. Similarly, the sensitivity of the algal culture itself should also be acknowledged, as phytoplankton species are not all immune to this compound as expected. Factors such as the growth phase may be exploited to minimise the nefarious effects of the presence of rotenone in non-target organisms.

References

Almeda R., Hyatt C., Buskey E.J., 2014. Toxicity of dispersant Corexit 9500A and crude oil to marine microzooplankton. *Ecotoxicol. Environ. Saf.*, **106**: 76-85.

Anderson R., Jürgens K., Hansen P.J., 2017. Mixotrophic phytoflagellate bacterivory field measurements strongly biased by standard approaches: a case study. *Front. Microbiol.*, **8**: 1398.

Arora V.K., Boer G.J., Friedlingstein P., Eby M., Jones C.D., Christian J.R., Bonan G., Bopp L., Brovkin V., Cadule P., 2013. Carbon–concentration and carbon–climate feedbacks in CMIP5 Earth system models. *J. Climate*, **26**: 5289-5314.

Beal D.L., Anderson R.V., 1993. Response of zooplankton to rotenone in a small pond. *Bull. Environ. Contam. Toxicol.*, **51**: 551-556.

Beisner B.E., Grossart H.-P., Gasol J.M., 2019. A guide to methods for estimating phago-mixotrophy in nanophytoplankton. *J. Plankton Res.*, **41**: 77-89.

Berge T., Hansen P.J., 2016. Role of the chloroplasts in the predatory dinoflagellate *Karlodinium armiger*. *Mar. Ecol. Prog. Ser.*, **549**: 41-54.

Broglio E., Saiz E., Calbet A., Trepat I., Alcaraz M., 2004. Trophic impact and prey selection by crustacean zooplankton on the microbial communities of an oligotrophic coastal area (NW Mediterranean Sea). *Aquat. Microb. Ecol.*, **35**: 65-78.

Calbet A., Bertos M., Fuentes-Grünewald C., Alacid E., Figueroa R., Renom B., Garcés E., 2011. Intraspecific variability in *Karlodinium veneficum*: Growth rates, mixotrophy, and lipid composition. *Harmful Algae*, **10**: 654-667.

Calbet A., Isari S., Martínez R.A., Saiz E., Garrido S., Peters J., Borrat R.M., Alcaraz M., 2013. Adaptations to feast and famine in different strains of the marine heterotrophic dinoflagellates *Gyrodinium dominans* and *Oxyrrhis marina*. *Mar. Ecol. Prog. Ser.*, **483**: 67-84.

Calbet A., Landry M.R., 2004. Phytoplankton growth, microzooplankton grazing, and carbon cycling in marine systems. *Limnol. Oceanogr.*, **49**: 51-57.

Dawson V.K., Gingerich W.H., Davis R.A., Gilderhus P.A., 1991. Rotenone persistence in freshwater ponds: effects of temperature and sediment adsorption. *N. Am. J. Fish Manag.*, **11**: 226-231.

Dortch Q., Roberts T.L., Clayton Jr J.R., Ahmed S.I., 1983. RNA/DNA ratios and DNA concentrations as indicators of growth rate and biomass in planktonic marine organisms. *Mar. Ecol. Prog. Ser.*, **13**: 61-71.

El-Sayed W.M.M., Van Ginkel S.W., Igou T., Ibrahim H.A., Abdul-Raouf U.M., Chen Y., 2018. Environmental influence on rotenone performance as an algal crop protective agent to prevent pond crashes for biofuel production. *Algal Res.*, **33**: 277-283.

Faure E., Not F., Benoiston A.-S., Labadie K., Bittner L., Ayata S.-D., 2019. Mixotrophic protists display contrasted biogeographies in the global ocean. *ISME J.*, .

Fenchel T., Finlay B.J., 1983. Respiration rates in heterotrophic, free-living protozoa. *Microb. Ecol.*, **9**: 99-122.

Fenchel T., Hansen P.J., 2006. Motile behaviour of the bloom-forming ciliate *Mesodinium rubrum*. *Mar. Biol. Res.*, **2**: 33-40.

Flynn K.J., Mitra A., Anestis K., Anschütz A.A., Calbet A., Ferreira G.D., Gypens N., Hansen P.J., John U., Martin J.L., Mansour J.S., Maselli M., Medić N., Norlin A., Not F., Pitta P., Romano F., Saiz E., Schneider L.K., Stolte W., Traboni C., 2019. Mixotrophic protists and a new paradigm for marine ecology: where does plankton research go now? *J. Plankton Res.*, **41**: 375-391.

Flynn K.J., Stoecker D.K., Mitra A., Raven J.A., Glibert P.M., Hansen P.J., Granéli E., Burkholder J.M., 2013. Misuse of the phytoplankton–zooplankton dichotomy: the need to assign organisms as mixotrophs within plankton functional types. *J. Plankton Res.*, **35**: 3-11.

Fok A.K., Valin E.L., 1983. Effects of dimethylsulfoxide (DMSO) on the digestive-lysosomal system in *Paramecium caudatum*. *Eur. J. Cell Biol.*, **32**: 45-51.

Fredrickson K.A., Strom S.L., 2008. The algal osmolyte DMSP as a microzooplankton grazing deterrent in laboratory and field studies. *J. Plankton Res.*, **31**: 135-152.

Frost B.W., 1972. Effects of size and concentration of food particles on the feeding behavior of the marine planktonic copepod *Calanus pacificus*. *Limnol. Oceanogr.*, **17**: 805-815.

Hansen P.J., Moldrup M., Tarangkoon W., Garcia-Cuetos L., Moestrup Ø., 2012. Direct evidence for symbiont sequestration in the marine red tide ciliate *Mesodinium rubrum*. *Aquat. Microb. Ecol.*, **66**: 63-75.

Heinbokel J.F., 1978. Studies on the functional role of tintinnids in the Southern California Bight. I. Grazing and growth rates in laboratory cultures. *Mar. Biol.*, **47**: 177-189.

Hinson D., 2000. Rotenone characterization and toxicity in aquatic systems. *Principles of Environmental Toxicity*. University of Idaho, Moscow.

Ignatiades L., 2012. Mixotrophic and heterotrophic dinoflagellates in eutrophic coastal waters of the Aegean Sea (eastern Mediterranean Sea). *Bot. Mar.*, **55**: 39-48.

Jeong H.J., Yoo Y.D., Kim J.S., Seong K.A., Kang N.S., Kim T.H., 2010. Growth, feeding and ecological roles of the mixotrophic and heterotrophic dinoflagellates in marine planktonic food webs. *Ocean Sci. J.*, **45**: 65-91.

Johnson J.G., Janech M.G., Van Dolah F.M., 2014. Caspase-like activity during aging and cell death in the toxic dinoflagellate *Karenia brevis*. *Harmful Algae*, **31**: 41-53.

Kim J.S., Jeong H.J., 2004. Feeding by the heterotrophic dinoflagellates *Gyrodinium dominans* and *G. spirale* on the red-tide dinoflagellate *Prorocentrum minimum*. *Mar. Ecol. Prog. Ser.*, **280**: 85-94.

Kim M., Drumm K., Daugbjerg N., Hansen P.J., 2017. Dynamics of sequestered cryptophyte nuclei in *Mesodinium rubrum* during starvation and refeeding. *Front. Microbiol.*, **8**.

Kohzuma K., Froehlich J.E., Davis G.A., Temple J.A., Minhas D., Dhingra A., Cruz J.A., Kramer D.M., 2017. The role of Light–Dark regulation of the chloroplast ATP Synthase. *Front . Plant Sci.*, **8**.

Landry M.R., Hassett R.P.I., 1982. Estimating the grazing impact of marine micro-zooplankton. *Mar. Biol.*, **67**: 283-288.

Leles S.G., Mitra A., Flynn K.J., Stoecker D.K., Hansen P.J., Calbet A., McManus G.B., Sanders R.W., Caron D.A., Not F., 2017. Oceanic protists with different forms of acquired phototrophy display contrasting biogeographies and abundance. *Proc. R. Soc. B*, **284**: 20170664.

Lewin J.C., 1953. Heterotrophy in diatoms. *J. Gen. Microbiol.*, **9**: 305-313.

Li A., Stoecker D.K., Coats D.W., Adam E.J., 1996. Ingestion of fluorescently labeled and phycoerythrin-containing prey by mixotrophic dinoflagellates. *Aquat. Microb. Ecol.*, **10**: 139-147.

López-Sandoval D.C., Rodríguez-Ramos T., Cermeño P., Sobrino C., Marañón E., 2014. Photosynthesis and respiration in marine phytoplankton: relationship with cell size, taxonomic affiliation, and growth phase. *J. Exp. Mar. Biol. Ecol.*, **457**: 151-159.

Martinez-Garcia M., Brazel D., Poulton N.J., Swan B.K., Gomez M.L., Masland D., Sieracki M.E., Stepanauskas R., 2012. Unveiling in situ interactions between marine protists and bacteria through single cell sequencing. *ISME J.*, **6**: 703-707.

Martínez R.A., Isari S., Calbet A., 2014. Use of live, fluorescently-labeled algae for measuring microzooplankton grazing in natural communities. *J. Exp. Mar. Biol. Ecol.*, **457**: 59-70.

Mitra A., Flynn K.J., Burkholder J.M., Berge T., Calbet A., Raven J.A., Granéli E., Glibert P.M., Hansen P.J., Stoecker D.K., Thingstad F., Tillmann U., Våge S., Wilken S., Zubkov M.V., 2014. The role of mixotrophic protists in the biological carbon pump. *Biogeosciences*, **11**: 995-1005.

Mitra A., Flynn K.J., Tillmann U., Raven J.A., Caron D., Stoecker D.K., Not F., Hansen P.J., Hallegraeff G., Sanders R.W., Wilken S., McManus G., Johnson M., Pitta P., Våge S., Berge T., Calbet A., Thingstad F., Jeong H.J., Burkholder J., Glibert P.M., Granéli E., Lundgren V., 2016. Defining planktonic protist functional groups on mechanisms for energy and nutrient acquisition: incorporation of diverse mixotrophic strategies. *Protist*, **167**: 106-120.

Moeller H.V., Johnson M.D., Falkowski P.G., 2011. Photoacclimation in the phototrophic marine ciliate *Mesodinium rubrum* (ciliophora). *J. Phycol.*, **47**: 324-332.

Naess T., 1991. Tolerance of marine calanoid resting eggs: effects of freezing, desiccation and rotenone exposure-a field and laboratory study. *Mar. Biol.*, **111**: 455-459.

Palmer G., Horgan D.J., Tisdale H., Singer T.P., Beinert H., 1968. Studies on the respiratory chain-linked reduced nicotinamide adenine dinucleotide dehydrogenase XIV. Location of the sites of inhibition of rotenone, barbiturates, and piericidin by means of electron paramagnetic resonance spectroscopy. *J. Biol. Chem.*, **243**: 844-847.

Plagányi É.E., 2007. Models for an ecosystem approach to fisheries. *FAO (Food and Agriculture Organization of the United Nations) Fisheries Technical Paper*, .

Rajini P.S., Krishnakumari M.K., Majumder S.K., 1989. Cytotoxicity of certain organic solvents and organophosphorus insecticides to the ciliated protozoan *Paramecium caudatum*. *Microbios*, **59**: 157-163.

Rose J.M., Caron D.A., Sieracki M.E., Poulton N., 2004. Counting heterotrophic nanoplanktonic protists in cultures and aquatic communities by flow cytometry. *Aquat. Microb. Ecol.*, **34**: 263-277.

Saiz E., Griffell K., Calbet A., Isari S., 2014. Feeding rates and prey: predator size ratios of the nauplii and adult females of the marine cyclopoid copepod *Oithona davisae*. *Limnol. Oceanogr.*, **59**: 2077-2088.

Schmoker C., Hernández-León S., Calbet A., 2013. Microzooplankton grazing in the oceans: impacts, data variability, knowledge gaps and future directions. *J. Plankton Res.*, **35**: 691-706.

Schmoker C., Russo F., Drillet G., Trottet A., Mahjoub M.-S., Hsiao S.-H., Larsen O., Tun K., Calbet A., 2016. Effects of eutrophication on the planktonic food web dynamics of marine coastal ecosystems: the case study of two tropical inlets. *Mar. Environ. Res.*, **119**: 176-188.

Smith M., Hansen P.J., 2007. Interaction between *Mesodinium rubrum* and its prey: importance of prey concentration, irradiance and pH. *Mar. Ecol. Prog. Ser.*, **338**: 61-70.

Srivastava P., Panda D., 2007. Rotenone inhibits mammalian cell proliferation by inhibiting microtubule assembly through tubulin binding. *FEBS J.*, **274**: 4788-4801.

Stoecker D., Pierson J., 2019. Predation on protozoa: its importance to zooplankton revisited. *J. Plankton Res.*, **41**: 367-373.

Stoecker D.K., Hansen P.J., Caron D.A., Mitra A., 2017. Mixotrophy in the marine plankton. *Annu. Rev. Mar. Sci.*, **9**: 311-335.

Stoecker D.K., Li A., Coats D.W., Gustafson D.E., Nannen M.K., 1997. Mixotrophy in the dinoflagellate *Prorocentrum minimum*. *Mar. Ecol. Prog. Ser.*, **152**: 1-12.

Van Ginkel S.W., Bidwell M., Igou T., Gijon-Felix R., Salvi E.J.N.R., De Oliveira S.H.R., Duarte L.H.K., Steiner D., Hu Z., Johnston R., 2016. The prevention of saltwater algal pond contamination using the electron transport chain disruptor, rotenone. *Algal Res.*, **18**: 209-212.

Van Ginkel S.W., Igou T., Hu Z., Narode A., Cheruvu S., Doi S., Johnston R., Snell T., Chen Y., 2015. Taking advantage of rotifer sensitivity to rotenone to prevent pond crashes for algal-biofuel production. *Algal Res.*, **10**: 100-103.

Wilken S., Yung C.C.M., Hamilton M., Hoadley K., Nzongo J., Eckmann C., Corrochano-Luque M., Poirier C., Worden A.Z., 2019. The need to account for cell biology in characterizing predatory mixotrophs in aquatic environments. *Phil. Trans. R. Soc. B*, **374**: 20190090.

Yool A., Popova E.E., Anderson T.R., 2013. MEDUSA-2.0: an intermediate complexity biogeochemical model of the marine carbon cycle for climate change and ocean acidification studies. *Geosci. Model Dev.*, **6**: 1767-1811.

Zar J.H., 2010. Biostatistical Analysis. 5th Edition. Pearson Prentice-Hall, Upper Saddle River, New Jersey, USA, 960 p.

Paper III

Integrating phago-mixotrophy in dilution grazing experiments

Guilherme D. Ferreira, Filomena Romano, Nikola Medić, Paraskevi Pitta, Per J. Hansen, Kevin J. Flynn, Aditee Mitra, Albert Calbet

Abstract

It remains unclear as to how mixoplankton (coupled phototrophy and phagotrophy in one cell) affects the estimation of grazing rates obtained from the widely used dilution grazing technique. To address this issue, we prepared laboratory-controlled dilution experiments with known mixtures of phyto-, protozoo-, and mixoplankton, operated under different light regimes and species combinations. Our results evidenced that chlorophyll is an inadequate proxy for phytoplankton when mixoplankton are present. Conversely, species-specific cellular counts could assist (although not fully solve) in the integration of mixoplanktonic activity in a dilution experiment. Moreover, cell counts can expose prey selectivity patterns and intraguild interactions among grazers. Our results also demonstrated that whole community approaches mimic reality better than single-species laboratory experiments. We also confirmed that light is required for protozoo- and mixoplankton to correctly express their feeding activity, and that overall diurnal grazing is higher than nocturnal. Thus, we recommend that a detailed examination of initial and final plankton communities should become routine in dilution experiments, and that incubations should preferably be started at the beginning of both day and night periods. Finally, we hypothesize that *in silico* approaches may help disentangle the contribution of mixoplankton to the community grazing of a given system.

Introduction

The dilution grazing technique (Landry & Hassett 1982) is the most widely used method to measure microplankton grazing in the field, with more than one hundred studies on the topic throughout the world (Schmoker *et al.* 2013). It provides the rates of "phytoplankton" growth and "microzooplankton" grazing with a relatively simple experimental design. The rationale behind the method comes from the decrease in the encounter rates between predators and their prey as the whole community is diluted. Additionally, it assumes that phytoplankton growth is affected neither by the dilution factor nor by the presence of other phytoplankton species/individuals (Schmoker *et al.* 2013).

The technique is, however, beset by various problems, which have been extensively discussed in several papers (see Calbet & Saiz 2013, Schmoker *et al.* 2013, Calbet & Saiz 2018, and references therein). A particular challenge, and one that is often neglected, is the consequences of the presence of mixoplankton in the incubations (Calbet *et al.* 2012, Schmoker *et al.* 2013). Mixoplankton are protists that combine photo-autotrophy, osmo-heterotrophy, and phago-heterotrophy (Flynn *et al.* 2019); organisms that combine the former two modes of nutrient acquisition are termed phytoplankton whereas combining the latter two results in protozooplankton (Flynn *et al.* 2019).

In the original description of the dilution technique (Landry & Hassett 1982), the growth of the "phytoplankton" prey was assessed by using chlorophyll *a* (Chl *a*) as a proxy for its biomass, and grazing was assumed to be exclusively due to predatory activity of "microzooplankton" (i.e., *de facto* protozooplankton). Classic methods for estimating primary or secondary productivity do not recognise the complexity of involving mixoplankton growth (Mitra *et al.* 2014), and the numerous approaches to quantify grazing fail to distinguish mixoplanktonic and protozooplanktonic activities (Flynn *et al.* 2019, Wilken *et al.* 2019). Thus, the presence of mixoplankton includes "phytoplankton-like" phototrophic and "microzooplankton-like" phagotrophic activities simultaneously, effectively rendering the dilution grazing technique blind to this form of mixotrophy (Paterson *et al.* 2008, Calbet *et al.* 2012).

The presence of mixoplankton during the dilution incubations would not represent a serious shortcoming if mixoplankton were seldom present in the studied water. However, mixoplankton are not only ubiquitous (Leles *et al.* 2017, Leles *et al.* 2019), but also phylogenetically diverse, and can be found across a wide size spectrum (Flynn *et al.* 2019). Therefore, mixoplankton are expected to be very important grazers in marine

systems, and even dominant in some (Mitra *et al.* 2014). Nonetheless, the studies that quantify their grazing impact *in situ* are not very common (e.g., for bacterivory – Unrein *et al.* 2014, Anderson *et al.* 2017; for herbivory – Li *et al.* 1996, Calbet *et al.* 2012, Martínez *et al.* 2014) due to methodological difficulties (Wilken *et al.* 2019).

Another criticism of the dilution grazing technique is the incongruence between grazing rates derived from the technique and those obtained in the laboratory with single-species predator-prey experiments (Dolan & McKeon 2005). In the laboratory, the experimental determination of feeding rates typically involves the direct measurement of prey and predator abundances over a given period (Frost 1972). In the field, however, the complexity of the system poses a significant challenge for the accurate estimation of response function parameters for microzooplankton (Sandhu *et al.* 2019) as these cannot be directly measured (Landry & Hassett 1982, Calbet & Saiz 2013). This discrepancy is not surprising because of the multitude of biological interactions that take place within a given water column, which can (and likely will) alter individual and community grazing rates. Some of these major biological factors include the production of allelopathic compounds (e.g., Berge *et al.* 2012, Rasmussen *et al.* 2017), intraguild predation and trophic cascades (e.g., Hansen *et al.* 1994, Calbet & Saiz 2013, Yoo *et al.* 2013), and prey selectivity (e.g., Hansen *et al.* 1994, Ryabov *et al.* 2015, Maselli *et al.* 2020). Given the omnipresent nature of these features in marine ecosystems, it becomes clear that they cannot be ignored when interpreting dilution grazing experiments. The presence of mixoplankton, for the above-mentioned reasons, further complicates the situation.

With these matters in mind, we conducted several dilution grazing experiments in the laboratory, with mixtures of phyto-, protozoo- and mixoplankton species. The experiments were conducted under regular diel light cycle conditions and also in complete darkness because light can act both as a resource for phototrophic growth and as a modulating factor for grazing (Arias *et al.* 2020a, Morison *et al.* 2020). Dark incubations could serve to provide information on the contribution of mixoplanktonic activity into dilution grazing experiments. Additionally, we prepared control treatments (that cannot be included in field experiments) containing only prey, and combinations of a single predator with the prey, to explore individual dynamics during the incubation. These additional experiments, as controlled scenarios, provide added information for interpreting the otherwise hidden dynamics of multi-organism dilution grazing experiments and could ultimately, be used for *in silico* simulations of dilution grazing experiments.

Methods

We constructed several artificial food webs involving protozooplanktonic and mixoplanktonic predators to gain insights into the dynamics of dilution grazing experiments. Being a laboratory experiment, we were able to control variables and unknowns that cannot be controlled in field experiments. In particular, we included prey controls and ascertained single grazer rates at the experimental conditions. These additions enabled us to determine the species-specific contributions to the concentration of chlorophyll and grazing in the mixed dilution grazing experiment. We conducted our experiments with and without light and sampled the bottles at several time points to have a better representation of the grazer and prey dynamics during the incubation.

Cultures

We conducted the experiments with the protozooplanktonic dinoflagellate *Gyrodinium dominans* (strain ICM-ZOO-GD001) and ciliate *Strombidium arenicola* (strain ICM-ZOO-SA001), the CM dinoflagellate *Karlodinium armiger* (strain ICM-ZOO-KA001), and the ciliated pSNCM *Mesodinium rubrum* (strain DK-2009). As prey for all experiments, we used the cryptophyte *Rhodomonas salina* (strain K-0294) and the diatom *Conticribra weissflogii* (strain CCAP 1085/18). We found red chloroplasts inside several *M. rubrum* cells after incubating these predators with the diatom (**Figure SIII-1a**; under blue light excitation, cryptophyte chloroplasts glow orange due to the presence of phycoerythrin- e.g., Li *et al.* (1996), i.e., red chloroplasts likely belonged to the diatom). In these trials, we also confirmed that *G. dominans* was able to engulf *C. weissflogii* (**Figure SIII-1b**) and found no direct evidence of ingestion, neither in *K. armiger* nor in *S. arenicola*.

The predators were fed and maintained as described by Ferreira & Calbet (2020) during the up-scale and pre-experimental maintenance. *M. rubrum* was maintained on *Teleaulax amphioxeia* (strain K-1837) however, 1 day before the experiments, we allowed all predators to deplete their prey to extinction to reset their feeding history. Both *R. salina* and *T. amphioxeia* were kept in f/2 medium (Guillard 1975) and irradiated at ca. 150 µmol photons m^{-2} s^{-1} provided by cool white fluorescent lights. *C. weissflogii* was kept under the same conditions with the addition of silicate to the medium. All predators were kept in autoclaved 0.1 µm-filtered seawater. Protozooplankton were maintained at ca. 35 µmol photons m^{-2} s^{-1} whereas mixoplankton were kept at ca. 65 µmol photons m^{-2} s^{-1}. The

stock cultures were up-scaled and maintained using a discontinuous culture (pseudo-chemostat) approach, i.e., the cultures were diluted every 1-2 days with the respective medium (between 20 and 50 % of the total volume), to maintain them under exponential growth (and within target concentrations) at any moment. Additionally, to avoid an increase in the pH beyond the limits for exponential growth, all cultures were bubbled with 0.2 µm-filtered air (Berge *et al.* 2010). We used a very slow cadence of bubbles (flow rate not measured) to diminish the chances of stressing the predators (Berge *et al.* 2010). The direct effect of the bubbling process on the growth of the protists was not determined however if any, it was likely minor as we confirmed that all cultures were healthy and actively feeding before starting the experiments. All cultures were kept in a temperature-controlled room at 19°C with a 10:14 L/D cycle at a salinity of 38.

Dilution grazing experiments

The dilution grazing experiments were conducted with a paired mixture of predators at a time; i.e., *G. dominans* simultaneously with *K. armiger*, and *S. arenicola* concurrently with *M. rubrum* (for a summary of the experimental design, see **Table SIII-1** in the Supplementary Information). Both experiments were conducted with a mixture of *R. salina* and *C. weissflogii* as prey, in an equivalent C concentration. The initial concentration of prey was ca. 2.5 x 10^4 (both species combined) as we were aiming at saturating food conditions for mixoplanktonic predators (see **Figure SIII-2**), as a way to increase their overall grazing impact in the system. Carbon values for all species were obtained from the average volume and C:µm^3 ratio provided by Traboni *et al.* (2020). As previously mentioned, all predators were allowed to deplete their co-occurring prey before starting the experiment, to reset their feeding history. Like this, we ensured a non-acclimated scenario which is typical in standard field dilution experiments, as organisms are never adapted to the dilution itself.

Two dilution series of 60, 30, and 15 % were prepared from the 100 % treatment, in duplicated 1100 mL transparent polycarbonate bottles (Thermo Scientific Nalgene). All bottles contained 200 mL of f/2 medium + Si per litre of suspension to reach a final concentration equivalent to f/10 medium + Si (Guillard 1975). The actual level of dilution was determined from the initial concentration of prey in each dilution relative to the initial concentration of prey in the 100 %. One of the dilution series was incubated with a 10:14 L/D cycle at 100 µmol photons m^{-2} s^{-1} (hereafter termed L/D treatment). The second series was wrapped in aluminium foil and covered with an opaque box (i.e. incubated in

complete darkness) during the whole period (hereafter termed D treatment). It took us ca. 1 h between the preparation of the experimental suspension of organisms and the collection of the initial sample. As such, we avoided the typical hunger response and consequent vacuole replenishment of starved predators (Calbet *et al.* 2013), and diminished the consequences of photoacclimation in the chlorophyll content of the phototrophs, as this is an almost immediate process (Jokel *et al.* 2018, Zhou *et al.* 2021). The times of sampling were the only sources of culture vessel mixing during the incubation.

Additionally, a second, third, and fourth set of duplicated 100 % bottles were prepared under the same prey, nutrient and light conditions mentioned before for the dilution grazing experiments. The second set contained the two prey and no predators (termed 100prey). These bottles were used as a control and accounted for the net growth rate (both in cell numbers and Chl *a*) of each prey in the absence of grazing. The third and the fourth set of 100 % bottles comprised the two prey and only one of the predators (in the dinoflagellate experiment, 100gyro and 100karlo, or 100strom and 100meso in the ciliate experiment). These bottles eased the interpretation of the more complex mixed experiment by providing the outcome of the presence of a single predator.

All treatments were prepared with a final volume of 1 L per bottle. In the dilution series, the bottles from every dilution level were sampled after 0, 2, 4, 8, and 24 h for both Chl *a* (150 mL) and cell counts (70 mL, 2 % acidic Lugol's solution final concentration). The control bottles were sampled after 0, 8, and 24 h (150 mL for Chl *a* and 50 mL for cell counts). Samples collected after 2 and 4 h were only used to calculate Chl *a* per cell concentrations and are, therefore, not going to be further discussed. For the detailed cell counts and Chl *a* concentrations for each time point, see **Figures SIII-3** to **SIII-12** in the Supplementary Information. The 8 h sample of both L/D and D bottles were collected immediately before the beginning of the night period (i.e., Day period = 0 to 8 h samples; Night period = 8 to 24 h samples). For the D treatment, this did not imply any change in the light conditions despite effectively representing a day sample.

The samples preserved with acidic Lugol's solution were stored in the dark at 4 °C for 1-6 months before being counted. After stabilising the samples to room temperature (21±3 °C), the bottles were rotated softly and used to fill 10 mL methacrylate sedimentation chambers. The Utermöhl (1958) method was employed to analyse the samples after 24 h on an inverted microscope (XSB-1A) using a 25× objective. A

minimum of 200 individuals of each species were counted per replicate count, being each sample counted twice.

Chlorophyll, growth, and grazing analysis

The total chlorophyll *a* (Chl *a*, µg L^{-1}) was determined by filtering 150 mL of water from every bottle as specified before. The samples were collected into dark bottles and filtered through Whatman GF/C glass fibre filters under dim light conditions immediately after collection. The filters were folded in half twice, wrapped in aluminium foil and then kept at -20 °C for ca. 5 months until the extraction of pigments with 6 mL of acetone 90 %. The extraction was conducted in the dark at 4 °C and lasted ca. 24 h, thus avoiding the need to grind the filters (Holm-Hansen & Riemann 1978). The samples were measured before and after the addition of 100 µL of HCl 10 % (final concentration in the extract ca. 0.05 M) on a Turner Designs Fluorometer (Yentch & Menzel 1963) to account for the concentration of phaeophytin. The fluorometer was calibrated against a pure Chl *a* standard (2.13 mg Chl *a* L^{-1}) of cyanobacterial origin (DHI, Hørsholm, Denmark). Phaeopigments (µg L^{-1}) were determined by dividing the chlorophyll concentration by the acid factor ratio between fluorescence values before and after acidification.

We determined individual species contribution to the total Chl *a* mathematically for each time point in the control bottles. First, 100prey bottles were used to determine Chl *a* content of *R. salina* and *C. weissflogii*. These concentrations of pigment were then integrated into the controls with one predator and in the dilution series bottles to determine the pigment concentrations within each predator cell. We estimated the intermediate time points (those not directly assessed from control bottles) using linear progression.

Growth, clearance, and grazing rates were calculated for every time point using Frost (1972) equations as modified by Heinbokel (1978). If one uses these equations considering the 100prey bottles as controls and the 100gyro, 100karlo, 100strom or 100meso bottles as experimental, ingestion rates for each individual predator can be obtained. Thus, one would expect that, when mixed together, the total ingestion rate would be the average of the one calculated for each individual predator. This average yields an estimated value. Alternatively, if the control bottles are the same but one considers the 100 % bottles as the experimental (i.e., with both predators together), a real calculation of the average ingestion rate per predator (not specified) can be determined. Therefore, we considered this value to be the observed ingestion rate in our experiments. Finally, a third estimate of grazing can be obtained by measuring the slope of the linear

regression that correlates the fraction of undiluted water and the apparent growth rates based on the changes in the concentration of prey during the incubation (Landry & Hassett 1982). This slope yields the grazing coefficient (g), which can be converted into clearance rates by dividing it by the average predator concentration throughout the incubation. Ingestion rates are obtained by multiplying the average prey concentration by the clearance rate of the predators. This was defined as the dilution-measured ingestion rate.

The results of some incubations denoted the presence of saturated feeding responses. Accordingly, under these circumstances, prey growth rates (μ, Chl *a* Chl a^{-1} h^{-1}) were determined from the interception of linear regression with the 3 most diluted treatments. The grazing coefficients (g) were then calculated using **Equation III.1**

K (Chl *a* Chl a^{-1} h^{-1}) being the apparent growth rates obtained in the undiluted bottles (Gallegos 1989, Dolan *et al.* 2000). We followed the same procedure to determine cell-specific grazing rates with the difference that cell counts were used instead of Chl *a*. For the sake of clarity, we decided to show only the regressions whose slope was significantly ($p < 0.05$) different from zero. Nevertheless, we calculated μ and g for all experiments as recommended by Latasa (2014) and Landry (2014).

Results

Dilution grazing experiments

The majority of the dilution grazing incubations yielded non-significant grazing rates (P > 0.05) when based on Chl *a* (**Figure III-1**). The only exceptions were the experiment with dinoflagellates (**Figure III-1a,c**), but the slopes of the linear regressions were positive on both instances. In the occasions where mixoplankton represent a relevant shear of the pigmented community, it is thus challenging to determine the actual grazing mortality using the traditional dilution approach of tracking only Chl *a*. Species-specific Chl *a* content can be found in **Table III-1** for each sampling point.

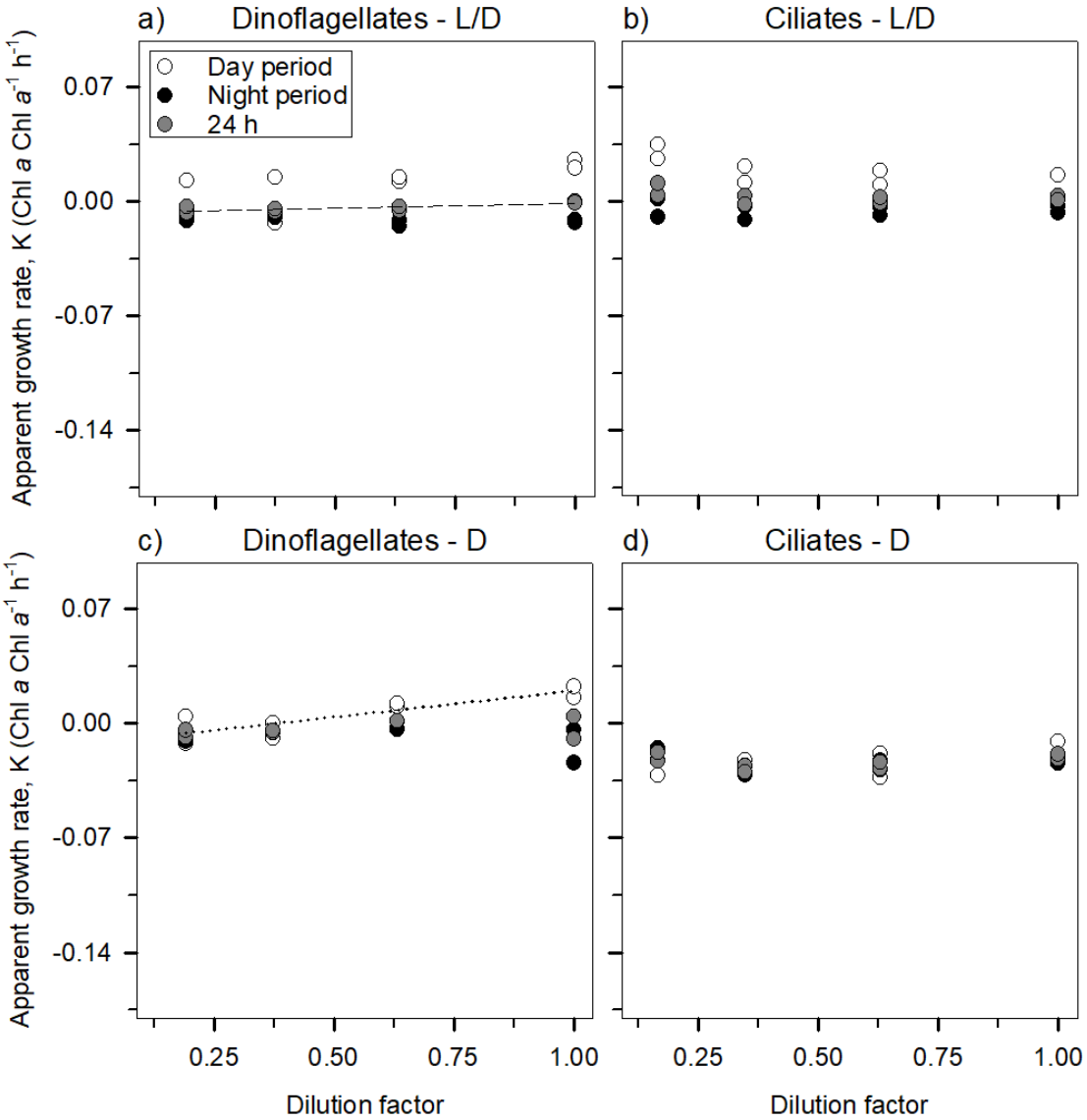

Figure III-1 Chl *a*-based dilution grazing experiment results. The left panels (a and c) show experiments with dinoflagellates and the right panels (b and d) correspond to experiments with ciliates. The top section is relative to the L/D treatment whereas the bottom one relates to the Dark (D) treatment. Plotted linear regressions imply a significant slope (P < 0.05). Dotted regression lines correspond to the day period and dashed lines to the integrated 24 h incubations.

Table III-1 Chl *a* content (pg Chl *a* Cell^{-1} ± se) of the target species at each sampling point as calculated from the control bottles. Columns highlighted in grey correspond to the Dark (D) treatment whereas the others relate to the L/D treatment. The initial samples were the same for both treatments. The + indicates that the calculations yielded a negative value and, as an impossible solution, the value was forced to 0.

Species	Sampling points				
	t = 0 h	t = 8 h	t = 8 h	t = 24 h	t = 24 h
Rhodomonas salina	0.63	1.66 ± 0.11	1.38 ± 0.17	1.22 ± 0.23	1.58 ± 0.11
Conticribra weissflogii	5.59	4.65 ± 0.66	3.40 ± 0.35	3.07 ± 0.51	3.30 ± 1.37
Karlodinium armiger	6.71	10.94 ± 0.05	6.70 ± 0.27	17.38 ± 0.80	8.16 ± 0.13
Mesodinium rubrum	19.98	21.97 ± 1.14	12.50 ± 2.82	19.97 ± 2.09	15.22 ± 0.74
Gyrodinium dominans	19.88	15.23 ± 3.90	6.69 ± 0.52	2.74 ± 0.78	1.84 ± 4.58
Strombidium arenicola	10.22	0.62 ± 6.44	13.06 ± 0.24	0.00^{+}	4.52 ± 1.13

Cell-based dilution regressions for dinoflagellates showed very distinct patterns for the two prey (**Figure III-2**). *R. salina* (**Figure III-2a,b**) was always ingested irrespective of the period of the day and light conditions (although it had a higher grazing mortality during the day in the presence of light), but the diatom *C. weissflogii* was not (**Figure III-2c,d**). In fact, the diatom seemed to benefit from the presence of predators, as suggested by the significantly positive slopes both in the L/D and D treatments (see the Methods Section for the experimental conditions of each treatment). When the predator community was composed of ciliates instead of dinoflagellates (**Figure III-3**), *R. salina* was subject to significant grazing mortalities (i.e., negative slope) during the day in both L/D and D treatments, and in the integrated 24 h in the D treatment (**Figure III-3a,b**).

All four species of predators showed a lack of response of growth rates to the dilution of the community (**Figure III-2e,g,h** and **III-3e-h**), except for *K. armiger* in the D bottles (**Figure III-2f**). It seems then that *K. armiger* was actively ingested by *G. dominans* in the D treatments as ascertained by the significant grazing mortality ($P < 0.05$). A summary of the species-specific growth and grazing rates can be found in **Table III-2**.

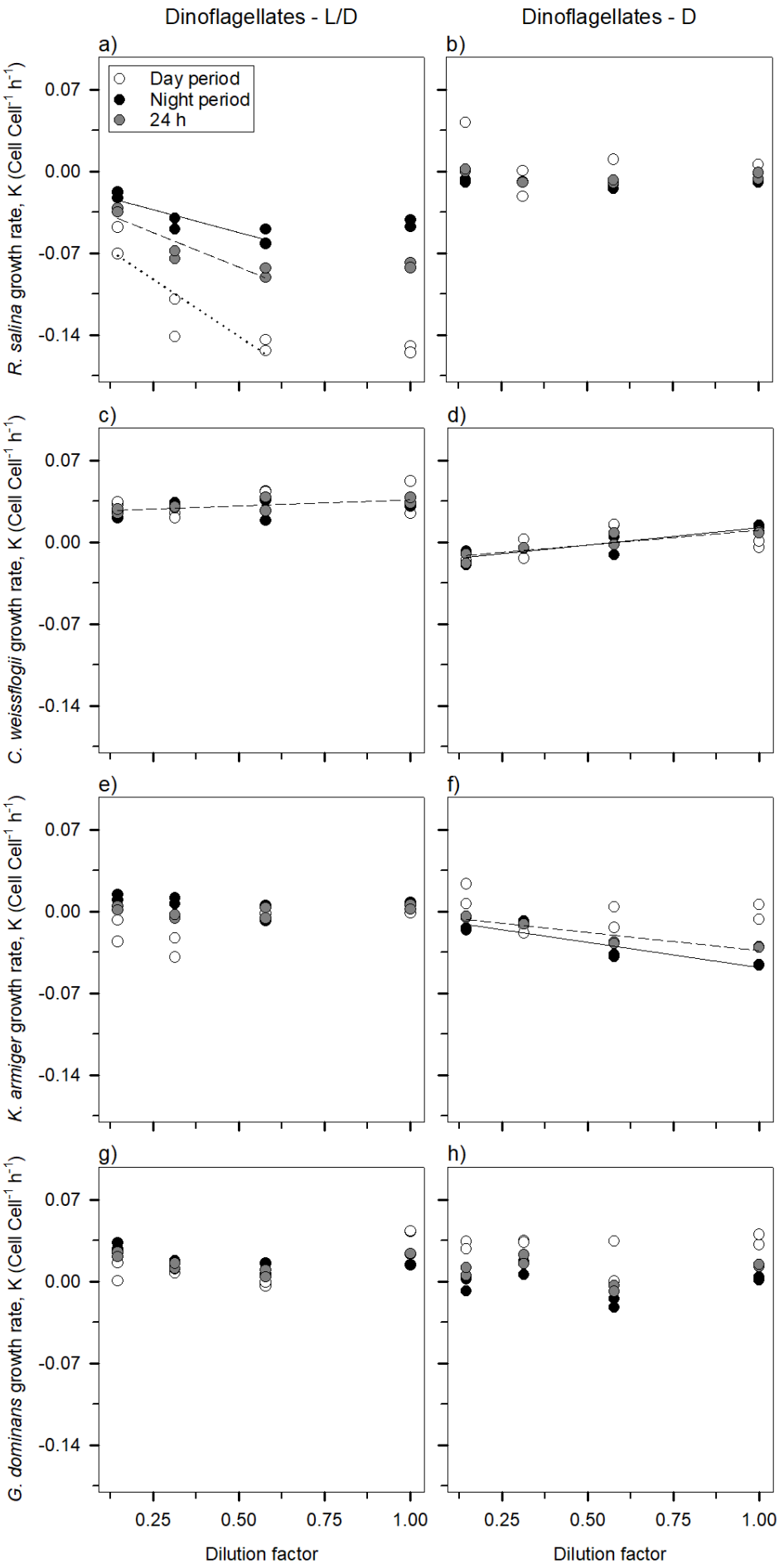

Figure III-2 Cell-based dilution grazing experiment with dinoflagellates. The left panels (a, c, e, and g) depict the L/D bottles and the right ones (b, d, f, and h) correspond to the Dark (D) bottles. Only linear regressions with a slope significantly ($P < 0.05$) different from zero are plotted. Dotted regression lines, dashed regressions lines, and solid regression lines correspond to the day period, integrated 24 h incubations, and night period, respectively.

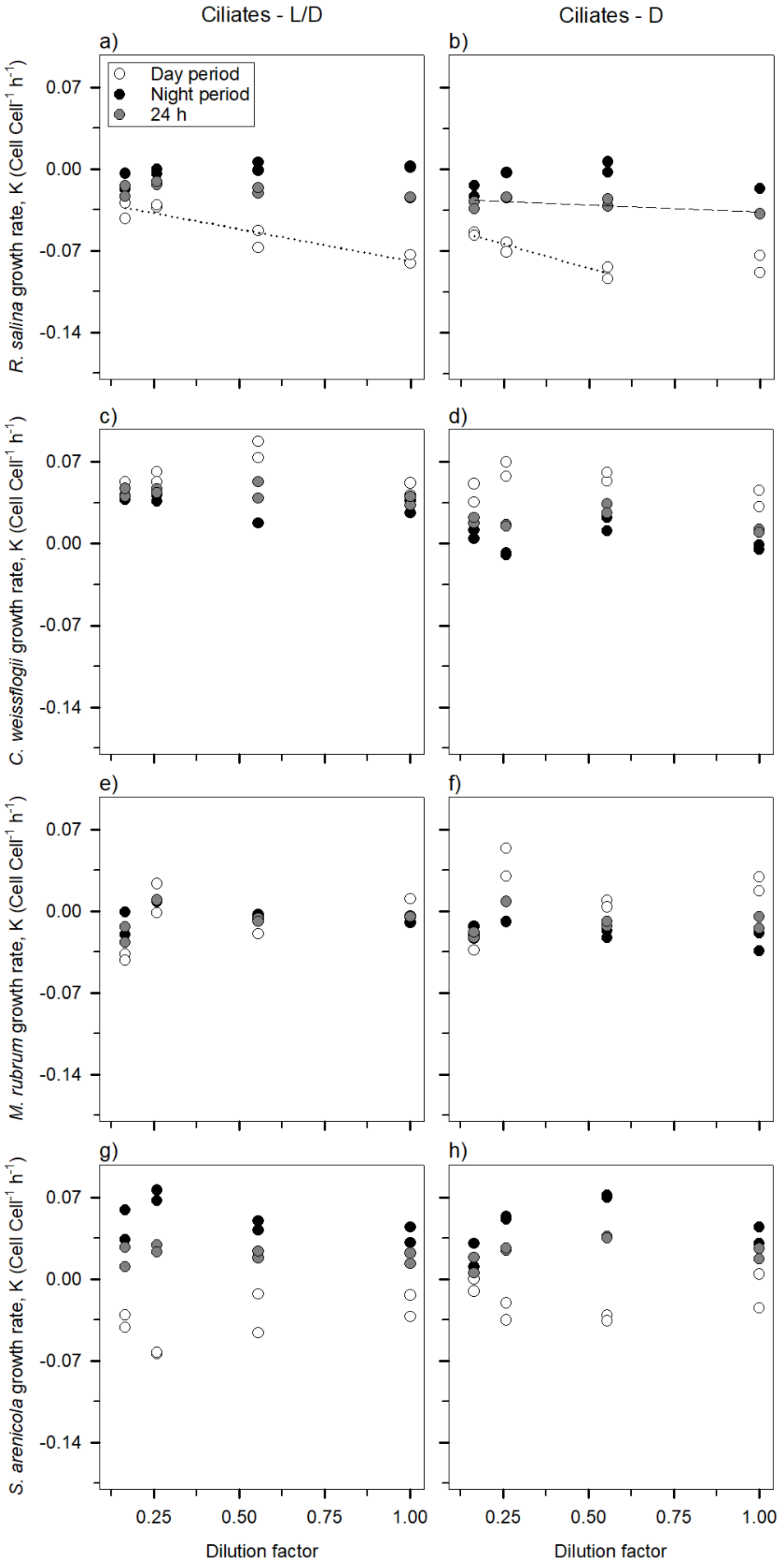

Figure III-3 Cell-based dilution grazing experiment with ciliates. Legend as in **Figure III-2**.

Exp	Rate, Species	Day	R^2	Day	R^2	Night	R^2	Night	R^2	24 h	R^2	24 h	R^2
Dinoflagellates	μ, Total Chl *a*	-0.0059	0.47	-0.0121	0.74**	-0.0081	0.31	-0.0032	0.13	-0.0071	0.60*	-0.0061	0.12
	g, Total Chl *a*	-0.0285		-0.0321		0.0049		0.0079		-0.0059		-0.0053	
	μ, *R. salina*	-0.0431	0.77*	0.0065	0.03	-0.0132	0.80*	-0.0102	0.06	-0.0229	0.85**	-0.0039	0.03
	g, *R. salina*	0.1091#		0.0102		0.0311#		-0.0025		0.0575#		0.0025	
	μ, *C. weissflogii*	0.0280	0.15	-0.0107	0.21	0.0249	0.19	-0.0172	0.76**	0.0259	0.50*	-0.0150	0.79**
	g, *C. weissflogii*	-0.0126		-0.0167		-0.0089		-0.0296		-0.0104		-0.0253	
	μ, *K. armiger*	-0.0278	0.48	0.0022	0.03	0.0110	0.23	-0.0049	0.81**	-0.0019	0.09	-0.0024	0.87**
	g, *K. armiger*	-0.0311		0.0073		0.0096		0.0431		-0.0039		0.0312	
	μ, *G. dominans*	-0.0043	0.49	0.0285	0.00	0.0249	0.33	-0.0004	0.01	0.0152	0.01	0.0093	0.00
	g, *G. dominans*	-0.0377		-0.0019		0.0147		0.0028		-0.0027		0.0012	
Ciliates	μ, Total Chl *a*	0.0277	0.36	-0.0281	0.13	-0.0056	0.00	-0.0233	0.00	0.0052	0.16	-0.0248	0.03
	g, Total Chl *a*	0.0171		-0.0087		0.0001		0.0010		0.0047		-0.0022	
	μ, *R. salina*	-0.0241	0.87**	-0.0432	0.92**	-0.0081	0.36	-0.0075	0.01	-0.0134	0.42	-0.0247	0.51*
	g, *R. salina*	0.0548		0.0382+		-0.0122		0.0033		0.0103		0.0120	
	μ, *C. weissflogii*	0.0585	0.00	0.0582	0.17	0.0417	0.24	0.0043	0.01	0.0474	0.27	0.0224	0.09
	g, *C. weissflogii*	0.0014		0.0152		0.0131		0.0025		0.0092		0.0068	
	μ, *M. rubrum*	-0.0225	0.17	-0.0028	0.11	0.0002	0.10	-0.0097	0.49	-0.0073	0.01	-0.0073	0.00
	g, *M. rubrum*	-0.0266		-0.0275		0.0089		0.0168		-0.0030		0.0020	
	μ, *S. arenicola*	-0.0540	0.33	-0.0204	0.00	0.0625	0.28	0.0404	0.03	0.0235	0.08	0.0200	0.07
	g, *S. arenicola*	-0.0322		-0.0024		0.0243		-0.0098		0.0053		-0.0075	

Table III-2 Summary of growth (μ, h^{-1}) and grazing (g, h^{-1}) rates calculated from the slopes of dilution grazing experiments at the different periods of the day. The significance of the slope of the linear regressions is also listed. Columns highlighted in grey correspond to the Dark (D) treatment whereas the remaining correspond to the L/D ones. Values marked with an # showed saturation and g was then calculated according to Gallegos (1989) and Dolan *et al.* (2000). R^2 values marked with a * or ** are significant, i.e., $P < 0.05$ and $P < 0.01$ respectively.

Incubation experiments

By having control bottles held under the same conditions as the dilution series, we were able to determine individual grazing rates for each predator species. Therefore, it was possible to i) calculate the individual ingestion rate of each predator on both prey (**Table III-3**), ii) average the previous information to estimate the combined ingestion rate per pair of predators, iii) calculate the actual ingestion rate for each pair of grazers by comparing data from the 100 % bottles and controls without grazers, and iv) calculate the ingestion rates based on the slopes of the dilution regressions.

Table III-3 Carbon-specific ingestion rates (pg C pg C^{-1} h^{-1} ± se) for each predator on both prey items during the day and the night. These values were ascertained using the control bottles with a single predator. NS implies that the measured ingestion rate was not significantly different from 0. Columns highlighted in grey correspond to the Dark (D) treatment whereas the remaining relate to the L/D treatment. Different letters within a given prey row imply statistically significant differences between treatments (One-Way ANOVA, Tukey HSD, P < 0.05).

Predator	Prey	Ingestion rates (pg C pg C^{-1} h^{-1})			
		Day	Day	Night	Night
Karlodinium armiger	*R. salina*	0.04±0.00^{a}	0.03±0.00^{a}	0.04±0.00^{a}	NS
	C. weissflogii	-0.02±0.01^{a}	NS	0.02±0.00^{a}	-0.01±0.00^{a}
Mesodinium rubrum	*R. salina*	0.03±0.02^{a}	NS	-0.02±0.00^{b}	0.01±0.01^{a,b}
	C. weissflogii	-0.10±0.01^{a}	-0.08±0.06^{a}	NS	-0.07±0.03^{a}
Gyrodinium dominans	*R. salina*	0.17±0.02^{a}	0.02±0.01^{b}	0.02±0.00^{b}	NS
	C. weissflogii	-0.02±0.01^{a}	0.00±0.00^{a}	NS	-0.01±0.00^{a}
Strombidium arenicola	*R. salina*	0.16±0.01^{a}	0.21±0.00^{b}	0.06±0.00^{c}	0.02±0.00^{d}
	C. weissflogii	-0.04±0.00^{a}	0.02±0.01^{a}	0.02±0.01^{a}	-0.04±0.03^{a}

Most comparisons resulted in non-significant (i.e., not different from 0, two-tailed Student's t-test, P > 0.05) ingestion rates on *C. weissflogii*, except for *S. arenicola* in some treatments, and *K. armiger* during the night-time in the L/D treatment (**Table III-3**). In the L/D treatment, *G. dominans* consumed more *R. salina* during the day than at night (Tukey HSD, P < 0.05), a pattern shared by all grazers except *K. armiger*, whose differences between day and night periods were negligible. *M. rubrum* was the species with the largest day/night differences, as it was the only species displaying a significantly negative ingestion rate on *R. salina* during the night.

The D treatments affected the grazers differently: *G. dominans* and *K. armiger* decreased their ingestion rates during the day (despite being significant only in the former) and displayed non-significant ingestion rates at night. Conversely, *S. arenicola* benefitted from the D treatment during the day (Tukey HSD, $P < 0.05$) despite having its ingestion rate decreased during the night (Tukey HSD, $P < 0.05$). Finally, ingestion rates by *M. rubrum* decreased to negligible levels during day-time in the D treatments (two-tailed Student's t-test, $P > 0.05$). The nightly ingestion rates of the D treatment were significantly positive whereas the same period in L/D yielded significantly negative ingestion rates (**Table III-3**), however, this difference was not significant due to the high variability of the data (Tukey HSD, $P > 0.05$). Protozooplankton displayed higher 24 h integrated ingestion rates on *R. salina* than did mixoplankton regardless of the light conditions. This difference was more evident in the presence of light but not negligible in its absence. In the L/D treatment, *G. dominans* exhibited carbon-specific ingestion rates ca. 1.5 times higher than *K. armiger*, and *S. arenicola* completely outcompeted *M. rubrum* with an ingestion rate ca. 21.4 times superior. In the D treatment, the differences were only ca. 1.3 and 6.7 times, respectively for dinoflagellates and ciliates.

A diagram that summarises the interactions found between our protist species can be found in **Figure III-4**. On this conceptual model, we can see the trophic interactions that took place in our experiments. Following our pre-experiment trials, we expected to find ingestion on the cryptophyte *R. salina* and on the diatom *C. weissflogii* by every protist grazer. Indeed, we were able to quantify ingestion rates on the cryptophyte by all predator species studied, and in all the light conditions tested. However, ingestion on the diatom was only detected for *S. arenicola*. Unexpectedly, the diatom even seemed to benefit from the combined presence of the grazers in the dinoflagellate experiment. Finally, we confirmed that the protozooplanktonic predators within each experiment were able to feed on their mixoplanktonic counterparts although *K. armiger* decreased the growth rates of its competitor, *G. dominans*, likely through allelopathy.

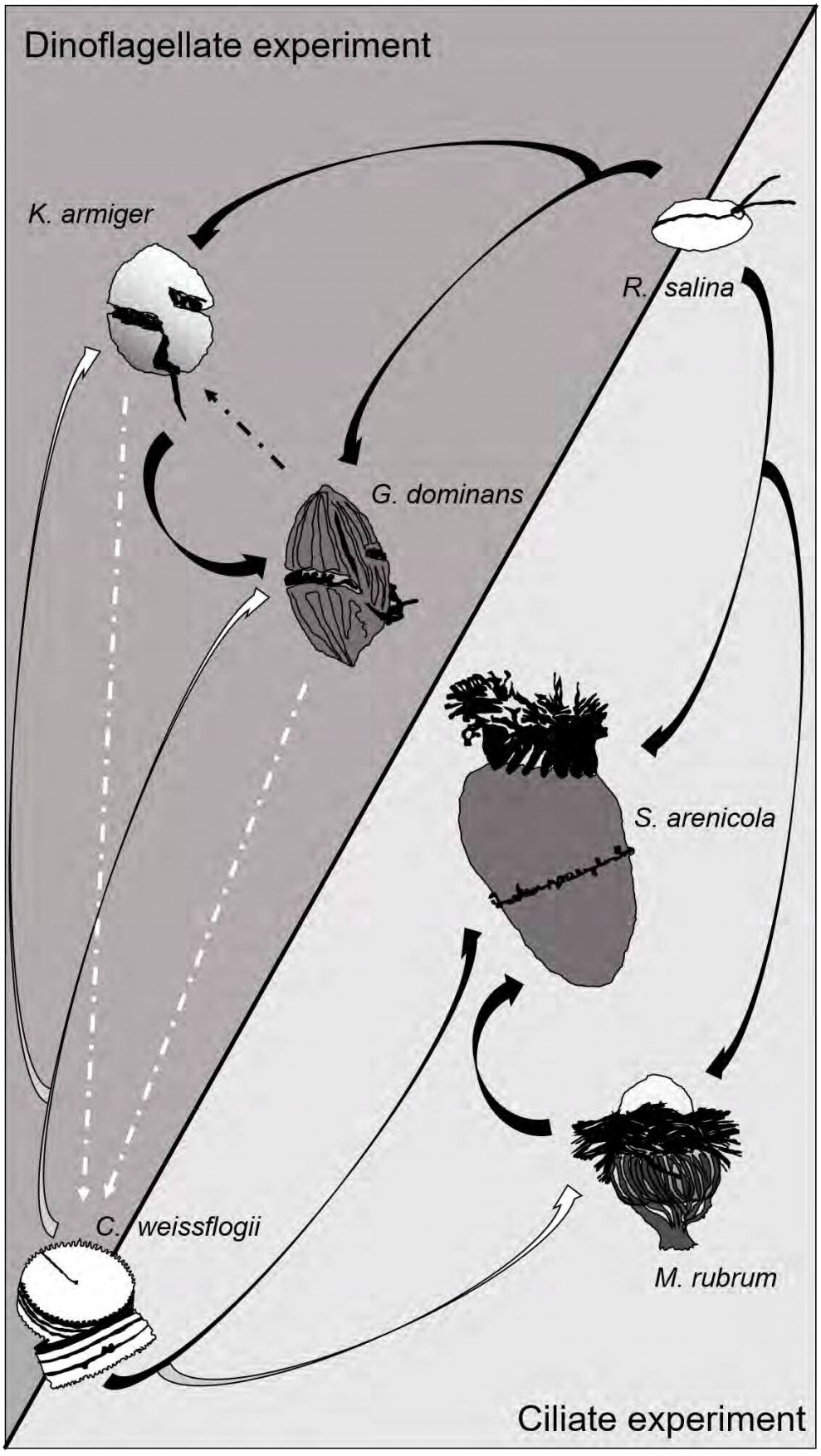

Figure III-4
Schematic representation of the interactions found between the protist species used in the present study. Phytoplankton species are depicted in white and protozooplankton in dark grey. Mixoplankton are shown in a gradient tone between the latter two. The tip of the arrow points to the organism benefitting from the interaction. Thick black arrows mean that the ingestion was observed in the dilution grazing experiment, whereas thick white arrows denote that the ingestion was expected (based on previous trials using single predator-prey interactions) but not confirmed. The black dashed arrow implies allelopathy. The white dashed arrows between the dinoflagellates and the diatom indicate that the latter benefits from the presence of these predators though the exact mechanism behind this interaction is unknown.

The integrated 24 h period grazing for each predator tandem calculated as explained before is summarised in **Figure III-5**. Since *C. weissflogii* was often not consumed in the experiments, we have shown only the data regarding *R. salina*. The estimated ingestion rates (obtained from the grazing impact of each grazer) were higher than those measured in the undiluted bottles against the respective controls. Additionally, ingestion rates calculated from the dilution slope (without controls) tend to be lower than those measured using the control bottles containing both grazers. However, the differences between methods used to ascertain ingestion rates were only significant in the L/D treatments.

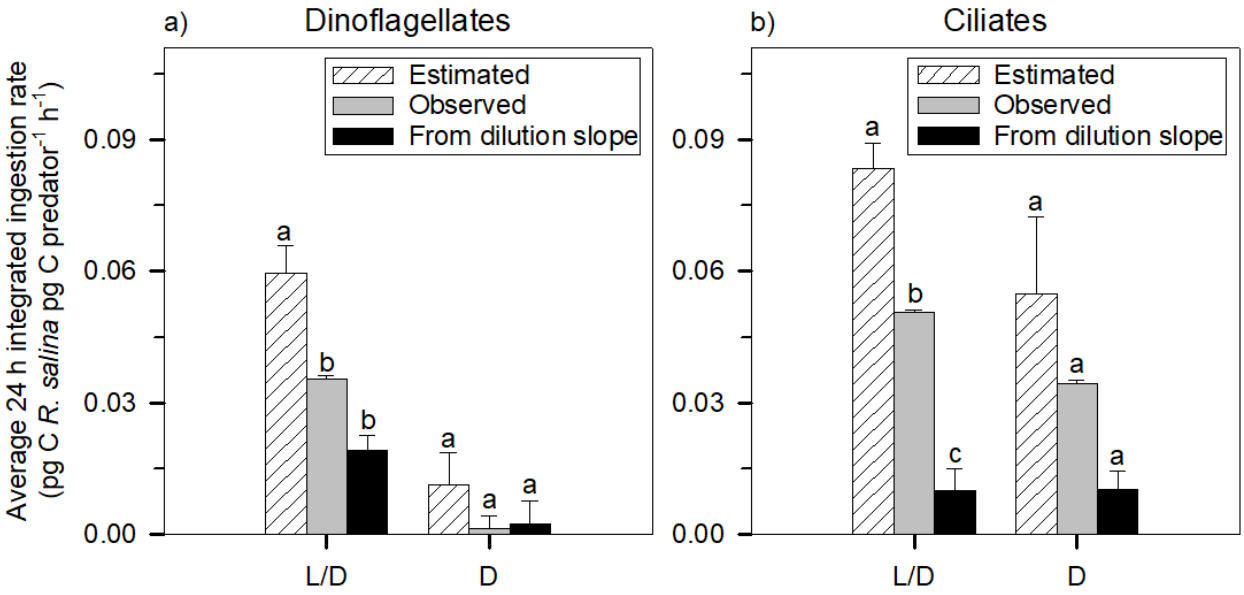

Figure III-5 Comparison between estimated (▨), observed (▩), and dilution-measured (■) ingestion rates (pg C *R. salina* pg C predator^{-1} h^{-1}) in the L/D and Dark (D) bottles over a 24 h period: a) experiment with dinoflagellates and b) experiment with ciliates. Notice that dilution-measured ingestion rates were calculated using g values listed in Table 2. See the Methods for a detailed explanation of the calculation of each value. Different letters within each group of bars (i.e., L/D evaluated independently from D bottles) imply statistically significant differences (One-Way ANOVA, Tukey HSD, $P < 0.05$). Error bars ± se.

To further understand the Chl *a* dynamics that shaped the outcome of the dilution experiments based on this proxy, we evaluated the contribution of each species to the total Chl *a* pool (**Figure III-6** and **III-7**) both in the undiluted and most diluted treatments. Regarding the dinoflagellate experiment (**Figure III-6**), both the diatom and *K. armiger* became more relevant to the total Chl *a* as time passed, in particular in the undiluted L/D treatment (**Figure III-6a**) where they increased their contribution to the total Chl *a* by ca. 9.3 and 31.7 % respectively.

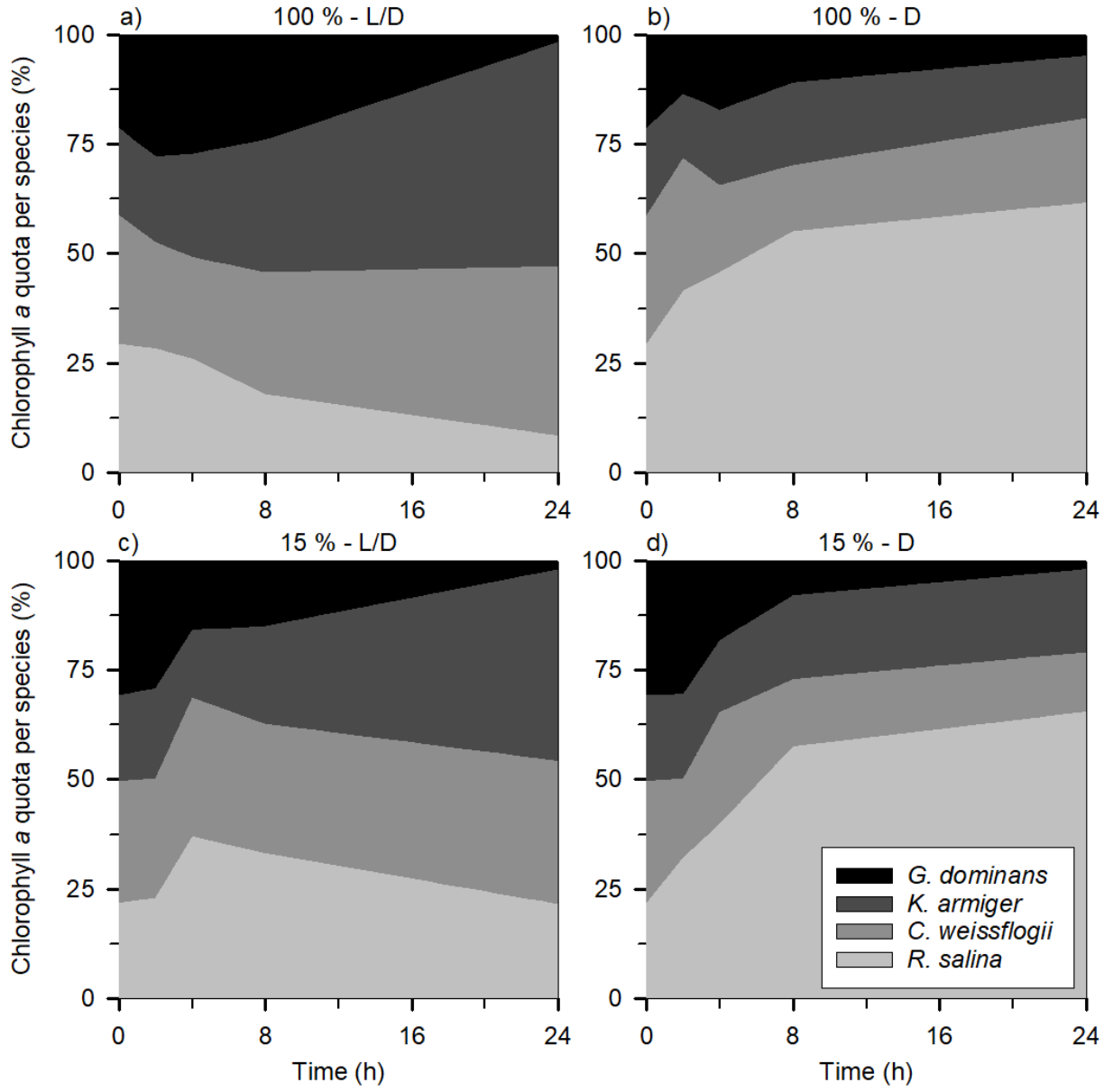

Figure III-6 The proportion of the total Chl *a* (%) represented by each species (in different colours) in the dinoflagellate experiment throughout the incubation: a and c) L/D treatment with the undiluted and most dilute communities respectively; b and d) Dark (D) treatment with the undiluted and most dilute communities respectively.

The D treatment has a completely different pattern, with *R. salina* benefiting the most, in particular when the predator concentration was low (**Figure III-6d**), becoming ca. 65.4 % of the total Chl *a* of the system at the end of the incubation (as compared to 21.8 % in the beginning). Irrespective of the light conditions, *G. dominans* displayed a particularly significant contribution to the total Chl *a* (up to 30.8 %) at the beginning of the incubation. The experiment with ciliates (**Figure III-7**) followed a similar trend for the diatom and the protozooplankton (**Figure III-7a**), albeit to a slightly larger extent in the

former (an increase of ca. 10.9 %) and smaller in the latter (maximum contribution of ca. 12.7 %).

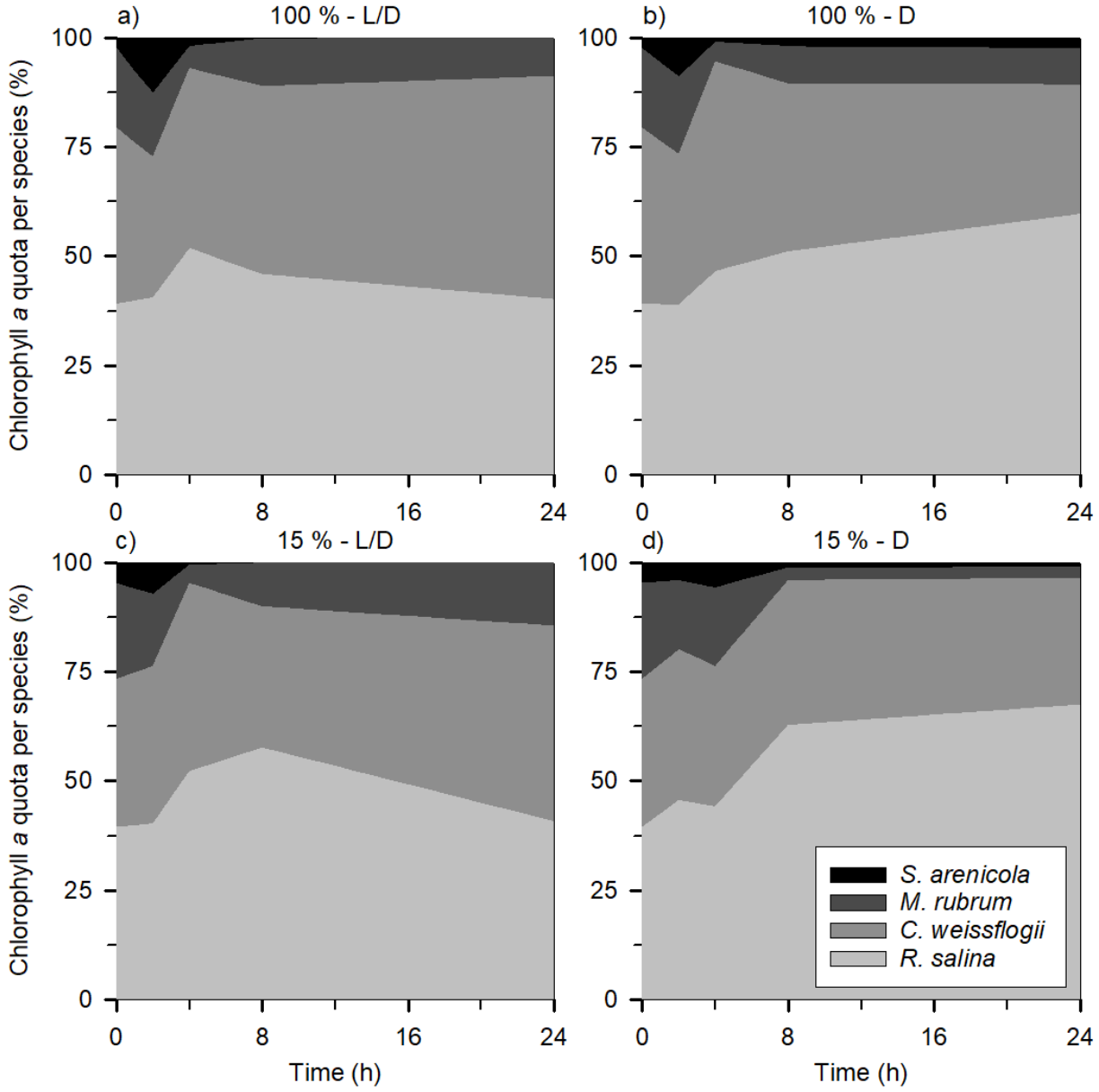

Figure III-7 The proportion of the total Chl *a* (%) represented by each species (in different colours) in the ciliate experiment throughout the incubation. Legend as in **Figure III-6**.

M. rubrum, in contrast with its dinoflagellate counterpart, decreased its contribution to the total Chl *a* by ca. 9.2 % (**Figure III-7a**). Concerning the D treatment, *R. salina* was also the species that fared better with an increase of ca. 28.0 % in the diluted treatment (**Figure III-7d**). In general, when the incubation contained only one predator species, the calculated individual Chl *a* content was, on average, ca. 8.5 % higher than when two predators were incubated together. Additionally, the magnitude of this effect differed between undiluted bottles, and the most diluted treatments (raw data not shown but incorporated in **Figures III-6** and **III-7**).

Discussion

Our results show that Chl *a* alone is not an adequate proxy for prey growth rates in dilution grazing experiments when mixoplankton are present (Paterson *et al.* 2008, Calbet *et al.* 2012). Chlorophyll is, in any case, a poor proxy for phototrophic plankton biomass (Kruskopf & Flynn 2006) because of inter-species variations, and also for the photoacclimation abilities of some species (for which very significant changes can occur within a few hours). The problem extends to the involvement of mixoplanktonic prey and grazers. Nevertheless, even very recent studies continue to rely on this parameter for quantifications of grazing despite acknowledging the dominance, both in biomass and abundance, of mixoplanktonic predators in their system (Morison *et al.* 2020). Moreover, the detailed analysis of the species-specific dynamics revealed that different prey species are consumed at very different rates. In our experiments, and contrarily to expectations (see Berge *et al.* 2008a, Nakamura *et al.* 1995, and **Figure SIII-1** in the Supplementary Information), *C. weissflogii* was only actively ingested in the ciliate experiment and, according to the results from the control bottles (**Table III-3**), not by *M. rubrum* (**Figure III-4**, and **Figure SIII-1a**).

Certainly, it is not the first time that a negative selection against diatoms has been seen; for example, Burkill *et al.* (1987) noticed that diatoms were less grazed than other phytoplankton species, as assessed by a dilution technique paired with High-Performance Liquid Chromatography for pigment analysis. Using the same method, Suzuki *et al.* (2002) reported that diatoms became the dominant phytoplankton group which suggests that other groups were preferentially fed upon. Calbet *et al.* (2011b), in the Arctic, also found only occasional grazing over the local diatoms. In our study, diatoms were not only not consumed, but the presence of dinoflagellates appeared to contribute to their growth (**Figure III-4**), this relationship being partly dependent on the concentration of the predator (see **Figure III-2c,d**). This result could be a direct consequence of assimilation and use of compounds (e.g. Admiraal *et al.* 1984, Armbrust *et al.* 2004, Olofsson *et al.* 2019) released by microplankton such as ammonium (e.g. Caperon *et al.* 1979, Gao *et al.* 2018) and urea (e.g. Solomon *et al*. 2010), which were not supplied in the growth medium, but which would have supported prey growth. Alternatively, this unexpected outcome may have been a consequence of the selective ingestion of *R. salina* by the two predators, relieving the competition for nutrients and light and resulting in a higher growth rate of the diatom in the presence of the predators. We

cannot rule out the fact that diatoms sink faster than flagellates which, as the bottles were immotile during most of the incubation period, may have also involuntarily decreased ingestion rates on *C. weissflogii*. Still, one *C. weissflogii* cell contains, on average, ca. 2.5 times more Chl *a* than one *R. salina* cell (initial value excluded, see **Table III-1**). Taken together with the preference for *R. salina* it is not surprising that the proportion of total Chl *a* represented by the diatoms increased over time, in particular in the L/D treatment (**Figures III-6a,c** and **III-7a,c**).

Another factor clearly highlighted by our experiments is that protozooplankton themselves contribute a significant portion of the total chlorophyll of the system (due to ingested Chl *a*), in particular at the beginning of the incubation (see **Figures III-6** and **III-7**); this being invariably ignored in a traditional dilution experiment. The high Chl *a* detected inside the protozooplanktonic grazers could suggest that the system was initially out of equilibrium and that this was the result of superfluous feeding (e.g., Calbet *et al.* 2013). Still, we required ca. 1 h to collect the initial sample (t = 0 h) after mixing all the organisms together (see the Methods Section). Previous studies like the one on *G. dominans* and *Oxyrrhis marina* by Calbet *et al.* (2013) showed that the hunger response and consequent vacuole replenishment occurred in ca. 1 h for very high prey concentrations and is expected to decrease at lower prey concentrations as the ones used in our study. Moreover, after 24 h, the first minutes of possible superfluous feeding would be irrelevant (e.g., Arias *et al.* 2017) and, therefore, we can assume that no hunger response was likely masking our experiments. In any case, as stated before, an actual field grazing dilution experiment also suffers from the same problem, because grazers and prey are suddenly diluted and not pre-adapted to distinct food concentrations. Nevertheless, this is not novel information, since Chl *a* and its degradation products have been found inside several protozooplankton species from different phylogenetic groups immediately after feeding (Kashiyama *et al.* 2012) and even after some days without food (Aristizábal 2009). An increase in intracellular Chl *a* concentrations immediately after feeding has also been found in mixoplankton (Johnson & Stoecker 2005, Berge & Hansen 2016), on which this increase is derived both from ingested prey as well as from new synthesis of their own Chl *a*. Additionally, several experiments with LFLA show that predators (irrespective of their trophic mode) seem to maximise the concentration of intracellular prey shortly after the initiation of the incubation (e.g. Rublee & Gallegos 1989, Setälä *et al.* 2005, **Paper I**). Indeed, some authors have even been able to measure

photosynthesis in protozooplankton, like the ciliates *Mesodinium pulex* (Tarangkoon & Hansen 2011) and *Strombidinopsis* sp. (Schoener & McManus 2017).

The fact that Chl *a* is a very poor indicator of phytoplankton biomass and the inherent consequences discussed so far can be solved by the quantification of the prey community abundance (e.g. Lawrence & Menden-Deuer 2012) by microscopy or by the use of signature pigments for each major phytoplankton group. The latter method, however, is not as thorough as the former, since rare are the cases where one pigment is exclusively associated with a single group of organisms (e.g. Jeffrey & Vesk 1997, Landry *et al.* 2000, Garcés *et al.* 2006). In any case, any pigment-based proxy is subject to the same problems, as identified by Kruskopf & Flynn (2006). Irrespective of the quantification method, it has been made evident that the different algae are consumed at different rates (e.g. pigments - Burkill *et al.* 1987, Suzuki *et al.* 2002, Paterson *et al.* 2008, Grattepanche *et al.* 2011; microscopy - Stelfox-Widdicombe *et al.* 2004, Calbet *et al.* 2011b, Arias *et al.* 2020b).

Prey selection in protistan grazers is a common feature (e.g. Flynn *et al.* 1996, Peltomaa & Johnson 2017, Johnson *et al.* 2018, Maselli *et al.* 2020). Given the diversity of grazers in natural communities and the array of preferred prey that each particular species possesses, it is logical to think that dilution experiments will capture the net community response properly. Likewise, grazers interact with each other through allelopathy, competition, and intraguild predation among other factors. An example of intraguild predation could be the observed on *K. armiger* by *G. dominans* (see **Figure III-2f** and **III-4**, and **Table III-2**), which caused an average loss of ca. 18.72 pg of *K. armiger* carbon per *G. dominans* per hour in the D treatment. Interestingly, in the same treatment, a slight negative effect of *K. armiger* on its predator *G. dominans* can also be deduced (i.e., positive g, **Table III-2**), resulting in an average loss of ca. 0.33 pg *G. dominans* carbon per *K. armiger* per hour. This could be a consequence of allelopathy since *K. armiger* is a known producer of karmitoxin (Rasmussen *et al.* 2017), whose presence can have negative effects even on metazoan grazers (Berge *et al.* 2012). Regarding ciliates, none of the species used is a known producer of allelopathic compounds, which suggests that the average loss of ca. 1.25 pg *M. rubrum* carbon per hour in the D treatment was due to *S. arenicola* predation. Altogether, it seems clear from our data that intraguild predation cannot be ignored when analysing dilution experiments (**Figure III-4**). Furthermore, our results clearly show that single functional responses

cannot be used to extrapolate community grazing impacts, as evidenced by the differences in estimated and measured ingestion rates based on the disappearance of prey in combined grazers experiments (**Figures III-5**). Nevertheless, this is a common procedure (e.g. Kim & Jeong 2004, Yih *et al.* 2004, Lee *et al.* 2014). Often in modelling approaches, individual predator's functional responses have been used to extrapolate prey selectivity and community grazing responses (Ryabov *et al.* 2015); in reality complex prey selectivity functions are required to satisfactorily describe prey selectivity and inter-prey allelopathic interactions (Mitra & Flynn 2006).

It is however also evident that the measured ingestion rates in combined grazers experiments were not the same as those calculated from the slope of the dilution grazing experiment. This raises the question of why was that the case. It is well known that phytoplankton cultures, when extremely diluted, show a lag phase of different duration (Fogg 1957, Aliyu *et al.* 2021) which has been attributed to the net leakage of metabolites (Flynn & Berry 1999). Assuming that the duration of the lag phase will be dependent on the level of dilution, it seems reasonable to deduce that after ca. 24 h the instantaneous growth rates (μ) in the most diluted treatments will be lower than that of the undiluted treatments. This has consequences, not only for the estimated prey growth rates but also for the whole assessment of the grazing rate, due to the flattening of the regression line (i.e., the decrease in the computed growth rate). This artefact may be more evident in cultures acclimated to very particular conditions (as the laboratory cultures used in this study) than in nature.

Another important finding of our research is the importance of light on the correct expression of the feeding activity by both mixoplankton and protozooplankton. We noticed that irrespective of the light conditions, all species exhibited a diurnal feeding rhythm (*R. salina* panels in **Figures III-2** and **III-3**), which is in accordance with earlier observations on protists (e.g. Strom 2001, Ng *et al.* 2017, Arias *et al.* 2020a, 2021). The presence of light typically increased the ingestion rates. Additionally, the ingestion rates differed during the night period between L/D and D treatments, which implies that receiving light during the day is also vital in modulating the night behaviour of protoozoo- and mixoplankton. In particular, mixoplankton grazing is usually affected by light conditions, typically increasing (e.g. Jakobsen *et al.* 2000, Li *et al.* 2000, Berge *et al.* 2008a, Kim *et al.* 2008), but also sometimes decreasing (Myung *et al.* 2006, McKie-Krisberg *et al.* 2015) in the presence of light. Different irradiance levels can also affect the magnitude of

ingestion rates both in protozoo- and mixoplankton (Moeller *et al.* 2019 and references therein).

For those reasons, we hoped for a rather consistent pattern among our protists that would help us discriminate mixoplankton in dilution grazing experiments. Based on the results from Arias *et al.* (2020a), we expected that in the dinoflagellate experiment, the D treatment would have inhibited only the grazing of *K. armiger*, enabling a simple discrimination between trophic modes. The reality did not meet the expectations since the day and night-time carbon-specific ingestion rates (as assessed using the control bottles, **Table III-3**) of *K. armiger* were respectively higher and equal than those of *G. dominans*. Conversely, in the ciliate experiment, protozooplankton were the major grazers in our incubations regardless of the day period and light conditions. This response was not as straightforward as one would expect it to be because *M. rubrum* has been recently suggested to be a species-complex containing at least 7 different species (Drumm *et al.* 2021 and references therein), which hinders any possible conjecture on their grazing impact. Indeed, the uneven responses found between and within trophic modes precluded such an optimistic hypothetical procedure.

The D treatment in the present paper illustrated the importance of mimicking natural light conditions, a factor also addressed in the original description of the technique by Landry & Hassett (1982). It is crucial for the whole interpretation of the dilution technique that incubations should be conducted in similar light (and temperature) conditions as the natural ones to allow for the continued growth of the phototrophic prey. However, here we want to stress another aspect of the incubations: should they start during the day or the night? Considering our (and previous) results on diel feeding rhythms, and on the contribution of each species to the total Chl a pool, it is clear that different results will be obtained if the incubations are started during the day or the night. Besides, whether day or night, organisms are also likely to be in a very different physiological state (either growing or decreasing). Therefore, we recommend that dilution experiments conducted in the field should always be started at the same period of the day to enable comparisons (see also Anderson *et al.* (2017) for similar conclusions on bacterivory exerted by small flagellates). Ideally, incubations would be started at different times of the day to capture the intricacies of the community dynamics on a diel cycle. Nevertheless, should the segmented analysis be impossible, we argue that the right time to begin the incubations would be during the night, as this is the time where ingestion

rates by protozooplankton are typically lower (e.g. Strom 2001, Ng *et al.* 2017, Arias *et al.* 2020a, 2021, this study) and would, consequently, reduce their quota of Chl *a* in the system.

Lastly, we want to stress that we are aware that our study does not represent natural biodiversity because our experiments were conducted in the laboratory with a few species. Nevertheless, we attempted to use common species of wide distribution for each major group of protists to provide a better institutionalisation of our conclusions. Indeed, our incubations contained cryptophytes and diatoms as prey, and both mixoplanktonic and pure protozooplanktonic predators, namely a dinoflagellate and a ciliate for each trophic mode (see **Figure III-4**). With these laboratory experiments, we have presented evidence calling for a revision of the use of chlorophyll in dilution grazing experiments (Paterson *et al.* 2008, Calbet *et al.* 2012), and we have highlighted the need to observe the organismal composition of both initial and final communities to better understand the dynamics during the dilution grazing experiments (Lawrence & Menden-Deuer 2012). This approach will not incorporate mixoplanktonic activity into the dilution technique *per se* however if combined with LFLA (see Calbet *et al.* 2012 and Martínez *et al.* 2014), a semi-quantitative approach to disentangle the contribution of mixoplankton to community grazing could be achieved (although not perfect, see the discussion on **Paper I**).

An alternative (and perhaps more elegant) solution could be the integration of the experimental technique with *in silico* modelling. The modelling approaches of the dilution technique have already been used, for example, to disentangle niche competition (Beckett & Weitz 2017) and to explore nonlinear grazer responses (Sandhu *et al.* 2019). We believe that our experimental design and knowledge of the previously indicated data could be of use for the configuration of a dilution grazing model, which could then be validated in the field (and, optimistically, coupled to the ubiquitous application of the dilution technique across the globe). We cannot guarantee that having a properly constructed model that mimics the dilution technique will be the solution to the mixoplankton paradigm. However, it may provide a step towards that goal as it could finally shed much-needed light on the mixo- and protozooplanktonic contributions to the grazing pressure of a given system. To quote from the commentary of Flynn *et al.* (2019), it could provide the answer to the question of whether mixoplankton are *de facto* “another of the Emperor’s New Suit of Clothes” or, “on the other hand (…) collectively worthy of more detailed inclusion in models”.

References

Admiraal W., Laane R.W.P.M., Peletier H., 1984. Participation of diatoms in the amino acid cycle of coastal waters; uptake and excretion in cultures. *Mar. Ecol. Prog. Ser.*, **15**: 303-306.

Anderson R., Jürgens K., Hansen P.J., 2017. Mixotrophic phytoflagellate bacterivory field measurements strongly biased by standard approaches: a case study. *Front. Microbiol.*, **8**: 1398.

Arias A., Saiz E., Calbet A., 2020a. Towards an understanding of diel feeding rhythms in marine protists: consequences of light manipulation. *Microb. Ecol.*, **79**: 64-72.

Arias A., Saiz E., Tiselius P., Calbet A., 2020b. Trophic interactions and diel feeding rhythms of microzooplankton in a productive Swedish Fjord. *ICES J. Mar. Sci.*, **77**: 2718-2728

Arias A., Selander E., Saiz E., Calbet A., 2021. Predator chemical cue effects on the diel feeding behaviour of marine protists. *Microb. Ecol.*, 10.1007/s00248-020-01665-9.

Aristizábal M., 2009. Potential respiration in *Oxyrrhis marina* and *Rhodomonas salina*, Universidad de Las Palmas de Gran Canaria, Las Palmas de Gran Canaria, Spain.

Beckett S.J., Weitz J.S., 2017. Disentangling niche competition from grazing mortality in phytoplankton dilution experiments. *PLoS One*, **12**: e0177517.

Berge T., Daugbjerg N., Andersen B.B., Hansen P.J., 2010. Effect of lowered pH on marine phytoplankton growth rates. *Mar. Ecol. Prog. Ser.*, **416**: 79-91.

Berge T., Hansen P.J., 2016. Role of the chloroplasts in the predatory dinoflagellate *Karlodinium armiger*. *Mar. Ecol. Prog. Ser.*, **549**: 41-54.

Berge T., Hansen P.J., Moestrup Ø., 2008. Feeding mechanism, prey specificity and growth in light and dark of the plastidic dinoflagellate *Karlodinium armiger*. *Aquat. Microb. Ecol.*, **50**: 279-288.

Berge T., Poulsen L.K., Moldrup M., Daugbjerg N., Hansen P.J., 2012. Marine microalgae attack and feed on metazoans. *ISME J.*, **6**: 1926-1936.

Burkill P.H., Mantoura R.F.C., Llewellyn C.A., Owens N.J.P., 1987. Microzooplankton grazing and selectivity of phytoplankton in coastal waters. *Mar. Biol.*, **93**: 581-590.

Calbet A., Martínez R.A., Isari S., Zervoudaki S., Nejstgaard J.C., Pitta P., Sazhin A.F., Sousoni D., Gomes A., Berger S.A., 2012. Effects of light availability on mixotrophy and microzooplankton grazing in an oligotrophic plankton food web: evidences from a mesocosm study in Eastern Mediterranean waters. *J. Exp. Mar. Biol. Ecol.*, **424**: 66-77.

Calbet A., Saiz E., 2013. Effects of trophic cascades in dilution grazing experiments: from artificial saturated feeding responses to positive slopes. *J. Plankton Res.*, **35**: 1183-1191.

Calbet A., Saiz E., 2018. How much is enough for nutrients in microzooplankton dilution grazing experiments? *J. Plankton Res.*, **40**: 109-117.

Calbet A., Saiz E., Almeda R., Movilla J.I., Alcaraz M., 2011. Low microzooplankton grazing rates in the Arctic Ocean during a *Phaeocystis pouchetii* bloom (Summer 2007): fact or artifact of the dilution technique? *J. Plankton Res.*, **33**: 687-701.

Caperon J., Schell D., Hirota J., Laws E., 1979. Ammonium excretion rates in Kaneohe Bay, Hawaii, measured by a 15N isotope dilution technique. *Mar. Biol.*, **54**: 33-40.

Dolan J.R., McKeon K., 2005. The reliability of grazing rate estimates from dilution experiments: Have we over-estimated rates of organic carbon consumption by microzooplankton? *Ocean Sci.*, **1**: 1-7.

Drumm K., Norlin A., Kim M., Altenburger A., Juel Hansen P., 2021. Physiological responses of *Mesodinium major* to irradiance, prey concentration and prey starvation. *J. Eukaryot. Microbiol.*, **n/a**: e12854.

Ferreira G.D., Calbet A., 2020. Caveats on the use of rotenone to estimate mixotrophic grazing in the oceans. *Sci. Rep.*, **10**: 3899.

Flynn K.J., Berry L.S., 1999. The loss of organic nitrogen during marine primary production may be significantly overestimated when using ^{15}N substrates. *Proc. R. Soc. B*, **266**: 641-647.

Flynn K.J., Mitra A., Anestis K., Anschütz A.A., Calbet A., Ferreira G.D., Gypens N., Hansen P.J., John U., Martin J.L., Mansour J.S., Maselli M., Medić N., Norlin A., Not F., Pitta P., Romano F., Saiz E., Schneider L.K., Stolte W., Traboni C., 2019. Mixotrophic protists and a new paradigm for marine ecology: where does plankton research go now? *J. Plankton Res.*, **41**: 375-391.

Fogg G.E., 1957. Relationships between metabolism and growth in plankton algae. *J. Gen. Microbiol.*, **16**: 294-297.

Frost B.W., 1972. Effects of size and concentration of food particles on the feeding behavior of the marine planktonic copepod *Calanus pacificus*. *Limnol. Oceanogr.*, **17**: 805-815.

Gallegos C.L., 1989. Microzooplankton grazing on phytoplankton in the Rhode River, Maryland: Nonlinear feeding kinetics. *Mar. Ecol. Prog. Ser.*, **57**: 23-33.

Gao H., Hua C., Tong M., 2018. Impact of *Dinophysis acuminata* feeding *Mesodinium rubrum* on nutrient dynamics and bacterial composition in a microcosm. *Toxins*, **10**: 443.

Guillard R.R.L., 1975. Culture of phytoplankton for feeding marine invertebrates. In: W.L. Smith, M.H. Chanley (Eds), Culture of marine invertebrate animals. Plenum Press, New York, NY, pp 29-60.

Hansen B., Bjørnsen P.K., Hansen P.J., 1994. The size ratio between planktonic predators and their prey. *Limnol. Oceanogr.*, **39**: 395-403.

Heinbokel J.F., 1978. Studies on the functional role of tintinnids in the Southern California Bight. I. Grazing and growth rates in laboratory cultures. *Mar. Biol.*, **47**: 177-189.

Holm-Hansen O., Riemann B., 1978. Chlorophyll a determination: improvements in methodology. *Oikos*, **30**: 438-447.

Johnson M.D., Stoecker D.K., 2005. Role of feeding in growth and photophysiology of *Myrionecta rubra*. *Aquat. Microb. Ecol.*, **39**: 303-312.

Kashiyama Y., Yokoyama A., Kinoshita Y., Shoji S., Miyashiya H., Shiratori T., Suga H., Ishikawa K., Ishikawa A., Inouye I., Ishida K.-i., Fujinuma D., Aoki K., Kobayashi M., Nomoto S., Mizoguchi T., Tamiaki H., 2012. Ubiquity and quantitative significance of detoxification catabolism of chlorophyll associated with protistan herbivory. *Proc. Natl. Acad. Sci.*, **109**: 17328.

Kim S., Kang Y.G., Kim H.S., Yih W., Coats D.W., Park M.G., 2008. Growth and grazing responses of the mixotrophic dinoflagellate *Dinophysis acuminata* as functions of light intensity and prey concentration. *Aquat. Microb. Ecol.*, **51**: 301-310.

Kruskopf M., Flynn K.J., 2006. Chlorophyll content and fluorescence responses cannot be used to gauge reliably phytoplankton biomass, nutrient status or growth rate. *New Phytol.*, **169**: 525-536.

Landry M.R., Constantinou J., Latasa M., Brown S.L., Bidigare R.R., Ondrusek M.E., 2000. Biological response to iron fertilization in the eastern equatorial Pacific (IronEx II). III. Dynamics of phytoplankton growth and microzooplankton grazing. *Mar. Ecol. Prog. Ser.*, **201**: 57-72.

Landry M.R., Hassett R.P.I., 1982. Estimating the grazing impact of marine micro-zooplankton. *Mar. Biol.*, **67**: 283-288.

Latasa M., 2014. Comment: A potential bias in the databases of phytoplankton growth and microzooplankton grazing rates because of the improper formulation of the null hypothesis in dilution experiments. *Limnol. Oceanogr.*, **59**: 1092-1094.

Lawrence C., Menden-Deuer S., 2012. Drivers of protistan grazing pressure: seasonal signals of plankton community composition and environmental conditions. *Mar. Ecol. Prog. Ser.*, **459**: 39-52.

Lee K.H., Jeong H.J., Jang T.Y., Lim A.S., Kang N.S., Kim J.-H., Kim K.Y., Park K.-T., Lee K., 2014. Feeding by the newly described mixotrophic dinoflagellate *Gymnodinium smaydae*: Feeding mechanism, prey species, and effect of prey concentration. *J. Exp. Mar. Biol. Ecol.*, **459**: 114-125.

Leles S.G., Mitra A., Flynn K.J., Stoecker D.K., Hansen P.J., Calbet A., McManus G.B., Sanders R.W., Caron D.A., Not F., 2017. Oceanic protists with different forms of acquired phototrophy display contrasting biogeographies and abundance. *Proc. R. Soc. B*, **284**: 20170664.

Leles S.G., Mitra A., Flynn K.J., Tillmann U., Stoecker D., Jeong H.J., Burkholder J., Hansen P.J., Caron D.A., Glibert P.M., 2019. Sampling bias misrepresents the biogeographical significance of constitutive mixotrophs across global oceans. *Glob. Ecol. Biogeogr.*, **28**: 418-428.

Li A., Stoecker D.K., Coats D.W., Adam E.J., 1996. Ingestion of fluorescently labeled and phycoerythrin-containing prey by mixotrophic dinoflagellates. *Aquat. Microb. Ecol.*, **10**: 139-147.

Martínez R.A., Isari S., Calbet A., 2014. Use of live, fluorescently-labeled algae for measuring microzooplankton grazing in natural communities. *J. Exp. Mar. Biol. Ecol.*, **457**: 59-70.

Maselli M., Altenburger A., Stoecker D.K., Hansen P.J., 2020. Ecophysiological traits of mixotrophic *Strombidium* spp. *J. Plankton Res.*, **42**: 485-496.

McKie-Krisberg Z.M., Gast R.J., Sanders R.W., 2015. Physiological responses of three species of Antarctic mixotrophic phytoflagellates to changes in light and dissolved nutrients. *Microb. Ecol.*, **70**: 21-29.

Mitra A., Flynn K.J., 2006. Accounting for variation in prey selectivity by zooplankton. *Ecol. Modell.*, **199**: 82-92.

Mitra A., Flynn K.J., Burkholder J.M., Berge T., Calbet A., Raven J.A., Granéli E., Glibert P.M., Hansen P.J., Stoecker D.K., Thingstad F., Tillmann U., Våge S., Wilken S., Zubkov M.V., 2014. The role of mixotrophic protists in the biological carbon pump. *Biogeosciences*, **11**: 995-1005.

Moeller H.V., Laufkötter C., Sweeney E.M., Johnson M.D., 2019. Light-dependent grazing can drive formation and deepening of deep chlorophyll maxima. *Nat. Commun.*, **10**: 1978.

Morison F., Franzè G., Harvey E., Menden-Deuer S., 2020. Light fluctuations are key in modulating plankton trophic dynamics and their impact on primary production. *Limnol. Oceanogr. Lett.*, **5**: 346-353.

Nakamura Y., Suzuki S.-Y., Hiromi J., 1995. Growth and grazing of a naked heterotrophic dinoflagellate, *Gyrodinium dominans*. *Aquat. Microb. Ecol.*, **9**: 157-164.

Olofsson M., Robertson E.K., Edler L., Arneborg L., Whitehouse M.J., Ploug H., 2019. Nitrate and ammonium fluxes to diatoms and dinoflagellates at a single cell level in mixed field communities in the sea. *Sci. Rep.*, **9**: 1424.

Paterson H.L., Knott B., Koslow A.J., Waite A.M., 2008. The grazing impact of microzooplankton off south west Western Australia: as measured by the dilution technique. *J. Plankton Res.*, **30**: 379-392.

Rasmussen S.A., Binzer S.B., Hoeck C., Meier S., de Medeiros L.S., Andersen N.G., Place A., Nielsen K.F., Hansen P.J., Larsen T.O., 2017. Karmitoxin: an amine-containing polyhydroxy-polyene toxin from the marine dinoflagellate *Karlodinium armiger*. *J. Nat. Prod.*, **80**: 1287-1293.

Rublee P.A., Gallegos C.L., 1989. Use of fluorescently labelled algae (FLA) to estimate microzooplankton grazing. *Mar. Ecol. Prog. Ser.*: 221-227.

Ryabov A.B., Morozov A., Blasius B., 2015. Imperfect prey selectivity of predators promotes biodiversity and irregularity in food webs. *Ecol. Lett.*, **18**: 1262-1269.

Sandhu S.K., Morozov A.Y., Mitra A., Flynn K., 2019. Exploring nonlinear functional responses of zooplankton grazers in dilution experiments via optimization techniques. *Limnol. Oceanogr.*, **64**: 774-784.

Schmoker C., Hernández-León S., Calbet A., 2013. Microzooplankton grazing in the oceans: impacts, data variability, knowledge gaps and future directions. *J. Plankton Res.*, **35**: 691-706.

Schoener D.M., McManus G.B., 2017. Growth, grazing, and inorganic C and N uptake in a mixotrophic and a heterotrophic ciliate. *J. Plankton Res.*, **39**: 379-391.

Solomon C.M., Collier J.L., Berg G.M., Glibert P.M., 2010. Role of urea in microbial metabolism in aquatic systems: a biochemical and molecular review. *Aquat. Microb. Ecol.*, **59**: 67-88.

Strom S.L., 2001. Light-aided digestion, grazing and growth in herbivorous protists. *Aquat. Microb. Ecol.*, **23**: 253-261.

Tarangkoon W., Hansen P.J., 2011. Prey selection, ingestion and growth responses of the common marine ciliate *Mesodinium pulex* in the light and in the dark. *Aquat. Microb. Ecol.*, **62**: 25-38.

Traboni C., Calbet A., Saiz E., 2020. Effects of prey trophic mode on the gross-growth efficiency of marine copepods: the case of mixoplankton. *Sci. Rep.*, **10**: 12259.

Unrein F., Gasol J.M., Not F., Forn I., Massana R., 2014. Mixotrophic haptophytes are key bacterial grazers in oligotrophic coastal waters. *ISME J.*, **8**: 164.

Utermöhl H., 1958. Zur vervollkommung der quantitativen phytoplankton methodik. *Mitt. Int.Verein. Theor. Angew. Limnol.*, **9**: 1-38.

Wilken S., Yung C.C.M., Hamilton M., Hoadley K., Nzongo J., Eckmann C., Corrochano-Luque M., Poirier C., Worden A.Z., 2019. The need to account for cell biology in characterizing predatory mixotrophs in aquatic environments. *Phil. Trans. R. Soc. B*, **374**: 20190090.

Yentsch C.S., Menzel D.W., 1963. A method for the determination of phytoplankton chlorophyll and phaeophytin by fluorescence. *Deep-Sea Res.*, **10**: 221-231.

Yoo Y.D., Yoon E.Y., Lee K.H., Kang N.S., Jeong H.J., 2013. Growth and ingestion rates of heterotrophic dinoflagellates and a ciliate on the mixotrophic dinoflagellate *Biecheleria cincta*. *Algae*, **28**: 343-354.

Page deliberately left in blank

Paper IV

The effect of short-term temperature exposure on key physiological processes of mixoplankton and protozooplankton grazers

Guilherme D. Ferreira, Afroditi Grigoropoulou, Enric Saiz, Albert Calbet

Abstract

Mixoplankton and protozooplankton are key components of marine food webs. As such, it is paramount to understand their physiological response to sudden environmental changes, like marine heatwaves, which are projected to become more intense and frequent. Here, we report the acute (24 h) growth and grazing responses to temperature changes (range 5-34°C) for four protistan grazers and their respective prey. Additionally, we determined respiration and photosynthetic rates over a 6°C variation for each grazer. The thermal performance curves showed that at higher temperatures ciliates performed better than dinoflagellates, and protozooplankton better than mixoplankton, whether grouped by taxonomy or trophic strategy, respectively. In addition, our results confirmed that irrespective of the species, warmer temperatures imply smaller cellular volumes. Our experiments also evidenced that grazing is the physiological rate that depends the most on temperature for protozooplankton. For mixoplankton however, grazing is impaired at warmer temperatures, whereas photosynthesis is increased. Therefore, our results contribute to the body of evidence calling for a reassessment of mixoplankton's placing within the Metabolic Theory of Ecology, as these organisms appear to become more phototrophic than phagotrophic in a warming scenario, unlike past conjectures. The short-term thermal performance of a given species is paramount for the correct parametrization of climate change models; however, future studies should also address the multigenerational response to temperature changes, besides determining the extent of different prey concentrations on the measured physiological rates.

Introduction

A mixoplanktonic species is defined by its potential to simultaneously express phototrophic and phagotrophic processes within a single cell (Flynn *et al.* 2019). Temperature is perhaps the most important abiotic factor that can affect the balance between phototrophy and phagotrophy on a given mixoplanktonic species, irrespective of its taxonomic group (e.g., Princiotta *et al.* 2016). In this regard, both autotrophic and heterotrophic processes (like photosynthesis and ingestion, respectively) are predicted to increase in response to temperature albeit at different rates (Regaudie-de-Gioux & Duarte 2012). In particular, the Metabolic Theory of Ecology (MTE, Gillooly *et al.* 2001, Brown *et al.* 2004) predicts that the Activation Energy (*Ea*) for the rate-limiting biochemical reactions of photosynthesis is significantly lower than the value for heterotrophic activities such respiration and grazing (Allen *et al.* 2005, López-Urrutia *et al.* 2006, Rose & Caron 2007, Regaudie-de-Gioux & Duarte 2012). Therefore, heterotrophic processes are expected to increase faster than autotrophic ones in response to increasing temperatures, which would shift the balance of photo/phagotrophy in mixoplankton towards the latter mode of nutrition. In fact, one of the major drivers motivating research on mixoplankton is the quantification of this balance on a given species among different groups of protists such as dinoflagellates (e.g., Adolf *et al.* 2006, Riisgaard & Hansen 2009, Berge & Hansen 2016) and ciliates (e.g., Stoecker *et al.* 1988, Stoecker & Michaels 1991, Yih *et al.* 2004). Such differences may strongly impact the flow of matter and energy within the food web and complicate their accurate integration into biogeochemical models (Mitra *et al.* 2014). Nevertheless, at the moment, the data on the effects of temperature on key physiological parameters of mixoplankton are rather scarce and contradictory (e.g., Wilken *et al.* 2013, Princiotta *et al.* 2016, Cabrerizo *et al.* 2019, González-Olalla *et al.* 2019).

One particular issue that brings temperature to the spotlight is the increasing evidence that climate change will have profound impacts on marine ecosystems, due to progressive temperature rise but also to short-term extreme climate events (such as marine heatwaves), which are projected to increase both in frequency and intensity (Oliver *et al.* 2019). To understand how short-term (ca. 24 h) changes in temperature affect mixoplankton and protozooplankton species, we measured growth, grazing, respiration, and photosynthetic rates. Through the comparison of the dependency of these processes on temperature, we hope to continue the (far from complete) process of

integrating mixoplankton within biogeochemical models, by placing them properly in the MTE.

Methods

Cultures

We conducted the experiments with the protozooplanktonic dinoflagellate *G. dominans* (strain ICM-ZOO-GD001) and ciliate *S. arenicola* (strain ICM-ZOO-SA001), the CM dinoflagellate *K. armiger* (strain ICM-ZOO-KA001), and the ciliated pSNCM *M. rubrum* (strain DK-2009). The two dinoflagellates and *S. arenicola* were provided the cryptophyte *R. salina* as prey *ad libitum* during the up-scale period. To avoid the depletion of *R. salina* in the predator cultures, we gave them fresh cryptophytes every second to third day depending on the predator species. *M. rubrum* was offered the cryptophyte *T. amphioxeia* (strain K-1837) as prey in a proportion of ca. 1:5 (Smith & Hansen 2007) during the up-scale process. Protozooplankton were maintained at ca. 35 µmol photons m^{-2} s^{-1} whereas mixoplankton were kept at ca. 65 µmol photons m^{-2} s^{-1}, both in 0.1 µm filtered seawater. Both cryptophyte prey were kept in f/2 medium (Guillard 1975) prepared using 0.1 µm filtered seawater, and irradiated at ca. 150 µmol photons m^{-2} s^{-1} provided by cool white fluorescent lights. The stock cultures were diluted every 1-2 days with the respective medium (between 20 and 50 % of the total volume), to maintain them under exponential growth (and within target concentrations) at any moment. All cultures were kept in a temperature-controlled room at 19°C with a 10:14 L/D cycle at a salinity of 38.

Thermal performance curves

To assess the acute effects of temperature on the growth and grazing rates of protozooplanktonic and mixoplanktonic grazers, we exposed them to a wide range of temperatures (5-34°C) for ca. 24 h without previous acclimation to the target temperature. Additionally, we also quantified the growth rates of the cryptophytes *R. salina* and *T. amphioxeia*, in the experiments. These temperatures were reached using recirculating water baths connected to individual aquarium chillers and heaters (TECO®). The experiments were conducted in triplicate experimental (predator and prey) and control (only prey) 132 mL Pyrex bottles. The bottles were submerged in the water baths during the incubation, being the temperature monitored continuously using an Onset HOBO data logger.

These suspensions were prepared with the addition of 100 mL of fresh f/2 medium per L of suspension (final nutrient concentration equivalent to f/20 medium – Guillard 1975). During these experiments, *K. armiger*, *G. dominans,* and *S. arenicola* were fed *R. salina*, whereas *M. rubrum* was fed *T. amphioxeia*. All experiments were conducted at saturating food concentrations (see **Table II-1** for the detailed predator and prey concentrations – Ferreira & Calbet 2020), to minimise the effect of different food concentrations on the measured ingestion rates. The bottles were filled gradually, in three to four steps, using a single experimental and/or control suspension, which was carefully mixed in between fillings. Additional experimental and control bottles were sacrificed at the beginning of the incubations to obtain the initial concentrations of the organisms. Growth and grazing rates were calculated after ca. 24 h using Frost (1972) and Heinbokel (1978) equations. Ingestion rates were deemed significant only when the prey growth rates in the control and experimental bottles were significantly different (two-tailed Student's t-test, $P < 0.05$) following the recommendations by Saiz *et al.* (2014).

The thermal performance curves were used to calculate the maximum optimal temperatures (T_{opt}) and thermal breadths ($T_{breadth}$). The former can be defined as the temperature which maximises a given rate whereas the latter comprises the (arbitrarily defined) temperature range where that rate is equal to or higher than 80 % of the rate at T_{opt} (Schulte *et al.* 2011). In the cases where the T_{opt} and the $T_{breadth}$ for growth and grazing rates differed, we averaged the two values as representative of the species.

Oxygen consumption and production rates

In addition to the feeding experiments, we conducted parallel experiments aiming to quantify the light and dark oxygen consumption/production rates. For that, we used optical oxygen sensors (OxygenDipping Probe DP-PSt3, PresensH) at the beginning and at the end of the incubations to determine oxygen concentrations. These experiments were conducted in triplicate experimental and control bottles, under a regular diel light cycle (light bottles) or under wrapped in aluminium foil through the entire incubation (dark bottles). The control bottles contained only 0.1 µm filtered seawater, whereas the experimental ones only contained a known concentration of each predator. The concentrations of prey in the predator stock solutions were adjusted to ensure their depletion on the night before the experiment, to ensure a good physiological condition of the predators while eliminating the possible artefacts that co-existing prey could induce (Almeda *et al.* 2011). Additionally, initial bottles were also prepared in triplicate to improve

the accuracy of the initial oxygen concentration and, consequently, of the oxygen consumption rate. The hourly oxygen consumption rates per hour of darkness (O_{Dark}, µmol O_2 L^{-1} h^{-1}) were obtained considering only the dark bottles (i.e., ca. 24 h of darkness) using **Equation IV.1**

where *Exp* corresponds to the oxygen concentration inside the experimental bottles and *Ctr* to the same parameter inside control bottles. The incubation time (h) for the experimental bottles is represented by t_{Exp} and for the control bottles by t_{Ctr}. The horizontal bars above some parcels of the equation mean that the average of the 3 replicates should be used. The letters *f* and *i* correspond to the final and initial values, respectively.

The oxygen consumption rates obtained using **Equation IV.1** were converted into *per capita* rates by diving O_{Dark} by the average concentration of cells inside each individual bottle, which was obtained using Frost (1972) and Heinbokel (1978) equations. At last, oxygen consumption rates per unit of carbon per hour of darkness (i.e., respiration rates, *R*, µmol O_2 pg C^{-1} h^{-1}) were obtained from the division of the last value by the average C concentration, *C* (pg C L^{-1}) in the same bottle, which was also calculated according to Frost (1972) and Heinbokel (1978).

To calculate oxygen consumption/production rates during the light period (O_{Light}, µmol O_2 L^{-1} h^{-1}) for both mixoplanktonic and protozooplanktonic grazers we considered only the light bottles. In addition, we assumed that the respiration rate *R* was the same in dark and light bottles (Wielgat-Rychert *et al.* 2017) and applied **Equation IV.2**

where 14 is the number of hours of darkness in our experimental setup. All other parcels are as described before. To notice that the calculation of *R* as previously described yields a negative value, thus justifying the use of the absolute value of *R* in **Equation IV.2**. *Per capita* and per unit of carbon values were obtained as described before.

For mixoplanktonic species, we used only the O_{Dark} for the determination of *R* and O_{Light} for the determination of photosynthetic rates, *P* (Wielgat-Rychert *et al.* 2017). For protozooplankton, O_{Light} resulted in negative values, i.e., oxygen consumption during the hours of light. These results were typically lower than in the dark incubations, i.e., there was residual photosynthesis still occurring due to the presence of algae food vacuoles inside protozooplanktonic grazers (Tarangkoon & Hansen 2011, Schoener & McManus 2017, **Paper III**). Yet, O_{Light} and O_{Dark} were not significantly different from each other (Student's t-test, $P > 0.05$) and, therefore, light bottles were considered replicates from the dark incubations and their average was used to determine *R* in protozooplankton.

Volumes and C-specific physiological rates

With the exception of *M. rubrum* and its prey, all remaining organisms were counted and their volumes assessed using a Beckman Coulter Multisizer III particle counter. *M. rubrum* may escape the current flow generated by the particle counter due to their shear sensitivity and fast jump responses (Fenchel & Hansen 2006). Therefore, cell counts of this ciliate using this instrument are often not representative of the concentration of the entire population. Accordingly, for the feeding and respiration experiments that contained *M. rubrum*, we sampled an aliquot to be fixed in acidic Lugol's (final concentration 2 %). A minimum of 300 cells of both predator and prey were counted using a Sedgwick-Rafter counting chamber. Additionally, 30 organisms were measured per replicate using the Fiji software (Schindelin *et al.* 2012) totalizing 90 cells measured per temperature, both for the feeding and respiration experiments. Their volumes were estimated from linear dimensions using simple geometric shapes. For *M. rubrum* we used the shape of a rotational ellipsoid whereas for the *T. amphioxeia* the chosen shape was the added volume of a hemisphere and a cone (Smith & Hansen 2007).

Since we noticed that *M. rubrum* and *T. amphioxeia* cells enlarged when fixed in Lugol's (using the previously described geometrical models), we conducted an independent trial where we sampled a single population of each species and ran an aliquot through the Beckman Coulter Multisizer III while fixing another in acidic Lugol's (final concentration 2 %). It is important to mention that despite not rendering trustable cell counts for *M. rubrum*, the electronic particle counter provides accurate volume estimations. From the fixed sample, we measured 200 organisms of each species and obtained a conversion factor to correct the Lugol's volumes into live volumes using the organisms (for *M. rubrum* $n > 1.0 \times 10^3$; for *T. amphioxeia* $n > 1.3 \times 10^6$) measured with

the electronic particle counter. For *M. rubrum*, Live ESD = 9.6389 $e^{0.0288}$ (Fixed ESD), whereas for *T. amphioxeia* Live ESD = 1.8759 $e^{0.1490}$ (Fixed ESD) (**Figure SIV-1** and **SIV-2**, respectively, Supplementary Information).

Carbon values for all species were obtained from the pg C:µm^3 ratio provided by Traboni *et al.* (2020) and used to determine C-specific rates. For the C-specific respiration, we multiplied *R* for the average respiratory quotient (moles of carbon dioxide produced per mole of oxygen consumed) of 0.89 (Williams & Robertson 1991, Williams & del Giorgio 2005). The exact opposite, i.e., the molar ratio of oxygen produced to fixed carbon dioxide via photosynthesis is called the photosynthetic quotient. Likewise, we multiplied *P* by the average value of 1.28 (Wielgat-Rychert *et al.* 2017) to obtain C-specific photosynthetic rates.

Activation energies and *Q*10s

The Metabolic Theory of Ecology (MTE) expresses a given metabolic rate as a function of body temperature and mass, as well as the *Ea* (given in eV) for the rate-limiting biochemical reaction that modulates that given rate. *Ea*s can be obtained from the slope of the linear regression between the natural logarithm of a given rate versus the inverse of the absolute temperature (given in K) multiplied by the Boltzmann's constant (8.62 x 10^{-5} eV K^{-1}) (Vaquer-Sunyer *et al.* 2010). This plot is commonly referred to as an Arrhenius plot. Therefore, each physiological rate must yield an individual Arrhenius plot for each species. A summary of the Arrhenius plots can be found in **Figure SIV-3**. To simplify the analysis of the data, we decided to convert *Ea* into *Q*10, which is the fold-increase in a given rate within a 10°C variation, using **Equation IV.3** (Raven & Geider 1988)

$$\frac{\quad}{\quad}$$

where *R* is the gas constant (8.314472 mol^{-1} K^{-1}) and *T* is the mean absolute temperature for the range over which *Q*10 was measured (upper and lower thermal extremes excluded – e.g., Eppley 1972). For this calculation, the *Ea* must be expressed in J mol^{-1} using a conversion factor of 96486.9 (Vaquer-Sunyer *et al.* 2010).

Results

The C-specific thermal performance curves for all six species are shown in **Figure IV-1** (for cell-specific rates, the reader is referred to **Figure SIV-3**) and a summary of the respective T_{opt} and $T_{breadth}$ can be found in **Table IV-1**.

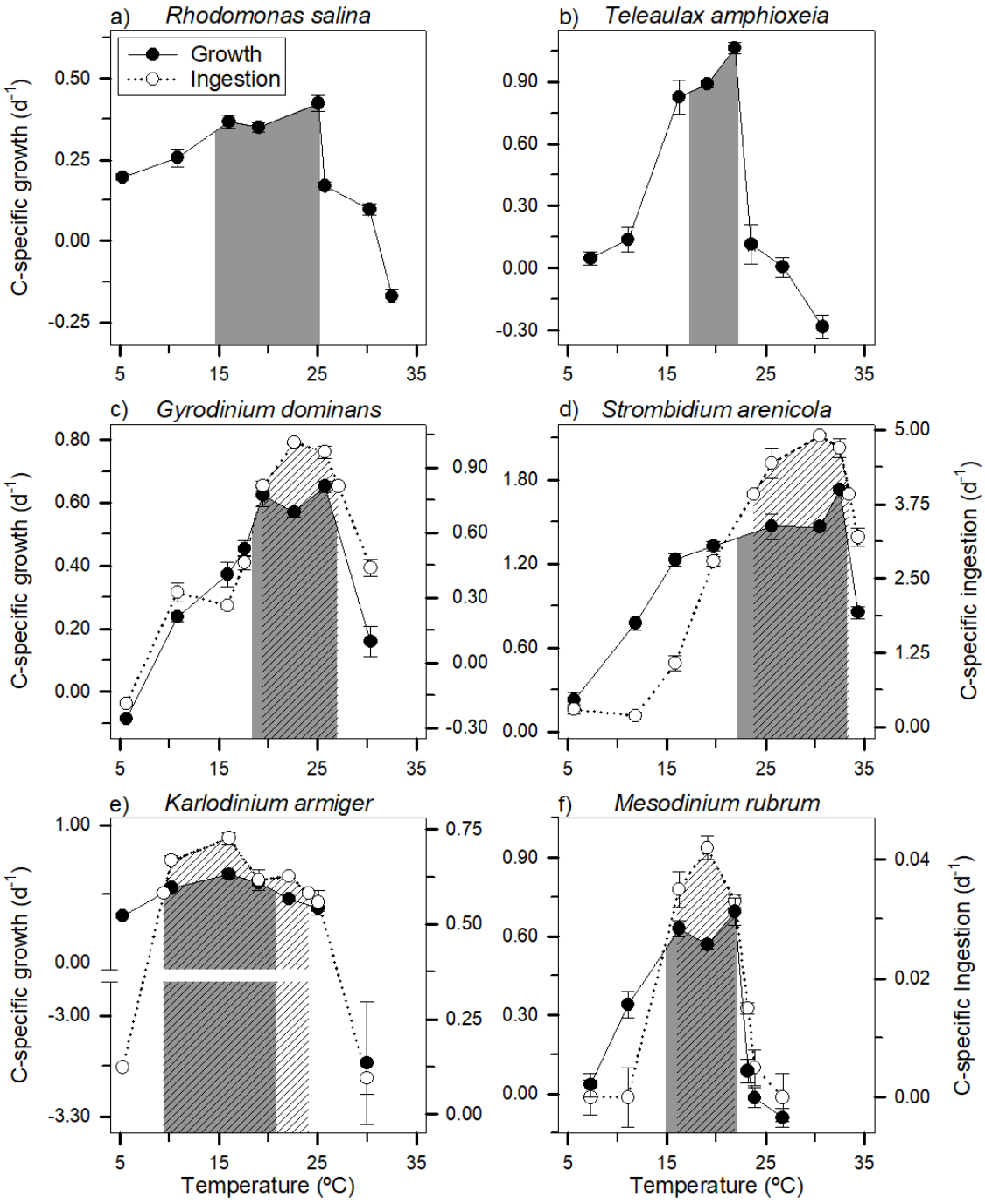

Figure IV-1 C-specific thermal performance curves for the studied protists in terms of growth (black circles with solid lines) and ingestion (white circles with dotted lines): a and b) the phytoplankton *R. salina* and *T. amphioxeia*; c and d) the protozooplankton *G. dominans* and *S. arenicola*; e and f) the mixoplankton *K. armiger* and *M. rubrum*. The shaded areas limit the $T_{breadth}$ for each species, defined as the temperature range where a given rate is equal to or higher than 80 % of the observed rate at the T_{opt} (Schulte *et al.* 2011). *M. rubrum* exhibited non-significant ingestion rates (two-tailed Student's t-test, $P > 0.05$) at some temperatures and, therefore, ingestion was considered 0 in these instances. Error bars ± se.

Table IV-1 Summary of T_{opt} and $T_{breadth}$ for each species obtained from the species-specific thermal performance curves displayed in **Figure IV-1**. NA = not applicable.

Species	T_{opt} Growth	$T_{breadth}$ Growth	T_{opt} Grazing	$T_{breadth}$ Grazing
Rhodomonas salina	25.07	10.61	NA	NA
Teleaulax amphioxeia	21.90	4.99	NA	NA
Gyrodinium dominans	25.74	8.63	22.62	7.67
Strombidium arenicola	32.52	11.05	30.49	9.71
Karlodinium armiger	16.01	11.39	16.01	14.65
Mesodinium rubrum	21.90	7.32	19.08	5.82

Five out of six species displayed a typical response to temperature by exhibiting a pronounced decline barely above the T_{opt} both in terms of C-specific growth and grazing rates. The only exception was *K. armiger* (**Figure IV-1e**), which displayed an exceptionally wide thermal performance around the T_{opt} (ca. 16°C for both rates). In fact, *K. armiger* was the species exhibiting the lowest T_{opt} and the only species whose T_{opt} was lower than the maintenance temperature (ca. 19°C) to which all species were exposed for years before the experiment. In addition, the widening of *K. armiger*'s curve resulted in the largest $T_{breadth}$ among all species, both in terms of growth and grazing rates (**Table IV-1**). Conversely, *M. rubrum* was the predator displaying the narrowest $T_{breadth}$. Yet, the species with the narrowest $T_{breadth}$ of all was the cryptophyte *T. amphioxeia* (**Table IV-1**). Indeed, it was only capable of growing at rates up to 80 % of the maximum rate between 17.3 and 22.3°C, despite showing positive growth rates between 7.3 and 26.7°C (**Figure IV-1b**). In this regard, the most sensitive species in our study was undeniably *M. rubrum*, whose range of temperatures yielding positive growth rates was narrower (between 7.3 and 23.2°C) than that of other species studied (**Figure IV-1f**). The opposite pattern (i.e., the widest temperature range for positive growth) was found in the protozooplanktonic ciliate *S. arenicola*, which exhibited positive growth rates at all temperatures tested (5.6 to 34.4°C), being followed by *G. dominans* (range broadens over 23°C difference). In addition, this ciliate was also the species displaying the highest T_{opt} for both rates (ca. 32.5°C and 30.5°C for growth and grazing, respectively – **Table IV-1**). *G. dominans* was the only species showing significantly negative ingestion rates ($P < 0.05$ at ca. 5.6°C), which were paired with negative growth rates. The thermal performance curves also enabled the assessment of the overall effect of temperature on volume (as relative to the

initial 19°C) of each target species (**Figure IV-2**). Absolute average volumes for each species can be found in **Figure SIV-4**.

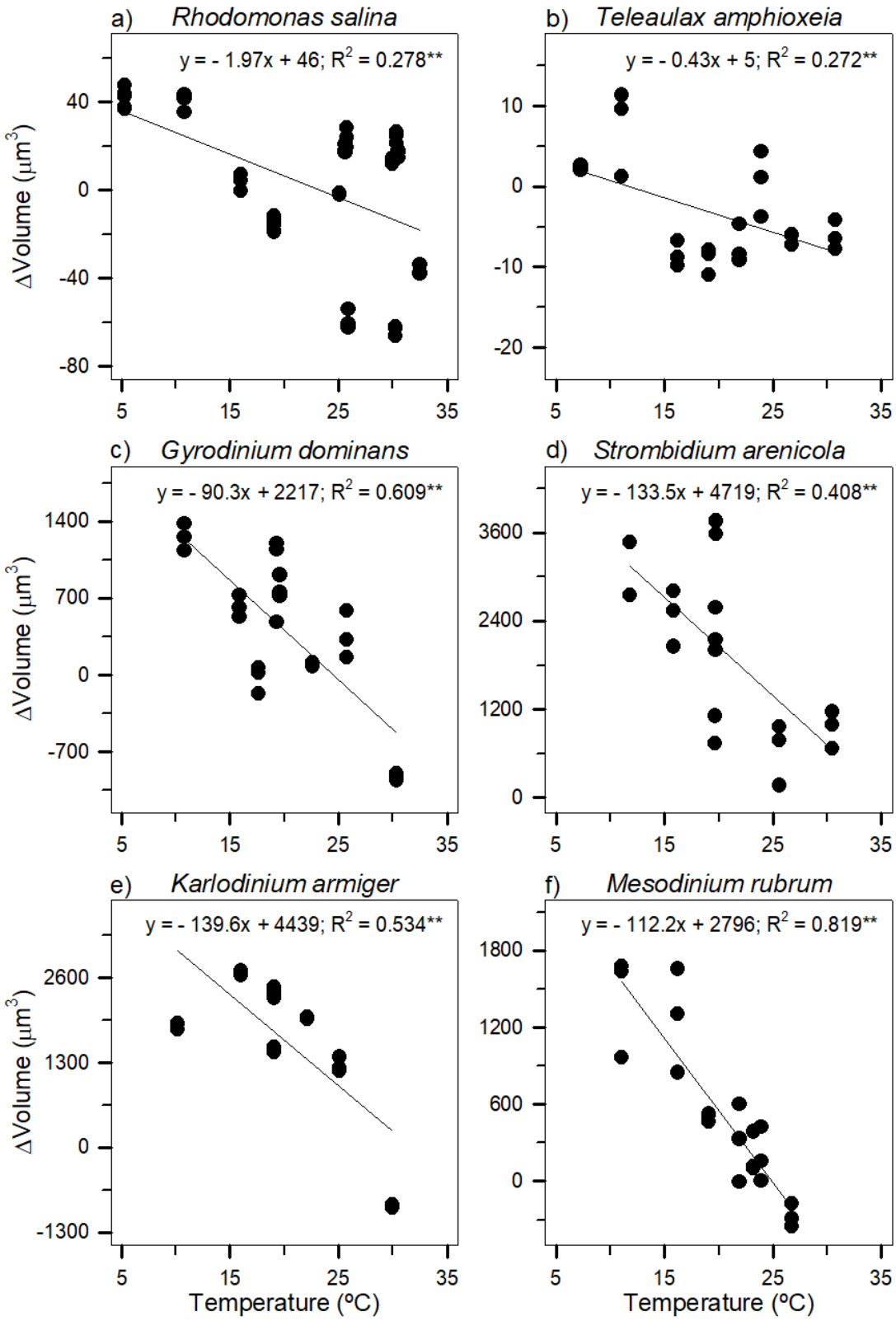

Figure IV-2 Relationship between temperature (°C) and changes in volume (µm^3, relative to the initial volume at 19°C) for a) *R. salina*, b) *T. amphioxeia*, c) *G. dominans*, d) *S. arenicola*, e) *K. armiger*, and f) *M. rubrum*. All relationships yielded significant negative slopes (** implies $P < 0.01$). The results for *R. salina* and *T. amphioxeia* were obtained from the control bottles, i.e., without predators.

The result was a conserved trend across all species, with a significant decrease in size ($P < 0.01$) at higher temperatures. Still, in order to properly interpret **Figure IV-2**, it is critical to know whether smaller volumes were a consequence of individual cell shrinkage (i.e., somatic decrease) or due to a higher cellular division rate (i.e., reproductive decrease). In addition, in the case of the grazers, changes in one's own volume can also be due to the ingestion of prey. Thus, we applied linear model regressions between ΔVolumes and each C-specific rate and summarized the results in **Table IV-2**.

Table IV-2 Linear regression model between changes in predator volumes (μm^3) and C-specific growth and ingestion rates. R^2 values marked with a * or ** imply a significant slope of the regression, i.e., $P < 0.05$ and $P < 0.01$, respectively. NA = not applicable. NS = not significant ($P > 0.05$).

Species	C-specific ingestion vs ΔVolume	ΔVolume vs C-specific growth
Rhodomonas salina	NA	NS
Teleaulax amphioxeia	NA	$y = -0.0318x + 0.27$, $R^2 = 0.17$*
Gyrodinium dominans	NS	$y = 0.0002x + 0.44$, $R^2 = 0.48$**
Strombidium arenicola	$y = -498x + 3348$, $R^2 = 0.43$**	$y = -0.0001x + 1.52$, $R^2 = 0.37$**
Karlodinium armiger	$y = 5393x – 1355$, $R^2 = 0.92$**	$y = 0.0011x – 1.68$, $R^2 = 0.86$**
Mesodinium rubrum	NS	$y = 0.0003x + 0.17$, $R^2 = 0.32$**

For both *M. rubrum* and *G. dominans*, ingestion could not explain the variation in volume ($P > 0.05$) however, the latter was positively correlated with growth ($P < 0.01$). Therefore, changes in cellular volume were not driven by ingestion rates and growth should be merely somatic (**Figure IV-2c,f**). For *R. salina* the regression between ΔVolume and C-specific growth was not significant ($P = 0.09$, **Table IV-2**), meaning that an increasing temperature diminishes *R. salina*'s volume (**Figure IV-2a**) likely due to somatic causes. Conversely, *T. amphioxeia* displayed a significantly negative correlation between ΔVolume and C-specific growth (**Table IV-2**) meaning that temperature decreases *T. amphioxeia*'s volume by increasing cellular division rate. The same pattern was observed in the ciliate *S. arenicola*, with the addition that ΔVolume was also negatively associated with ingestion (**Table IV-2**). Finally, *K. armiger* exhibited a unique pattern: the ΔVolume explained ca. 86 % of the observed changes in C-specific growth

and was itself highly dependent on the measured C-specific ingestion (**Table IV-2**). We also measured oxygen consumption/production rates across three different temperatures within the ascending part of the thermal performance curves for each grazer and converted them into C-specific rates using respiratory and photosynthetic quotients (**Figure IV-3**).

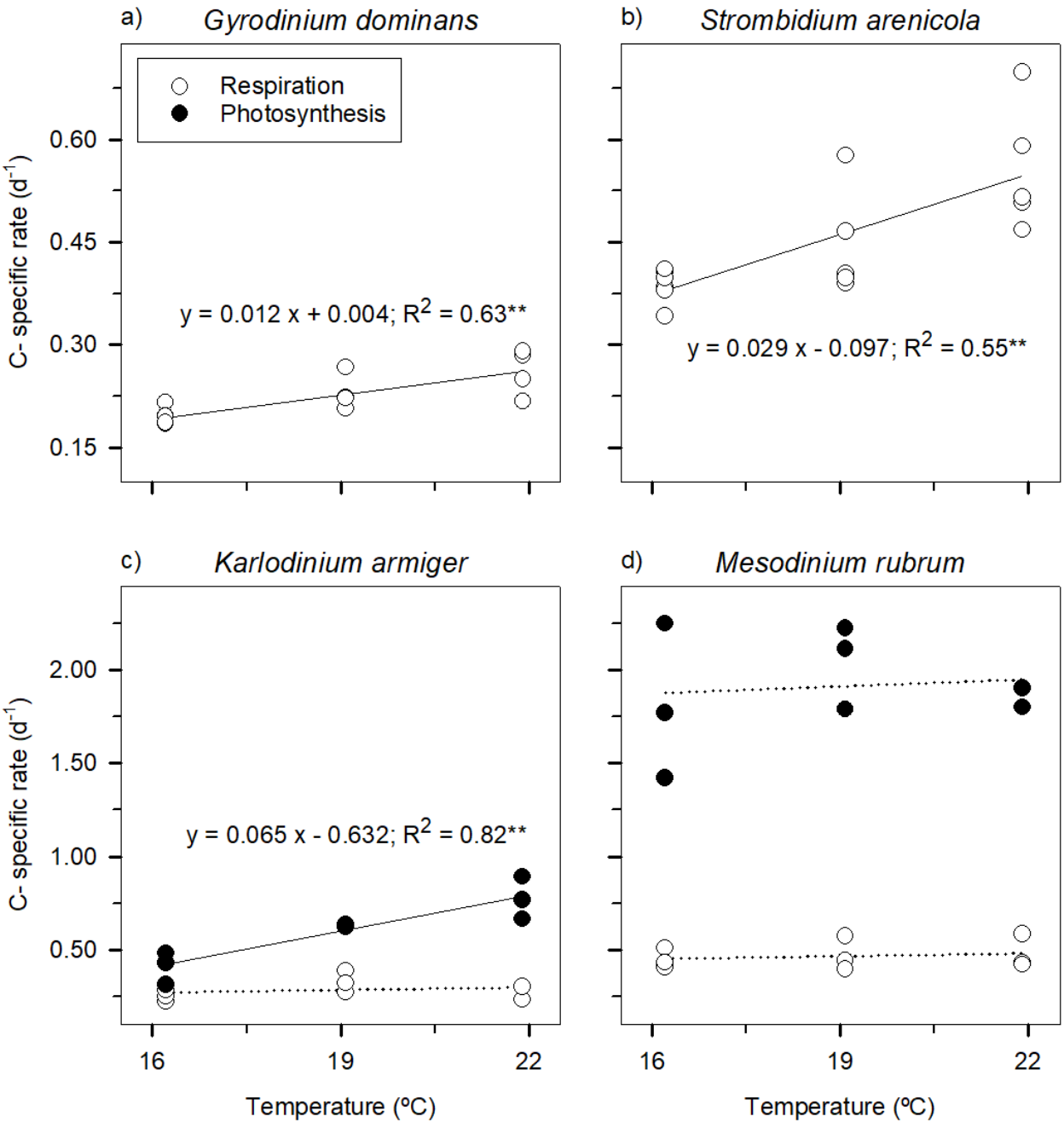

Figure IV-3 C-specific respiration (white circles) and photosynthetic (black circles) rates for a) *G. dominans*, b) *S. arenicola*, c) *K. armiger*, and d) *M. rubrum* for temperatures between 16 and 22°C. Respiration rates are in fact C losses thus the plotted points correspond to their absolute value to ease the comparison (see **Equations IV.1** and **IV.2**). Non-significant regressions (P > 0.05) are depicted with a dotted line whereas significant regressions are displayed with a solid line (** implies P < 0.01).

Regarding C-specific respiration rates, both protozooplanktonic grazers showed a significant increase ($P < 0.01$) in respiratory rates as temperature increased (**Figure IV-3a,b**), whereas mixoplanktonic grazers seemed unaffected (**Figure IV-3c,d**). For the ciliate *M. rubrum*, photosynthesis was also unaffected by temperature ($P > 0.05$, **Figure IV-3d**). However, for *K. armiger*, a change in temperature from 16.2 to 21.9°C nearly doubled the measured C-specific photosynthetic rates (from ca. 0.41 d^{-1} to ca. 0.78 d^{-1}, $P < 0.01$, **Figure IV-3c**). Within a given trophic mode of nutrition, ciliates demonstrated higher C-specific rates than dinoflagellates. Altogether, this information resulted in distinct overall responses to temperature, as summarized by the rate-specific *Q*10 (**Table IV-3**).

Table IV-3 *Q*10 for every physiological rate ascertained in this study for the predator species. *Q*10 was calculated using **Equation IV.3**. NA = not applicable.

Species	Growth	Grazing	Respiration	Photosynthesis
Gyrodinium dominans	2.01	2.66	1.67	NA
Strombidium arenicola	2.04	4.39	1.85	NA
Karlodinium armiger	0.80	0.88	1.19	3.16
Mesodinium rubrum	1.08	0.38	1.10	1.11

Growth, grazing, and respiration rates were higher in protozooplankton than in mixoplankton, being the *Q*10s of grazing rates much higher than the ones observed in the remaining parameters. In addition, the *Q*10s of this rate defined grazing as the parameter with the highest fold-difference between trophic modes, being ca. 5.60 times higher in protozooplankton than in mixoplankton. Conversely, photosynthesis was the physiological parameter that varied the most in mixoplankton in response to temperature changes, with *K. armiger* exhibiting the largest fold increase. Nevertheless, the mixoplanktonic dinoflagellate was the only species diminishing its growth rate in this temperature range, as seen by a *Q*10 < 1.

Discussion

One of the major objectives of this study was to assess the short-term physiological response of protists to a sudden variation in temperature (i.e., without previous acclimation to a given target temperature). In this regard, our study evidenced that several key physiological parameters are heavily modulated by temperature (**Figures IV-1** and **IV-3**), with grazing and photosynthesis being the highest temperature-dependent parameters in protozooplankton and mixoplankton, respectively (**Table IV-3**). In addition, we observed that higher temperatures imply smaller organisms (**Figure IV-2** and **Figure SIV-4**). The lack of an acclimation period is not a very common approach in studies aiming to determine the physiological consequences of temperature changes, as they oftentimes involve an acclimation period before the actual experiment (e.g., Lim *et al.* 2019, Ok *et al.* 2019, Kang *et al.* 2020). Still, there are studies where metabolic responses have been directly measured after an acclimation period of 15 min (see, for example, Padfield *et al.* 2016). Yet, the rationale behind our experimental design was to improve the similarities between our laboratory experiment and an extreme short-term temperature event in the field, such as marine heatwaves, whose frequency and intensity is projected to increase in the future (Oliver *et al.* 2019). Therefore, our data intend to address a specific question, and we must highlight that different time scales allow different processes to take place, which could imply different effects. Indeed, Franzé & Menden-Deuer (2020) state that physiological acclimation can take up to 2.5 d $°C^{-1}$ when transitioning towards lower temperatures and 1.25 d $°C^{-1}$ when temperatures increase. Thus, our experiments may have slightly overestimated the variations of the measured rates in response to temperature (when compared to larger time-scale studies), although these differences were likely minor (as per the differences in non-acclimated vs acclimated populations reported by Franzé & Menden-Deuer 2020).

Temperature effects on cellular volumes

Volume reductions as a consequence of temperature have been observed several times in the past (e.g., Montagnes *et al.* 2008, Morán *et al.* 2010, Franzé & Menden-Deuer 2020). In fact, decreasing cellular volumes have even been proposed as a universal ecological response to increasing ambient temperatures (Daufresne *et al.* 2009, Gardner *et al.* 2011, Sheridan & Bickford 2011), with its due physiological consequences. For instance, nutrient acquisition in phototrophs depends on the cellular surface/volume relationship (e.g., Pasciak & Gavis 1974). Likewise, ingestion rates for planktonic grazers

depend heavily on prey encounter rates, which is also a function of cell size (e.g., Kiørboe & MacKenzie 1995). In our study, we have demonstrated that the ciliate *S. arenicola* exhibited a significantly negative slope of the linear regressions between changes in volume and both C-specific growth and ingestion rates (**Table IV-2**). Therefore, it means that i) smaller *S. arenicola* grew faster than larger ones and that ii) smaller cells have higher C-specific ingestion rates. Being a protozooplanktonic grazer, the only substantial mechanism of C acquisition is through the ingestion of particulate matter. As such, we can conclude that the overall decrease in volume at higher temperatures (**Figure IV-2d**) is a result of an enhanced cellular division rate, which in turn can only be attained due to higher C-specific ingestion rates. Similarly, *T. amphioxeia* also became smaller due to faster growth rates at higher temperatures.

On the contrary, species like the dinoflagellate *G. dominans* and the ciliate *M. rubrum* exhibited a positive regression between ΔVolume and C-specific growth while displaying a non-significant relationship with C-specific ingestion rates (**Table IV-2**). Thus, it seems that the smaller cells, observed at higher temperatures (**Figure IV-2c,f**), are due to somatic reasons, i.e., higher temperatures shrink individual cells although not necessarily as a consequence of higher growth rates. On the other hand, the pattern detected in *K. armiger* was unique: both regressions (i.e., ΔVolume vs C-specific growth and C-specific ingestion vs ΔVolume) displayed significant positive slopes. This means that *K. armiger* increased ingestion rates due to temperature although it did not result in a faster division rate, producing an enlargement of the predator's cell (i.e., ingested cells were not digested). Hence, we can conclude that the pattern seen in **Figure IV-2e** was a consequence of the effect of temperature on grazing and not directly on *K. armiger*'s volume.

Temperature effects on physiological rates

A particular aspect in *K. armiger*'s response to temperature that must be highlighted is the wide $T_{breadth}$ that this species exhibited, both in terms of growth and ingestion (**Figure IV-1e** and **Table IV-1**), which was unlike any other pattern observed in this study (although *S. arenicola* followed a similar pattern regarding growth). Nevertheless, it is not the first time that a similar response is seen, as exemplified by its congener *Karlodinium veneficum* (Lin *et al.* 2018, Vidyarathna *et al.* 2020) and by other mixoplanktonic dinoflagellates (e.g., Lim *et al.* 2019, Ok *et al.* 2019, Kang *et al.* 2020).

The exact opposite (i.e., a narrow $T_{breadth}$) was found both in the ciliate *M. rubrum* and in the cryptophyte *T. amphioxeia* (**Figure IV-1b,f** and **Table IV-1**). In the work of Fiorendino *et al.* (2020), the $T_{breadths}$ for these two species were similar; however, T_{opts} were slightly higher than ours even though they used the same strains as in our experiments. Still, in this study, both species were adapted to a slightly higher temperature than in our experiments, besides being acclimated for 2 days for every °C until the experimental temperature was reached. Thus, this procedure may have increased their tolerance and performance at higher temperatures (e.g., Chakravarti *et al.* 2017, O'Donnell *et al.* 2018). Gaillard *et al.* (2020) found similar growth performances for *T. amphioxeia* in response to temperature. Thus, the combined analysis of our and other studies suggest that *M. rubrum* and its prey are tightly coupled in terms of thermal performance.

In addition, we have also confirmed that protozooplanktonic predators are better adapted to a sudden increase of temperature than their mixoplanktonic counterparts, as seen by the higher average T_{opts} (both in growth and ingestion rates) in the former group (**Table IV-1**). Regarding protozooplankton, we must highlight the negative ingestion and growth rates obtained at the lowest temperature in *G. dominans*' performance curve (**Figure IV-1c**). These results denote a higher growth of the prey in the presence of the dinoflagellate than when incubated alone and likely resulted from an increased nutrient pool originating from the dead grazers (e.g., Ferreira & Calbet 2020). We attempted to eliminate this possible artefact by the addition of nutrients to the experimental medium however, ammonium and urea, for example, can be released by microplankton (Caperon *et al.* 1979, Solomon *et al*. 2010, Gao *et al.* 2018) and may explain the increased growth of *R. salina*. A negative growth rate at similar temperatures has already been detected previously by Franzé & Menden-Deuer (2020), which suggests that there is a threshold temperature for *G. dominans* around 5-6°C. Finally, our results also indicate that our *R. salina* strain was better adapted to varying water temperatures than the one studied by Hammer *et al.* (2002), as seen by the better performance displayed at all temperatures.

According to *Q*10s, the species whose grazing rates increased the most in a sudden warming scenario was *S. arenicola*, being followed by *G. dominans*, then *K. armiger* and finally *M. rubrum*. This is in agreement with the maximum ingestion rates of their respective functional responses. Indeed, *S. arenicola* consumed as much as 120 *R. salina* predator^{-1} d^{-1} (**Figure SIII-2b**, Ferreira *et al.* submitted), whereas *M. rubrum* only

ate ca. 5 *T. amphioxeia* predator^{-1} d^{-1} (Smith & Hansen 2007). *G. dominans* and *K. armiger* stand in between the two ciliates, with the protozooplankter eating ca. 20 *R. salina* predator^{-1} d^{-1} (Calbet *et al.* 2013) and the mixoplankter ca. 10 *R. salina* predator^{-1} d^{-1} (Berge *et al.* 2008). Respiration and growth followed the same pattern, which agrees with the fact that all three parameters are integrated into an organism's C budget. Indeed, from the total ingested C (and photosynthesis in mixoplankton), a portion is egested as either particulate or dissolved organic C, and the remaining is assimilated by the organism; from the assimilated C, part is devoted to growth and the rest is lost to the environment through respiration. The respiration rates of mixoplanktonic species did not respond to warmer ambient temperatures, as opposed to the protozooplanktonic grazers studied. This is likely a consequence of their internal photosynthetic mechanisms, which oftentimes (if not always) prioritise internal C sources over external ones; i.e., there is internal recycling of C, which decreases their overall void of C (Flynn & Mitra 2009).

One interesting outcome of our experiments comes from the analysis of photosynthesis in both *K. armiger* and *M. rubrum*. From our data, it seems that the ciliate, whose mode of nutrition is primarily autotrophic (Smith & Hansen 2007), is not going to benefit much from a sudden increased of temperature (*Q*10 ca. 1.11, **Table IV-3**), as predicted by the MTE for autotrophic processes. *K. armiger*, on the other hand, increased its photosynthetic rate by ca. 1.9 times in less than 6°C, which resulted in a very high *Q*10 for this process in the dinoflagellate (ca. 3.16 – **Table IV-3**). Nevertheless, these results must not be considered standalone i.e., placement within the MTE framework requires the combined analysis of more physiological rates.

If we consider all rates, a critical aspect that is conserved in both mixoplanktonic predators is that photosynthesis is the rate that benefits the most from temperature (although the differences across rates are minor in *M. rubrum*). In addition, grazing was always hindered in a sudden warming scenario in both species (seen by a *Q*10 < 1). Moreover, digestion rates depend on the ambient temperature but vary similarly in mixoplanktonic and protozooplanktonic grazers (e.g., Fenchel 1975, Li *et al.* 2001). This particular combination of factors suggests that both mixoplanktonic species (irrespective of their taxonomic or functional group) increase their auto/heterotrophic ratio at higher temperatures, as opposed to the predictions of the MTE (Gillooly *et al.* 2001, Brown *et al.* 2004) and some experimental studies (e.g., Wilken *et al.* 2013, Cabrerizo *et al.* 2019). Nevertheless, our results are not the first to report an abnormal behaviour of mixoplankton

in light of the MTE projections. For example, a direct measurement of the contribution of grazing to the total metabolic budget in the bacterivore mixoplankter *Dinobryon sociale* resulted in a higher contribution of phototrophy at higher temperatures (Princiotta *et al.* 2016). Similarly, González-Olalla *et al.* (2019) assessed the effect of temperature on two bacterivores and concluded that warmer temperatures shifted the overall metabolism towards an increased phototrophy in both species. Also, Ok *et al.* (2019) studied the CM dinoflagellate *Takayama helix* (same family as *K. armiger*) and noticed increased growth rates paired with insignificant changes in ingestion rates in a wide temperature range. Lim *et al.* (2019) and Kang *et al.* (2020) noticed the same pattern in the CM dinoflagellates *Alexandrium pohangense* and *Yihiella yeosuensis*, respectively. Altogether, the results from these latter three works hint at a possibly higher phototrophic contribution to the overall metabolism in these dinoflagellate species, although this variable was not directly measured in their study.

Still, and perhaps surprising in light of the previous paragraph, our results do not question prior estimations of *Ea* in phototrophs and heterotrophs based on growth rates (e.g., Rose & Caron 2007, Chen *et al.* 2012), as the average *Q*10 for protozooplanktonic growth was more than twice that of mixoplankton. Nevertheless, recent evidence demonstrated that growth-due *Ea*s are widely variable among different taxonomic groups (Chen & Laws 2017). All of these discrepancies call for a revision of the general belief that the temperature sensitivity of phytoplankton is lower than that of protozooplankton (Wang *et al.* 2019). In addition, the nutritional plasticity of mixoplankton has been pointed as a possible source of error between theoretical and observed *Ea*s in microplankton (Wang *et al.* 2019). Therefore, as our results support an increased phototrophy in mixoplankton at higher temperatures, we are contributing to the body of literature that deviates mixoplankton from the MTE and strict auto/heterotrophic *Ea*s. This conclusion means that such a change in nutritional strategies will likely impact biogeochemical cycles and reinforces the need to integrate mixoplankton in current ecosystem models (Wilken *et al.* 2018). Indeed, recent simulations confirm that modelling phagotrophy in *K. veneficum* is critical for the accurate prediction of bloom dynamics in a future warming scenario (Lin *et al.* 2018).

Conclusion

Despite agreeing with multiple data sources on several aspects, we must stress the short-term nature of this study. Indeed, the data presented in this work can and should be used to assist in the comprehension of the effect of climate change in marine protistan communities regarding short-term temperature events such as marine heatwaves. Future studies should also address the multigenerational response to temperature changes since a general (and gradual) increase in the oceanic temperature is also expected as a consequence of climate change. Accordingly, adaptation is likely going to be reflected in the biological rates and overall metabolism, meaning that these changes must also be incorporated in future modelling predictions. In this regard, evidence from evolutionary studies suggests that, in spite of having a stronger temperature dependence, heterotrophic processes are balanced with autotrophic ones with passing generations, which culminates with higher C fixation rates in a future warming scenario (e.g., Padfield *et al.* 2016, Barton *et al.* 2020). Our short-term data agrees with these results as photosynthesis was the metabolic process which benefitted the most from an increased temperature in mixoplanktonic grazers. With this study, we are slowly contributing to the correct placement of mixoplankton within the MTE, which may be crucial for the accurate projection of climate change in the future.

References

Adolf J.E., Stoecker D.K., Harding Jr L.W., 2006. The balance of autotrophy and heterotrophy during mixotrophic growth of *Karlodinium micrum* (Dinophyceae). *J. Plankton Res.*, **28**: 737-751.

Allen A.P., Gillooly J.F., Brown J.H., 2005. Linking the global carbon cycle to individual metabolism. *Funct. Ecol.*, **19**: 202-213.

Almeda R., Alcaraz M., Calbet A., Saiz E., 2011. Metabolic rates and carbon budget of early developmental stages of the marine cyclopoid copepod *Oithona davisae*. *Limnol. Oceanogr.*, **56**: 403-414.

Barton S., Jenkins J., Buckling A., Schaum C-E., Smirnoff N., Raven J.A., Yvon-Durocher G., 2020. Evolutionary temperature compensation of carbon fixation in marine phytoplankton. *Ecol. Lett.*, **23**: 722-733.

Berge T., Hansen P.J., 2016. Role of the chloroplasts in the predatory dinoflagellate *Karlodinium armiger*. *Mar. Ecol. Prog. Ser.*, **549**: 41-54.

Berge T., Hansen P.J., Moestrup Ø., 2008. Prey size spectrum and bioenergetics of the mixotrophic dinoflagellate *Karlodinium armiger*. *Aquat. Microb. Ecol.*, **50**: 289-299.

Brown J.H., Gillooly J.F., Allen A.P., Savage V.M., West G.B., 2004. Toward a metabolic theory of ecology. *Ecology*, **85**: 1771-1789.

Cabrerizo M.J., González Olalla J.M., Hinojosa López V.J., Peralta Cornejo F.J., Carrillo P., 2019. A shifting balance: responses of mixotrophic marine algae to cooling and warming under UVR. *New Phytol.*, **221**: 1317-1327.

Calbet A., Isari S., Martínez R.A., Saiz E., Garrido S., Peters J., Borrat R.M., Alcaraz M., 2013. Adaptations to feast and famine in different strains of the marine heterotrophic dinoflagellates *Gyrodinium dominans* and *Oxyrrhis marina*. *Mar. Ecol. Prog. Ser.*, **483**: 67-84.

Caperon J., Schell D., Hirota J., Laws E., 1979. Ammonium excretion rates in Kaneohe Bay, Hawaii, measured by a 15N isotope dilution technique. *Mar. Biol.*, **54**: 33-40.

Chakravarti L.J., Beltran V.H., van Oppen M.J.H., 2017. Rapid thermal adaptation in photosymbionts of reef building corals. *Glob. Change Biol.*, **23**: 4675-4688.

Chen B., Landry M.R., Huang B., Liu H., 2012. Does warming enhance the effect of microzooplankton grazing on marine phytoplankton in the ocean? *Limnol. Oceanogr.*, **57**: 519-526.

Chen B., Laws E.A., 2017. Is there a difference of temperature sensitivity between marine phytoplankton and heterotrophs? *Limnol. Oceanogr.*, **62**: 806-817.

Daufresne M., Lengfellner K., Sommer U., 2009. Global warming benefits the small in aquatic ecosystems. *Proc. Natl. Acad. Sci.*, **106**: 12788-12793.

Eppley R.W., 1972. Temperature and phytoplankton growth in the sea. *Fish. Bull.*, **70**: 1063-1085.

Fenchel T., 1975. The quantitative importance of the benthic microfauna of an arctic tundra pond. *Hydrobiologia*, **46**: 445-464.

Fenchel T., Hansen P.J., 2006. Motile behaviour of the bloom-forming ciliate *Mesodinium rubrum*. *Mar. Biol. Res.*, **2**: 33-40.

Ferreira G.D., Calbet A., 2020. Caveats on the use of rotenone to estimate mixotrophic grazing in the oceans. *Sci. Rep.*, **10**: 3899.

Fiorendino J.M., Smith J.L., Campbell L., 2020. Growth response of *Dinophysis*, *Mesodinium*, and *Teleaulax* cultures to temperature, irradiance, and salinity. *Harmful Algae*, **98**: 101896.

Flynn K.J., Mitra A., 2009. Building the "perfect beast": modelling mixotrophic plankton. *J. Plankton Res.*, **31**: 965-992.

Flynn K.J., Mitra A., Anestis K., Anschütz A.A., Calbet A., Ferreira G.D., Gypens N., Hansen P.J., John U., Martin J.L., Mansour J.S., Maselli M., Medić N., Norlin A., Not F., Pitta P., Romano F., Saiz E., Schneider L.K., Stolte W., Traboni C., 2019. Mixotrophic protists and a new paradigm for marine ecology: where does plankton research go now? *J. Plankton Res.*, **41**: 375-391.

Franzè G., Menden-Deuer S., 2020. Common temperature-growth dependency and acclimation response in three herbivorous protists. *Mar. Ecol. Prog. Ser.*, **634**: 1-13.

Frost B.W., 1972. Effects of size and concentration of food particles on the feeding behavior of the marine planktonic copepod *Calanus pacificus*. *Limnol. Oceanogr.*, **17**: 805-815.

Gaillard S., Charrier A., Malo F., Carpentier L., Bougaran G., Hégaret H., Réveillon D., Hess P., Séchet V., 2020. Combined effects of temperature, irradiance, and pH on *Teleaulax amphioxeia* (Cryptophyceae) physiology and feeding ratio for its predator *Mesodinium rubrum* (Ciliophora). *J. Phycol.*, **n/a**.

Gao H., Hua C., Tong M., 2018. Impact of *Dinophysis acuminata* feeding *Mesodinium rubrum* on nutrient dynamics and bacterial composition in a microcosm. *Toxins*, **10**: 443.

Gardner J.L., Peters A., Kearney M.R., Joseph L., Heinsohn R., 2011. Declining body size: a third universal response to warming? *Trends Ecol. Evol.*, **26**: 285-291.

Gillooly J.F., Brown J.H., West G.B., Savage V.M., Charnov E.L., 2001. Effects of size and temperature on metabolic rate. *Science*, **293**: 2248-2251.

González Olalla J.M., Medina Sánchez J.M., Carrillo P., 2019. Mixotrophic trade off under warming and UVR in a marine and a freshwater alga. *J. Phycol.*, **55**: 1028-1040.

Guillard R.R.L., 1975. Culture of phytoplankton for feeding marine invertebrates. In: W.L. Smith, M.H. Chanley (Eds), Culture of marine invertebrate animals. Plenum Press, New York, NY, pp 29-60.

Hammer A., Schumann R., Schubert H., 2002. Light and temperature acclimation of *Rhodomonas salina* (Cryptophyceae): photosynthetic performance. *Aquat. Microb. Ecol.*, **29**: 287-296.

Heinbokel J.F., 1978. Studies on the functional role of tintinnids in the Southern California Bight. I. Grazing and growth rates in laboratory cultures. *Mar. Biol.*, **47**: 177-189.

Kang H.C., Jeong H.J., Lim A.S., Ok J.H., You J.H., Park S.A., Lee S.Y., Eom S.H., 2020. Effects of temperature on the growth and ingestion rates of the newly described mixotrophic dinoflagellate *Yihiella yeosuensis* and its two optimal prey species. *Algae*, **35**: 263-275.

Kimmance S.A., Atkinson D., Montagnes D.J.S., 2006. Do temperature–food interactions matter? Responses of production and its components in the model heterotrophic flagellate *Oxyrrhis marina*. *Aquat. Microb. Ecol.*, **42**: 63-73.

Kiørboe T., MacKenzie B., 1995. Turbulence-enhanced prey encounter rates in larval fish: effects of spatial scale, larval behaviour and size. *J. Plankton Res.*, **17**: 2319-2331.

Li A., Stoecker D.K., Coats D.W., 2001. Use of the 'food vacuole content' method to estimate grazing by the mixotrophic dinoflagellate *Gyrodinium galatheanum* on cryptophytes. *J. Plankton Res.*, **23**: 303-318.

Lim A.S., Jeong H.J., Ok J.H., You J.H., Kang H.C., Kim S.J., 2019. Effects of light intensity and temperature on growth and ingestion rates of the mixotrophic dinoflagellate *Alexandrium pohangense*. *Mar. Biol.*, **166**: 98.

Lin C.-H., Flynn K.J., Mitra A., Glibert P.M., 2018. Simulating effects of variable stoichiometry and temperature on mixotrophy in the harmful dinoflagellate *Karlodinium veneficum*. *Front. Mar. Sci.*, **5**: 320.

López-Urrutia Á., San Martin E., Harris R.P., Irigoien X., 2006. Scaling the metabolic balance of the oceans. *Proc. Natl. Acad. Sci.*, **103**: 8739-8744.

Mitra A., Flynn K.J., Burkholder J.M., Berge T., Calbet A., Raven J.A., Granéli E., Glibert P.M., Hansen P.J., Stoecker D.K., Thingstad F., Tillmann U., Våge S., Wilken S., Zubkov M.V., 2014. The role of mixotrophic protists in the biological carbon pump. *Biogeosciences*, **11**: 995-1005.

Montagnes D.J.S., Morgan G., Bissinger J.E., Atkinson D., Weisse T., 2008. Short-term temperature change may impact freshwater carbon flux: a microbial perspective. *Glob. Change Biol.*, **14**: 2823-2838.

Morán X.A.G., López Urrutia Á., Calvo Díaz A., Li W.K.W., 2010. Increasing importance of small phytoplankton in a warmer ocean. *Glob. Change Biol.*, **16**: 1137-1144.

O'Donnell D.R., Hamman C.R., Johnson E.C., Kremer C.T., Klausmeier C.A., Litchman E., 2018. Rapid thermal adaptation in a marine diatom reveals constraints and trade offs. *Glob. Change Biol.*, **24**: 4554-4565.

Ok J.H., Jeong H.J., Lim A.S., You J.H., Kang H.C., Kim S.J., Lee S.Y., 2019. Effects of light and temperature on the growth of *Takayama helix* (Dinophyceae): mixotrophy as a survival strategy against photoinhibition. *J. Phycol.*, **55**: 1181-1195.

Oliver E.C.J., Burrows M.T., Donat M.G., Gupta A.S., Alexander L.V., Perkins-Kirkpatrick S.E., Benthuysen J.A., Hobday A.J., Holbrook N.J., Moore P.J., Thomsen M.S., Wernberg T., Smale D.A., 2019. Projected marine heatwaves in the 21st Century and the potential for ecological impact. *Front. Mar. Sci.*, **6**: 734.

Padfield D., Yvon Durocher G., Buckling A., Jennings S., Yvon Durocher G., 2016. Rapid evolution of metabolic traits explains thermal adaptation in phytoplankton. *Ecol. Lett.*, **19**: 133-142.

Pasciak W.J., Gavis J., 1974. Transport limitation of nutrient uptake in phytoplankton. *Limnol. Oceanogr.*, **19**: 881-888.

Princiotta S.D., Smith B.T., Sanders R.W., 2016. Temperature dependent phagotrophy and phototrophy in a mixotrophic chrysophyte. *J. Phycol.*, **52**: 432-440.

Raven J.A., Geider R.J., 1988. Temperature and algal growth. *New Phytol.*, **110**: 441-461.

Regaudie-de-Gioux A., Duarte C.M., 2012. Temperature dependence of planktonic metabolism in the ocean. *Global Biogeochem. Cycles*, **26**.

Riisgaard K., Hansen P.J., 2009. Role of food uptake for photosynthesis, growth and survival of the mixotrophic dinoflagellate *Dinophysis acuminata*. *Mar. Ecol. Prog. Ser.*, **381**: 51-62.

Rose J.M., Caron D.A., 2007. Does low temperature constrain the growth rates of heterotrophic protists? Evidence and implications for algal blooms in cold waters. *Limnol. Oceanogr.*, **52**: 886-895.

Saiz E., Griffell K., Calbet A., Isari S., 2014. Feeding rates and prey: predator size ratios of the nauplii and adult females of the marine cyclopoid copepod *Oithona davisae*. *Limnol. Oceanogr.*, **59**: 2077-2088.

Schindelin J., Arganda-Carreras I., Frise E., Kaynig V., Longair M., Pietzsch T., Preibisch S., Rueden C., Saalfeld S., Schmid B., 2012. Fiji: an open-source platform for biological-image analysis. *Nat. Methods*, **9**: 676.

Schoener D.M., McManus G.B., 2017. Growth, grazing, and inorganic C and N uptake in a mixotrophic and a heterotrophic ciliate. *J. Plankton Res.*, **39**: 379-391.

Schulte P.M., Healy T.M., Fangue N.A., 2011. Thermal performance curves, phenotypic plasticity, and the time scales of temperature exposure. *Integr. Comp. Biol.*, **51**: 691-702.

Sheridan J.A., Bickford D., 2011. Shrinking body size as an ecological response to climate change. *Nat. Clim. Change*, **1**: 401-406.

Smith M., Hansen P.J., 2007. Interaction between *Mesodinium rubrum* and its prey: importance of prey concentration, irradiance and pH. *Mar. Ecol. Prog. Ser.*, **338**: 61-70.

Solomon C.M., Collier J.L., Berg G.M., Glibert P.M., 2010. Role of urea in microbial metabolism in aquatic systems: a biochemical and molecular review. *Aquat. Microb. Ecol.*, **59**: 67-88.

Stoecker D.K., Michaels A.E., 1991. Respiration, photosynthesis and carbon metabolism in planktonic ciliates. *Mar. Biol.*, **108**: 441-447.

Stoecker D.K., Silver M.W., Michaels A.E., Davis L.H., 1988. Obligate mixotrophy in *Laboea strobila*, a ciliate which retains chloroplasts. *Mar. Biol.*, **99**: 415-423.

Tarangkoon W., Hansen P.J., 2011. Prey selection, ingestion and growth responses of the common marine ciliate *Mesodinium pulex* in the light and in the dark. *Aquat. Microb. Ecol.*, **62**: 25-38.

Traboni C., Calbet A., Saiz E., 2020. Effects of prey trophic mode on the gross-growth efficiency of marine copepods: the case of mixoplankton. *Sci. Rep.*, **10**: 12259.

Vaquer-Sunyer R., Duarte C.M., Santiago R., Wassmann P., Reigstad M., 2010. Experimental evaluation of planktonic respiration response to warming in the European Arctic Sector. *Polar Biol.*, **33**: 1661-1671.

Vidyarathna N.K., Papke E., Coyne K.J., Cohen J.H., Warner M.E., 2020. Functional trait thermal acclimation differs across three species of mid-Atlantic harmful algae. *Harmful Algae*, **94**: 101804.

Wang Q., Lyu Z., Omar S., Cornell S., Yang Z., Montagnes D.J.S., 2019. Predicting temperature impacts on aquatic productivity: Questioning the metabolic theory of ecology's “canonical” activation energies. *Limnol. Oceanogr.*, **64**: 1172-1185.

Wielgat-Rychert M., Rychert K., Witek Z., Zalewski M., 2017. Calculation of the photosynthetic quotient (PQ) in the Gulf of Gdańsk (Southern Baltic). *Balt. Coast. Zone*, **21**: 51-60.

Wilken S., Huisman J., Naus Wiezer S., Van Donk E., 2013. Mixotrophic organisms become more heterotrophic with rising temperature. *Ecol. Lett.*, **16**: 225-233.

Wilken S., Soares M., Urrutia Cordero P., Ratcovich J., Ekvall M.K., Van Donk E., Hansson L.A., 2018. Primary producers or consumers? Increasing phytoplankton bacterivory along a gradient of lake warming and browning. *Limnol. Oceanogr.*, **63**: S142-S155.

Williams P.J.I.B., del Giorgio P.A., 2005. Respiration in aquatic ecosystems: history and background. In: P.A. del Giorgio, P.J.I.B. Williams (Eds), Respiration in Aquatic Ecosystems. Oxford University Press, Oxford University Press Inc., New York, pp 1-17.

Williams P.J.I.B., Robertson J.E., 1991. Overall planktonic oxygen and carbon dioxide metabolisms: the problem of reconciling observations and calculations of photosynthetic quotients. *J. Plankton Res.*, **13**: 153-169.

Yih W., Kim H.S., Jeong H.J., Myung G., Kim Y.G., 2004. Ingestion of cryptophyte cells by the marine photosynthetic ciliate *Mesodinium rubrum*. *Aquat. Microb. Ecol.*, **36**: 165-170.

Page deliberately left in blank

3. Conclusions and future perspectives

Being able to quantify how much herbivory is due to mixoplanktonic organisms is of utmost importance for the understanding of the marine food webs, and to produce correct modelling projections in marine ecosystems (e.g., Mitra *et al.* 2014). Nevertheless, we still lack a well-established technique to quantify the grazing impact of mixoplankton *in situ* (e.g., Beisner *et al.* 2019, Flynn *et al.* 2019). Accordingly, this thesis deepened into the issue of the quantification of mixoplanktonic grazing in mixed assemblages. Before investigating in the field, where complex interactions can occur, it seemed reasonable to conduct experiments in the laboratory, where a much larger degree of control can be exerted. Therefore, **Papers I** to **III**, explored three independent approaches to measure mixoplankton's grazing impact. Each of the tested methodologies had its own advantages and disadvantages, and can be listed in terms of its success rate towards the common objective as *in silico* dilution technique (**Paper III**) > LFLA (**Paper I**) > Rotenone (**Paper II**).

Starting with the least effective approach, **Paper II** concluded that rotenone could not be used to disentangle mixoplanktonic and protozooplanktonic grazing impact. Despite being conceptually simple, since protozooplankton and mixoplankton can rely on different organelles for the production of ATP (mitochondria for the former; mitochondria and chloroplasts for the latter), this approach determined that physiological differences between species were stronger discriminators than the trophic mode of nutrition. Therefore, in spite of being highly promising in theory, the results did not support the use of rotenone as an exclusive trophic deterrent for protozooplankton.

The intermediately effective solution to the determination of the grazing impact of mixoplankton was achieved in **Paper I**. This study evaluated the utility, in mixoplankton, of a previously developed method that uses LFLA as tracers for grazing (Li *et al.* 1996). This was not a novel approach. In fact, this method has been used numerous times before and even in studies targeting mixoplanktonic species. The results presented here corroborated the utility of the technique, but also highlighted several issues that call for caution when using this method. In particular, size and species selectivity can induce a massive bias in the measured protistan ingestion rates. This issue can be minimised if one decides to use two fluorochromes instead of one, and could be routinely applied in the field to determine mixoplanktonic grazing rates. That is, of course, if the species at

hand feed by engulfment and not by any other mechanism like peduncle or pallium feeding (only existent in dinoflagellates – Hansen & Calado 1999), as this severely impairs the results obtained with this technique.

Finally, the approach presented in **Paper III** was the most promising although not, *per se*, sufficient to obtain a definitive solution to the quantification of the grazing impact exerted by mixoplankton. This approach focused on the, currently, most used technique to quantify microplanktonic herbivory in the field, the dilution technique (Landry & Hassett 1982). Despite its robustness and extended use, the technique is conceptually not prepared to deal with mixoplankton, because they possess Chl *a*, and act both as grazers and prey. This problem could be partially solved by using other proxies besides Chl *a* to quantify prey dynamics during incubations. However, other factors, such as proper illumination, species selectivity, and intraguild predation contribute in shaping the outcome of the technique. Still, the major objective of this work was to provide an experimental framework on which a future *in silico* model can be built upon. Thus, the experiments consisted of known mixtures of cryptophytes and diatoms as prey, and both mixoplanktonic and protozooplanktonic predators, namely a dinoflagellate and a ciliate for each trophic mode. Therefore, the next step in this matter is the development of the *in silico* model *per se*. In a near-future, this model of the dilution technique can be coupled to the actual technique, and distributed for free for researchers to use at will. As the model relies on individual calculations for each trophic group, it should also be able to provide the actual grazing impact exerted by both mixoplankton and protozooplankton. For that, the model needs not only to be built, but also validated using independent field data.

Lastly, this thesis explored the effects of short-term temperature changes in the modulation of grazing (among other physiological parameters) in protistan predators (**Paper IV**). In terms of growth and ingestion rates, ciliates performed better than dinoflagellates of the same trophic mode of nutrition at higher temperatures, i.e., they displayed higher T_{opt} for both parameters. Using the same parameters, it appears that protozooplankton take better advantage of temperature than mixoplankton, when the grouping factor is the trophic mode of nutrition instead of taxonomy. Nevertheless, in terms of the optimal temperature range, this pattern was not retained, and the responses appeared to be species-specific. Indeed, *K. armiger* displayed a very wide $T_{breadth}$, which suggests that this species is prone to endure severe temperature changes and may explain its global success. On the other hand, *M. rubrum* did not seem very well adapted to temperature changes as seen by the low T_{opt} and $T_{breadth}$ for both growth and ingestion

rates. These results prompt the question as to how does this species endure polar winters (e.g., Moeller *et al.* 2011, van den Hoff & Bell 2015). Logic dictates that there must be severe adaptation processes who are responsible for the extreme differences observed between polar and our strains. In fact, massive phenotypic plasticity can be seen at relatively short time scales (see, for example, the loss of phagotrophy after three years of autotrophic growth in *Alexandrium pseudogonyaulax* – Blossom & Hansen 2021). An alternative explanation could be the fact that *M. rubrum* is in fact a species complex instead of a single species (Drumm *et al.* 2021). Irrespective of the explanation, there is an obvious immediate step to focus in the future, which concerns the intra-specific variability of a species. If previous results of intra-specific variation (e.g., Calbet *et al.* 2011) are taken into consideration, one can easily realise that in order to generalise results for a species, one must work with more than one strain. This aspect is likely transcendent to all the papers described in this thesis (i.e., it could improve the institutionalisation of the conclusions) although in no means diminishes its contribution to the advancement of the topic at hands.

Indeed, despite working with single strains, the **Paper IV** corroborated several (perchance universal?) behaviours that have been noticed by other authors. The strongest example concerns the cellular volume of a single organism, which, irrespective of the grouping factor, decreased at warmer temperatures (see also Daufresne *et al.* 2009, Gardner *et al.* 2011, Sheridan & Bickford 2011, among others). In addition, this study provided further evidence that mixoplanktonic grazers become more phototrophic in a warming scenario, as opposed to the predictions of the Metabolic Theory of Ecology (Gillooly *et al.* 2001, Brown *et al.* 2004) and some experimental works (e.g., Wilken *et al.* 2013, Cabrerizo *et al.* 2019). Accordingly, mixoplanktonic grazers are, apparently, exceptions within this universal theory for the scaling of metabolic rates (see also similar conclusions by Princiotta *et al.* 2016 and González-Olalla *et al.* 2019, and the studies of Kang *et al.* 2020, Lim *et al.* 2019 and Ok *et al.* 2019). It remains unknown as to what extent acclimation and adaptation affect the magnitude of these conclusions. Therefore, in the future, it seems reasonable to propose multigenerational studies, as adaptation may affect the biological rates and overall metabolism, meaning that these changes must also be incorporated in future modelling predictions. Altogether, with this thesis, I contributed to the ongoing process of unveiling the ecological role of mixoplankton, in particular in the situations where their grazing impact is concerned.

References

Adolf J.E., Stoecker D.K., Harding Jr L.W., 2006. The balance of autotrophy and heterotrophy during mixotrophic growth of *Karlodinium micrum* (Dinophyceae). *J. Plankton Res.*, **28**: 737-751.

Allen A.P., Gillooly J.F., Brown J.H., 2005. Linking the global carbon cycle to individual metabolism. *Funct. Ecol.*, **19**: 202-213.

Anderson R., Jürgens K., Hansen P.J., 2017. Mixotrophic phytoflagellate bacterivory field measurements strongly biased by standard approaches: a case study. *Front. Microbiol.*, **8**: 1398.

Arias A., Saiz E., Calbet A., 2020. Towards an understanding of diel feeding rhythms in marine protists: consequences of light manipulation. *Microb. Ecol.*, **79**: 64-72.

Arias A., Selander E., Saiz E., Calbet A., 2021. Predator chemical cue effects on the diel feeding behaviour of marine protists. *Microb. Ecol.*, 10.1007/s00248-020-01665-9.

Arora V.K., Boer G.J., Friedlingstein P., Eby M., Jones C.D., Christian J.R., Bonan G., Bopp L., Brovkin V., Cadule P., 2013. Carbon–concentration and carbon–climate feedbacks in CMIP5 Earth system models. *J. Climate*, **26**: 5289-5314.

Azam F., Fenchel T., Field J.G., Gray J.S., Meyer-Reil L.A., Thingstad F., 1983. The ecological role of water-column microbes in the sea. *Mar. Ecol. Prog. Ser.*, **10**: 257-263.

Beisner B.E., Grossart H.-P., Gasol J.M., 2019. A guide to methods for estimating phago-mixotrophy in nanophytoplankton. *J. Plankton Res.*, **41**: 77-89.

Berge T., Hansen P.J., 2016. Role of the chloroplasts in the predatory dinoflagellate *Karlodinium armiger*. *Mar. Ecol. Prog. Ser.*, **549**: 41-54.

Blossom H.E., Hansen P.J., 2021. The loss of mixotrophy in *Alexandrium pseudogonyaulax*: Implications for trade-offs between toxicity, mucus trap production, and phagotrophy. *Limnol. Oceanogr.*, **66**: 528-542.

Brown J.H., Gillooly J.F., Allen A.P., Savage V.M., West G.B., 2004. Toward a metabolic theory of ecology. *Ecology*, **85**: 1771-1789.

Cabrerizo M.J., González Olalla J.M., Hinojosa López V.J., Peralta Cornejo F.J., Carrillo P., 2019. A shifting balance: responses of mixotrophic marine algae to cooling and warming under UVR. *New Phytol.*, **221**: 1317-1327.

Calbet A., Bertos M., Fuentes-Grünewald C., Alacid E., Figueroa R., Renom B., Garcés E., 2011. Intraspecific variability in *Karlodinium veneficum*: Growth rates, mixotrophy, and lipid composition. *Harmful Algae*, **10**: 654-667.

Calbet A., Landry M.R., 2004. Phytoplankton growth, microzooplankton grazing, and carbon cycling in marine systems. *Limnol. Oceanogr.*, **49**: 51-57.

Calbet A., Martínez R.A., Isari S., Zervoudaki S., Nejstgaard J.C., Pitta P., Sazhin A.F., Sousoni D., Gomes A., Berger S.A., 2012. Effects of light availability on mixotrophy and microzooplankton grazing in an oligotrophic plankton food web: evidences from a mesocosm study in Eastern Mediterranean waters. *J. Exp. Mar. Biol. Ecol.*, **424**: 66-77.

Calbet A., Saiz E., 2013. Effects of trophic cascades in dilution grazing experiments: from artificial saturated feeding responses to positive slopes. *J. Plankton Res.*, **35**: 1183-1191.

Calbet A., Saiz E., 2018. How much is enough for nutrients in microzooplankton dilution grazing experiments? *J. Plankton Res.*, **40**: 109-117.

Daufresne M., Lengfellner K., Sommer U., 2009. Global warming benefits the small in aquatic ecosystems. *Proc. Natl. Acad. Sci.*, **106**: 12788-12793.

Dolan J.R., Gallegos C.L., Moigis A., 2000. Dilution effects on microzooplankton in dilution grazing experiments. *Mar. Ecol. Prog. Ser.*, **200**: 127-139.

Dolan J.R., McKeon K., 2005. The reliability of grazing rate estimates from dilution experiments: Have we over-estimated rates of organic carbon consumption by microzooplankton? *Ocean Sci.*, **1**: 1-7.

Drumm K., Norlin A., Kim M., Altenburger A., Juel Hansen P., 2021. Physiological responses of *Mesodinium major* to irradiance, prey concentration and prey starvation. *J. Eukaryot. Microbiol.*, **n/a**: e12854.

El-Sayed W.M.M., Van Ginkel S.W., Igou T., Ibrahim H.A., Abdul-Raouf U.M., Chen Y., 2018. Environmental influence on rotenone performance as an algal crop protective agent to prevent pond crashes for biofuel production. *Algal Res.*, **33**: 277-283.

Faure E., Not F., Benoiston A.-S., Labadie K., Bittner L., Ayata S.-D., 2019. Mixotrophic protists display contrasted biogeographies in the global ocean. *ISME J.*, .

Fenchel T., 2008. The microbial loop – 25 years later. *J. Exp. Mar. Biol. Ecol.*, **366**: 99-103.

Ferreira G.D., Calbet A., 2020. Caveats on the use of rotenone to estimate mixotrophic grazing in the oceans. *Sci. Rep.*, **10**: 3899.

Flynn K.J., Berry L.S., 1999. The loss of organic nitrogen during marine primary production may be significantly overestimated when using ^{15}N substrates. *Proc. R. Soc. B*, **266**: 641-647.

Flynn K.J., Hansen P.J., 2013. Cutting the canopy to defeat the "selfish gene"; conflicting selection pressures for the integration of phototrophy in mixotrophic protists. *Protist*, **164**: 811-823.

Flynn K.J., Mitra A., Anestis K., Anschütz A.A., Calbet A., Ferreira G.D., Gypens N., Hansen P.J., John U., Martin J.L., Mansour J.S., Maselli M., Medić N., Norlin A., Not F., Pitta P., Romano F., Saiz E., Schneider L.K., Stolte W., Traboni C., 2019. Mixotrophic protists and a new paradigm for marine ecology: where does plankton research go now? *J. Plankton Res.*, **41**: 375-391.

Fuhrman J.A., McManus G.B., 1984. Do bacteria-sized marine eukaryotes consume significant bacterial production? *Science*, **224**: 1257-1260.

Gallegos C.L., 1989. Microzooplankton grazing on phytoplankton in the Rhode River, Maryland: Nonlinear feeding kinetics. *Mar. Ecol. Prog. Ser.*, **57**: 23-33.

Gardner J.L., Peters A., Kearney M.R., Joseph L., Heinsohn R., 2011. Declining body size: a third universal response to warming? *Trends Ecol. Evol.*, **26**: 285-291.

Gillooly J.F., Brown J.H., West G.B., Savage V.M., Charnov E.L., 2001. Effects of size and temperature on metabolic rate. *Science*, **293**: 2248-2251.

González Olalla J.M., Medina Sánchez J.M., Carrillo P., 2019. Mixotrophic trade off under warming and UVR in a marine and a freshwater alga. *J. Phycol.*, **55**: 1028-1040.

Hansen P.J., Calado A.J., 1999. Phagotrophic mechanisms and prey selection in free living dinoflagellates *J. Eukaryot. Microbiol.*, **46**: 382-389.

Jakobsen H.H., Strom S.L., 2004. Circadian cycles in growth and feeding rates of heterotrophic protist plankton. *Limnol. Oceanogr.*, **49**: 1915-1922.

Jeong H.J., Yoo Y.D., Kim J.S., Seong K.A., Kang N.S., Kim T.H., 2010. Growth, feeding and ecological roles of the mixotrophic and heterotrophic dinoflagellates in marine planktonic food webs. *Ocean Sci. J.*, **45**: 65-91.

Kamiyama T., 2000. Application of a vital staining method to measure feeding rates of field ciliate assemblages on a harmful alga. *Mar. Ecol. Prog. Ser.*, **197**: 299-303.

Kang H.C., Jeong H.J., Lim A.S., Ok J.H., You J.H., Park S.A., Lee S.Y., Eom S.H., 2020. Effects of temperature on the growth and ingestion rates of the newly described mixotrophic dinoflagellate *Yihiella yeosuensis* and its two optimal prey species. *Algae*, **35**: 263-275.

Kohzuma K., Froehlich J.E., Davis G.A., Temple J.A., Minhas D., Dhingra A., Cruz J.A., Kramer D.M., 2017. The role of Light–Dark regulation of the chloroplast ATP Synthase. *Front . Plant Sci.*, **8**.

Landry M.R., Hassett R.P.I., 1982. Estimating the grazing impact of marine micro-zooplankton. *Mar. Biol.*, **67**: 283-288.

Leles S.G., Mitra A., Flynn K.J., Stoecker D.K., Hansen P.J., Calbet A., McManus G.B., Sanders R.W., Caron D.A., Not F., 2017. Oceanic protists with different forms of acquired phototrophy display contrasting biogeographies and abundance. *Proc. R. Soc. B*, **284**: 20170664.

Leles S.G., Mitra A., Flynn K.J., Tillmann U., Stoecker D., Jeong H.J., Burkholder J., Hansen P.J., Caron D.A., Glibert P.M., 2019. Sampling bias misrepresents the biogeographical significance of constitutive mixotrophs across global oceans. *Glob. Ecol. Biogeogr.*, **28**: 418-428.

Lewin J.C., 1953. Heterotrophy in diatoms. *J. Gen. Microbiol.*, **9**: 305-313.

Li A., Stoecker D.K., Coats D.W., Adam E.J., 1996. Ingestion of fluorescently labeled and phycoerythrin-containing prey by mixotrophic dinoflagellates. *Aquat. Microb. Ecol.*, **10**: 139-147.

Lim A.S., Jeong H.J., Ok J.H., You J.H., Kang H.C., Kim S.J., 2019. Effects of light intensity and temperature on growth and ingestion rates of the mixotrophic dinoflagellate *Alexandrium pohangense*. *Mar. Biol.*, **166**: 98.

López-Urrutia Á., San Martin E., Harris R.P., Irigoien X., 2006. Scaling the metabolic balance of the oceans. *Proc. Natl. Acad. Sci.*, **103**: 8739-8744.

Martínez R.A., Isari S., Calbet A., 2014. Use of live, fluorescently-labeled algae for measuring microzooplankton grazing in natural communities. *J. Exp. Mar. Biol. Ecol.*, **457**: 59-70.

Mitra A., Flynn K.J., Burkholder J.M., Berge T., Calbet A., Raven J.A., Granéli E., Glibert P.M., Hansen P.J., Stoecker D.K., Thingstad F., Tillmann U., Våge S., Wilken S., Zubkov M.V., 2014. The role of mixotrophic protists in the biological carbon pump. *Biogeosciences*, **11**: 995-1005.

Mitra A., Flynn K.J., Tillmann U., Raven J.A., Caron D., Stoecker D.K., Not F., Hansen P.J., Hallegraeff G., Sanders R.W., Wilken S., McManus G., Johnson M., Pitta P., Våge S., Berge T., Calbet A., Thingstad F., Jeong H.J., Burkholder J., Glibert P.M., Granéli E., Lundgren V., 2016. Defining planktonic protist functional groups on mechanisms for energy and nutrient acquisition: incorporation of diverse mixotrophic strategies. *Protist*, **167**: 106-120.

Moeller H.V., Johnson M.D., Falkowski P.G., 2011. Photoacclimation in the phototrophic marine ciliate *Mesodinium rubrum* (ciliophora). *J. Phycol.*, **47**: 324-332.

Morison F., Franzè G., Harvey E., Menden-Deuer S., 2020. Light fluctuations are key in modulating plankton trophic dynamics and their impact on primary production. *Limnol. Oceanogr. Lett.*, **5**: 346-353.

Newell S.Y., Sherr B.F., Sherr E.B., Fallon R.D., 1983. Bacterial response to presence of eukaryote inhibitors in water from a coastal marine environment. *Mar. Environ. Res.*, **10**: 147-157.

Ng W.H.A., Liu H., Zhang S., 2017. Diel variation of grazing of the dinoflagellate *Lepidodinium* sp. and ciliate *Euplotes* sp. on algal prey: the effect of prey cell properties. *J. Plankton Res.*, **39**: 450-462.

Ok J.H., Jeong H.J., Lim A.S., You J.H., Kang H.C., Kim S.J., Lee S.Y., 2019. Effects of light and temperature on the growth of *Takayama helix* (Dinophyceae): mixotrophy as a survival strategy against photoinhibition. *J. Phycol.*, **55**: 1181-1195.

Oliver E.C.J., Burrows M.T., Donat M.G., Gupta A.S., Alexander L.V., Perkins-Kirkpatrick S.E., Benthuysen J.A., Hobday A.J., Holbrook N.J., Moore P.J., Thomsen M.S., Wernberg T., Smale D.A., 2019.

Projected marine heatwaves in the 21st Century and the potential for ecological impact. *Front. Mar. Sci.*, **6**: 734.

Palmer G., Horgan D.J., Tisdale H., Singer T.P., Beinert H., 1968. Studies on the respiratory chain-linked reduced nicotinamide adenine dinucleotide dehydrogenase XIV. Location of the sites of inhibition of rotenone, barbiturates, and piericidin by means of electron paramagnetic resonance spectroscopy. *J. Biol. Chem.*, **243**: 844-847.

Plagányi É.E., 2007. Models for an ecosystem approach to fisheries. *FAO (Food and Agriculture Organization of the United Nations) Fisheries Technical Paper*, .

Princiotta S.D., Smith B.T., Sanders R.W., 2016. Temperature dependent phagotrophy and phototrophy in a mixotrophic chrysophyte. *J. Phycol.*, **52**: 432-440.

Regaudie-de-Gioux A., Duarte C.M., 2012. Temperature dependence of planktonic metabolism in the ocean. *Global Biogeochem. Cycles*, **26**.

Riisgaard K., Hansen P.J., 2009. Role of food uptake for photosynthesis, growth and survival of the mixotrophic dinoflagellate *Dinophysis acuminata*. *Mar. Ecol. Prog. Ser.*, **381**: 51-62.

Rose J.M., Caron D.A., 2007. Does low temperature constrain the growth rates of heterotrophic protists? Evidence and implications for algal blooms in cold waters. *Limnol. Oceanogr.*, **52**: 886-895.

Rublee P.A., Gallegos C.L., 1989. Use of fluorescently labelled algae (FLA) to estimate microzooplankton grazing. *Mar. Ecol. Prog. Ser.*: 221-227.

Sanders R.W., Porter K.G., 1986. Use of metabolic inhibitors to estimate protozooplankton grazing and bacterial production in a monomictic eutrophic lake with an anaerobic hypolimnion. *Appl. Environ. Microbiol.*, **52**: 101-107.

Schmoker C., Hernández-León S., Calbet A., 2013. Microzooplankton grazing in the oceans: impacts, data variability, knowledge gaps and future directions. *J. Plankton Res.*, **35**: 691-706.

Schoener D.M., McManus G.B., 2012. Plastid retention, use, and replacement in a kleptoplastidic ciliate. *Aquat. Microb. Ecol.*, **67**: 177-187.

Sheridan J.A., Bickford D., 2011. Shrinking body size as an ecological response to climate change. *Nat. Clim. Change*, **1**: 401-406.

Sherr B.F., Sherr E.B., Andrew T.L., Fallon R.D., Newell S.Y., 1986. Trophic interactions between heterotrophic protozoa and bacterioplankton in estuarine water analyzed with selective metabolic inhibitors. *Mar. Ecol. Prog. Ser.*, **32**: 169-179.

Stoecker D.K., Hansen P.J., Caron D.A., Mitra A., 2017. Mixotrophy in the marine plankton. *Annu. Rev. Mar. Sci.*, **9**: 311-335.

Stoecker D.K., Michaels A.E., 1991. Respiration, photosynthesis and carbon metabolism in planktonic ciliates. *Mar. Biol.*, **108**: 441-447.

Stoecker D.K., Silver M.W., Michaels A.E., Davis L.H., 1988. Obligate mixotrophy in *Laboea strobila*, a ciliate which retains chloroplasts. *Mar. Biol.*, **99**: 415-423.

Strom S.L., 2001. Light-aided digestion, grazing and growth in herbivorous protists. *Aquat. Microb. Ecol.*, **23**: 253-261.

van den Hoff J., Bell E., 2015. The ciliate *Mesodinium rubrum* and its cryptophyte prey in Antarctic aquatic environments. *Polar Biol.*, **38**: 1305-1310.

Van Ginkel S.W., Bidwell M., Igou T., Gijon-Felix R., Salvi E.J.N.R., De Oliveira S.H.R., Duarte L.H.K., Steiner D., Hu Z., Johnston R., 2016. The prevention of saltwater algal pond contamination using the electron transport chain disruptor, rotenone. *Algal Res.*, **18**: 209-212.

Van Ginkel S.W., Igou T., Hu Z., Narode A., Cheruvu S., Doi S., Johnston R., Snell T., Chen Y., 2015. Taking advantage of rotifer sensitivity to rotenone to prevent pond crashes for algal-biofuel production. *Algal Res.*, **10**: 100-103.

Wilken S., Huisman J., Naus Wiezer S., Van Donk E., 2013. Mixotrophic organisms become more heterotrophic with rising temperature. *Ecol. Lett.*, **16**: 225-233.

Wilken S., Yung C.C.M., Hamilton M., Hoadley K., Nzongo J., Eckmann C., Corrochano-Luque M., Poirier C., Worden A.Z., 2019. The need to account for cell biology in characterizing predatory mixotrophs in aquatic environments. *Phil. Trans. R. Soc. B*, **374**: 20190090.

Yih W., Kim H.S., Jeong H.J., Myung G., Kim Y.G., 2004. Ingestion of cryptophyte cells by the marine photosynthetic ciliate *Mesodinium rubrum*. *Aquat. Microb. Ecol.*, **36**: 165-170.

Yool A., Popova E.E., Anderson T.R., 2013. MEDUSA-2.0: an intermediate complexity biogeochemical model of the marine carbon cycle for climate change and ocean acidification studies. *Geosci. Model Dev.*, **6**: 1767-1811.

SUPPLEMENTARY INFORMATION

Supplementary Information for Paper I

Table SI-1 Detailed experimental conditions for the first experiment with LFLA. The fluorescently labelled species was always *Isochrysis galbana*. The cryptophyte was *Rhodomonas salina* for all species except *Karlodinium veneficum* and *Mesodinium rubrum*, which were incubated with *Teleaulax amphioxeia* instead. Saturating and non-saturating food conditions were determined using functional responses for each grazer according to the footnote. The exact percentages of *I. galbana* and *T. amphioxeia* were not assessed on the respective predator's incubations because the ESD of both prey is very similar (ca. 4.5 and ca. 4.7 µm respectively). Accordingly, we assumed that the mixture contained, on average, 28.92 % LFLA. For the two ciliates, *Mesodinium rubrum* and *Strombidium arenicola*, we only tested a saturating food concentration.

Species	[Prey] = Low			[Prey] = High		
	Total prey mL^{-1}	LFLA %	Cryptophyte %	Total prey mL^{-1}	LFLA %	Cryptophyte %
Oxyrrhis marina[1]	4759	29.74	70.26	87797	26.41	73.59
Gyrodinium dominans[1]	4216	42.86	57.14	91785	30.97	69.03
Karlodinium veneficum[2]	5080	------	------	17454	------	------
Karlodinium armiger[3]	8440	23.89	76.11	114187	20.91	79.09
Mesodinium rubrum[4]	------	------	------	9134	------	------
Strombidium arenicola[5]	------	------	------	73725	27.67	72.33

[1]Calbet *et al.* 2013;

[2]Calbet *et al.* 2011a;

[3]Berge *et al.* 2008b;

[4]Smith & Hansen 2007;

[5]Ferreira *et al.* submitted – **Paper III**.

a)

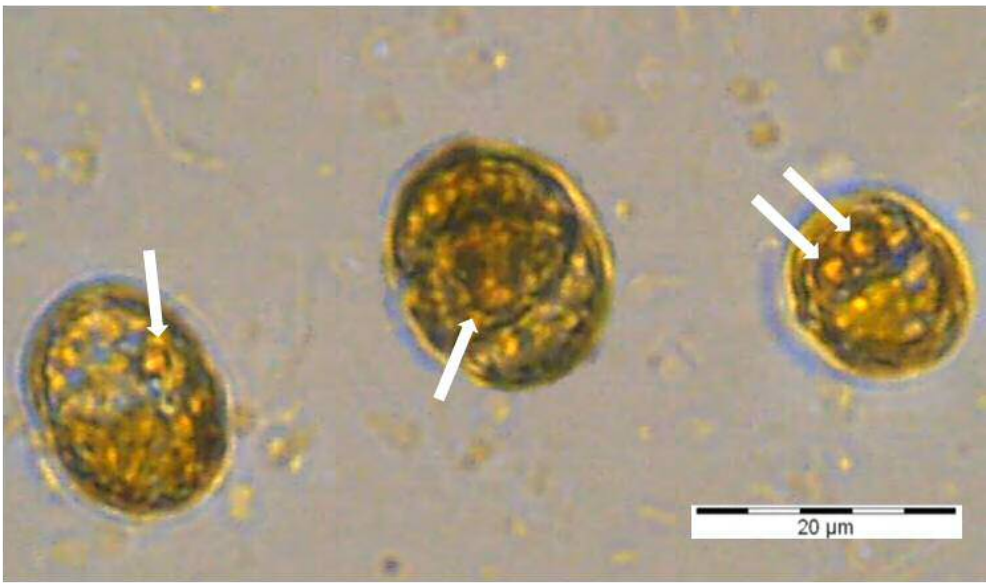

b)

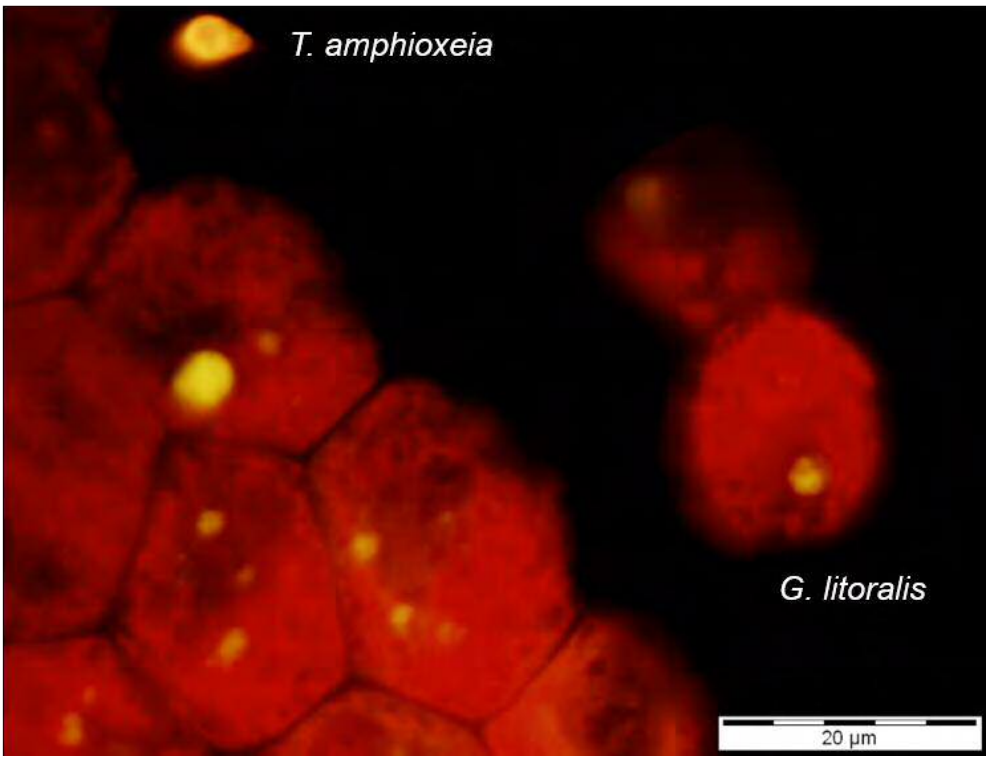

Figure SI-1 Detection of food vacuoles inside the previously unknown CM *Gymnodinium litoralis*: a) live pictures obtained after keeping a monoculture under complete darkness for two days (cannibalism); b) using epifluorescence microscopy under UV light excitation to detect *Teleaulax amphioxeia*. Cryptophytes such as *T. amphioxeia* contain phycoerythrin, i.e., seen as orange fluorescent inclusions as opposed to chlorophyll which glows in a bright red tone.

Supplementary Information for Paper III

Table SIII-1 The experimental design used in the dinoflagellate experiment. The whole community comprised *Gyrodinium dominans* and *Karlodinium armiger* as predators, and *Conticribra weissflogii* and *Rhodomonas salina* as prey. The sampling points include one sample for Chlorophyll *a* and one for cell counts. The ciliate experiment followed the same scheme with the difference that the whole community contained *Strombidium arenicola* and *Mesodinium rubrum* as predators, being the controls adjusted accordingly.

Treatment[1]		Sampling points (hours)				
		0	2	4	8	24
Dilution series[2]	100 %	✓	✓	✓	✓	✓
	60 %	✓	✓	✓	✓	✓
	30 %	✓	✓	✓	✓	✓
	15 %	✓	✓	✓	✓	✓
Controls	100prey	✓			✓	✓
	100gyro	✓			✓	✓
	100karlo	✓			✓	✓

[1]The same design was used under a regular diel light cycle and complete darkness

[2]Executed with the whole community

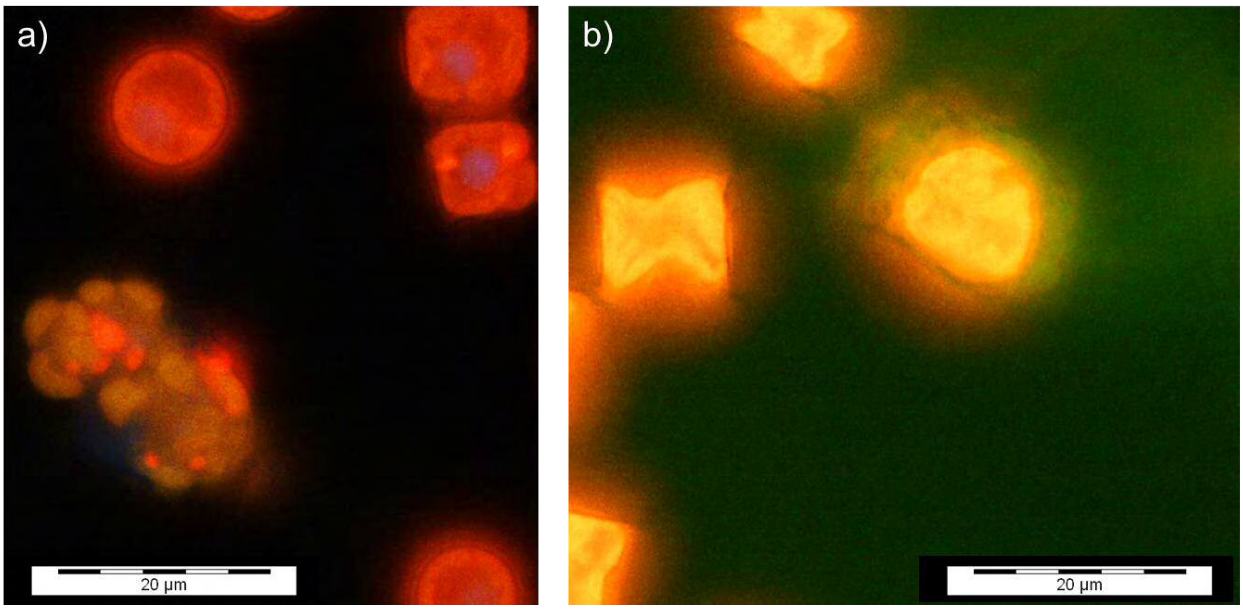

Figure SIII-1 Epifluorescence photographs of a trial conducted before the dilution grazing experiment: a) *Mesodinium rubrum* with red chloroplasts inside (blue light excitation) and b) *Gyrodinium dominans* with a *Conticribra weissflogii* inside (green light excitation). Both images were obtained after incubating both species together for ca. 24 h under regular diel light conditions.

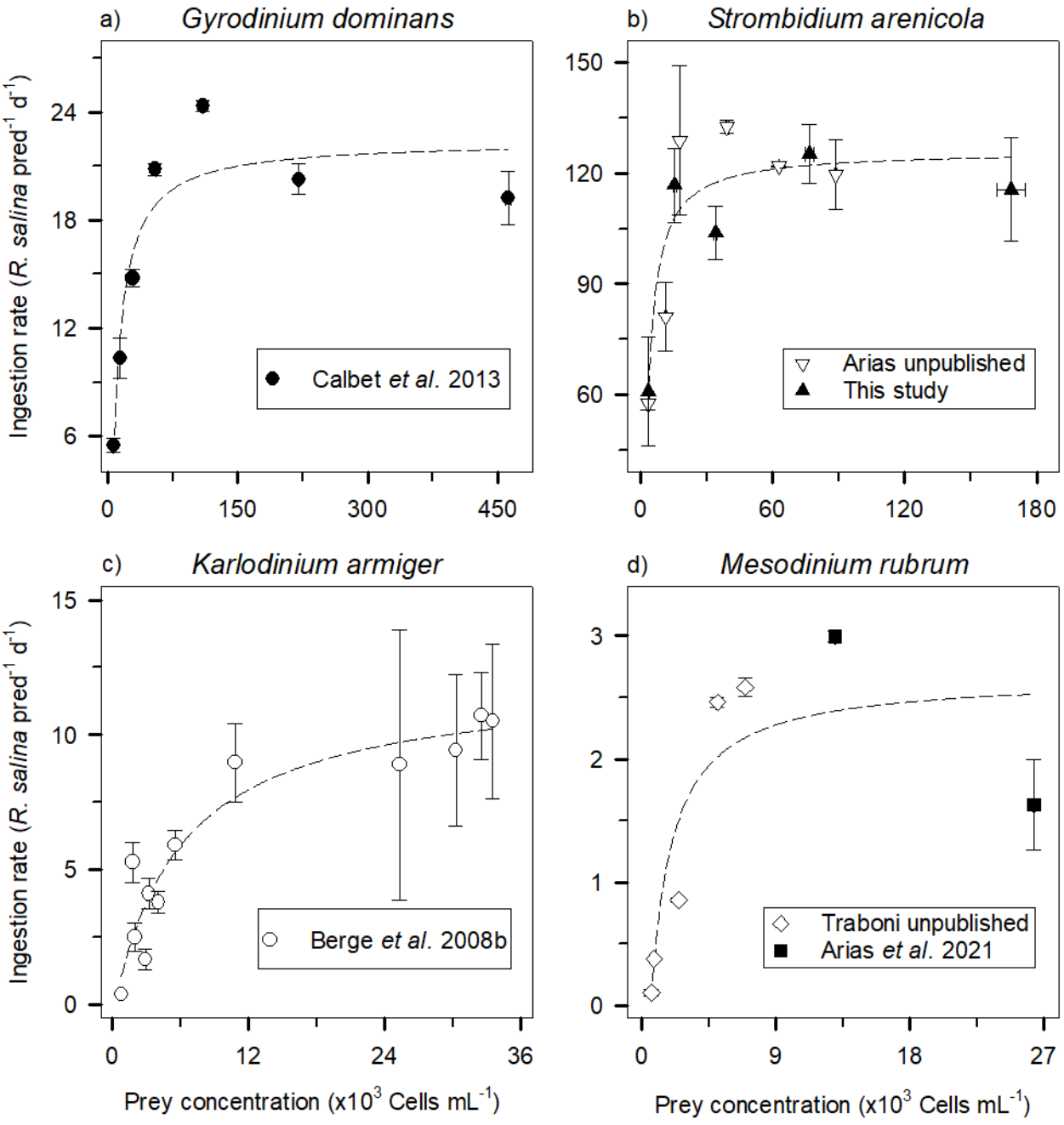

Figure SIII-2 Ingestion rate (Cells predator^{-1} d^{-1}) of a) *Gyrodinium dominans*, b) *Strombidium arenicola*, c) *Karlodinium armiger*, and d) *Mesodinium rubrum* on the cryptophyte *Rhodomonas salina*. The original data source is indicated in each panel of the figure. The curve fits were obtained by applying Michaelis-Menten kinetics to the data. Error bars ± se.

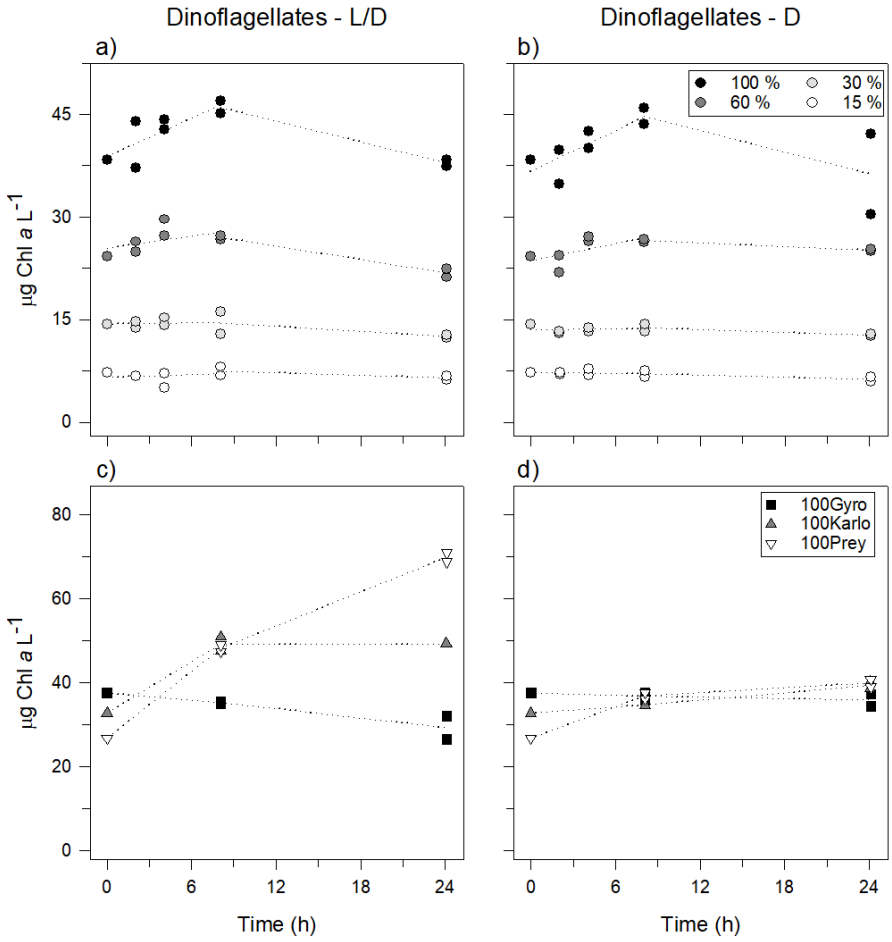

Figure SIII-3 Chl *a* over time for the experiment with dinoflagellates: a and b) dilution series in the L/D and D treatments respectively; c and d) control bottles series in the L/D and D treatments respectively.

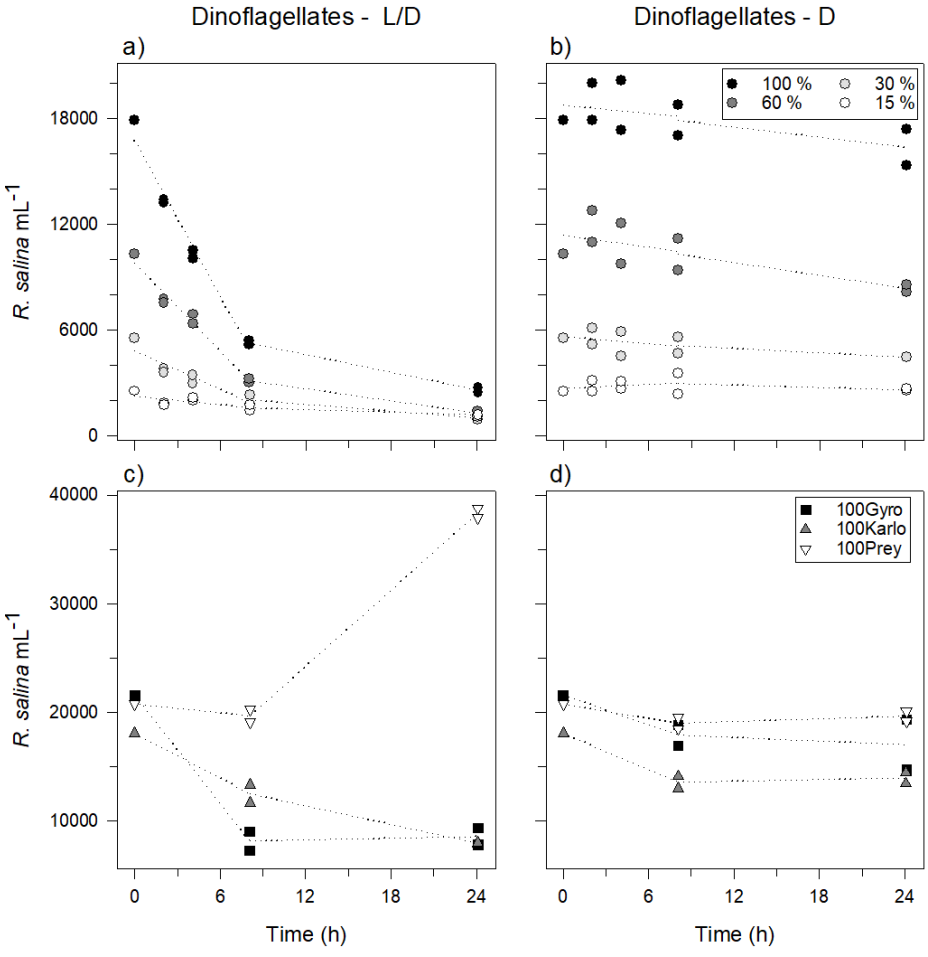

Figure SIII-4 Abundance of *Rhodomonas salina* over time for the experiment with dinoflagellates: a and b) dilution series in the L/D and D treatments respectively; c and d) control bottles series in the L/D and D treatments respectively.

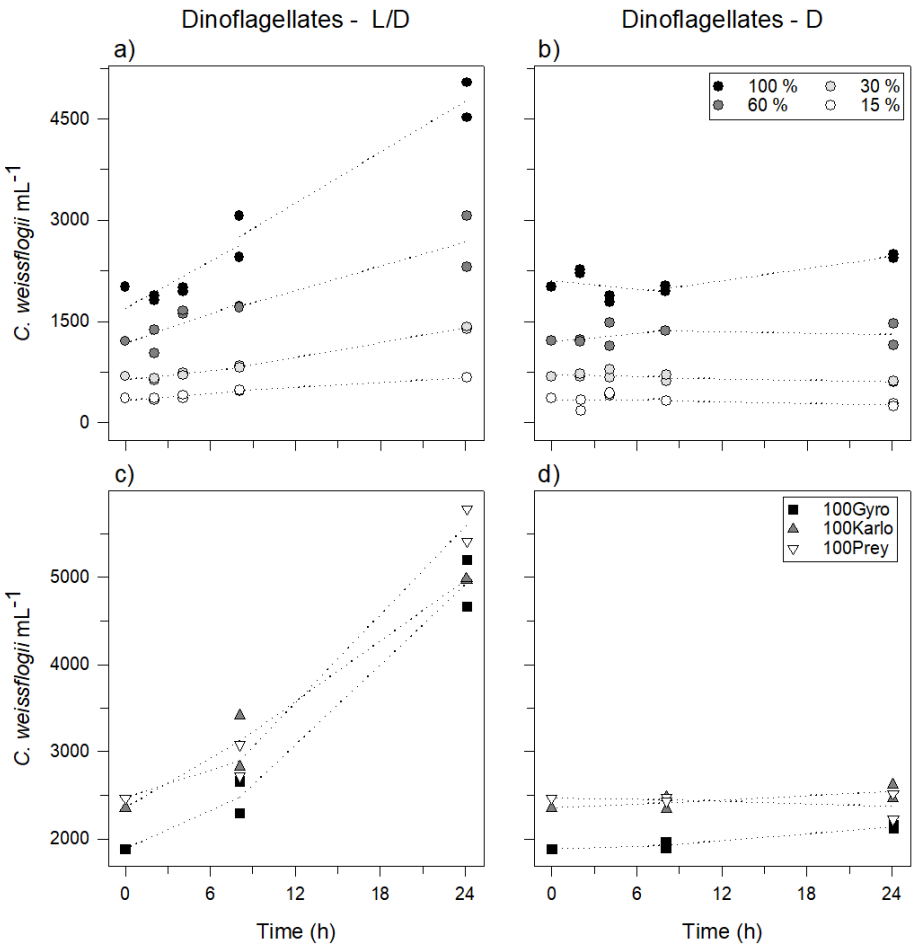

Figure SIII-5 Abundance of *Contricriba weissflogii* over time for the experiment with dinoflagellates: a and b) dilution series in the L/D and D treatments respectively; c and d) control bottles series in the L/D and D treatments respectively.

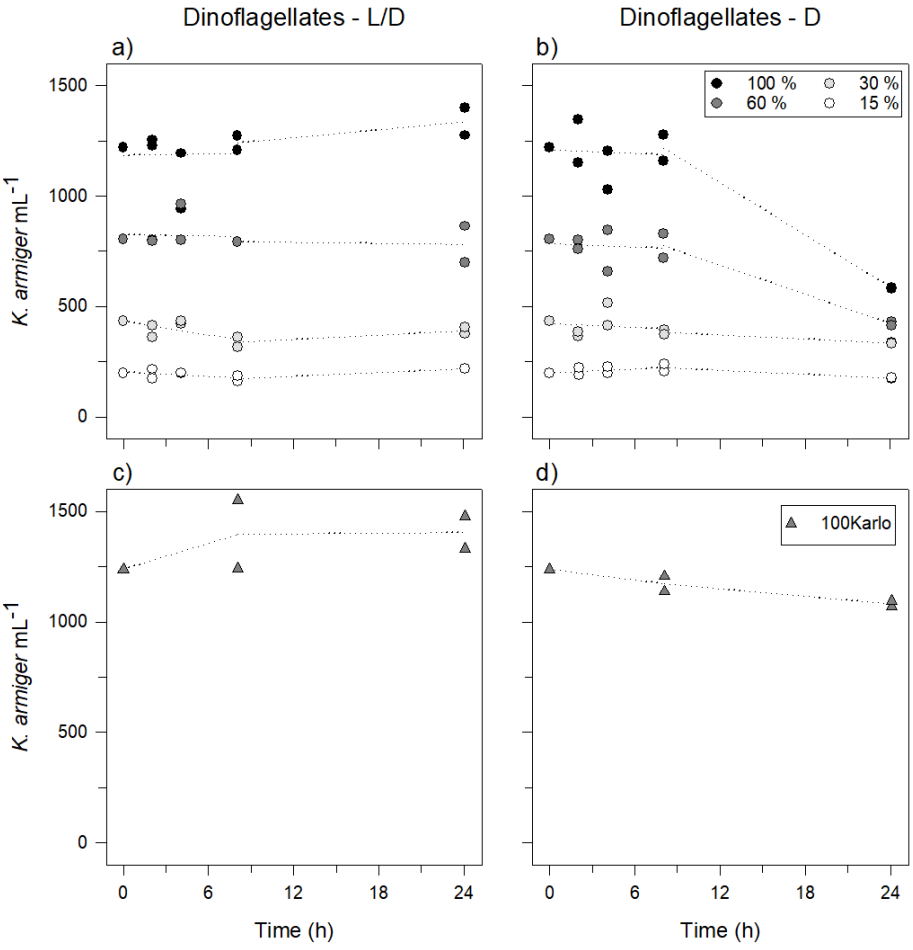

Figure SIII-6 Abundance of *Karlodinium armiger* over time for the experiment with dinoflagellates: a and b) dilution series in the L/D and D treatments respectively; c and d) control bottles series in the L/D and D treatments respectively.

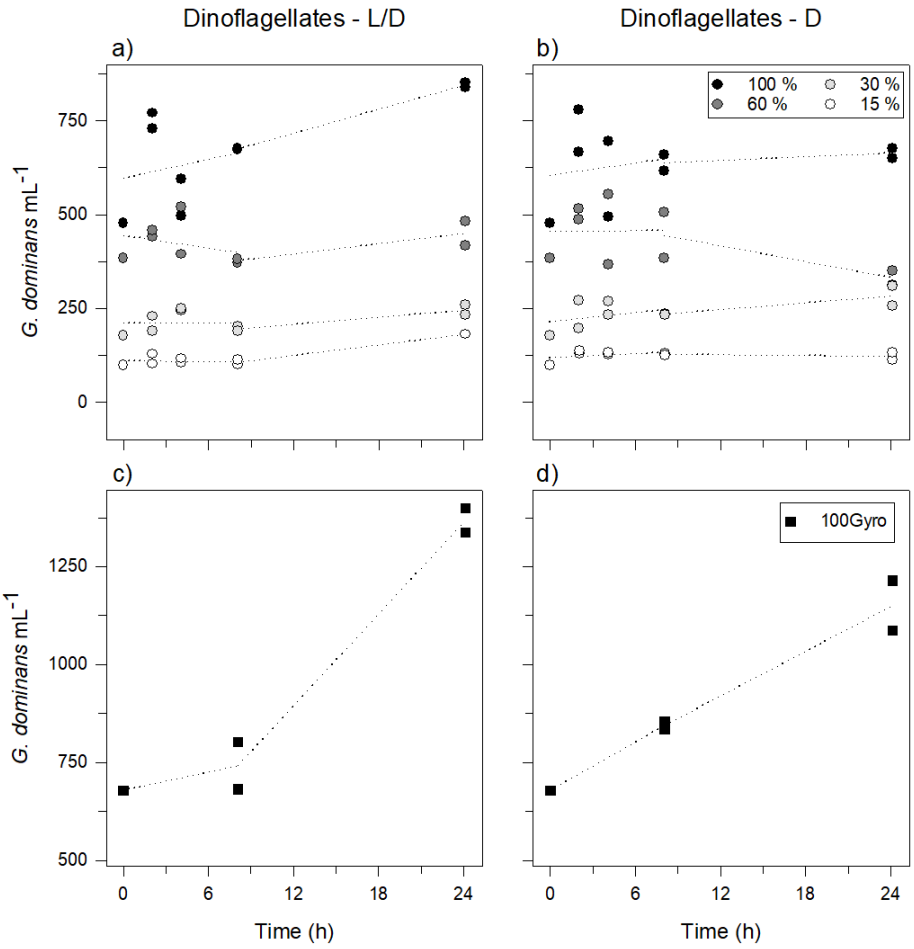

Figure SIII-7 Abundance of *Gyrodinium dominans* over time for the experiment with dinoflagellates: a and b) dilution series in the L/D and D treatments respectively; c and d) control bottles series in the L/D and D treatments respectively.

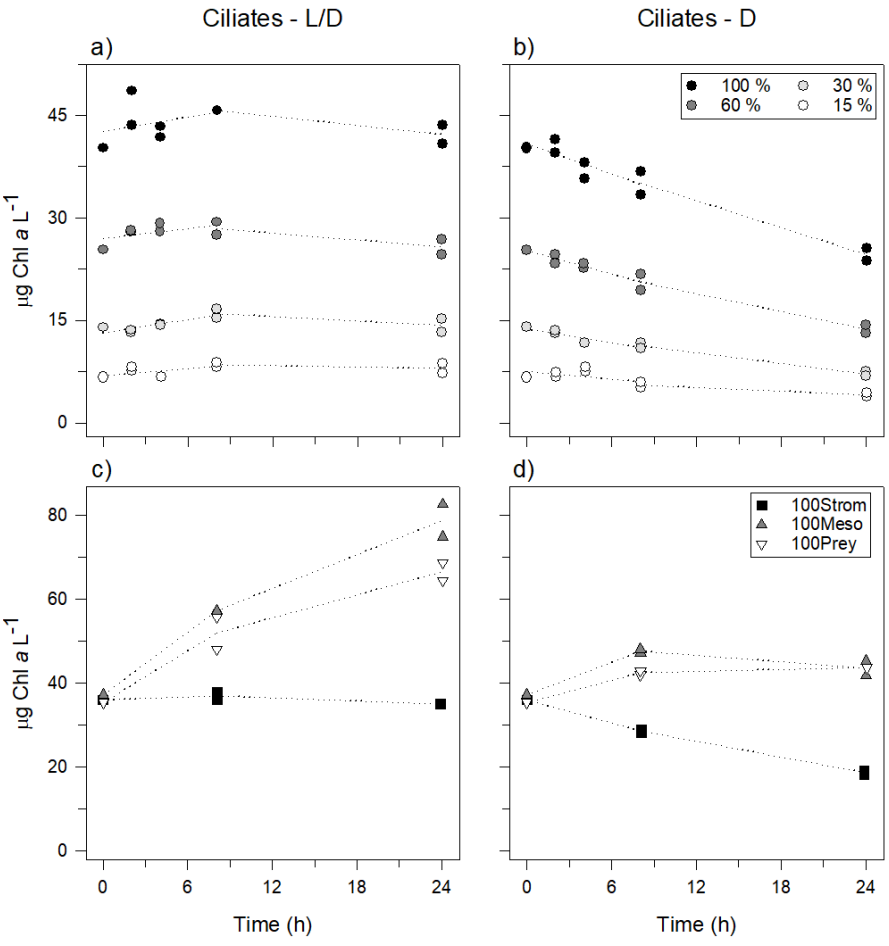

Figure SIII-8 Chl *a* over time for the experiment with ciliates: a and b) dilution series in the L/D and D treatments respectively; c and d) control bottles series in the L/D and D treatments respectively.

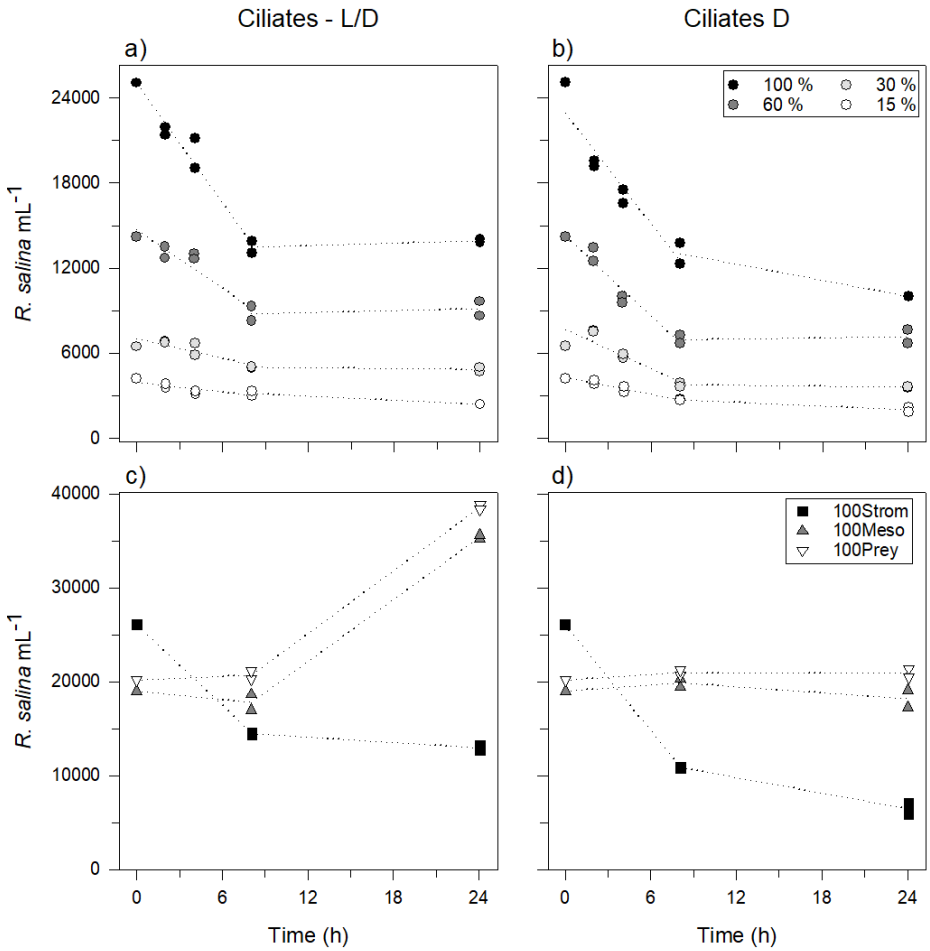

Figure SIII-9
Abundance of *Rhodomonas salina* over time for the experiment with ciliates: a and b) dilution series in the L/D and D treatments respectively; c and d) control bottles series in the L/D and D treatments respectively.

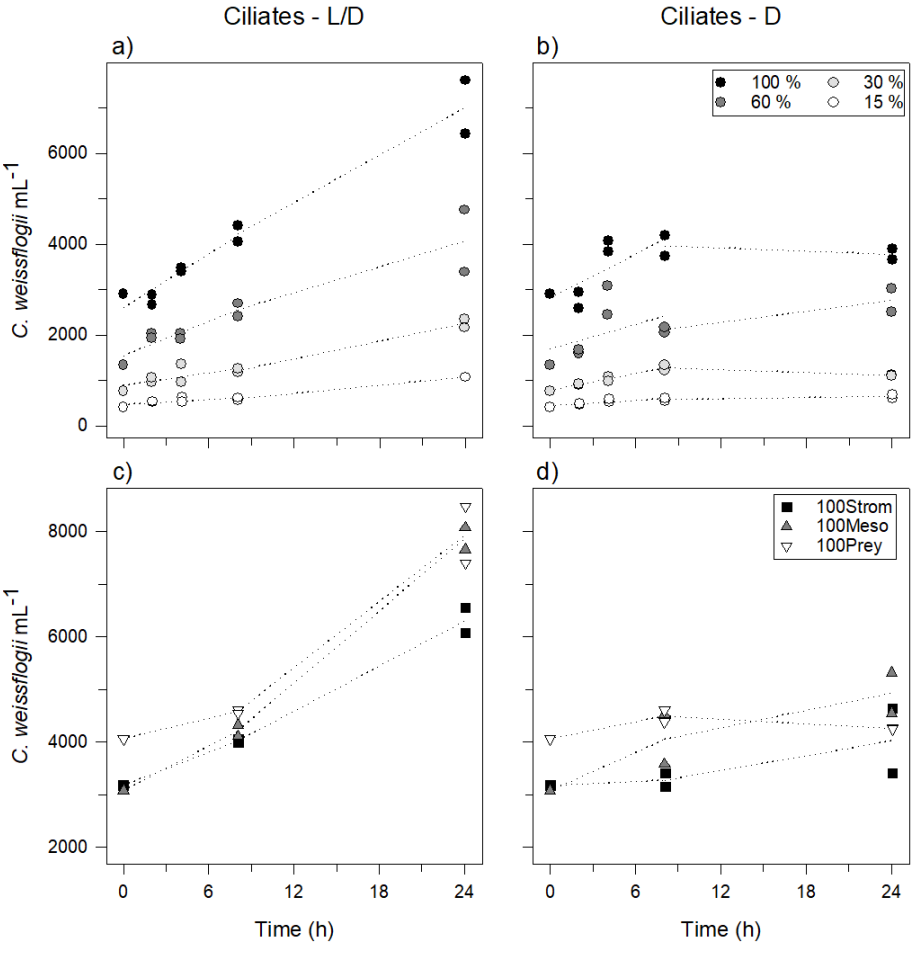

Figure SIII-10
Abundance of *Conticribra weissflogii* over time for the experiment with ciliates: a and b) dilution series in the L/D and D treatments respectively; c and d) control bottles series in the L/D and D treatments respectively.

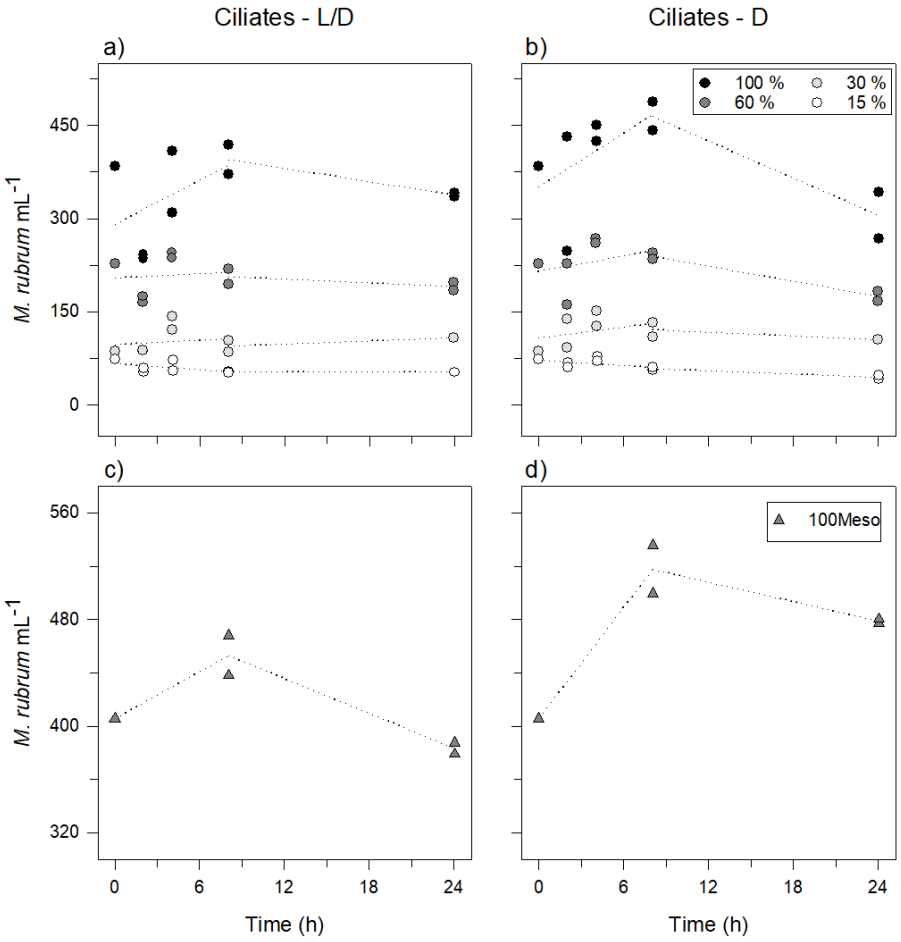

Figure SIII-11 Abundance of *Mesodinium rubrum* over time for the experiment with ciliates: a and b) dilution series in the L/D and D treatments respectively; c and d) control bottles series in the L/D and D treatments respectively.

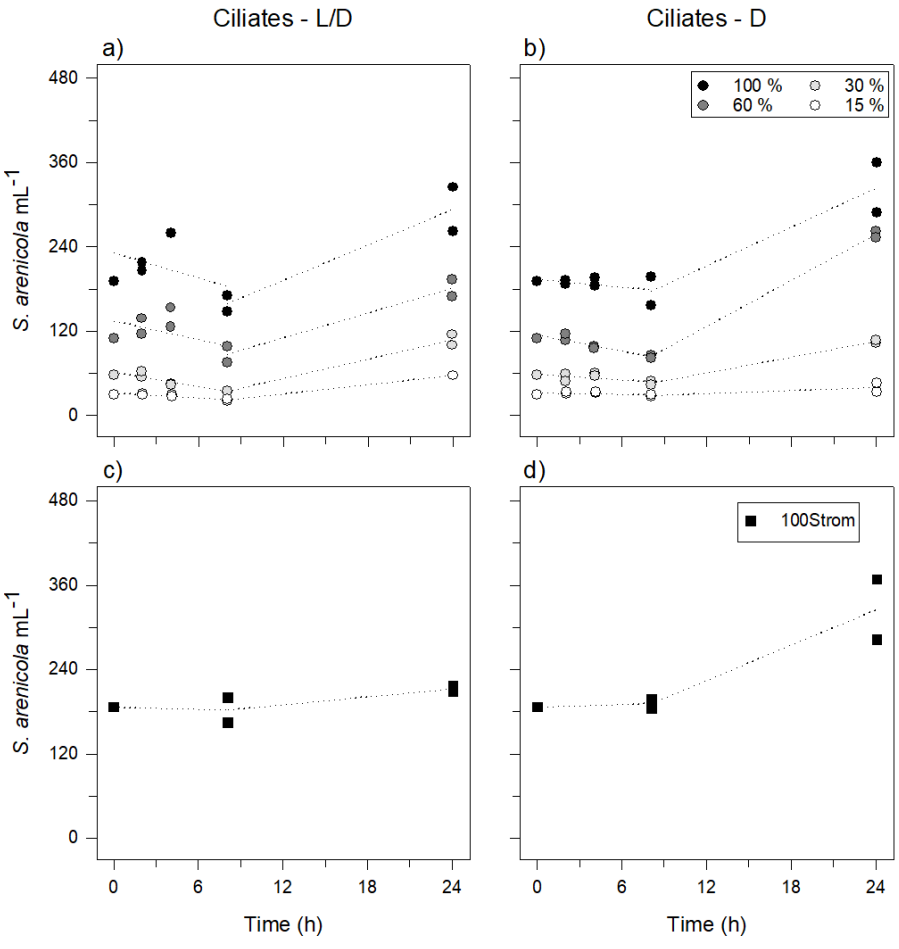

Figure SIII-12 Abundance of *Strombidium arenicola* over time for the experiment with ciliates: a and b) dilution series in the L/D and D treatments respectively; c and d) control bottles series in the L/D and D treatments respectively.

Supplementary Information for Paper IV

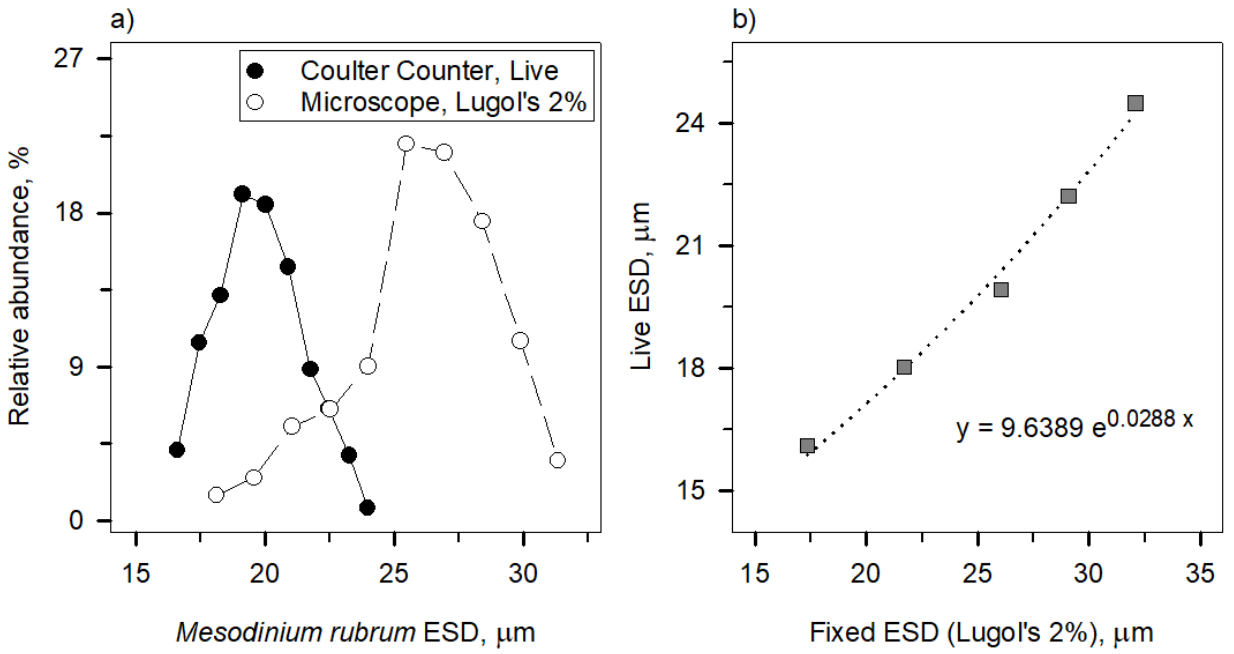

Figure SIV-1 Volume differences between a single population of *Mesodinium rubrum*, live (n > 1.0 x 10^3) and after fixation in 2 % Lugol's (n = 200). a) relative abundance of ESDs; b) exponential correction between fixed and live ESDs.

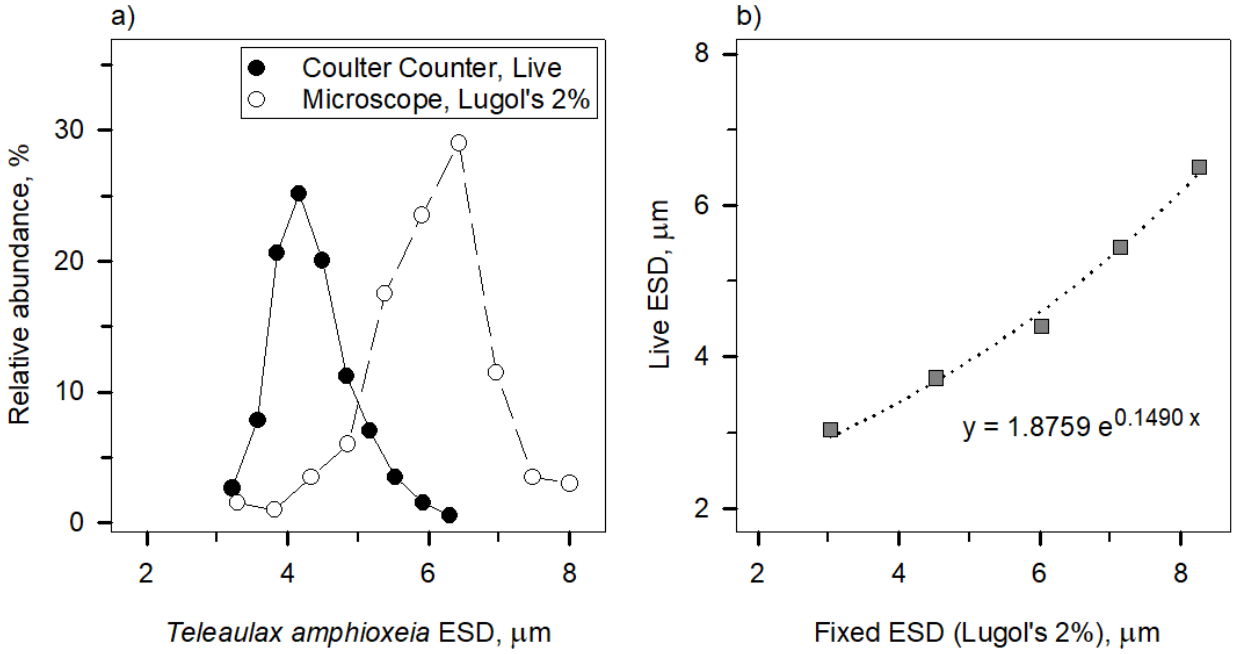

Figure SIV-2 Volume differences between a single population of *Teleaulax amphioxeia*, live (n > 1.3 x 10^6) and after fixation in 2 % Lugol's (n = 200). a) relative abundance of ESDs; b) exponential correction between fixed and live ESDs.

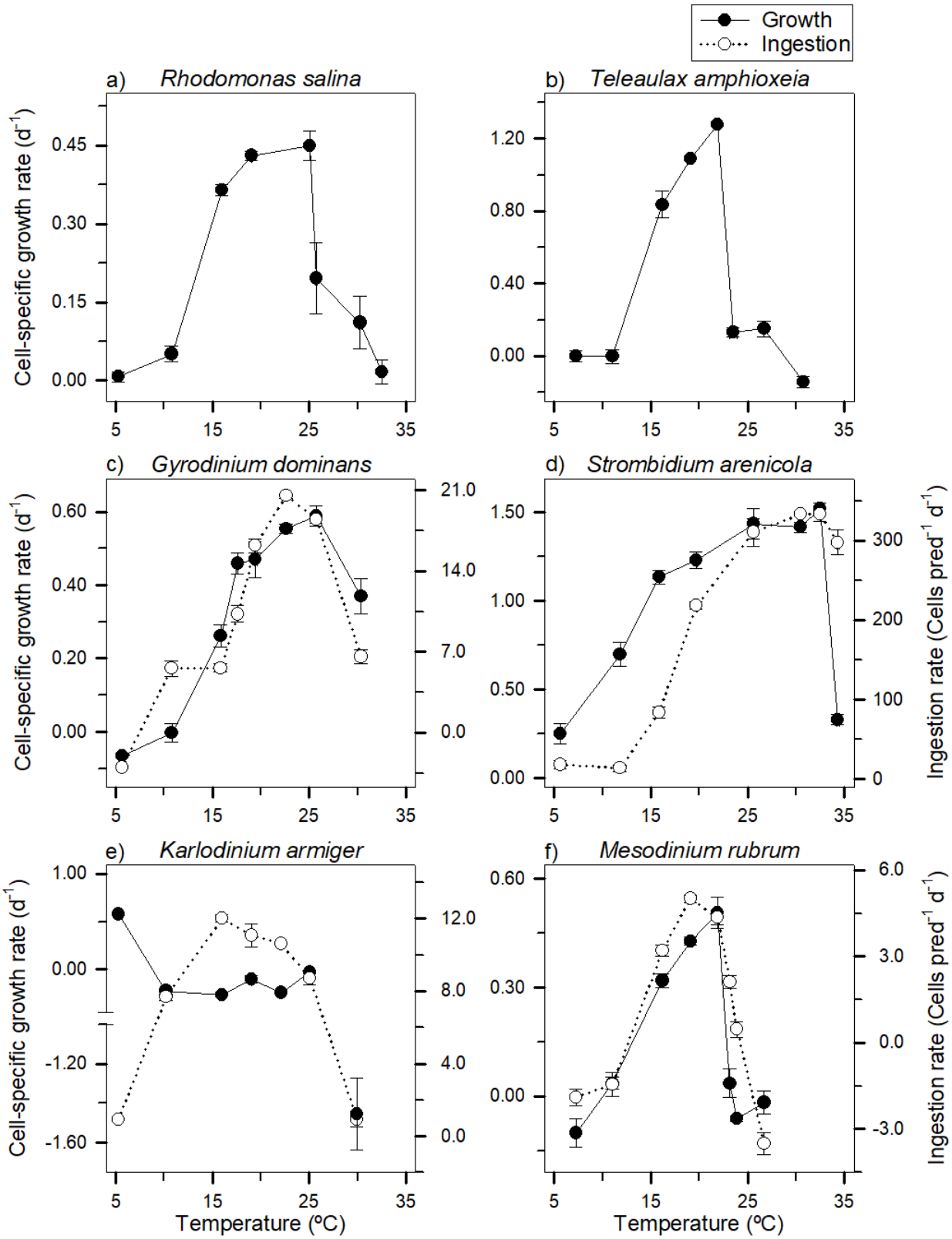

Figure SIV-3 Cell-specific thermal performance curves for the studied protists in terms of growth (black circles with solid lines) and ingestion (white circles with dotted lines): a and b) the phytoplankton *R. salina* and *T. amphioxeia*; c and d) the protozooplankton *G. dominans* and *S. arenicola*; e and f) the mixoplankton *K. armiger* and *M. rubrum*. Error bars ± se.

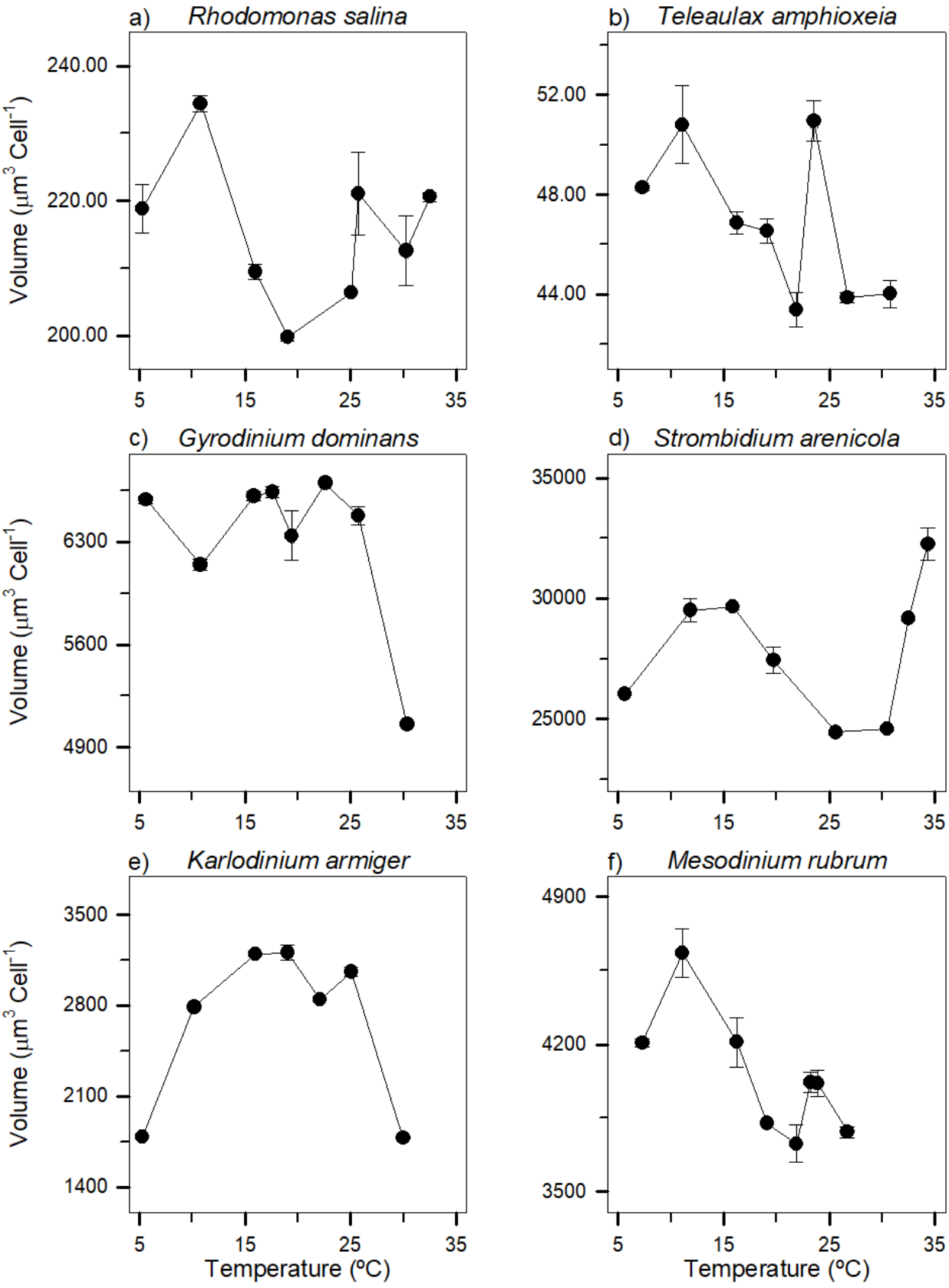

Figure SIV-4 Relationship between temperature (°C) and Volume (µm^3 Cell^{-1}) for a) *R. salina*, b) *T. amphioxeia*, c) *G. dominans*, d) *S. arenicola*, e) *K. armiger*, and f) *M. rubrum*. The results for *R. salina* and *T. amphioxeia* were obtained from the control bottles, i.e., without predators.

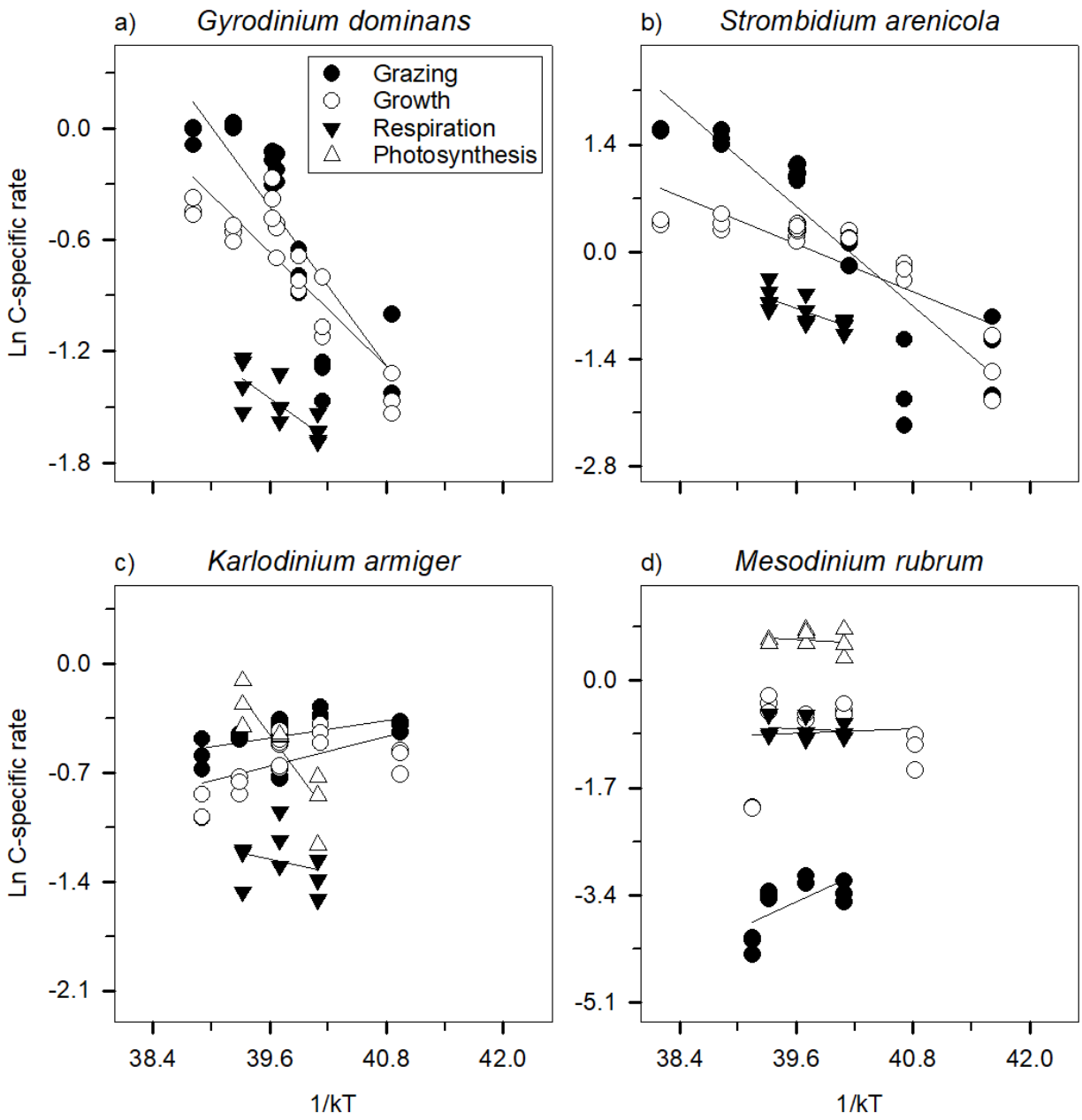

Figure SIV-5 Arrhenius plots for the C-specific physiological rates of the a and b) protozooplankton *Gyrodinium dominans* and *Strombidium arenicola*, respectively, c and d) mixoplankton *Karlodinium armiger* and *Mesodinium rubrum*, respectively. Photosynthesis was only measurable in mixoplankton.

Table SIV-1 Activation energies (eV) for every physiological rate ascertained in this study. *Ea*s were calculated from the slope of the Arrhenius plot for each parameter.

Species	Growth	Grazing	Respiration	Photosynthesis
Gyrodinium dominans	0.5145	0.7186	0.3765	NA
Strombidium arenicola	0.5229	1.0850	0.4533	NA
Karlodinium armiger	-0.1603	-0.0937	0.1295	0.8468
Mesodinium rubrum	0.0573	-0.7126	0.0695	0.0741

Acknowledgments

I must start by thanking Albert for you are the main reason why this thesis has been sucessful. We started our journey with an immesurable knowledge gap between the two of us (which remains today ahaha) but you have always listened to me and made me feel like my opinion mattered. Even when I showed you my first-ever manuscript draft and your comments were somewhere down the line of “let us pretend that this did not exist”. I am truly grateful for your support, constructive criticism, and for not being afraid to show your claws to stand up for me.

I must also thank Per with all my heart even though we did not have the opportunity to spend as much time together. Still, I think that you were a fundamental piece in my PhD. Not only scientifically speaking but also personally. There was a time, during my secondment at Helsingør, when I was feeling completely beaten down for numerous reasons, and you, your never-ending optimism, and ridiculous dedication (the good kind of ridiculous) somehow lifted me up. And again! And again in other occasions too ahaha.

A special thanks is also due to Kevin Flynn and Aditee Mitra, not only for the numerous scientific advices, but also for bringing together the MixITiN Consortium which has been a tremendous source of inspiration and friendship throughout these past years. Worthy of a particular recognition within the Consortium are my colleague-turned-friends, the 10 ESRs which embarked on this adventure with me. One way or another, you may be certain that you have left your mark on me and that I am grateful for not having missed the day we met. Hoping that no one gets offended, I must individually acknowledge Andreas, Nikola, and Maira, for all the good moments that we lived together, and Mena and Anna, for all the meals, conversations, and opinions that we shared.

To Barcelona, for giving me Anna, Manu, Deju, Queralt, Kaiene and Enric. Your companionship and assistance have been paramount for the success of this work. To Claudia for the unexpected friendship which I did not know I needed but became so important during this period. Also, for the otherwordly cover page for my thesis.

I must also thank my friends from my home country for the continued reminder that I was not forgotten in their life. To my family, for all the support that they have given me throughout my life. I know that you will always be there for me. Always.

Finally, I could not have finished this journey if my wife, Cátia, hadn’t been beside me the whole time. Either telling me that I was great, or that I could be better. By standing silent next to me while I pretend to write. For holding my hand. Thank you!

APPENDIX